

Electronic Thesis and Dissertation Repository

---

3-2-2011 12:00 AM

## The Behaviour of Cement Stabilized Clay At High Water Contents

Saeed Sasanian

*The University of Western Ontario*

Supervisor

Dr. Timothy A. Newson

*The University of Western Ontario*

Graduate Program in Civil and Environmental Engineering

A thesis submitted in partial fulfillment of the requirements for the degree in Doctor of  
Philosophy

© Saeed Sasanian 2011

Follow this and additional works at: <https://ir.lib.uwo.ca/etd>



Part of the [Geotechnical Engineering Commons](#)

---

### Recommended Citation

Sasanian, Saeed, "The Behaviour of Cement Stabilized Clay At High Water Contents" (2011). *Electronic Thesis and Dissertation Repository*. 110.

<https://ir.lib.uwo.ca/etd/110>

This Dissertation/Thesis is brought to you for free and open access by Scholarship@Western. It has been accepted for inclusion in Electronic Thesis and Dissertation Repository by an authorized administrator of Scholarship@Western. For more information, please contact [wlsadmin@uwo.ca](mailto:wlsadmin@uwo.ca).

# **THE BEHAVIOUR OF CEMENT STABILIZED CLAY AT HIGH WATER CONTENTS**

(Thesis Format: Integrated-Article)

by:

Saeed Sasanian

Department of Civil and Environmental Engineering  
Faculty of Engineering Science

A thesis submitted in partial fulfillment  
of the requirements for the degree of  
Doctor of Philosophy

The School of Graduate and Postdoctoral Studies  
The University of Western Ontario  
London, Ontario, Canada

© Saeed Sasanian, 2011

**THE UNIVERSITY OF WESTERN ONTARIO  
THE SCHOOL OF GRADUATE AND POSTDOCTORAL STUDIES**

**CERTIFICATE OF EXAMINATION**

Supervisor

\_\_\_\_\_  
Dr. Timothy A. Newson

Examiners

\_\_\_\_\_  
Dr. Ernest K. Yanful

\_\_\_\_\_  
Dr. Moncef L. Nehdi

\_\_\_\_\_  
Dr. Sean D. Hinchberger

\_\_\_\_\_  
Dr. James A. Blatz

The thesis by  
Saeed Sasanian

Entitled

**THE BEHAVIOUR OF CEMENT STABILIZED CLAY AT HIGH WATER  
CONTENTS**

is accepted in partial fulfillment of the  
requirements for the degree of  
Doctor of Philosophy

Date \_\_\_\_\_

\_\_\_\_\_  
Chair of the Thesis Examination Board

## **ABSTRACT**

Artificial cementation of soft clays has been used for several years for different ground improvement projects. Although considerable work has been done to develop advanced machinery and techniques for the implementation of artificial cementation, less knowledge is available on the mechanisms involving the formation of the artificial structure and the resulting mechanical behaviour. The primary objectives of the present work were to investigate the formation of microstructure in artificially cemented material with Portland cement, find the relationships between cementitious bonding and clay mineralogy, and create constitutive frameworks for predicting the mechanical behaviour of cement-treated clays.

Qualitative and quantitative microstructural characterisation of reconstituted and cemented material has been performed using scanning electron microscopy (SEM) and mercury intrusion porosimetry (MIP). The results confirmed the transformation of the void microstructure from a bimodal, dispersed material into a unimodal, flocculated material due to artificial cementation. The addition of cement was found to reduce the amount of macro-pores within the cemented material, resulting in a significant reduction in hydraulic conductivity.

A further parametric study was conducted on data obtained in the laboratory by the author combined with those found in the literature, to investigate the effect of clay mineralogy on artificial cementation. The results indicated the major influence of the activity of the clay, along with the cement and water content, on the results of the cement treatment. The observed variations in the mechanical behaviour with respect to mineralogy and the important effect of curing time have been explained in terms of the

pozzolanic reactions, and the limitations of applying Abrams' law to cement-admixed clays are discussed.

In addition, an experimental study has been conducted to investigate the yielding and stress-strain behaviour of artificially cemented Ottawa clay and to compare it with the behaviour of the same soil in its naturally structured state. The results indicate that although the natural clay exhibits a meta-stable structure, resulting in an abrupt post-yield loss of strength, the artificially cemented material undergoes a more gradual breakage of the cementitious bonds. This allows for the use of the critical state concept, along with a pseudo-normal compression line, to develop a constitutive model for the artificially cemented material.

**Keywords:** reconstituted clay, artificially cemented clay, microstructure, inter-aggregate, intra-aggregate, activity, cement-water ratio, hydration reactions, pozzolanic reactions, critical state, yield locus, elastic and plastic deformations, stiffness

## **CO-AUTHORSHIP**

This work was carried out by Saeed Sasanian under the direct supervision of Professor Timothy A. Newson. The laboratory experimental work and the literature review were conducted by Saeed Sasanian, and Dr. Timothy A. Newson assisted in the design of the experimental program, the interpretation of the acquired data, and the preparation of the final papers. Dr. Timothy A. Newson will be a co-author in all of the publications emerging from this thesis. The details of the publications are as follows:

### **Chapter 2: Use of Mercury Intrusion Porosimetry for Microstructural Investigation of Reconstituted Clays**

S. Sasanian and T.A. Newson

A version of this chapter has been submitted to the journal of “*Engineering Geology*”

### **Chapter 3: The Development of Microstructure in Artificially Cemented Canadian Clays**

S. Sasanian and T.A. Newson

A version of this chapter has been submitted to the “*Journal of Geotechnical and Geoenvironmental Engineering*”

### **Chapter 4: Basic Parameters Governing the Behaviour of Cement-treated Clays**

S. Sasanian and T.A. Newson

A version of this chapter has been submitted to the “*Soils and Foundations*” journal

**Chapter 5: A Framework for Yielding and Stress-strain Behaviour of Artificially  
Cemented Clays**

S. Sasanian and T.A. Newson

A version of this chapter will be submitted to the “*Canadian Geotechnical Journal*”

**To my wife, Bahareh**  
**And to the memory of my mother**



## **ACKNOWLEDGEMENT**

I would like to express my deep gratitude to Dr. Timothy A. Newson for giving me the opportunity to work in his group, providing me with his unlimited and unconditioned support, and having endless patience and understanding. His commitment to excellence, together with his excellent knowledge, has been essential for the accomplishment of this work. I have truly enjoyed being his student and friend and wish to have the opportunity to work with him again in the future.

Appreciation is also expressed to the Natural Sciences and Engineering Research Council of Canada, NSERC, and The University of Western Ontario, for providing financial support for this work.

I would like to express sincere appreciation to the faculty and staff in the department of civil engineering at the University of Western Ontario. In particular, I am grateful to Wilbert Logan and Tim Stephens for their assistance during the laboratory work and their efforts to provide a safe a working environment.

I would like to also thank all of my colleagues and friends for providing me with such a pleasant work environment and for contributing to my work in numerous ways. Special thanks are due to my good friends Erol Tas, Mohammadreza Dehghani-Najvani, Kimberly Rasmussen, Lisa K. Reipas, Alireza Varshoi, Saeed Ahmed, Mohamed Elkasabgy, Africa M. Geremew, and Joon K. Lee.

Finally, I would like to express deepest appreciations to my family, especially my beloved wife, Bahareh, whose continuous kindness and support have greatly empowered me throughout the course of my studies.

# TABLE OF CONTENTS

<b>Certificate of Examination</b> .....	<b>ii</b>
<b>Abstract</b> .....	<b>iii</b>
<b>Co-Authorship</b> .....	<b>v</b>
<b>Acknowledgement</b> .....	<b>viii</b>
<b>Table of Contents</b> .....	<b>ix</b>
<b>List of Tables</b> .....	<b>xiii</b>
<b>List of Figures</b> .....	<b>xiv</b>
<b>Nomenclature</b> .....	<b>xxi</b>
<b>1 Introduction</b> .....	<b>1</b>
1.1 General.....	1
1.2 Objectives of the Research .....	7
1.3 Structure of the Thesis .....	8
1.4 References.....	11
<b>2 Use of Mercury Intrusion Porosimetry for Microstructural Investigation of Reconstituted Clays</b> .....	<b>20</b>
2.1 Introduction.....	20
2.2 Literature Review .....	20
2.3 Experimental Design .....	24
2.3.1 Material properties .....	24
2.3.2 Specimen preparation and testing programme .....	25
2.4 Test Results and Analysis .....	26
2.5 Discussion on MIP analysis for soft and slurried clays .....	33

2.6	Summary and Conclusions .....	38
2.7	Acknowledgments .....	39
2.8	References.....	39
<b>3</b>	<b>The Development of Microstructure in Artificially Cemented Canadian Clays...54</b>	
3.1	Introduction.....	54
3.2	Literature Review .....	56
3.3	Experimental Design .....	59
3.3.1	Material properties .....	59
3.3.2	Specimen preparation and testing programme.....	60
3.4	Results and Analysis.....	64
3.4.1	SEM analysis of undisturbed, reconstituted, and artificially cemented specimens.....	64
3.4.2	Pore size distribution: the effect of artificial cementation by Portland cement and gypsum .....	70
3.4.3	The effects of the developed microstructure on the mechanical behaviour of artificially cemented clays.....	78
3.5	Summary and Conclusions .....	82
3.6	Acknowledgments .....	84
3.7	References.....	84
<b>4</b>	<b>Basic Parameters Governing the Behaviour of Cement-treated Clays.....110</b>	
4.1	Introduction.....	110
4.2	Literature Review .....	111
4.3	Description of Laboratory Studies and Data Analysis.....	115

4.3.1	Experimental work .....	115
4.3.2	Specimen preparation and testing procedures .....	115
4.3.3	Additional database compilation .....	117
4.3.4	Material properties .....	118
4.4	Analysis of the Data .....	119
4.4.1	Hardening of cemented clays with time .....	119
4.4.2	Shear strength of artificially cemented clays: state parameters .....	122
4.4.3	Predicting the behaviour of artificially cemented clays .....	125
4.4.3.1	Undrained shear strength: Unconfined compression .....	125
4.4.3.2	Undrained shear strength: Triaxial .....	126
4.4.3.3	Compressibility and vertical yield stress: Oedometer .....	127
4.5	Discussion .....	134
4.6	Summary and Conclusions .....	140
4.7	Acknowledgements .....	143
4.8	References .....	143
<b>5</b>	<b>A Framework for Yielding and Stress-strain Behaviour of Artificially Cemented Clays .....</b>	<b>179</b>
5.1	Introduction .....	179
5.2	Literature Review .....	180
5.3	Experimental Design .....	187
5.3.1	Material properties .....	187
5.3.2	Specimen preparation .....	188
5.3.3	Testing programme .....	189

5.4 Results and Analysis.....	191
5.4.1 General volumetric behaviour and hardening.....	191
5.4.2 Yielding and critical state.....	196
5.4.3 Stiffness and deformations.....	208
5.5 Conclusions.....	215
5.6 Acknowledgements.....	217
5.7 References.....	217
<b>6 Conclusions and Recommendations .....</b>	<b>253</b>
6.1 Summary and conclusions .....	253
6.2 Recommendations for future research .....	257
6.3 References.....	260
<b>Curriculum Vitae .....</b>	<b>262</b>

## LIST OF TABLES

<b>Table 2-1.</b> Basic geotechnical properties of the two types of clay used in this study.....	45
<b>Table 2-2.</b> The calculated inter-aggregate and intra-aggregate pore volumes for samples of Nanticoke clay at different moisture contents.....	46
<b>Table 2-3.</b> The calculated inter-aggregate and intra-aggregate pore volumes for samples of EPK kaolin at different moisture contents .....	47
<b>Table 3-1.</b> Basic geotechnical properties of the three types of clay used in this study....	92
<b>Table 4-1.</b> Geotechnical properties of the four types of clay tested by the authors .....	151
<b>Table 4-2.</b> Properties of the cemented soil samples from the literature used in the time analysis (Fig. 4-3).....	152
<b>Table 4-3.</b> Properties of the cemented soil samples from the literature used in the parametric study .....	153
<b>Table 5-1.</b> Summary of laboratory triaxial experiments performed on artificially cemented Ottawa clay.....	223
<b>Table 5-2.</b> Parameters defining the isotropic and $K_0$ compression and the critical state line for the artificially cemented Ottawa clay .....	224
<b>Table 5-3.</b> Parameters defining the elastic isotropic compression and unloading-reloading lines for the artificially cemented Ottawa clay.....	225
<b>Table 5-4.</b> Parameters required to define the proposed yield loci for samples with different cement contents .....	226
<b>Table 5-5.</b> The measured average $K_0$ coefficients and calculated Poisson's ratios of the artificially cemented Ottawa clay.....	227

## LIST OF FIGURES

<b>Fig. 1-1.</b> Micrographs of two Ottawa clay specimens with a similar moisture content: (a) reconstituted, $c_u < 2$ kPa; (b) artificially cemented (6.4% cement), $c_{u,28 \text{ days}} = 160$ kPa .....	17
<b>Fig. 1-2.</b> Deep mixing: (a) dual mixing shafts; (b) an excavation supported by deep mixed retaining wall (Coastal Development Institute of Technology, 2002) .....	18
<b>Fig. 1-3.</b> Jet grouting: (a) the steps of a large diameter jet grouting technique; (b) jet grouting nozzle; (c) & (d) cemented columns made by jet grouting (Raito, 2010)	19
<b>Fig. 2-1.</b> Particle size distribution of the three clays used in this study .....	48
<b>Fig. 2-2.</b> Pore size distribution of reconstituted Naticoke clay specimens with different liquidity indices: (a) cumulative distribution; (b) log-differential distribution .....	49
<b>Fig. 2-3.</b> Pore size distribution of reconstituted EPK kaolin specimens with different liquidity indices: (a) cumulative distribution; (b) log-differential distribution .....	50
<b>Fig. 2-4.</b> Pore size distribution of freeze-dried and air-dried reconstituted Naticoke clay at LI=3 (a) cumulative distribution; (b) log-differential distribution .....	51
<b>Fig. 2-5.</b> Pore size distribution of freeze-dried and air-dried reconstituted EPK specimens at different liquidity indices: (a) cumulative distribution; (b) log-differential distribution.....	52
<b>Fig. 2-6.</b> MIP derived moisture contents versus the measured moisture contents .....	53
<b>Fig. 3-1.</b> X-ray diffraction analysis of (a) Naticoke clay; (b) Ottawa clay.....	93
<b>Fig. 3-2.</b> Particle size distribution of the three clays used in this study .....	94
<b>Fig. 3-3.</b> Scanning electron micrographs of <i>undisturbed</i> Naticoke clay, $w = 28\%$ , $LI = 0.2$ (the numbers in figure b mark the explained minerals).....	95

<b>Fig. 3-4.</b> Scanning electron micrographs of Nanticoke clay treated with 8.7% Portland cement, w = 98%, LI = 3 (the circles in figure b mark some of the bonded contacts) .....	96
<b>Fig. 3-5.</b> Scanning electron micrographs of <i>undisturbed</i> Ottawa clay, w = 80%, LI = 2 (the circle in figure d marks a clast of calcium carbonate).....	97
<b>Fig. 3-6.</b> Scanning electron micrographs of reconstituted specimens of Ottawa clay, w = 80%, LI = 2.....	98
<b>Fig. 3-7.</b> Scanning electron micrographs of Ottawa clay treated with 3.1% Portland cement, w = 80%, LI = 2.....	99
<b>Fig. 3-8.</b> Scanning electron micrographs of Ottawa clay treated with 6.4% Portland cement, w = 80%, LI = 2.....	100
<b>Fig. 3-9.</b> Scanning electron micrographs of EPK Kaolin treated with 6.4% Portland cement, w = 61%, LI = 1 (the circles in figure c mark some of the bonded contacts) .....	101
<b>Fig. 3-10.</b> Scanning electron micrographs of EPK Kaolin treated with 6.4% Portland cement and 25% gypsum, w = 61%, LI = 1 .....	102
<b>Fig. 3-11.</b> Pore size distribution of cement treated Nanticoke clay specimens with LI=3 (w=98%) at different cement contents: (a) cumulative distribution; (b) log-differential distribution.....	103
<b>Fig. 3-12.</b> Pore size distribution of undisturbed, reconstituted, and cement treated Ottawa clay specimens: (a) cumulative distribution; (b) log-differential distribution.....	104
<b>Fig. 3-13.</b> Pore size distribution of reconstituted and cement treated EPK kaolin: (a) cumulative distribution; (b) log-differential distribution .....	105



<b>Fig. 3-14.</b> Pore size distribution of freeze-dried and air-dried cement treated Nanticoke clay specimens with LI=3 (w=98%) at different cement contents: (a) cumulative distribution; (b) log-differential distribution .....	106
<b>Fig. 3-15.</b> Pore size distribution of cement and gypsum treated EPK kaolin: (a) cumulative distribution; (b) log-differential distribution .....	107
<b>Fig. 3-16.</b> Permeability of undisturbed, reconstituted, and cement treated specimens of (a) Nanticoke clay; (b) Ottawa clay .....	108
<b>Fig. 3-17.</b> The effect of cement content on (a) undrained shear strength, and (b) sensitivity of Nenticoke, EPK, and Ottawa clay specimens with different moisture contents.....	109
<b>Fig. 4-1.</b> Shear strength of artificially cemented Nanticoke clay (LI=3, w=98%) with curing time.....	154
<b>Fig. 4-2.</b> Normalized undrained shear strength of cemented Nanticoke clay (LI=3, w=98%) versus curing time.....	155
<b>Fig. 4-3.</b> Normalized undrained shear strength of various clays cemented with Portland cement versus curing time .....	156
<b>Fig. 4-4.</b> Sensitivity of artificially cemented Nanticoke clay (LI=3, w=98%) with curing time .....	157
<b>Fig. 4-5.</b> Normalized sensitivity of three cemented clays versus curing time .....	158
<b>Fig. 4-6.</b> The relationship between liquidity index and undrained shear strength for soils with different cement contents .....	159
<b>Fig. 4-7.</b> The relationship between cement content and undrained shear strength for soils with different liquidity indices .....	160

<b>Fig. 4-8.</b> Variations in undrained shear strength with cement-moisture ratio (c/w).....	161
<b>Fig. 4-9.</b> Variations in sensitivity with cement-moisture ratio (c/w).....	162
<b>Fig. 4-10.</b> The effect of cement-moisture ratio (c/w) and activity number (A) on undrained shear strength.....	163
<b>Fig. 4-11.</b> The effect of cement-moisture ratio (c/w) and activity number (A) on sensitivity.....	164
<b>Fig. 4-12.</b> Undrained shear strength of various cemented clays versus cement-moisture ratio.....	165
<b>Fig. 4-13.</b> Undrained shear strength of various clays versus the $\beta$ parameter.....	166
<b>Fig. 4-14.</b> Comparison between undrained shear strengths obtained for consolidated triaxial specimens and those obtained for unconfined specimens.....	167
<b>Fig. 4-15.</b> Undrained shear strength from CIU triaxial tests versus the $\beta$ parameter.....	168
<b>Fig. 4-16.</b> Vertical yield stress versus undrained shear strength.....	169
<b>Fig. 4-17.</b> The relationship between the plasticity index and the $c_u/\sigma'_y$ ratio.....	170
<b>Fig. 4-18.</b> The relationship between vertical yield stress and $\beta$ .....	171
<b>Fig. 4-19.</b> One dimensional compression curves for undisturbed, artificially cemented, and reconstituted Ottawa clay.....	172
<b>Fig. 4-20.</b> Idealized compression behaviour of artificially cemented clays (after Horpibulsuk et al., 2004b).....	173
<b>Fig. 4-21.</b> The relationship between $C_c$ (the slope of the compression line) and $e_\lambda$ (void ratio at $\sigma'_v = 1$ kPa).....	174
<b>Fig. 4-22.</b> The effect of variations in (a) initial void ratio; and (b) vertical effective yield stress, on the slope of the pseudo-normal compression line.....	175

<b>Fig. 4-23.</b> The relationship between the slope of the compression line, $C_c$ , and $\alpha$ .....	176
<b>Fig. 4-24.</b> The relationship between $e_\lambda$ (void ratio at $\sigma'_v=1$ ) and $\alpha$ .....	177
<b>Fig. 4-25.</b> The relationship between the slope of the swelling line, $C_s$ , and $\beta$ .....	178
<b>Fig. 5-1.</b> The direction of the drained probing triaxial tests performed on specimens with 4.2% cement content .....	228
<b>Fig. 5-2.</b> One dimensional compression of undisturbed, reconstituted, and artificially cemented Ottawa clay.....	229
<b>Fig. 5-3.</b> Isotropic compression of undisturbed and artificially cemented Ottawa clay .	230
<b>Fig. 5-4.</b> Volumetric response of artificially cemented specimens due to loading and unloading in different stress paths.....	231
<b>Fig. 5-5.</b> Modeling of the volumetric behaviour with changes in the mean effective stress ( $p'$ ) of artificially cemented Ottawa clays: (a) $c=3.1\%$ ; (b) $c=4.2\%$ ; (c) $c=6.4\%$ .	232
<b>Fig. 5-6.</b> The critical state lines on the volumetric plane of the naturally and artificially structured Ottawa clay.....	233
<b>Fig. 5-7.</b> The critical state lines on the $p'$ - $q$ plane of the naturally and artificially structured Ottawa clay.....	234
<b>Fig. 5-8.</b> Images of the sheared specimens: (a) Undisturbed, $p'_i=25$ kPa; (b) Undisturbed, $p'_i=600$ kPa; (c) artificially cemented ( $c=3.1\%$ ), $p'_i=600$ kPa.....	235
<b>Fig. 5-9.</b> The derivation of the yield states for tests performed along different stress paths .....	236
<b>Fig. 5-10.</b> Normalised yielding states of the artificially cemented specimens with different cement contents .....	237

<b>Fig. 5-11.</b> (a) The experimental yielding states, and (b) the proposed model for the artificially cemented specimen with 4.2% cement content .....	238
<b>Fig. 5-12.</b> The experimental yielding states and the proposed model for the artificially cemented specimen with: (a) $c=3.1\%$ ; (b) $c=6.4\%$ .....	239
<b>Fig. 5-13.</b> The determination of the size of the yield locus using oedometer test results: (a) $c=3.1\%$ ; (b) $c=4.2\%$ ; (c) $c=6.4\%$ .....	240
<b>Fig. 5-14.</b> The amount of work required to cause yielding in specimens with 4.2% cement content versus the direction of the drained probing tests (all started at $p'_i=75\text{kPa}$ ) .....	241
<b>Fig. 5-15.</b> The expansion of the yield surface along different stress paths in the artificially cemented specimen with 4.2% cement content .....	242
<b>Fig. 5-16.</b> The variations in the work input during the unloading-reloading of the specimens with 4.2% cement content along different stress paths.....	243
<b>Fig. 5-17.</b> The state boundary surface of artificially cemented specimens with: (a) $c=3.1\%$ ; (b) $c=4.2\%$ ; (c) $c=6.4\%$ .....	244
<b>Fig. 5-18.</b> Theoretical and experimental critical state lines in normalized stress space.	245
<b>Fig. 5-19.</b> Normalized stress paths obtained for undisturbed Ottawa clay: (a) using the equivalent pressure ( $p'_e$ ); (b) using the isotopic yield stress ( $p'_o$ ).....	246
<b>Fig. 5-20.</b> Gradual versus brittle failure of artificially cemented clay ( $c=4.2\%$ ) in drained compression and extension: (a) normalized deviator stress versus shear strain; (b) normalized shear modulus versus shear strain .....	247

**Fig. 5-21.** Undrained shear behaviour of the artificially cemented Ottawa clay ( $c=4.2\%$ ):  
(a) normalized deviator stress versus shear strain; (b) normalized shear modulus  
versus shear strain..... 248

**Fig. 5-22.** Undrained shear behaviour of undisturbed Ottawa clay: (a) normalized  
deviator stress versus shear strain; (b) normalized shear modulus versus shear strain  
..... 249

**Fig. 5-23.**  $K_0$  stress paths for artificially cemented specimens with: (a)  $c=3.1\%$ ; (b)  
 $c=4.2\%$ ; (c)  $c=6.4\%$ ..... 250

**Fig. 5-24.** Experimentally determined yield loci along with plastic strain increment  
vectors: (a)  $c=3.1\%$ ; (b)  $c=4.2\%$ ; (c)  $c=6.4\%$ ..... 251

**Fig. 5-25.** The deviation from normality versus the stress ratio ..... 252

## NOMENCLATURE

A	Activity
$C_c$	Compression index
$C_s$	Swelling index
$c_u$	Undrained shear strength ( $L^{-1}MT^{-2}$ )
$c_{u, 28 \text{ da}}$	Undrained shear strength after curing for 28 days ( $L^{-1}MT^{-2}$ )
c	Cement content (%)
$D_i$	Pore diameter (L)
e	Void ratio
$e_o$	After curing void ratio
$e_n$	Normalizing void ratio
$e_L$	Void ratio on 1-D compression line corresponding to liquid limit
$e_\lambda$	Void ratio on 1-D compression line at $\sigma'_v = 1$ kPa
$e_{100}$	Void ratio on 1-D compression line at $\sigma'_v = 100$ kPa
$G_s$	Specific gravity
$G_{\text{sec}}$	Secant shear modulus ( $L^{-1}MT^{-2}$ )
$G'$	Effective shear modulus ( $L^{-1}MT^{-2}$ )
$G_u$	Undrained shear modulus ( $L^{-1}MT^{-2}$ )
$K_o$	Coefficient of earth pressure at rest
$K'$	Effective bulk modulus ( $L^{-1}MT^{-2}$ )
LI	Liquidity index
LL	Liquid limit (%)
l	Mean effective stress on the yield surface at the critical state ( $L^{-1}MT^{-2}$ )

$M_s$	Mass of dry solids (M)
$M$	Slope of the critical state line in $p'$ - $q$ plane
$m$	Slope of the stress path in $p'$ - $q$ plane
$N$	Specific volume on the isotropic compression line at $p'=1$ kPa
$P$	Applied mercury pressure ( $L^{-1}MT^{-2}$ )
$P_a$	Atmospheric pressure ( $L^{-1}MT^{-2}$ )
$PI$	Plasticity index (%)
$PL$	Plastic limit (%)
$p'$	Mean effective stress ( $L^{-1}MT^{-2}$ )
$p'_i$	Isotropic consolidation pressure ( $L^{-1}MT^{-2}$ )
$p'_o$	Isotropic yield stress ( $L^{-1}MT^{-2}$ )
$p'_e$	Equivalent pressure ( $L^{-1}MT^{-2}$ )
$p'_f$	Mean effective stress corresponding to failure ( $L^{-1}MT^{-2}$ )
$p'_t$	Mean effective stress on the yield surface equivalent to $\eta=3$ ( $L^{-1}MT^{-2}$ )
$q$	Deviator stress ( $L^{-1}MT^{-2}$ )
$R$	Yield surface parameter, $(p'_o - l)/(Ml)$
$S$	Degree of saturation
$S_t$	Sensitivity
$S_{t, 28 \text{ days}}$	Sensitivity after curing for 28 days
$s$	Length of the stress path ( $L^{-1}MT^{-2}$ )
$t$	Time past curing (T)
$t_{28}$	Time past curing corresponding to 28 days (T)
$V_s$	Volume of solids ( $L^3$ )

$V_v$	Volume of voids ( $L^3$ )
$V_m$	MIP measured total pore volume ( $L^3M^{-1}$ )
$V_i$	Intruded volume corresponding to pore diameter $D_i$ ( $L^3M^{-1}$ )
$V_{cumulative}$	Cumulative intruded pore volume ( $L^3M^{-1}$ )
$V_{log-differential}$	Log-differential intruded pore volume ( $L^3M^{-1}$ )
$v$	Specific volume
$v_\kappa$	Specific volume on the unloading-reloading line at $p'=1$ kPa
$v_\lambda$	Specific volume on the compression line at $p'=1$ kPa
$v_{cs}$	Specific volume corresponding to the critical state
$W$	Work input per unit volume ( $L^{-1}MT^{-2}$ )
$w$	Moisture content
$w_r$	Measured gravimetric moisture content
$w_e$	Error related to the MIP derived moisture content
$w_m$	MIP derived moisture content
$\alpha$	Newly defined parameter, $LI.c.A^{3.2}$
$\beta$	Newly defined parameter, $(c/w)A^{3.2}$
$\Delta W_{yield}$	Work input corresponding to the yield state ( $L^{-1}MT^{-2}$ )
$\delta\epsilon_q$	Incremental shear strain (%)
$\delta\epsilon_q^e$	Incremental elastic shear strain (%)
$\delta\epsilon_q^p$	Incremental plastic shear strain (%)
$\delta\epsilon_p$	Incremental volumetric strain (%)
$\delta\epsilon_p^e$	Incremental elastic volumetric strain (%)
$\delta\epsilon_p^p$	Incremental plastic volumetric strain (%)



$\varepsilon_a$	Axial strain (%)
$\varepsilon_r$	Radial strain (%)
$\varepsilon_p$	Volumetric strain (%)
$\varepsilon_q$	Shear strain (%)
$\varepsilon_{p,y}$	Volumetric strain at yield (%)
$\varepsilon_{q,y}$	Shear strain at yield (%)
$\Gamma$	Specific volume on the critical state line at $p'=1$ kPa
$\gamma$	Surface tension of mercury ( $MT^{-2}$ )
$\eta$	Stress ratio
$\kappa$	Slope of the unloading-reloading line in $p'$ - $v$ plane
$\lambda$	Slope of the compression line in $p'$ - $v$ plane
$\nu'$	Effective Poisson's ratio
$\sigma'_a$	Effective axial stress ( $L^{-1}MT^{-2}$ )
$\sigma'_r$	Effective radial stress ( $L^{-1}MT^{-2}$ )
$\sigma'_v$	Vertical effective stress ( $L^{-1}MT^{-2}$ )
$\sigma'_y$	Vertical effective yield stress ( $L^{-1}MT^{-2}$ )
$\sigma'_{y, 28 \text{ days}}$	Vertical effective yield stress after curing for 28 days ( $L^{-1}MT^{-2}$ )
$\theta$	Angle defining the stress path in $p'$ - $q$ plane (degrees)
$\theta_d$	Deviation angle from normality (degrees)
$\theta_c$	Solid-liquid contact angle (degrees)
$\rho_w$	Density of water ( $L^{-3}M$ )
$\zeta$	Incremental stress ratio

# 1 INTRODUCTION

## 1.1 General

Modification of soils to enhance their engineering behaviour using cementing agents is well established and extensively practiced. Early methods of surface stabilization for compacted soils, in particular for sub-base construction of roads, were developed to improve the mechanical behaviour and reduce the total thickness of the base course (e.g. Noble and Plaster, 1970; Mitchell, 1986). Increased knowledge of artificial cementation techniques widened the range of applications and led to the development of new methods employed to stabilize soft or slurried material (Bergado et al., 1996). For instance, with growing environmental concerns, artificial cementation has been employed for solidification and isolation of contaminated sediments. Several reports indicate successful stabilization of wastes, mine tailings, dredged soils, and sludge basins with cementing agents (e.g. Adaska et al., 1992; Bodine and Trevino, 1996; Loest and Wilk, 1998; Wareham and Mackechnie, 2006; Nehdi and Tariq, 2007; Wilk, 2007; Beeghly and Schrock, 2010). In addition, of particular interest in recent years has been the improvement of engineering properties of soft clays with cementitious additives (e.g. Nagaraj and Miura, 2001).

Soft clays cover large areas of earth including many low-land and coastal regions, where many urban and industrial hubs are located, and are frequently encountered in civil engineering projects. The presence of soft material can be problematic in many different ways. A naturally high liquidity index is a notable characteristic of such material,

resulting in high compressibility and low shear strength. If proper engineering measures are not taken, a structure built on a soft clay could undergo excessive settlements or even failure (e.g. Eden and Bozozuk, 1962; Crawford et al., 1995). Soil subsidence due to the withdrawal of ground water is another issue related to the presence of soft clays, especially in many low-land regions of South East Asia (Nagaraj and Miura, 2001). Due to increased urbanization and industrialization of some populated areas of the planet, marine and inland soft clays are also encountered in several land reclamation projects (e.g. Chen and Tan, 2002). In addition, sensitive soft clay materials in Eastern Canada can lose a large portion of their strength due to mechanical disturbance. This can result in catastrophic or progressive failure of embankments and structures, and the creation of landslides due to seismic or blast loadings (e.g Skempton and Northey, 1952; Bjerrum, 1954; Penner, 1965; Sangrey, 1972a).

There are two common ways of tackling the problems associated with the presence of soft or sensitive clays. One effective approach is to pre-consolidate the clay using vertical drains and surcharge to reduce its water content and improve its mechanical properties. However, due to timing and cost related issues, preconsolidation is not the most suitable method in many engineering projects. As an alternative, soft clays can be solidified by the artificial production of cementitious bonding within the material (Nagaraj and Miura, 2001). This can be achieved by the addition to the clay of bonding agents, such as lime, Portland cement, gypsum, or fly ash (e.g. Croft, 1967; Bergado et al., 1996; Graham et al., 2005). The cementing agents gradually react with water and clay minerals to form bonds between and within the clay aggregates (Bergado et al., 1996). At

the same moisture content, the produced cemented material will have significantly higher strength and stiffness than the remoulded clay (e.g. Fig. 1-1).

There are a number of parameters, such as cement type, curing time, cement/water content, temperature, soil mineralogy, and activity, that affect these reactions and hence control the strength and stiffness development in an artificially cemented clay (Bergado et al., 1996). Similar to naturally structured sensitive clays, the artificially cemented material could still undergo large deformations due to its high water content. However, the different nature of the cementation process and cementitious bonds in artificially cemented soft clay reduces the tendency of the material to display a meta-stable behaviour and enables it to sustain higher stresses without undergoing excessive settlements (Nagaraj and Miura, 2001).

The choice of the cementing agent for a particular purpose depends on several factors, including the required increase in strength and stiffness, availability, workability, durability, working climate, and cost (Ismail et al., 2002). Amongst the cementing agents commonly used for artificial cementation, Portland cement is most commonly adopted because of its higher availability and effectiveness, lower cost, and easier storage (Bergado et al., 1996). Two main types of chemical reaction, i.e. hydration and pozzolanic reactions, govern the formation of cementitious bonds within a Portland cement-admixed clay. Hydration reactions, which take place between the cementing agent and water, generally start faster and are deemed to be responsible for a larger share of the total strength gain. In contrast, pozzolanic reactions occur between hydration products and clay minerals. They only commence after enough calcium hydroxide is produced due to hydration reactions and usually continue for a longer time (Bergado et

al., 1996). In addition to the aforementioned reactions, the rapid ion exchange that occurs due to the introduction of calcium ions to the soil results in the flocculation of the remoulded material (Bergado et al., 1996).

Although the mechanisms involved in the formation of cementitious bonding and the development of strength and stiffness are not fully understood, artificial cementation of clays has been used for at least three decades in soil improvement projects. Deep mixing and jet grouting techniques have been developed during the past twenty years to produce cemented columns in soft ground for the stabilization of roads, excavations, and lightly loaded foundations (e.g Tatsuoka et al., 1997; Bergado et al., 1996). Unlike shallow mixing, which transforms the entire volume into cemented material, these deep mixing techniques only produce discrete cemented columns, leaving a large portion of the soft clay untouched (Nagaraj and Miura, 2001). The resulting composite material, however, will have higher resistance to settlement and applied loading. In most of these methods, the cementing agent is introduced deep into the ground by either mechanical or high pressure grout mixing (e.g. Fig. 1-2 and Fig. 1-3). The original deep mixing techniques have been modified with time, and combined methods using both mechanical and high pressure mixing have been developed, to increase the flexibility and effectiveness of the mixing process (Nagaraj and Miura, 2001). The majority of mixing techniques remould the *in-situ* material and therefore destroy the natural structure while introducing the artificial cementation (Nagaraj and Miura, 2001).

Unfortunately, although extensively used, and studied in East and South East Asia, cement stabilization of Canadian clays is not common and has not been given much attention in the literature. In addition, despite the developments of the associated field

techniques and the extensive use of artificially cemented material in engineering projects, the effect of some of the controlling parameters, such as soil properties and curing time, on the mechanical behaviour is not fully understood. In particular, despite a large amount of experimental data on the behaviour of artificially cemented clays being available in the literature (e.g. Uddin et al., 1997; Tremblay et al., 2001; Rotta et al., 2003; Horpibulsuk et al., 2003; Lorenzo and Bergado, 2004; Kamruzzaman et al., 2009), limited work has been done to assess the effect of clay mineralogy and soil activity on artificial cementation. Therefore, the available data that is obtained for certain types of clay cannot be confidently applied to different clay soils. Due to this lack of knowledge, the application of *in-situ* mixing techniques without a relatively extensive laboratory and field testing program is not possible (Nagaraj and Miura, 2001). Better understanding of the dominant parameters, especially those related to clay mineralogy, could lead to the introduction of predictive models that reduce the time and cost required to design an appropriate mix in a particular project by minimizing the number of trials needed to find the proper quantity of admixed cement and the required curing period (Horpibulsuk et al., 2003). Moreover, further investigation of the behaviour of artificially cemented Canadian clays can improve knowledge and introduce new opportunities for using these promising techniques to improve soft and sensitive Canadian clay soils.

The term “structure” is usually used for both naturally and artificially cemented clays to describe the combined effect of fabric and bonding (Mitchell and Soga, 2005). The presence of structure in natural clays has captured the attention of researchers for a number of decades. Given the relatively large amount of research that has been conducted on the issue, it is surprising that there is not yet a consensus among researchers about the

source of this natural cementation (e.g. Sangrey, 1972b; Bentley and Smalley, 1978; Yong et al., 1979; Quigley, 1980; Torrance, 1995; Boone and Lutenecker, 1997). Nonetheless, several works have been conducted to understand the yielding behaviour of natural clays, and constitutive models have been proposed to predict the mechanical behaviour of the structured and cemented material (e.g. Mitchell, 1970; Wong and Mitchell, 1975; Graham et al., 1983; Rouainia and Muir Wood, 2000; Cotecchia and Chandler, 2000; Liu and Carter, 2002; Baudet and Stallebrass, 2004). Some of these models have been later applied to artificially cemented clays (e.g. Horpibulsuk et al., 2010) and some other models have been proposed for both naturally and artificially cemented clays (e.g. Vatsala et al., 2001), without properly addressing the nature of the structuration and the manner in which it breaks down under loading, which can be different for artificially cemented materials. Thus, there is a need to understand microstructural and mechanical differences of these two types of cemented materials, so that more representative models can be assigned to each type of “structured” clay. Doing so requires proper investigation of the microstructural changes undergone by the remoulded clay during and after the addition of cementing agents, and of the yielding behaviour of the resulting cemented material. Finding these differences and similarities in behaviour could also help researchers better exploit artificially cemented samples to represent naturally cemented clays in laboratory testing, avoiding the costs and technical problems related to obtaining undisturbed specimens of naturally cemented clays and providing sufficient specimen consistency required to conduct full parametric studies.

## 1.2 Objectives of the Research

The aims of this study were to investigate the changes in the microstructure during the transformation from remoulded to artificially cemented states, the dominant parameters affecting the observed mechanical behaviour of the resulting cemented clays, and the suitability of constitutive frameworks to predict the yielding, compressibility, and shearing behaviour of such material. In accordance with these overall aims, the specific objectives of this research can be summarized as follows:

- To investigate the micro-fabric of reconstituted clayey soils and to examine changes in the microstructure due to variations in the water content.
- To evaluate the potential transformations occurring to the micro-fabric of reconstituted clays due to the addition of Portland cement and to find links between clay mineralogy and the observed microstructural changes.
- To investigate the differences between the micro-fabric and mechanical behaviour of artificially cemented clays and those of naturally structured materials.
- To assess the existence of potential connections between the observed changes in the microstructure and the strength and permeability of the artificially cemented material.
- To study the effect of clay mineralogy on the effectiveness of artificial cementation, and to identify pertinent parameters for predicting the strength, stiffness, sensitivity, and other important characteristics of soft clays cemented with Portland cement.



- To experimentally study the yield states and stiffness of a soft clay stabilized by Portland cement, find the yield envelope, and check the validity of the hardening law and associated flow rule.

### **1.3 Structure of the Thesis**

This thesis is divided into of six chapters and is presented in an integrated-article format. Except for the introductory and concluding chapters, which also have their own bibliography, every chapter has its own introduction, literature review, list of references, tables, and figures. Detailed organization of the thesis can be summarized as follows:

Chapter 1 is an introductory chapter providing preliminary information about the artificial cementation of clays and recognizes the areas in need of more research. It also outlines the objectives and contributions of the thesis, along with its structure.

Chapter 2 shows the results of a series of mercury intrusion porosimetry tests on reconstituted specimens of two types of clay with different water contents. It explains the changes in the pore size distribution due to variations in the water content for a relatively large range of liquidity indices. Then it discusses technical issues related to the use of mercury intrusion porosimetry for clay specimens with high moisture contents.

Chapter 3 provides the results of a number of scanning electron microscopy and mercury intrusion porosimetry tests on three types of clay admixed with Portland cement. It explains how the development of cementitious changes the micro-fabric of the material, and confirms the existence of some by-products within the cemented soft clay.

Chapter 4 presents a comprehensive parametric study of the test data obtained by the author for four types of clay, as well as those found in the literature for other clay

mineralogies. Based on these data, a number of relationships, incorporating the effect of mineralogy and activity on the observed mechanical behaviour, are developed. These are followed by a critical discussion explaining the possible reasons behind the observed behaviour.

Chapter 5 further explores the mechanical behaviour by presenting the results of several triaxial experiments on artificially cemented specimens of a sensitive Leda clay. These are added to test results for the undisturbed specimens of the same clay to explain the differences between the natural and artificial cementation. Moreover, a simple constitutive framework, describing the yielding and shearing behaviour of artificially cemented clays, is proposed and evaluated based on the experimental data.

Chapter 6 presents the major conclusions drawn from this work, along with recommendations for further related studies.

## **1.4 Significant Contributions**

This research involved extensive laboratory testing, coupled with statistical and empirical formulation and theoretical analysis and modelling. Various experiments were conducted on a number of different clays treated with Portland cement, and the results were used either independently or together with test data from the literature to achieve the aforementioned objectives. The major contributions of this research are as follows:

- Microstructural analysis showed that variations in the moisture content of reconstituted clays are primarily accompanied by changes in the volume of inter-aggregate rather than intra-aggregate pores. It also proved that artificial

- cementation results in the flocculation of the material, converting the observed bimodal pore size distribution of reconstituted clays to unimodal.
- It was observed that a greater degree of microstructural modifications due to artificial cementation is accompanied by higher gain of strength and loss of hydraulic conductivity in the material.
  - It was shown that although providing some useful information about the micro-fabric of the material, the mercury intrusion porosimetry technique can underestimate the total volume of the pores for saturated clay specimens with moisture contents higher than 50%.
  - The hardening of artificially cemented clays was found to continue with a considerable rate with curing time. A new relationship was suggested to predict the developed strength for a certain curing time.
  - The activity number ( $A$ ) of the clay was recognized as a pertinent parameter, along with the cement and water contents. Empirical relationships were proposed to estimate the undrained shear strength, vertical effective yield stress, and compression index of clay stabilized by Portland cement.
  - The results showed that contrary to the general belief, the effect of the secondary reactions on the developed strength and stiffness is significant. A critical review of the literature provided possible reasons for the importance of these reactions in the cementation process.
  - It was shown that the compression behaviour of artificially cemented clays can be represented by a bilinear model. A general relationship was found to be usually true for the compression of both reconstituted and artificially cemented clays.

- The results indicated gradual destructuration and more isotropic behaviour of artificially cemented clays compared to naturally structured material. The structure was found to be preserved even when the artificially cemented material underwent significant volumetric strains due to compression.
- A combination of the elliptical cap and modified Cam-clay models were used to represent the yield locus of the artificially cemented clays. The proposed envelope was suggested to be bounded in  $p'$ - $q$  plane by the unconfined compression path. It was also shown that using the critical state concept, the parameters required to find the yield envelope for a soft clay stabilized by Portland cement can be obtained.

## 1.5 References

- Adaska, W.S., Ten Bruin, W., and Day, S.R. (1992), "Remediation of oil refinery sludge basin." *Cement Industry Solutions to Waste Management*, Calgary, Canada October 7-9, 119–134.
- Baudet, B., and Stallebrass, S. (2004). "A constitutive model for structured clays." *Geotechnique* , 54(4) , 269–278.
- Beeghly, J., and Schrock, M. (2010). "Dredge material stabilization using the pozzolanic or sulfo-pozzolanic reaction of lime by-products to make an engineered structural fill." *International Journal of Soil, Sediment and Water*, 3(1), 1–21.
- Bentley, S.P., and Smalley, I.J. (1978). "Inter-particle cementation in Canadian post-glacial clays and the problem of high sensitivity ( $St > 50$ ).” *Sedimentology*, 25, 297–302.

- Bergado, D.T., Anderson, L.R., Miura, N., and Balasubramaniam, A.S. (1996). "Soft ground improvement in lowland and other environments." American Society of Civil Engineers (ASCE) Press, New York, U.S.A.
- Bjerrum, L. (1954). "Geotechnical properties of Norwegian marine clays." *Geotechnique*, 4(2), 49–69.
- Bodine, D.G., and Trevino, F.M. (1996). "RCRA closure of refinery sludge basin using in-situ solidification and containment". Proceedings of the Fourth Great Lakes Geotechnical/Geoenvironmental Conference on In-Situ Remediation of Contaminated Sites, Chicago, IL, May 17, 49–74.
- Boone, S.J., and Lutenecker, A.J. (1997). "Carbonates and cementation of glacially derived cohesive soils in New York State and southern Ontario." *Canadian Geotechnical Journal*, 34, 534–550.
- Chen, C.S., and Tan, S.M. (2002). "A case history of a coastal land reclamation project." *GSM-IEM Forum on Engineering Geology and Geotechnics in Coastal Development*, Bangunan IEM, P.J., Oct 23.
- Coastal Development Institute of Technology (CDIT). (2002). "The deep mixing method: principle, design and construction." Balkema, Rotterdam, The Netherlands.
- Cotecchia, F., and Chandler, R.J. (2000). "A general framework for the mechanical behaviour of clays." *Geotechnique*, 50(4), 431–447.
- Crawford, C.B., Fannin, R.J., and Kern, C.B. (1995). "Embankment failure at Vernon, British Columbia." *Canadian Geotechnical Journal*, 32(2), 271–284.

- Croft, J.B. (1967). "The structures of soils stabilized with cementitious agents." *Engineering Geology*, 2(2), 63–80.
- Eden, W.J., and Bozozuk, M. (1962). "Foundation failure of a silo on varved clay." *The Engineering Journal*, 45(9), 54–57.
- Graham, J., Noonan, M. L., and Lew, K. V. (1983). "Yield states and stress-strain relationships in a natural plastic clay." *Canadian Geotechnical Journal*, 20(3), 502–516.
- Graham, J., Man, A., Alfaro, M., Blatz, J.A., and Van Gulck, J. (2005). "Gypsum Cementation and Yielding in Plastic Clay." *Proceedings of the 16th International Conference on Soil Mechanics and Geotechnical Engineering*, Osaka, Japan, 507–512.
- Horpibulsuk, S., Miura, N., and Nagaraj, T.S. (2003). "Assessment of strength development in cement-admixed high water content clays with Abrams' law as a basis." *Geotechnique*, 53(4), 439–444.
- Horpibulsuk, S., Liu, M.D., Liyanapathirana, D.S., and Suebsuk, J. (2010). "Behaviour of cemented clay simulated via the theoretical framework of the Structured Cam Clay model." *Computers and Geotechnics*, 37(1-2), 1–9.
- Ismail, M.A., Joer, H.A., Sim, W.H., and Randolph, M.F. (2002). "Effect of cement type on shear behavior of cemented calcareous soil." *Journal of Geotechnical and Geoenvironmental Engineering*, 128(6), 520–529.
- Kamruzzaman, A.H.M., Chew, S.H., and Lee, F.H. (2009). "Structuration and Destructuration Behavior of Cement-Treated Singapore Marine Clay Cement-

- Treated Singapore Marine Clay.” *Journal of Geotechnical and Geoenvironmental Engineering*, 135(4), 573–589.
- Liu, M.D., and Carter, J.P. (2002). “A Structured Cam Clay model.” *Canadian Geotechnical Journal*, 39(6), 1313–1332.
- Loest, K., and Wilk, C.M. (1998). “Brownfield reuse of dredged New York Harbor sediment by cement based solidification/stabilization.” *Proceedings of the 91st Annual Meeting and Exhibition*, Air and Waste Management Association.
- Lorenzo, G.A., and Bergado, D.T. (2004). Fundamental parameters of cement-admixed clay – New approach.” *Journal of Geotechnical and Geoenvironmental Engineering*, 130(10), 1042–1050.
- Mitchell, R. J. (1970). “On the yielding and mechanical strength of Leda clays.” *Canadian Geotechnical Journal*, 7, 297–312.
- Mitchell J. K. (1986). “Practical problems from surprising soil behaviour.” *Journal of Geotechnical Engineering (ASCE)*, 112(3), 259–289.
- Mitchell, J.K., and Soga, K. (2005). “Fundamentals of Soil Behavior, 3rd Ed.” John Wiley & Sons, Hoboken, New Jersey.
- Nagaraj, T.S., and Miura, N. (2001). “Soft clay behaviour – analysis and assessment.” A.A. Balkema, Rotterdam, The Netherlands.
- Nehdi, M., and Tariq, A. (2007). “Stabilization of sulphidic mine tailings for prevention of metal release and acid drainage using cementitious materials: a review.” *Journal of Environmental Engineering and Science*, 6(4), 423–436.

Noble, D.F., and Plaster, R.W. (1970). "Reactions in Portland cement – clay mixtures."  
Final report, Virginia Highway Research Council, Charlottesville.

Penner, E. (1965). "A study of sensitivity in Leda clay." *Canadian Journal of Earth Sciences*, 2(5), 425–441.

Quigley, R.M. (1980). "Geology, mineralogy, and geochemistry of Canadian soft soils: a geotechnical perspective." *Canadian Geotechnical Journal*, 17(2), 261–285.

Raito Corporation. (2010). Jet grouting brochure, Dec. 15, <http://www.raito.co.jp/english>.

Rotta, G.V., Consoli, N.C., Prietto, P.D.M., Coop, M.R., and Grahams, J. (2003).  
"Isotropic yielding in an artificially cemented soil cured under stress."  
*Geotechnique*, 53(5), 493–501.

Rouainia, M., and Muir Wood, D. (2000). "A kinematic hardening constitutive model for natural clays with loss of structure." *Geotechnique*, 50(2), 153–164.

Sangrey, D.A. (1972a). "Naturally cemented sensitive clays." *Geotechnique*, 22(1), 139–152.

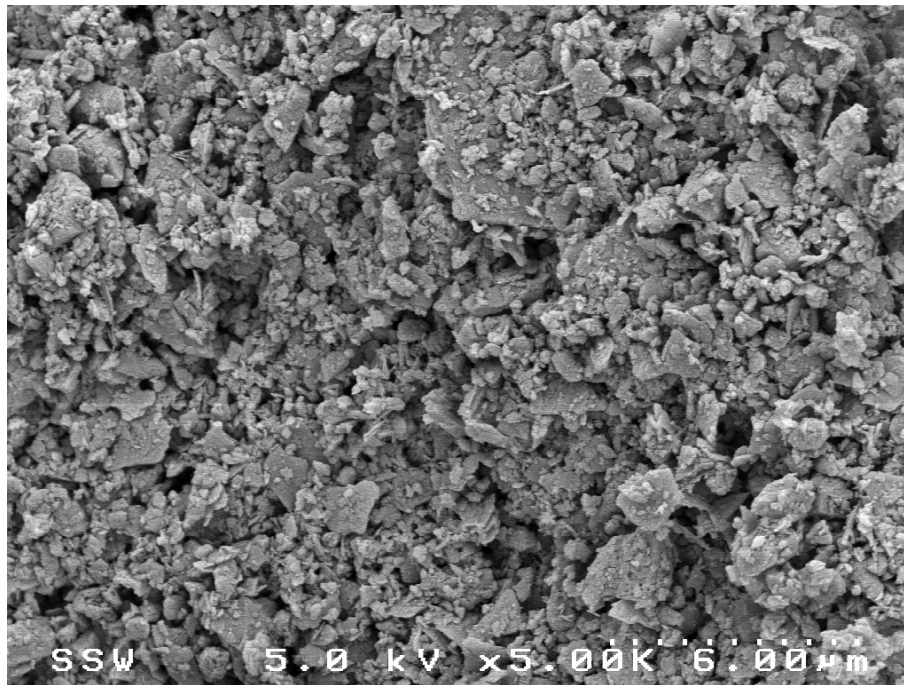
Sangrey, D.A. (1972b). "On the causes of natural cementation in sensitive soils."  
*Canadian Geotechnical Journal*, 9(1), 117–119.

Skempton, A.W., and Northey, R.D. (1952). "The Sensitivity of Clays." *Geotechnique*, 3, 30–53.

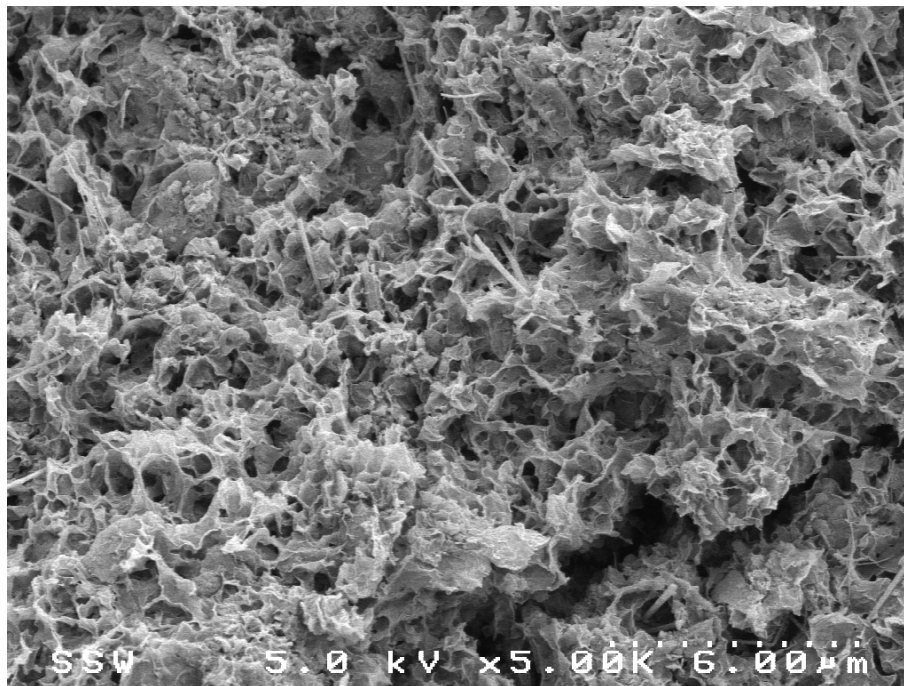
Tatsuoka, F., Uchida, K., Imai, K., Ouchi, T., and Kohata, Y. (1997). "Properties of cement treated soils in the Trans-Tokyo Bay Highway project." *Ground Improvement*, 1(1), 37–57.



- Torrance, J.K. (1995). "On the paucity of amorphous minerals in the sensitive postglacial marine clays." *Canadian Geotechnical Journal*, 32(3), 535–538.
- Tremblay, H., Leroueil, S., and Locat, J. (2001). "Mechanical improvement and vertical yield stress prediction of clayey soils from eastern Canada treated with lime or cement." *Canadian Geotechnical Journal*. 38, 567–579.
- Uddin, K., Balasubramaniam, A.S., and Bergado, D.T. (1997). "Engineering behavior of cement-treated Bangkok soft clay." *Geotechnical Engineering Journal*, 28(1), 89–119.
- Vatsala, A., Nova, R., and Srinivasa Murthy, B.R. (2001). "Elastoplastic model for cemented soils." *Journal of Geotechnical and Geoenvironmental Engineering*, 127(8): 679–687.
- Wareham, D.G., and Mackechnie, J.R. (2006). "Solidification of New Zealand Harbor Sediments Using Cementitious Materials." *Journal of Materials in Civil Engineering*, 18(2), 311–315.
- Wilk, C.M. (2007). "Principles and use of solidification/stabilization treatment for organic hazardous constituents in soil, sediment, and waste." Presented at *WM'07 Conference*, Tuscan, AZ, Feb 25–Mar 01.
- Wong, P.K.K., and Mitchell, R.J. (1975). "Yielding and plastic flow of sensitive cemented clay." *Geotechnique*, 25, 763–782.
- Yong, R.N., Sethi, A.J., and Larochelle, P. (1979). "Significance of amorphous material relative to sensitivity in some Champlain clays." *Canadian Geotechnical Journal*, 16, 511–520.



(a)



(b)

**Fig. 1-1.** Micrographs of two Ottawa clay specimens with a similar moisture content: (a) reconstituted,  $c_u < 2$  kPa; (b) artificially cemented (6.4% cement),  $c_{u,28 \text{ days}} = 160$  kPa

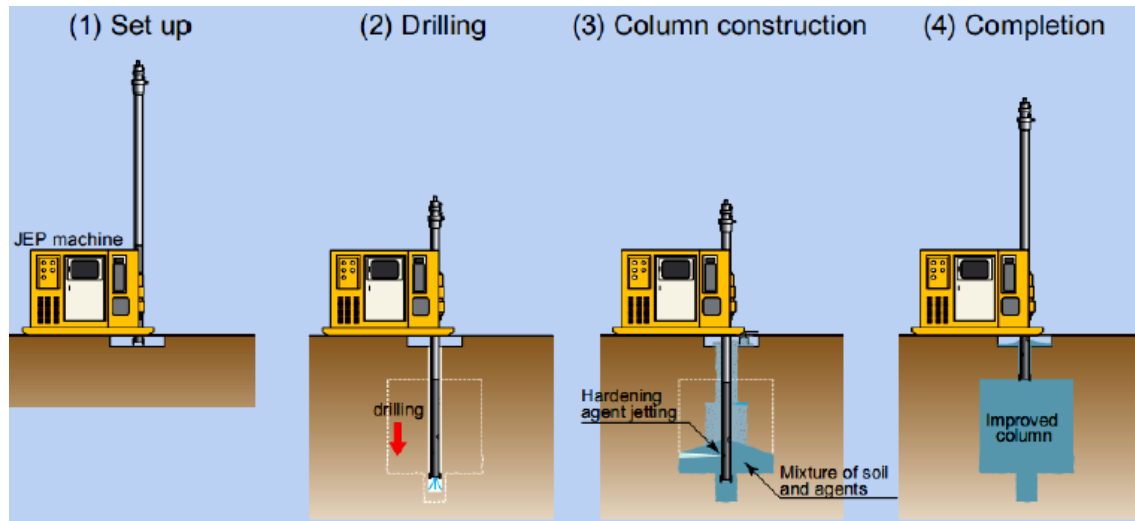


(a)

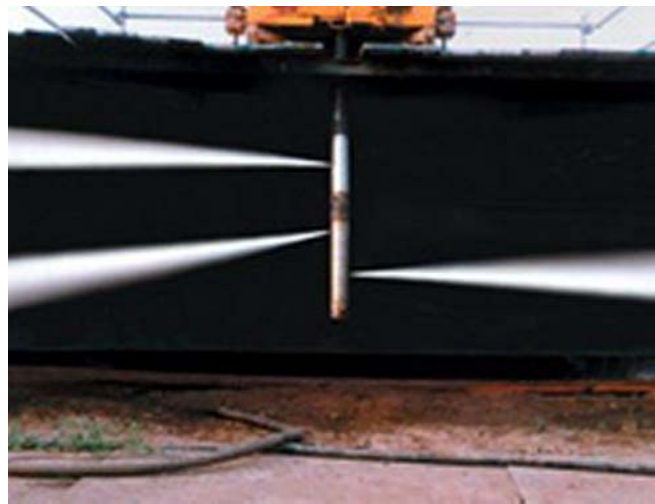


(b)

**Fig. 1-2.** Deep mixing: (a) dual mixing shafts; (b) an excavation supported by deep mixed retaining wall (Coastal Development Institute of Technology, 2002)



(a)



(b)



(c)



(d)

**Fig. 1-3.** Jet grouting: (a) the steps of a large diameter jet grouting technique; (b) jet grouting nozzle; (c) & (d) cemented columns made by jet grouting (Raito, 2010)

## **2 USE OF MERCURY INTRUSION POROSIMETRY FOR MICROSTRUCTURAL INVESTIGATION OF RECONSTITUTED CLAYS**

### **2.1 Introduction**

Mercury intrusion porosimetry (MIP) has been used by a number of researchers to study the structure developed in clays under various conditions, i.e. natural, remoulded, compacted, or consolidated states. However, there is very little information in the literature about the fabric developed in reconstituted clayey soils and slurries. Studying the fabric of these types of soil can provide valuable information about the processes governing the formation of natural soils and hydraulic fills, and can give insights into the link between micro-structure and fundamental geotechnical characteristics, such as hydraulic conductivity, strength, and compressibility. Since MIP is a relatively new technique, the limitations of performing this type of analysis on saturated clays are currently not well defined. Hence, the present study has two main objectives: to investigate changes in the micro-fabric of reconstituted clayey soils due to variations in moisture content and to assess the effectiveness of using mercury intrusion porosimetry on saturated clays with high moisture contents.

### **2.2 Literature Review**

Soil aggregates or peds are often described as “packings” of clay particles, which behave as compressible, crushable single particles and interact to create strength, stiffness, and flow responses in clays (Mitchell and Soga, 2005). Although early works

considered the interactions between individual clay platelets to play a central role in the mechanical behaviour of clays (Terzaghi, 1925; Casagrande, 1932; Lamb, 1953; Lamb, 1958), researchers later confirmed the importance of clay clusters in understanding the behaviour of such material. Aylmore and Quirk (1960) investigated dried specimens of an illite clay from South Australia and suggested that the clay mass consisted of a series of parallel crystals, called “domains”. They concluded that the pore space of the dried material was “almost exclusively” within these domains and that the inter-domain porosity was negligible. Olsen (1962) described the discrepancies between the measured hydraulic flow rates of saturated clays and those predicted from Darcy’s law as being fully explainable in terms of the “cluster” concept. He postulated that the clay pores are not of equal sizes and almost all of the flow passes through the larger pores existing between clay aggregates. After studying the microfabric of a variety of normally consolidated and lightly overconsolidated clays by scanning electron microscopy, Collins and McGown (1974) suggested that single clay platelets rarely exist within clayey material, while groups of platey particles, which interact with each other in various forms, are abundant. They also classified the pore spaces observed in different soils into four broad groups: intra-elemental, intra-assemblage, inter-assemblage, and trans-assemblage pores. The cluster concept has also provided a basis for recent dual porosity/dual permeability models used to simulate water movement and solute transport in porous media. These models assume that the total porosity of the soil is divided into two independent, but interacting domains, i.e. macropores and micropores, and use a coupled set of parameters and equations to describe the hydraulic properties of each domain (e.g. Gerke and van Genuchten, 1993; Jarvis, 1994).

Mercury intrusion porosimetry has been used previously for examining the micro-fabric of various porous media and can provide quantitative information on the distribution of pores within the material (e.g. Choquette et al., 1987; Delage et al., 1996; Locat et al., 1996; Ninjgarav et al., 2007; Romero and Simms, 2008; Koliji et al., 2010). Such information can significantly improve the understanding of the macroscopic and engineering behaviour of soils (Romero and Simms, 2008). Diamond (1970) was one of the first to investigate the pore size distribution of clays using MIP analysis. He measured mercury contact angles for different clay minerals and performed MIP analysis on clays from various geological origins and for different structural states. Garcia-Bengochea et al. (1979) performed MIP analysis on compacted silty clay and observed a bimodal pore size distribution in the tested material. They showed that variations in the compaction effort and moisture content were only accompanied by changes in the volume of the macropores and suggested that the large pores alone are responsible for the permeability of the material. However, Lapierre et al. (1990) later measured the mercury intrusion and permeability of Louiseville clay and contended that permeability cannot be predicted by exclusively using the pore size distribution data, since other factors also control flow through a porous medium. Delage and Lefebvre (1984) used combined SEM and MIP results to describe the microstructure of a sensitive Champlain clay in undisturbed and remoulded states. They suggested that two different porosity regimes, i.e. intra-aggregate and inter-aggregate, existed in remoulded specimens of a Champlain clay from St. Marcel. They also showed that consolidation of the clay resulted in the collapse of its inter-aggregate pores, leaving its intra-aggregate pores almost intact. This was further confirmed by test results for four different types of clay reported by Griffiths and Joshi

(1989). Romero et al. (1999) also performed MIP and scanning electron microscopy analyses on compacted Boom clay and reported that at high compressive stresses, the clay aggregates fuse as the inter-aggregate porosity collapses.

A clay specimen should be depleted of all of its pore moisture, prior to performing mercury intrusion porosimetry. This can be achieved with various methods including air/oven-drying, freeze-drying or critical-point-drying; an effective drying method will impose minimal disturbance to the soil fabric. Gillott (1970) investigated the fabric of Leda clays and showed that although all of these drying techniques had detectable influence on fabric, air-drying caused the greatest disturbance. Air-drying also causes significant disturbance to the fabric of saturated clayey soils with high water contents, since it results in considerable pore shrinkage in the material (Mitchell and Soga, 2005). Oven-drying may result in less fabric changes, since the shorter drying time limits the ability of particles to rearrange. However, there is still some fabric disturbance, as well as breakage of particle clusters, in such samples due to thermal stresses induced by the oven-drying (Mitchell and Soga, 2005). Delage and Lefebvre (1984) showed that oven drying resulted in a dense packing of the particles and significantly modified the microstructure of a Champlain clay. Cuisinier and Laloui (2004) also reported that oven drying induced a significant porosity reduction in specimens of a compacted silt. However, by using the freeze-drying or critical-point drying technique, the fabric disruption caused by the other two conventional drying methods can be minimized (Mitchell and Soga, 2005). Freeze-drying is the more commonly used method, and if implemented properly, can essentially preserve the initial structure of the soil material (Romero et al., 1999; Cuisinier and Laloui, 2004). Thompson et al. (1985) investigated



the effects of drying treatment on porosity of three types of clay. They reported that although both freeze-drying and oven-drying caused a porosity reduction in the material, oven drying resulted in more sample disturbance than freeze-drying.

Despite its potential effectiveness, mercury intrusion porosimetry has been rarely used to examine the microstructure developed in slurried and reconstituted clays. This method, if accompanied with a proper sample preparation technique, can therefore shed some light on fabric development in reconstituted soft clays and enrich the current understanding of the role of particles and aggregates in the mechanical behaviour of clay soils.

## **2.3 Experimental Design**

### **2.3.1 Material properties**

Reconstituted samples of two types of clay: EPK kaolin and Nanticoke clay were prepared for this study. EPK kaolin is a commercially available pulverized kaolin clay from Georgia, U.S. Air-dried clay powder was also obtained from block samples of a stiff, fissured clay with a glacio-lacustrine origin taken from 3 m depth in a test pit in Nanticoke, Ontario. X-ray diffraction analysis showed that the Nanticoke clay had primary clay minerals of illite and chlorite and primary non-clay minerals of quartz, feldspar, calcite, and dolomite. Table 2-1 summarizes the basic geotechnical properties of the two types of clay used in this study and Fig. 2-1 shows their grain size distribution obtained in compliance with ASTM D422.

### 2.3.2 Specimen preparation and testing programme

All of the samples used in this study were obtained from the aforementioned powdered material. EPK Kaolin was already available in a powder form. To prepare the powdered Nanticoke clay, the original soil was cut into small pieces and dried at room temperature. Then it was finely pulverized into a powder (100% passing Sieve No. 40) using a rubber hammer to avoid crushing the soil particles. The prepared powder was then used to make reconstituted specimens.

For the preparation of the reconstituted samples, two different methods were used depending on the target moisture content of the specimen. To make specimens with a moisture content *higher* than the plastic limit, powdered clay was added to the amount of water needed to reach the target moisture content. The resulting mixture was blended for a few minutes and was left to soak for 24 hours in a sealed container before it was mixed again and used for testing. To prepare specimens with a moisture content *equal* to the plastic limit, an initial clay-water mixture with a liquidity index of 0.5 was made. The moisture content of the resulting paste was then reduced to that of the plastic limit, using the same method described in ASTM D4318 for obtaining the plastic limit of soils. For all reconstituted samples, the moisture content of a portion of the specimen was measured before performing the experiments to ensure that the target moisture content was reached. Distilled, deionized water was used in the preparation of all of the reconstituted clay specimens.

Mercury intrusion porosimetry (MIP) was carried out on the reconstituted samples of clay with an AutoPore IV, a porosimeter manufactured by Micromeritics and capable of providing a maximum mercury pressure of 414 MPa. To carry out the tests, a sample

of the dried soil was placed in an MIP penetrometer, and the sealed penetrometer was inserted into the low pressure port of the equipment. In the first phase, the air was evacuated and was then replaced by mercury in increments until a mercury pressure of 172 kPa was reached. Next, the penetrometer, now filled with mercury, was removed from the low pressure port, weighed, and placed in the high pressure port, where it was pressurized incrementally up to the maximum pressure of 414 MPa. The mass of the dried specimens used in the MIP analysis ranged from 1.0 to 3.0 g depending on the stem volume of the penetrometer and the expected total pore volume of the sample.

The samples were prepared for the MIP analysis with two methods: air-drying and freeze-drying. To air-dry the specimens, they were left to dry at room temperature (25°C) for a few days, before they were completely dried in a desiccator under an absolute pressure of 4 Pa. For freeze-drying, very small pieces or drops (depending on the liquidity index) of the reconstituted specimens were placed on wax paper to prevent them from sticking to the specimen holder. Next, the samples were placed in a specimen holder and dipped for about one minute into a container filled with isopentane that had been previously cooled to its melting point (-160°C) in liquid nitrogen (-196°C). After freezing, the pore water was removed by sublimation with the use of a vacuum pump capable of providing an absolute pressure of 4 Pa. The dried specimens were then kept in a desiccator under vacuum until tested.

## **2.4 Test Results and Analysis**

Mercury intrusion porosimetry was conducted on the reconstituted specimens of Nanticoke clay and EPK kaolin at different liquidity indices (ranging from 0 to 3).

Although most of the experiments were performed on freeze-dried samples, a few tests were also conducted on air-dried specimens, to investigate the effect of air-drying on pore size distribution and to compare air-dried and freeze-dried material. Washburn's equation (Washburn 1921), which is derived for capillary flow of a liquid in a cylindrical tube, was employed to calculate pore diameters based on the applied mercury pressures:

$$r = \frac{-2\gamma \cos \theta_c}{P} \quad (2.1)$$

Where  $r$  is the pore radius,  $P$  is the applied mercury pressure,  $\gamma$  is the surface tension of mercury, and  $\theta_c$  is the solid-liquid contact angle. Based on the recommendation of Diamond (1970) for kaolinite and illite, a mercury contact angle of  $147^\circ$  and also a surface tension of 485 dynes/cm were used in the calculations. If the calculated pore diameters are successively numbered, cumulative and log-differential pore volumes can be obtained for each calculated pore diameter,  $D_i$ , as follows:

$$V_{cumulative} = \sum_i \Delta V_i \quad (2.2)$$

$$V_{\log-differential} = \frac{-\Delta V_i}{\Delta \log D_i} \quad (2.3)$$

Where  $V_i$  is the measured total intruded pore volume corresponding to the diameter,  $D_i$ . Logarithmic differential distribution, which provides a qualitative measurement of the distribution of the pores, is typically used, rather than the incremental distribution, to eliminate the experimental point spacing effect that usually makes the latter curve uneven.

Fig. 2-2 shows the pore size distribution of reconstituted Nanticoke clay specimens with different moisture contents at liquidity indices of 0, 0.5, 1, 2, and 3. The

distribution is shown for a diameter range of 3 nm to 0.1 mm. Since all cumulative curves (Fig. 2-2a) become essentially flat at diameters less than 10 nm, we can assume that regardless of the moisture content of the specimens, almost all of the pores in reconstituted Nanticoke clay have a diameter larger than 3 nm. Thus, the cumulative volume reading at a diameter of 3 nm represents the total pore volume of the sample. As expected, the total pore volume increases with an increase in the moisture content (Fig. 2-2a). Note the trimodal behaviour observed in Fig. 2-2b is due to switchover errors related to the MIP test procedure. Thus, the local minimum that is observed in all of the curves at a diameter of about 7 microns (7,000 nm) is an experimental artefact due to the transition of the test from the low to high pressure systems (Giesche, 2006). Thus without that local minimum, the actual pore size distribution (in the log-differential curves) is bimodal with a first peak roughly between 70,000 and 400 nm and a second one between 300 and 10 nm.

The bimodal pattern observed in the log-differential curves indicates that two different mechanisms are involved in forming the pores within the material. We can attribute the peak with a larger dominant diameter to the free water existing between soil aggregates and the peak with a smaller dominant diameter to the water trapped within the aggregates and on the surface of clay particles (Garcia-Bengochea et al., 1979; Lapierre et al., 1990; Romero et al., 1999). With this assumption, the total volume of inter-aggregate and intra-aggregate pores can be obtained by calculating the area underneath the first (70,000 to 400 nm) and second (300 to 10 nm) peaks plotted in incremental space, respectively (Table 2-2). As moisture content increases, the first peak (between 70,000 and 400 nm) shifts towards the larger pores (the right side of the figure) and also

covers a larger area in Fig. 2-2b (larger inter-aggregate pore volume in Table 2-2), indicating that the inter-aggregate pores, which are occupied by the free pore water, expand in diameter and volume. In contrast, an increase in moisture content only causes slight movement of the position of the peak associated with intra-aggregate pores (between 300 and 10 microns). As the moisture content increases from 23 to 98%, the position of this peak translates from 65 to 160 nm (Fig. 2-2b). Similarly, with changes in moisture content, the area covered by the second peak in Fig. 2-2b (the total volume of intra-aggregate pores) remains almost constant at about 0.18 ml/g (Table 2-2). This suggests that most of the water added to Nanticoke clay at moisture contents higher than (or equal to) the plastic limit stays between, rather than within, the clay aggregates. As will be discussed later, the total volume of the pores trapped inside the clusters of clay appears to be essentially constant.

Fig. 2-3 illustrates the pore size distribution of reconstituted EPK specimens with different moisture contents at liquidity indices of 0, 0.5, 1 and 2. It can be seen that with an increase in the moisture content, the position of the peak associated with the intra-aggregate pores (between 300 and 10 microns) moves very little, although the peak associated with the inter-aggregate pores (between 70,000 and 400 nm) shifts significantly towards higher diameters. Moreover, in common with Nanticoke clay, the reconstituted samples of EPK kaolin with different moisture contents have the same intra-aggregate pore volumes. Table 2-3 summarizes the calculated inter-cluster and intra-cluster pore volumes for this clay. For all of the specimens, the volume of the intra-aggregate pores is very close to the average value of 0.26 ml/g, which is higher than that measured for Nanticoke clay (0.18 ml/g), implying that a higher amount of pores exists

within the kaolin clusters in a reconstituted state. This is due to the size, shape and inter-particle forces of the kaolin platelets being different from those of the illite and chlorite particles in the Nanticoke clay. Both the reconstituted Nanticoke clay and EPK kaolin hold all of the added water in the layers between clay aggregates, rather than within the aggregates themselves. At high liquidity indices, this free pore water is likely to be responsible for the higher permeability and the fluid behaviour of the reconstituted material.

Comparing the two figures, the effect of clay mineralogy on the pore size distribution can be seen; the two dominant peaks are more clearly separated in reconstituted EPK kaolin than in Nanticoke clay. The peaks associated with intra-aggregate pores are sharper and have a higher maximum value in the EPK kaolin. In addition, the dominant inter-aggregate pore diameter ranges from 30 to 10 microns in EPK kaolin, while it covers a wider range (from 30 to 1.5 microns) in the Nanticoke clay. In both clays, however, as the liquidity index reduces to zero, the material is first depleted of smaller inter-aggregate pores (within a diameter range of 0.4 to 10 microns) rather than the larger pores.

If left to dry at room temperature, a soft clay specimen will shrink until it reaches the shrinkage limit, after which the clay will dry without further volume change. Therefore, by causing substantial particle rearrangements within the clayey material (Aylmore and Quirk, 1960), air-drying would noticeably change the pore size distributions and total pore volume of a soft clay specimen. Comparing pore size distributions and total pore volumes of two originally identical reconstituted specimens, one air-dried and one freeze-dried, can therefore provide us with useful information about

the microstructure of the soil. The results of MIP analysis on air-dried and freeze-dried specimens of reconstituted Nanticoke clay and EPK kaolin are presented in Fig. 2-4 and Fig. 2-5, respectively. The Nanticoke clay specimen has lost a large portion of its pore volume due to shrinkage. As Fig. 2-4b shows, almost all of the pores with a diameter larger than 160 nm have disappeared from the air-dried Nanticoke sample. In addition, regardless of their initial moisture contents, all of the EPK specimens shrink to a similar total pore volume as they dry. Fig. 2-5b shows that almost all of the remaining pores in the air-dried kaolin are smaller in diameter than 400 nm, although there are still some voids with diameters higher than 10,000 nm (10 micron) left in the material. This confirms the previous observation that reducing the moisture content leads to the smaller inter-aggregate pores disappearing faster than the larger ones (Fig. 2-2 and Fig. 2-3). The total pore volumes remaining in the air-dried specimens (residual pore volume) are given in Table 2-2 and Table 2-3 along with the inter- and intra- aggregate pore volumes of the air-dried samples. The residual pore volumes of EPK kaolin and Nanticoke clay, which contains illite and chlorite clay minerals, are about 0.34 and 0.21 ml/g, respectively. Therefore, the moisture contents of 34% and 21% deduced based on the MIP results for air-dried EPK and Nanticoke clays, respectively, should be related to the shrinkage properties of the two clays. Further explanation about this deduction is provided in the discussion section.

Several researchers (Garcia-Bengochea et al., 1979; Delage and Lefebvre, 1984; Griffiths and Joshi, 1989; Lapierre et al., 1990; Delage et al., 1996; Romero et al., 1999; Simms and Yanful, 2002; Cuisinier and Laloui, 2004; Romero et al., 2005; and Ninjarav et al., 2007) have previously shown that a reduction in void ratio due to consolidation or



compaction only changes the inter-aggregate pore volume and that the volume of intra-aggregate pores remains almost constant during volumetric compression. Koliji et al. (2010) suggest that any structural degradation in aggregated clay due to mechanical loading or moisture changes leads to changes in the macro-pore structure and leaves the micro-pores unaffected. As Table 2-2 and Table 2-3 indicate, the intra-aggregate pore volume for each clay is almost constant regardless of the moisture content of the samples. The inter-aggregate pore volume is close to zero for the air-dried condition and increases proportionately with the moisture content. Thus, there appears to be a strong link between residual pore volumes for the EPK and Naticoke clays and the moisture content at the shrinkage limit. It is therefore postulated that regardless of the clay soil moisture content, the volume of the pores within its aggregates is approximately constant. Hence, the intra-aggregate pores are more closely related to clay mineralogy, particle size distribution, and pore water chemistry.

Table 2-1 shows that the liquid limits of Naticoke clay and EPK kaolin are 48 and 61%, respectively. Despite this difference, the inter-aggregate pore volumes of both clays, at a moisture content equal to the liquid limit ( $LI=1$ ), are almost equal (0.28 ml/g and 0.27 ml/g for Naticoke and EPK clays, respectively). This can be explained with the cluster model developed by Olsen (1962) and is consistent with the suggestion by Nagaraj et al. (1991) that different clays, at a moisture content equal to the liquid limit, have approximately the same hydraulic conductivity (Mitchell and Soga, 2005). It is also generally accepted that various clays have approximately the same undrained shear strength ( $c_u \sim 2.0$  kPa) at the liquid limit (Mitchell and Soga, 2005). This link suggests that the mechanical behaviour of remoulded and reconstituted soils, e.g. hydraulic

conductivity and shear strength, is closely related to the volume of inter-aggregate pores, supporting the concept that clay aggregates behave like single particles and inter-cluster pore sizes govern the interactions between different aggregates.

## **2.5 Discussion on MIP analysis for soft and slurried clays**

Mercury intrusion porosimetry has the potential to be an effective tool for studying the microstructure of porous material. However, there are certain aspects associated with the MIP test procedure that may affect the results. In particular, for MIP analysis of soft clays, structural damage that may occur within the specimen while its pore moisture is being depleted during drying could be significant. This section discusses this issue and other factors of importance for accurate measurement of microstructure for clays at high moisture content.

Being saturated and having high a moisture content, soft and slurried clays possess a highly porous and potentially collapsible structure. Therefore, an accurate MIP analysis of such material is impossible without an effective drying method. The size of the specimens is a major factor in uniform drying of soft and slurried clays. Clays usually have a poor thermal conductivity, exacerbated in soft clays by the high volume of the pores (Abu-Hamdeh and Reeder, 2000). Using a large specimen can result in improper freezing of the moisture existing deep inside the specimen or in melting and recrystallization of the ice in the core of the specimen before sublimation is complete. Attempts to freeze-dry samples with a thickness of about 10 mm failed as the specimens went through non-uniform freezing and drying, creating a two-phase dried specimen with a freeze-dried soft outer shell and an air-dried stiff inner core. Hence, the size of the

samples used for freeze-drying should be as small as possible (Mitchell and Soga, 2005, suggest a thickness of 3 mm), and the outer part rather than the core of the dried specimens should be used for MIP testing.

One approach to evaluating the intactness of a dried specimen is to compare the total pore volume measured by MIP analysis,  $V_m$ , with the moisture content of the sample before drying. If the obtained cumulative curves become flat at very small diameters, the total MIP measured pore volume,  $V_m$ , which is equal to the cumulative reading at the smallest measured diameter, will correspond to the volume of all of the pores within the specimen. The void ratio,  $e$ , can be related to the pore volume,  $V_v$ , using:

$$e = \frac{V_v \cdot G_s \cdot \rho_w}{M_s} \quad (2.4)$$

Where  $M_s$  is the mass of dry solids,  $G_s$  is the specific gravity, and  $\rho_w$  is the density of water. Void ratio can also be obtained from the following equation:

$$e = \frac{G_s \cdot w}{S} \quad (2.5)$$

Where  $w$  is the moisture content of the soil and  $S$  is its degree of saturation. Combining Eqs. (2.4) and (2.5) gives:

$$\frac{V_v}{M_s} = \frac{w}{S \cdot \rho_w} \quad (2.6)$$

The MIP measured pore volume,  $V_m$ , is the volume of intruded mercury in millilitres per one gram of dried specimen. Therefore, assuming that the sample used in the MIP analysis has been thoroughly dried:

$$V_m = \frac{V_v}{M_s} \quad (2.7)$$

Assuming that the clay has been completely saturated prior to drying ( $S=1$ ) leads to a direct correspondence between the MIP measured pore volume,  $V_m$ , and moisture content:

$$V_m = \frac{w}{\rho_w} \quad (2.8)$$

Since the density of the pore water,  $\rho_w$ , is approximately  $1 \text{ g/cm}^3$ , if given in millilitres per gram, the total measured pore volume,  $V_m$ , will be equal to the moisture content. Delage and Lefebvre (1984) used this same method to check the link between the natural moisture content of a soft clay and the total intruded pore volume measured by MIP analysis. Using Eq. (2.8) to evaluate MIP test results, it is found that some data provided in the literature for specimens obtained by freeze-drying or critical-point-drying are proposing moisture contents far below the gravimetric moisture content of the soil, indicating that the drying method may not have been successfully implemented (e.g. Kamruzzaman et al., 2009). In addition, some other data in the literature are presented in terms of percentage (ratio of intruded volume to the measured total pore volume), making it impossible to assess the effectiveness of the drying method and hence the validity of the data (e.g. Yamadera et al., 1998; Chew et al., 2004; Prashant and Penumadu, 2007).

Eq. (2.8) was used to calculate MIP derived moisture contents of reconstituted Nanticoke clay and EPK kaolin. The MIP derived moisture contents,  $w_m$ , are plotted against the measured gravimetric moisture content of the specimens,  $w_r$ , in Fig. 2-6. It can be seen that a bilinear relationship exists, i.e. below  $w_r$  of 50%, the MIP derived and measured moisture contents are equal, while at values higher than 50%, the MIP derived moisture contents are lower than expected. The difference between the two increases with

further increase in the moisture content. The variance between the two lines in Fig. 2-6 represents the amount of error in MIP results. This error may be estimated using the following relationships:

$$\begin{aligned} \text{For } w_r < 50\% : \quad w_e &= 0 \\ \text{For } w_r > 50\% : \quad w_e &= 0.5w_r - 25 \end{aligned} \quad (2.9)$$

Where  $w_e$  is the difference between the MIP derived and measured gravimetric moisture contents.

Other researchers have also reported that for void ratios in excess of a certain threshold, the void ratio of their specimens has been underestimated by MIP analysis (Cuisinier and Laloui, 2004; Ninjarav et al., 2007; Simms and Yanful, 2004; Romero and Simms, 2008; Koliji et al., 2010). As Fig. 2-6 shows, the points corresponding to the two different clays follow a similar path, indicating that the observed error should be systematic and independent of the type of clay. As discussed previously, the shrinking characteristics of clays are highly dependent on their mineralogy. Hence, the observed error is not due to ineffective drying. Romero and Simms (2008) suggested the following additional sources of error in MIP analysis of porous materials:

- The presence in the material of isolated pores surrounded by solids (enclosed porosity);
- The presence in the material of large pores that are only accessible via smaller ones (constricted porosity);
- The maximum practical pressure of the apparatus, possibly leaving some miniature pores unintruded (non-intruded porosity);

- The minimum practical pressure of the apparatus, making it unable to measure the volume of large pores (non-detected porosity).

However, Romero and Simms (2008) also suggested that the amount of enclosed porosity is generally insignificant in soils. Constricted porosity is also thought to only affect the measured pore size distribution, but not the measured total pore volume. Since all cumulative curves presented in this study flatten at diameters less than 10 nm (indicating that there is no pore with a lower diameter), the effect of non-intruded porosity on MIP results is also likely to be minimal. Consequently, the only plausible explanation for the variance in moisture contents measured by the MIP analysis at high moisture contents seems to be the limitation of MIP for detecting large pores (pores larger than 100 microns in diameter). This is supported by the observation that higher errors are found for samples with higher moisture contents, which would potentially have more inter-aggregate macropores. Koliiji et al. (2010), who used MIP to investigate the microstructure of unsaturated clays, used an ultra-macropore kit in the low pressure unit of their porosimeter, enabling them to detect pore diameters as large as 600  $\mu\text{m}$ . They compared the pore size distributions measured for a specific soil sample with and without the ultra-macropore kit and demonstrated that 22.5% of the total pore volume of the specimen was not detected when the ultra-macropore kit was not used. In common with Simms and Yanful (2004) and Cuisinier and Laloui (2004), they also attributed this error to the limitation of conventional MIP testing for detecting very large pores.

## 2.6 Summary and Conclusions

Mercury intrusion porosimetry analysis was used to evaluate the microstructural changes in reconstituted clays due to variations in the moisture content. The results of this study have indicated that:

- A bimodal distribution of pore sizes exists in all of the reconstituted specimens. The peak associated with larger diameters represented inter-cluster pores, while the one associated with smaller diameters corresponded to intra-cluster pores.
- The volume of the pores trapped within the clay aggregates was found to be independent of the moisture content. Although constant with variations in the moisture content, the intra-aggregate pore volume differed between clay types.
- Conversely, the volume of the pores existing between clay aggregates changed proportionately with changes in the moisture content. A reduction in the moisture content predominantly affected the volume of smaller inter-aggregate pores rather than larger ones.
- Air-drying resulted in the disappearance of almost all of the inter-aggregate pores from the material. However, even complete air-drying did not change the intra-aggregate pore volume of the specimens.
- At high moisture contents, MIP underestimated the void ratio of the saturated material. This error was attributed to the limitation of the MIP analysis in recognizing pores with a large pore diameter.
- Since higher amounts of error were observed in specimens with a higher void ratio, results of MIP analysis for such material states should be viewed with caution.

## 2.7 Acknowledgments

The authors would like to express their gratitude to the Natural Sciences and Engineering Research Council of Canada, NSERC, and The University of Western Ontario for providing financial support for this work.

## 2.8 References

- Abu-Hamdeh, N.H., and Reeder, R.C. (2000). "Soil thermal conductivity: effects of density, moisture, salt concentration and organic matter." *Soil Science Society of America Journal*, 64, 1285–1290.
- Aylmore, L.A.G., and Quirk, J.P. (1960). "Domain or turbostratic structure of clays." *Nature*, 187, 1046–1048.
- Casagrande, A. (1932). "The structure of clay and its importance in foundation engineering." *Boston Society Civil Engineers Journal*, 19(4), 168–209.
- Chew, S.H., Kamruzzaman, A.H.M., and Lee, F.H. (2004). "Physicochemical and Engineering Behavior of Cement Treated Clays." *Journal of Geotechnical and Geoenvironmental Engineering*, 130(7), 696–706.
- Choquette, M., Marc-André Bérubé, and Locat, J. (1987). "Mineralogical and microtextural changes associated with lime stabilization of marine clays from eastern Canada." *Applied Clay Science*, 2(3), 215–232.
- Collins, K., and McGown, A. (1974). "The form and function of microfabric features in a variety of natural soils." *Geotechnique*, 24(2), 223–254.



- Cuisinier, O., and Laloui, L. (2004). "Fabric evolution during hydromechanical loading of a compacted silt." *International Journal for Numerical and Analytical Methods in Geomechanics*, 28, 483–499.
- Delage P., and Lefebvre, G. (1984). "Study of the structure of a sensitive Champlain clay and of its evolution during consolidation." *Canadian Geotechnical Journal*, 21, 21–35.
- Delage, P., Audiguier, M., Cui, Y.-J., and Howat, M.D. (1996). "Microstructure of a compacted silt." *Canadian Geotechnical Journal*, 33(1), 150–158.
- Diamond, S. (1970). "Pore size distribution in clays." *Clays and Clay Minerals*, 18, 7–23.
- Garcia-Bengochea, I., Lovell, C.W., and Altschaeffl, A.G., (1979). "Pore distribution and permeability of silty clays." *Journal of the Geotechnical Engineering Division (ASCE)*, 105(7), 839–856.
- Gerke, H.H., van Genuchten, M.T. (1993). "A dual-porosity model for simulating the preferential movement of water and solutes in structured porous media." *Water Resources Research*, 29(2), 305–319.
- Giesche, H. (2006). "Mercury porosimetry: A general (practical) overview." *Particle & Particle Systems Characterization*, 23, 9–19.
- Gillott, J.E. (1970). "Fabric of Leda clay investigated by optical, electron-optical, and X-ray diffraction methods." *Engineering Geology*, 4(2), 133–153.
- Griffiths, F.J., and Joshi, R.C. (1989). "Change in pore size distribution due to consolidation of clays." *Geotechnique*, 39(1), 159–167.

- Jarvis, N. (1994). "The MACRO model Version 3.1: technical description and sample simulations." Reports and Dissertations, No 19, Department of Soil Science, Swedish University of Agricultural Sciences, Uppsala, Sweden.
- Kamruzzaman, A.H.M., Chew, S.H., and Lee, F.H. (2009). "Structuration and Destructuration Behavior of Cement-Treated Singapore Marine Clay Cement-Treated Singapore Marine Clay." *Journal of Geotechnical and Geoenvironmental Engineering*, 135(4), 573–589.
- Koliji, A., Vulliet, L., and Laloui, L. (2010). "Structural characterization of unsaturated aggregated soil." *Canadian Geotechnical Journal*, 47(3), 297–311.
- Lamb, T.W. (1953). "The structure of inorganic soils." *Proceedings of the American Society of Civil Engineers*, 79, Separate No. 315.
- Lamb, T.W. (1958). "The structure of compacted clay." *Proceedings of the American Society of Civil Engineers*, 84, SM2, 1–34.
- Lapierre, C., Leroueil, S., and Locat, J., (1990). "Mercury intrusion and permeability of Louisville clay." *Canadian Geotechnical Journal*, 27, 761–773.
- Locat, J., Tremblay, H., and Leroueil, S. (1996). "Mechanical and hydraulic behaviour of a soft inorganic clay treated with lime." *Canadian Geotechnical Journal*, 33(4), 654–669.
- Mitchell, J.K., and Soga, K. (2005). "Fundamentals of Soil Behavior, 3rd Ed." John Wiley & Sons, Hoboken, New Jersey.

- Nagaraj, T.S., Pandian, N.S., and Narasimha Raju, P. S. R. (1991). “An approach for prediction of compressibility and permeability behaviour of sand-bentonite mixes.” *Indian Geotechnical Journal*, 21(3), 271–282.
- Ninjarav, E., Chung, S.-G., Jang, W.-Y., and Ryu, C.-K. (2007). “Pore Size Distribution of Pusan Clay Measured by Mercury Intrusion Porosimetry.” *Journal of Civil Engineering (KSCE)*, 11(3), 133–139.
- Olsen, H. W. (1962). “Hydraulic flow through saturated clays.” *Proceedings of the Ninth National Conference on Clays and Clay Minerals*, Pergamon Press, West Lafayette, IN, 131–161.
- Prashant, A., and Penumadu, D. (2007). “Effect of Microfabric on Mechanical Behavior of Kaolin Clay Using Cubical True Triaxial Testing.” *Journal of Geotechnical and Geoenvironmental Engineering*, 133(4), 433–444.
- Romero, E., Gens, A., and Lloret, A. (1999). “Water permeability, water retention and microstructure of unsaturated compacted Boom clay.” *Engineering Geology*, 54, 117–127.
- Romero, E., Hoffmann C., Castellanos E., Suriol J., and Lloret A. (2005). “Microstructural changes of compacted bentonite induced by hydro-mechanical actions.” *Proceedings of International Symposium on Large Scale Field Tests in Granite*, Sitges, Spain, 12–14th November, In: Advances in understanding engineered clay barriers. Alonso, E.E., Ledesma, A. (eds.). Taylor & Francis Group, London, 193–202.

- Romero, E. and Simms, P.H. (2008). "Microstructure investigation in unsaturated soils: A review with special attention to contribution of mercury intrusion porosimetry and environmental scanning electron microscopy." *Geotechnical and Geological Engineering*, 26, 705–727.
- Simms, P.H. and Yanful, E.K. (2002). "Predicting soil—water characteristic curves of compacted plastic soils from measured pore-size distributions." *Geotechnique*, 52(4), 269–278.
- Simms, P.H. and Yanful, E.K. (2004). "A discussion of the application of mercury intrusion porosimetry for the investigation of soils, including an evaluation of its use to estimate volume change in compacted clayey soils." *Geotechnique*, 54(6), 421–426.
- Terzaghi, K. (1925). "Erdbaumechanik auf boden physikalischer grundlage." F. Deuticke, Vienna.
- Thompson, M.L., McBride, J.F., and Horton, R. (1985). "Effects of drying treatment on porosity of soil materials." *Soil Science Society of America Journal*, 49, 1360–1364.
- Washburn, E.W. (1921). "Note on a method of determining the distribution of pore sizes in a porous material." *Proceedings of the National Academy of Sciences, USA*, 7(4), 115–116.
- Yamadera, A., Nagaraj, T.S., and Miura, N. (1998). "Prediction of strength development in cement stabilized marine clay." *In Proceedings of the Geotechnical*

*Engineering Conference, Asian Institute of Technology, Bangkok, Thailand. 1,*  
141–153.

**Table 2-1.** Basic geotechnical properties of the two types of clay used in this study

Soil Characteristic	Nanticoke clay	EPK kaolin
Liquid limit, LL (%)	48	61
Plastic limit, PL (%)	23	36
Plasticity Index, PI (%)	25	25
Specific Gravity, $G_s$	2.73	2.61
Clay fraction (<2 $\mu\text{m}$ , %)	48	53
Activity, A	0.52	0.47

**Table 2-2.** The calculated inter-aggregate and intra-aggregate pore volumes for samples of Nanticoke clay at different moisture contents

Liquidity index, LI	Moisture content, w (%)	Total pore volume (ml/g)	Inter-aggregate pore volume (ml/g)	Intra-aggregate pore volume (ml/g)
3	98	0.77	0.57	0.20
2	73	0.58	0.37	0.21
1	48	0.46	0.28	0.18
0.5	35.5	0.34	0.17	0.17
0	23	0.23	0.07	0.16
N/A	Air-dried	0.21	0.04	0.17

**Table 2-3.** The calculated inter-aggregate and intra-aggregate pore volumes for samples of EPK kaolin at different moisture contents

Liquidity index, LI	Moisture content, w (%)	Total pore volume (ml/g)	Inter-aggregate pore volume (ml/g)	Intra-aggregate pore volume (ml/g)
2	86	0.68	0.42	0.26
1	61	0.55	0.27	0.28
0.5	48.5	0.49	0.22	0.27
0	36	0.35	0.1	0.25
N/A	Air-dried	0.34	0.09	0.25



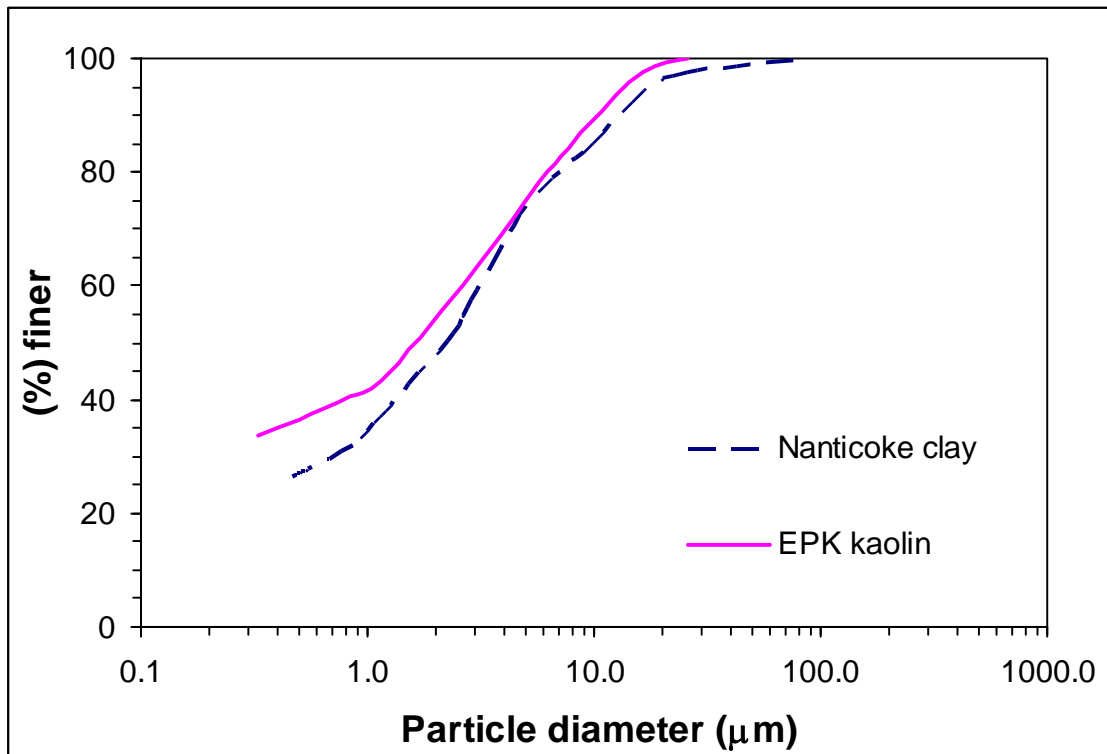
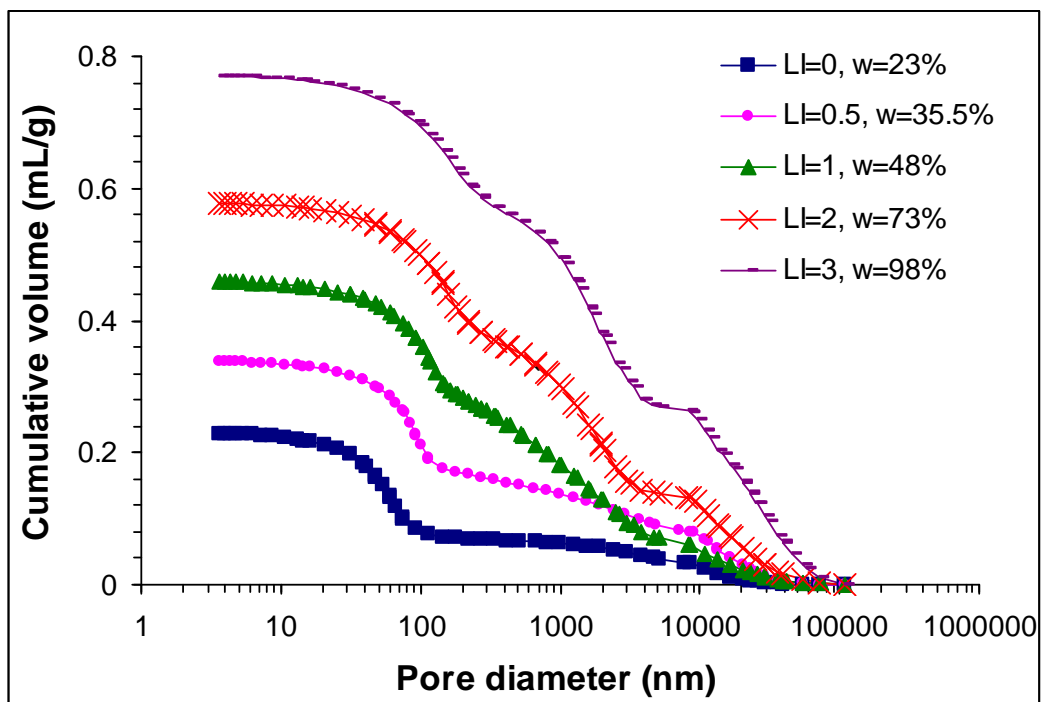
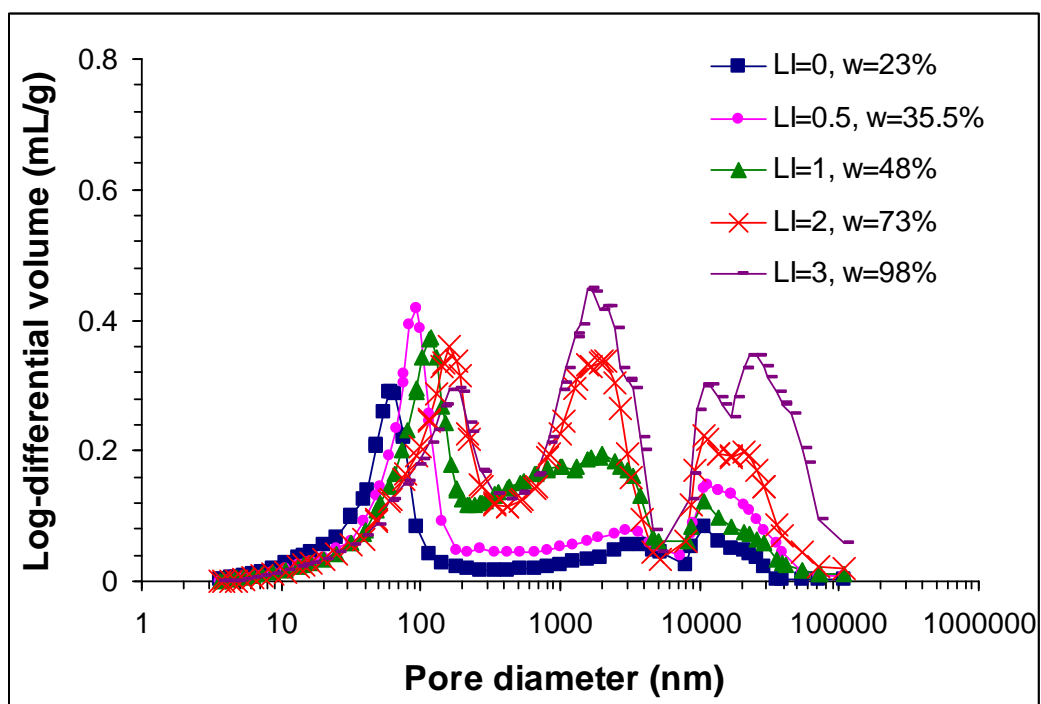


**Fig. 2-1.** Particle size distribution of the three clays used in this study

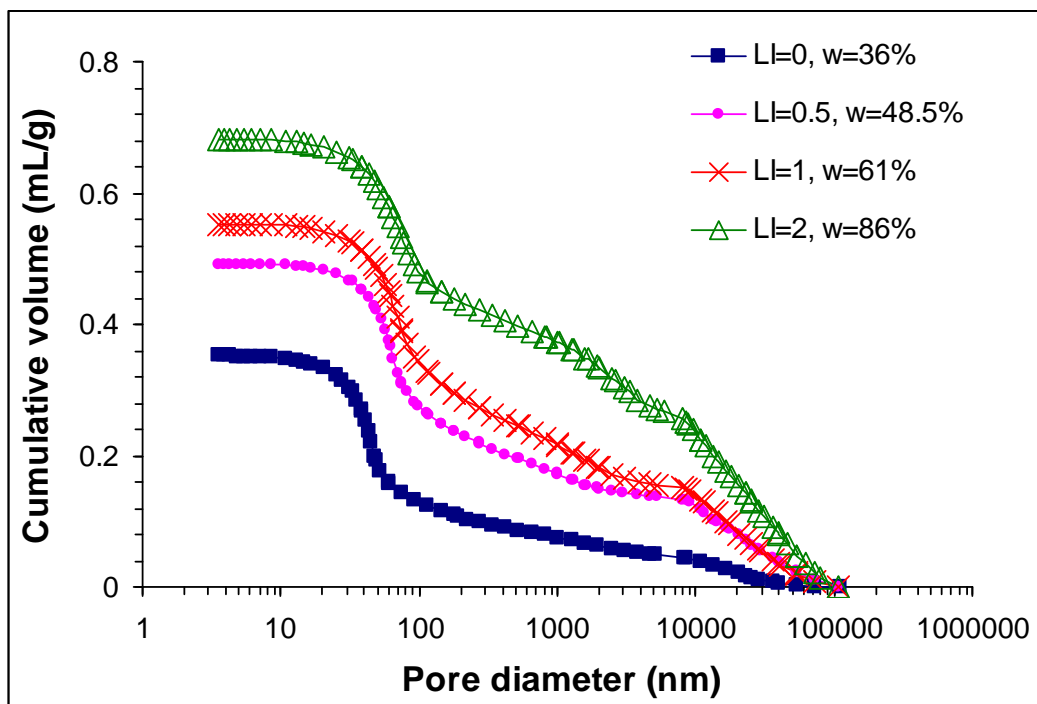


(a)

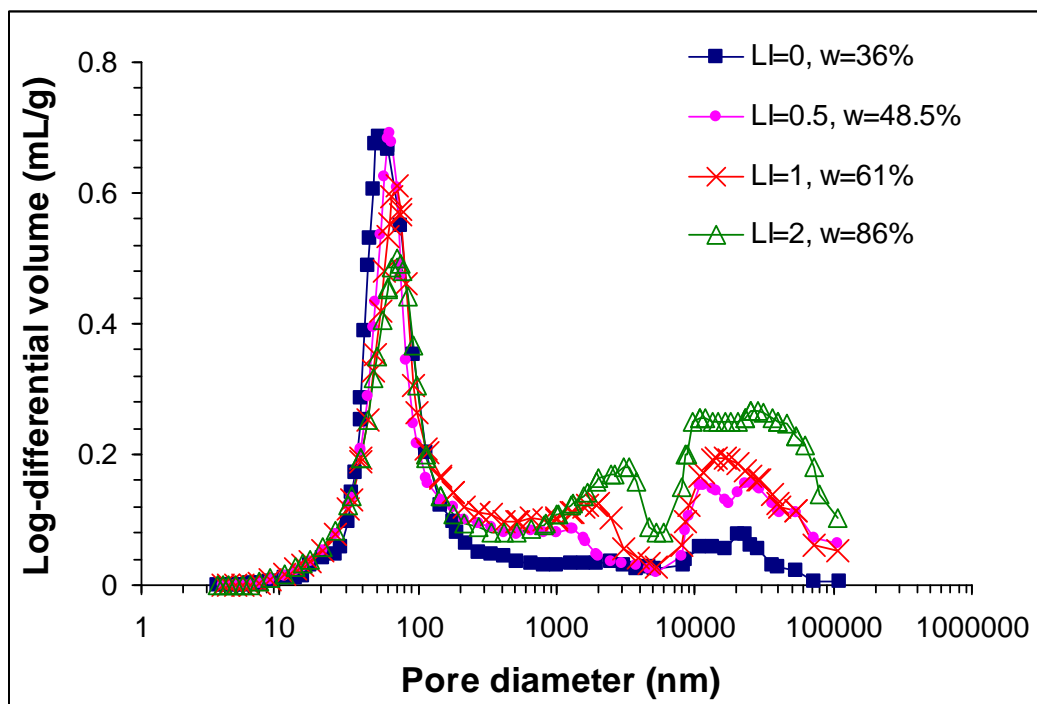


(b)

**Fig. 2-2.** Pore size distribution of reconstituted Nanticoke clay specimens with different liquidity indices: (a) cumulative distribution; (b) log-differential distribution

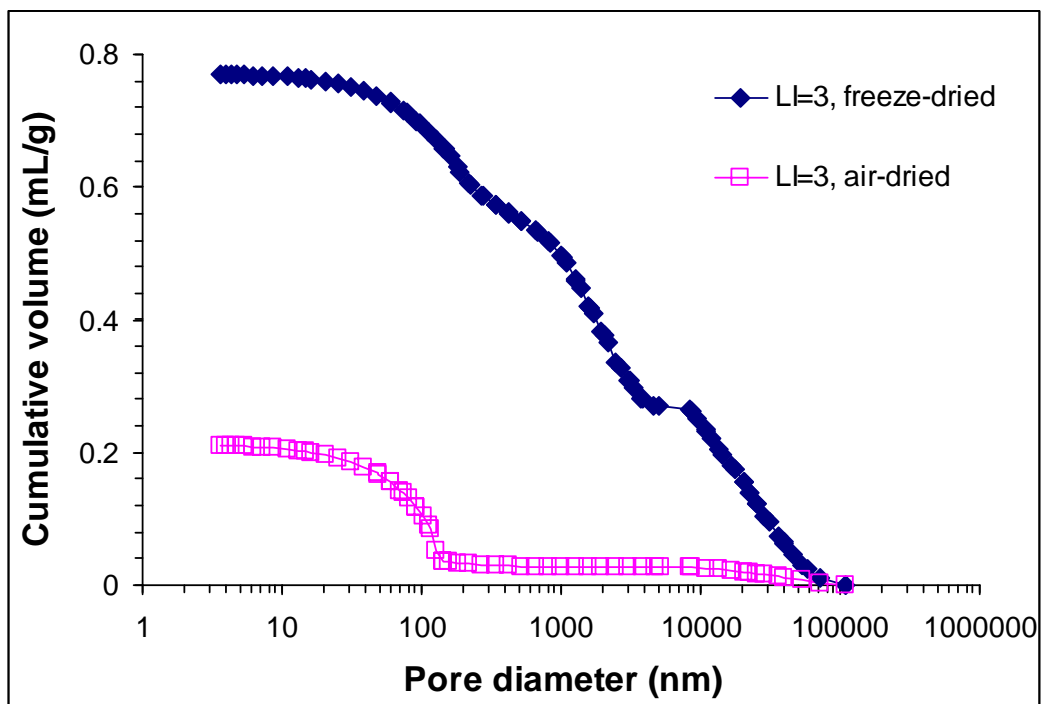


(a)

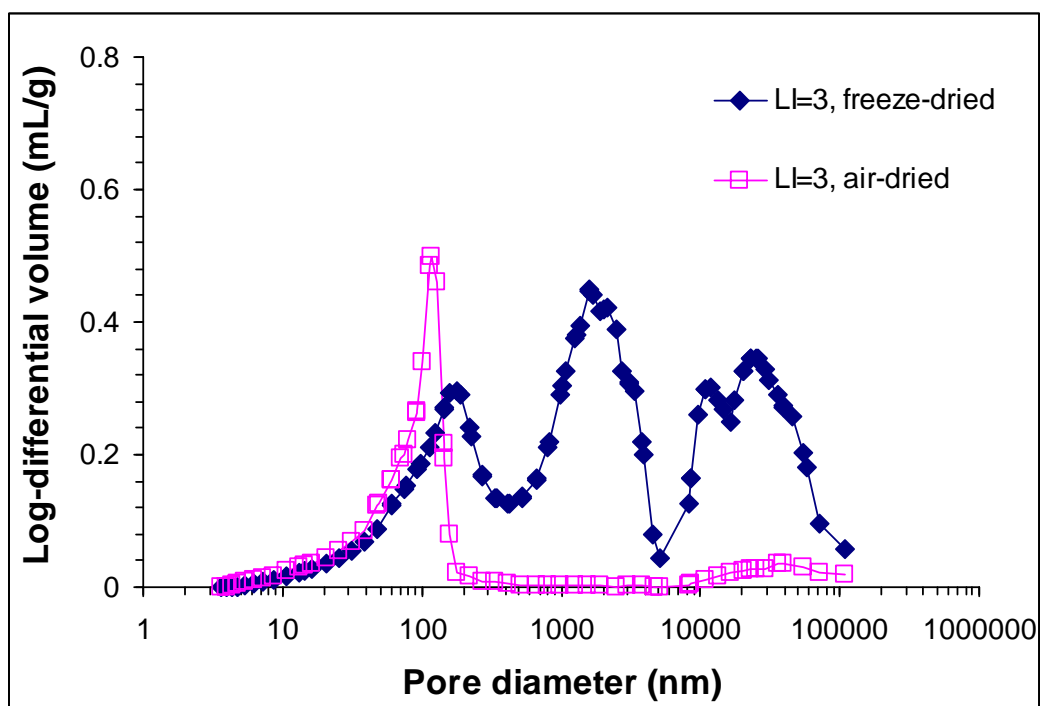


(b)

**Fig. 2-3.** Pore size distribution of reconstituted EPK kaolin specimens with different liquidity indices: (a) cumulative distribution; (b) log-differential distribution

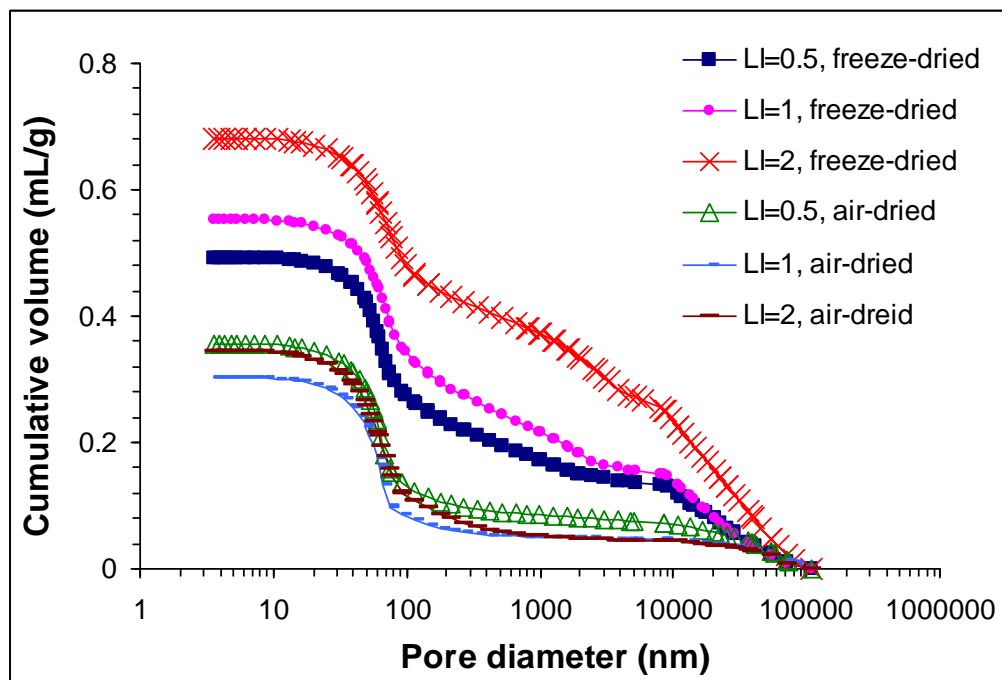


(a)

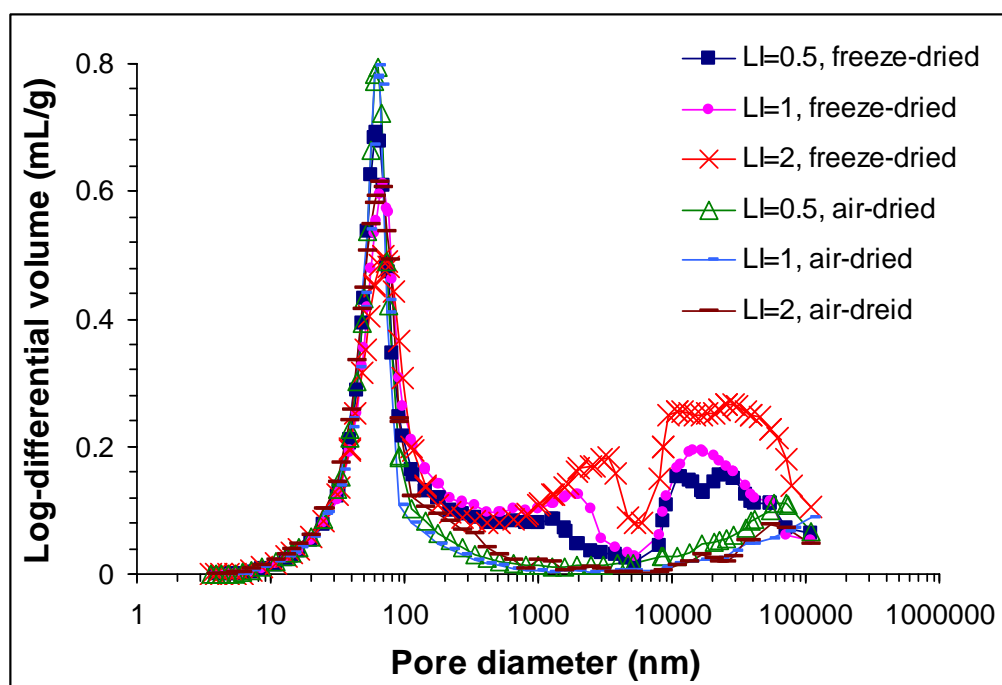


(b)

**Fig. 2-4.** Pore size distribution of freeze-dried and air-dried reconstituted Naticoke clay at LI=3 (a) cumulative distribution; (b) log-differential distribution



(a)



(b)

**Fig. 2-5.** Pore size distribution of freeze-dried and air-dried reconstituted EPK specimens at different liquidity indices: (a) cumulative distribution; (b) log-differential distribution

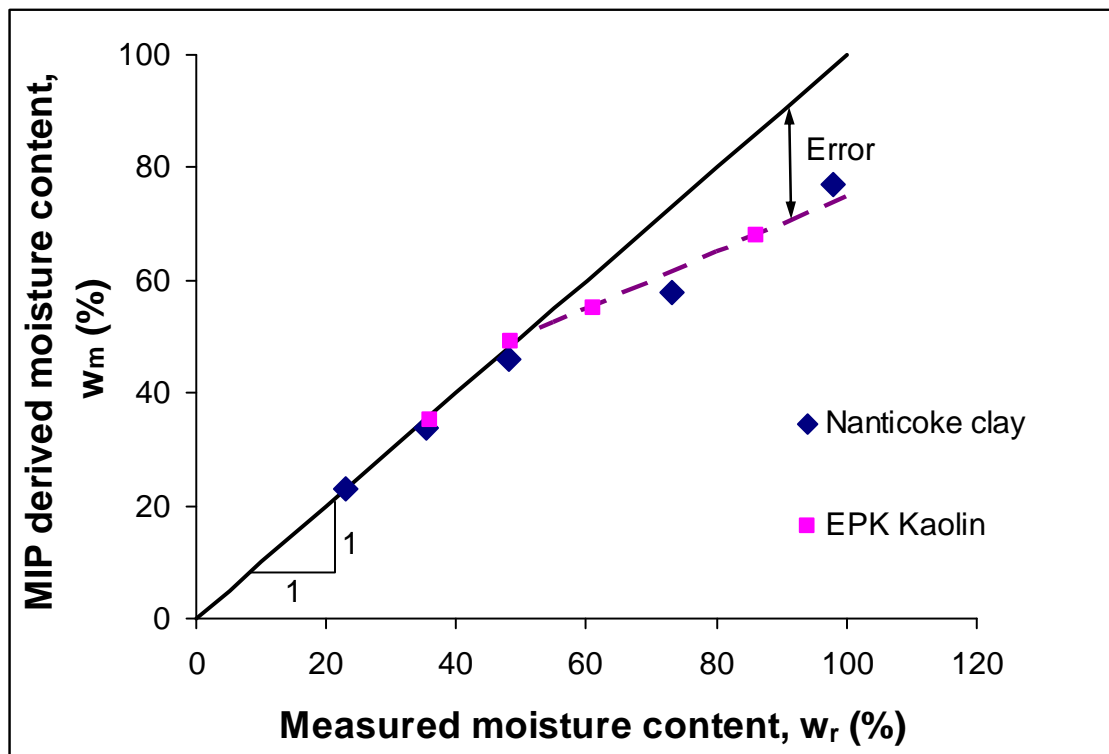


Fig. 2-6. MIP derived moisture contents versus the measured moisture contents

### **3 THE DEVELOPMENT OF MICROSTRUCTURE IN ARTIFICIALLY CEMENTED CANADIAN CLAYS**

#### **3.1 Introduction**

Artificial cementation is becoming increasingly important for the stabilization and treatment of soft clayey soils. Cemented, dredged and waste soils are often employed in land reclamation and rehabilitation projects. Cementitious additives are also extensively used to improve mechanical properties of soft ground underlying roads and railways. Deep mixed concrete columns are becoming more common as alternatives to piles for stabilized slopes, trenches and deep excavations in soft ground (Bergado et al., 1996). Cementitious additives are also used to stabilize mine wastes for underground disposal (e.g. MacKay and Emery, 1992). The major aim of the aforementioned application of artificial cementation is the creation of bonding between soil particles, thereby increasing the strength and reducing the compressibility of the materials (e.g. Fischer et al., 1978; Uddin et al., 1997; Tremblay et al., 2001; Ismail et al., 2002a; Lo and Wardani, 2002; Chew et al., 2004; Kamruzzaman et al., 2009). Whilst the mechanical behaviour of cemented clays is becoming better understood, the nature of the bonding and the microstructure developed in artificially cemented clays are still poorly described in the literature.

Many features of artificial cementation in clays are also characteristic of cementation in natural clay deposits (e.g. Loiselle et al., 1971; Sangrey, 1972; Boone and Lutenecker, 1997; Graham et al., 2005). Evidence of natural cementation is found in many sensitive soils, especially those located in parts of Canada (e.g. Sangrey, 1972;

Bentley and Smalley, 1978; Quigley, 1980; Graham et al., 2005). Investigation of the effect of natural cementation on soil behaviour has been enhanced by the use of artificially cemented samples created in the laboratory (e.g. Graham et al., 2005). This approach avoids the cost and technical difficulties associated with obtaining undisturbed naturally cemented specimens and can provide insight into the processes forming natural soils and weak rocks. In addition, the development of constitutive models for naturally and artificially cemented soils requires good understanding of the initial microstructure and bonding that occurs during the formation, and the subsequent breakdown of this structure during loading.

It is therefore important to study the microstructural changes and bonding of the soil due to the addition of cementitious binders and to investigate the links between the resulting microstructural changes and mechanical behaviour of the material. The behaviour of cemented clays has been found to be dependent on bonding, composition, and fabric (Mitchell and Soga, 2005). It is also thought to be dependent on the mineralogy and activity of the soil and the type of cement (Croft, 1967a; Croft, 1967b; Noble and Plaster, 1970; Osula, 1996; Tremblay, et al. 2001; Ismail et al., 2002a; Ismail et al., 2002b; Bhattacharja et al., 2003; Wareham and Mackechnie, 2006). However, these latter aspects have been less well investigated for cement-treated clays.

The objective of this study was to investigate the development of cementation for kaolinite and two Ontario clays with Portland cement additives, to better understand the effects of clay mineralogy and activity on the resulting microstructure and bonding. Qualitative and quantitative data have been utilised, from scanning electron microscopy and mercury porosimetry, and microstructural descriptions have been correlated to the



mechanical behaviour of the material. The effect of gypsum on Portland cement-soil mixtures has also been investigated. These aspects are discussed with the potential consequences for the use of cementitious binders for soil stabilization and improvement.

### **3.2 Literature Review**

Soil aggregates or clusters are often described as “assemblages” of clay particles, which behave as compressible, crushable macro-particles and interact to create strength and stiffness in clays (Mitchell and Soga, 2005). Despite soil-cement mixtures being thoroughly blended, clay particles will often form aggregates enclosed by the cement slurry (Croft, 1967b; Bergado et al., 1996). Due to its availability and relative inexpensiveness, Portland cement is the most commonly used cementing agent in geotechnical projects. Adding Portland cement to soil results in a hydration reaction in the cement, followed by a pozzolanic reaction between the calcium hydroxide supplied by the cement and the silica in the soil (e.g. Herzog and Mitchell, 1963; Croft, 1967a; Bergado et al., 1996; Bhattacharja et al., 2003). Both hydration and pozzolanic reactions lead to the creation of gelatinous and amorphous hydrated calcium silicates and calcium aluminates. These products later crystallize to form inter-aggregate and inter-particle bonds (Croft, 1967a), giving an apparent cohesion to the resulting composite material. The hydration reactions take place with a faster rate than the pozzolanic reactions and occur mainly in the space between the soil aggregates, forming a strong matrix enclosing the non-bonded particles and aggregates. Conversely, the pozzolanic reactions take place between the produced calcium hydroxide and the silica and alumina, dissolved from the clay surfaces, to bond the particles within the clay aggregates (Bergado et al., 1996;

Bhattacharja et al., 2003). These two forms of reactions combine to produce inter-aggregate and intra-aggregate bridges, creating a strongly bonded fabric within the soil body.

Gypsum is another effective cementing agent and is well-known for its workability and slow hardening rate after initial setting. When mixed with water, the calcium sulphate hemihydrate powder changes to its dihydrate form (gypsum), developing a rigid crystal lattice within the desired material (Amaratunga, 1995). Unlike cement-based mixtures, hydrated gypsum remains relatively soft for a long time after mixing; gypsum is often added as a compound to Portland cement to prevent flash setting. Although it can significantly increase the strength and stiffness of granular soils (Huang and Airey, 1998), adding gypsum alone to soft clays with high moisture contents does not improve their shear strength or compressibility characteristics. However, if added to cement and clay mixtures, gypsum can noticeably change the properties of the cemented clay. Both of these binders can change the microstructure of the clay; they produce a flocculated structure in the material, as they increase the calcium content of the soil. Moreover, both cement and gypsum hydration reactions consume pore water and are exothermic, i.e. they produce heat. However, the formation of gypsum crystals is also accompanied by volumetric expansion in the soil (Sereda et al., 1965).

Scanning electron microscopy and mercury intrusion porosimetry have been used previously for examining the micro-fabric of various porous materials (e.g. Choquette et al., 1987; Delage et al., 1996; Locat et al., 1996; Ninjgarav et al., 2007; Romero and Simms, 2008; Koliji et al., 2010). When used in combination, SEM and MIP can provide coupled qualitative and quantitative information on the arrangement and distribution of

particles and pores within the material. Such information can improve the understanding of the macroscopic and engineering behaviour of soils (Romero and Simms, 2008). Despite their potential effectiveness, these two characterization methods are infrequently used together to examine the microstructure developed in clays, especially those treated by Portland cement or gypsum. Lapierre et al. (1990) used MIP results to find the relationships between pore size distribution and permeability of a Leda clay and suggested that no unique correlation between the two parameters can be found.

Choquette et al. (1987) studied the effects of artificial cementation with quick lime on microtexture and mineralogy of marine clays from eastern Canada. They concluded that the addition of lime results in immediate agglomeration of clay particles and that the flocculated structure is maintained with development of cementitious bonds. They also suggested that lime stabilization results in the production of platy minerals, which partition the inter-aggregate space within the soil material and increase the volume of the micropores. They observed a correlation between the amount of structural change due to the addition of lime and the measured strength of the treated clay.

Locat et al. (1996) investigated the mechanical and hydraulic behaviour of a lime-treated clay, suggesting that if the lime content is high enough (greater than 3%) to provoke pozzolanic reactions in the soil (for a constant void ratio), the produced cementitious material will fill the pore space and can reduce the hydraulic conductivity by up to an order of magnitude. Chew et al. (2004) and Kamruzzaman et al. (2009) investigated the development of microstructure in cement-treated Singapore marine clay by performing SEM and MIP analyses and detected an increase in the degree of flocculation at higher cement contents. Based on the MIP results for the cement-treated

samples, Kamruzzaman et al. (2009) also suggested that among specimens prepared at the same initial moisture content, those having a higher cement content will also have a higher volume of macropores, as well as a higher total pore volume. Horpibulsuk et al. (2010) performed MIP analysis on compacted specimens of a silty clay treated with 10% Portland cement. They showed that in the pore diameter range of 10 to 100 nm, the pore size distributions of samples with different moisture contents are essentially the same.

### **3.3 Experimental Design**

#### **3.3.1 Material properties**

Artificially cemented samples of three types of clay: EPK kaolin, Nanticoke clay, and Ottawa clay, were prepared for this study. EPK kaolin is a commercially available pulverized kaolin clay from Georgia, U.S. Air-dried clay powders were also obtained from block samples of a stiff, fissured clay with a glacio-lacustrine origin taken from 3 m depth in a test pit in Nanticoke, Ontario, and from samples of a sensitive Leda/Champlain clay (St~20) also taken from 3 m depth in a borehole in Ottawa, Ontario. X-ray diffraction analysis showed that the Nanticoke and Ottawa clays had primary clay minerals of illite and chlorite. Traces of vermiculite were also found in the Ottawa clay. The primary non-clay minerals of these soils are quartz, feldspar, calcite, and dolomite. Additional pyrite was found in the Ottawa clay (Fig. 3-1). Both clays appear to have almost similar clay minerals. However, since they have been deposited in different geological periods and depositional environments, Nanticoke and Ottawa clays do not necessarily have a unique mineralogy and structure (Locat et al., 1985). For instance, the two clays have different colors, activities, and clay contents. Quigley (1980) suggests that

the Nanticoke clay, which can be considered among the Lake Erie basin clays, has been formed in freshwater glacial lakes around 13,000 years BP. However, the Ottawa clay is a Champlain Sea clay mainly deposited in a marine environment approximately between 12,500 to 10,000 BP (Quigley, 1980). Hence, unlike the Nanticoke material, the Ottawa clay has been formed in an environment with an approximate salinity of 35 g/L. The Nanticoke and Ottawa clay specimens used in this study had natural moisture contents of 28 and 80%, indicating liquidity indices of 0.2 and 2, respectively. Table 3-1 summarizes the basic geotechnical properties of the three types of clay used in this study, and Fig. 3-2 shows their grain size distribution conducted according to ASTM D422. Note that the particle size distribution curves for the three clays are relatively similar.

Two types of binders were used in this study. Ordinary Portland cement (type I according to ASTM C150) was used as the primary cementing agent to produce cementitious bonding within the specimens. Plaster of Paris (calcium sulphate hemihydrate) was also added to some of the mixtures of EPK kaolin, to investigate the microstructure and strength developed in gypsum treated material.

### **3.3.2 Specimen preparation and testing programme**

Except for the undisturbed specimens of Ottawa and Nanticoke clays, all other samples used in this study were obtained from powdered material. EPK Kaolin is already available in powder form. To prepare the powdered Nanticoke and Ottawa clays, the soil obtained from the block samples was cut into small pieces and dried at room temperature. Then the soil was finely pulverized into a powder (100% passing Sieve No. 40) using a rubber hammer to avoid crushing any soil particles. For each clay type, prepared powder was then used to make cemented or reconstituted specimens.

To make the cemented samples, clay powders were added to de-ionised water to form a slurry with a water content close to the desired value. The slurry was then mixed in a commercial mixer until it was uniform. Next, the required amount of cement and water was added to the mixture to increase the water content to the desired level. If needed, a certain amount of gypsum (in powder form) was also added to the mixture, so that the required combination of soil-cement-gypsum was obtained. The slurry was then gently mixed for a maximum of 15 minutes, to ensure that the mixing process would not break any produced bonds. The mixture was then poured into plastic cups, 70 mm in diameter and 120 mm in height. Trapped air bubbles were removed from the specimens by gently tapping on the walls of each cup, and some water was added above the slurry surface in every cup, to provide it with moisture throughout the curing period. The cups were then covered by plastic wrap and placed in a temperature controlled room to be cured at a constant temperature of 25°C. All cemented samples were cured for a period of 28 days before being used for testing. Cemented samples were prepared with different moisture content,  $w$  (%), cement content,  $c$  (%), and gypsum content,  $g$  (%). Cement and gypsum contents were defined as the ratio of mass of cement or plaster to the mass of dry soil in terms of a percentage, respectively.

For the preparation of the reconstituted samples, powdered clay was added to the amount of water needed to reach the target moisture content. The resulting mixture was blended for a few minutes and was left to soak for at least 24 hours in a sealed container before it was mixed again and used for testing. For all reconstituted samples, the moisture content of a portion of the specimen was measured prior to performing experiments to ensure that the target moisture content was reached.

To analyse the microstructure developed in the cemented clays, mercury intrusion porosimetry (MIP) and scanning electron microscopy (SEM) were carried out on undisturbed, reconstituted, or cemented samples of EPK kaolin, Nanticoke clay, and Ottawa clay. The scanning electron microscopy analysis was conducted using a Hitachi S-4500 field emission SEM with a Quartz XOne EDX system. For the SEM/EDX analysis, very small dried pieces of the clay sample were secured on aluminum mounting stubs by an adhesive carbon conductive tab and were sputter coated with a thin layer of gold, before placement in the SEM device. SEM images were taken at different levels of magnification in the range of 1000x to 25,000x. Mercury intrusion porosimetry tests were carried out with an AutoPore IV, a porosimeter manufactured by Micromeritics and capable of providing a maximum mercury pressure of 414 MPa. This porosimeter conducts MIP experiments in two stages; i.e. a low pressure stage followed by a high pressure stage. To carry out the tests, a sample of the dried soil was placed in an MIP penetrometer, and the sealed penetrometer was inserted into the low pressure port of the equipment. In this stage, the air was evacuated and was then replaced by mercury in increments until a mercury pressure of 172 kPa was reached. Next, the penetrometer, now filled with mercury, was removed from the low pressure port, weighed, and placed in the high pressure port, where it was pressurized, incrementally up to the maximum pressure of 414 MPa. The mass of the dried specimens used in the MIP analysis ranged from 1.0 to 1.7 g, depending on the stem volume of the penetrometer and the expected total pore volume of the sample.

For preparation of the samples for the SEM and MIP analyses, a freeze-drying method was employed to remove the pore water with minimum disturbance to the pore

structure. To freeze-dry the specimens, samples were cut into small cubes (about 5 mm in each linear dimension) to avoid disturbance due to non-uniform freezing (Mitchell and Soga, 2005). Next, they were placed in a specimen holder and dipped for about one minute into a container filled with isopentane that had been previously cooled to its melting point ( $-160^{\circ}\text{C}$ ) in liquid nitrogen ( $-196^{\circ}\text{C}$ ). This sudden reduction in temperature (to values lower than  $-130^{\circ}\text{C}$ ) prevents the formation of crystalline ice in the sample and avoids any volume expansion. In addition, dipping the samples in cooled isopentane prevents the delay in freezing that would happen to samples dipped directly into liquid nitrogen because of the development of thermally insulating gaseous bubbles around the specimens (Rowe, 1960). After freezing, the pore water was removed by sublimation with the use of a vacuum pump capable of providing an absolute pressure of 4 Pa. The dried samples were then kept in a desiccator under vacuum until tested. A number of specimens used in MIP analysis were prepared by air-drying rather than freeze-drying. To air-dry the samples, they were left to dry at room temperature ( $25^{\circ}\text{C}$ ) for a few days before they were completely dried in a desiccator under an absolute pressure of 4 Pa.

Oedometer tests on undisturbed, reconstituted, and cemented specimens of Nanticoke and Ottawa clays were used to measure the hydraulic conductivity. All oedometer tests and calculations were performed in accordance with ASTM D2435, and the hydraulic conductivity values were obtained using the square root of time method (Head, 1982). In addition, the undrained shear strengths of cemented EPK, Nanticoke and Ottawa clays with different cement contents were measured with a laboratory shear vane. The vane had a diameter and height of 19 and 28 mm, respectively. The tests were carried out with an approximate rate of one complete revolution per minute to avoid the



influence of shearing rate on the test results. To measure the peak shear strength,  $c_{up}$ , the vane was inserted into the plastic cups filled with the cemented soil and was rotated until the sample reached failure. The residual shear strength,  $c_{ur}$ , of the material was measured after multiple rotations of the vane.

## **3.4 Results and Analysis**

### **3.4.1 SEM analysis of undisturbed, reconstituted, and artificially cemented specimens**

Scanning electron microscopy provides a useful tool for visual characterisation of particle structure and bonding agents developed between soil particles due to artificial cementation. SEM analysis was performed on freeze-dried samples of intact, reconstituted or cemented clay to identify differences between these materials and states. Fig. 3-3 shows the images taken from an undisturbed sample of Nanticoke clay at different magnifications. The clay sample was highly overconsolidated with an apparent vertical preconsolidation stress of almost 500 kPa, explaining the compacted and dispersed structure observed in Fig. 3-3a, b, and d. EDX analysis confirmed the presence of silt size quartz and feldspar crystals, which are marked in Fig. 3-3b with the numbers 1 and 2, respectively. The smaller platy clay particles (Fig. 3-3b and d) gather in approximately parallel arrangements to form a dispersed structure. Calcite clasts were also observed in the intact soil. The calcite particle identified by EDX analysis can be recognized from its striated surface in Fig. 3-3b (point 3) and c (at a higher level of magnification). Although trace amounts of carbonates were also seen on the EDX scans

performed on the entire sample, it is difficult to identify whether the majority of carbonates are discrete clasts or are disseminated through the soil body.

In contrast, Fig. 3-4 shows SEM micrographs at different magnifications taken from the surface of Nanticoke clay treated with 8.7% Portland cement. Comparing this figure with Fig. 3-3, it can be seen that a more open structure exists in the cemented clay. This is a consequence of the introduction of cement into the soil; the concentration of calcium ions,  $\text{Ca}^{2+}$ , in the pore fluid increases rapidly due to the commencement of hydration reactions. Gartner et al. (1985) reported that the aqueous phase of Portland cement pastes with a w/c ratio of 0.5 became super-saturated with respect to calcium within 12 minutes of curing. This increase in the concentration of calcium ions leads to the substitution of calcium, which is a divalent cation, for the monovalent cations, such as  $\text{Na}^+$  and  $\text{K}^+$ , which have been previously adsorbed to clay surfaces within the double layer (Bergado et al., 1996; Bhattacharja et al., 2003). The cation exchange increases the concentration of positively charged calcium ions in the vicinity of particle surfaces and causes flocculation (Herrin and Mitchell, 1961; Herzog and Mitchell, 1963; Choquette et al., 1987). Resulting from the hydration and pozzolanic reactions, the rapid formation of cementing bonds at points of contacts between the particles and aggregates helps maintain this open structure over time. Choquette et al. (1987) suggest that a similar phenomenon occurs in lime treated clays. The addition of quick lime to clay gives rise to instantaneous agglomeration of clay particles. They showed that the soil keeps the instantly formed flocculated structure throughout the maturation process. Careful investigation of Fig. 3-4b shows cementitious bridges, marked by dashed circles, connecting the platy clay particles to each other.

Furthermore, it can be seen in Fig. 3-4 that the process of cementation has been accompanied by the formation of small needle-like precipitated crystals between the particles. These crystals, which are scattered throughout the surface individually or in the form of clusters, have a high aspect ratio with a maximum length and diameter of 4 and 0.3  $\mu\text{m}$ , respectively. EDX analysis showed that in comparison to the soil particles, these crystals contain substantial amounts of calcium, sulphide, and aluminum ions. Thus these crystals are most likely to be calcium sulfoaluminate or Ettringite. Ettringite forms as a reaction product of the lime produced during the cement hydration and aluminium provided by clay or other minerals (e.g. aluminosilicate feldspar). The release of calcium into the soil increases the pH of the medium, so silica and alumina dissolve from clay surfaces into the pore water and combine with the calcium and sulphate added to the soil to produce the Ettringite (Mitchell, 1986; Wang, 2002; Bhattacharja et al., 2003; Wang et al., 2005). The crystallization of Ettringite begins in the early stages of curing as soon as water is added to the cement-clay powder and the calcium hydroxide required for its formation starts to be produced. Wang et al. (2005) showed that the length and diameter of Ettringite crystals increase gradually with the curing time. They also suggested that the larger crystals form in a low pH environment. The formation of Ettringite crystals is often accompanied by considerable volumetric expansion, which could impose substantial damage to the surrounding soil structures. However, in the case of soft clays, the production of Ettringite is less problematic because of the relatively high void ratio of the soil. The primary problem regarding sulphate attack in cement treated soft clays is that it hinders the production of CSH and CAH, by consuming the two main ingredients needed for the progression of pozzolanic reactions, namely silica/alumina and calcium ions, and

also by depleting the material of lime, hence dropping the pH and making silica and alumina insoluble.

Fig. 3-5 shows SEM images at different magnifications of undisturbed Ottawa clay, which is a medium plasticity moderately sensitive clay (St~20) with a liquidity index of almost 2 in its natural state. It can be seen that tightly packed arrangements of clay particles have formed aggregates that exist in an open and flocculated structure with respect to each other. Several explanations, such as natural cementation, weathering, thixotropic hardening, and leaching/ion exchange, have been proposed for the sensitivity of North American and Scandinavian post-glacial clays (Mitchell and Soga, 2005). A number of researchers have attributed the card-house arrangement of the particles in post-glacial clays, partly to the existence of platy silt-sized crystals mainly composed of quartz (Gillott, 1979; Smalley et al., 1973; Krinsley and Smalley, 1973). Compared to spherical particles, these flat particles tend to form a more open structure, increasing the soil potential for sudden collapse (Krinsley and Smalley, 1973). Such platy particles, which have different orientations and are not bigger than 10  $\mu\text{m}$  in length, can be recognized in Fig. 3-5b and c. As can be seen in the figures, these particles help form a metastable fabric in the soil by acting as bridges between clay aggregates. Delage and Lefebvre (1984) also observed silt-size platy minerals, which interacted with clay platelets and helped form bridge crossings between the aggregates, in a sensitive Champlain clay. Quigley et al. (1981) suggested that the pyrite mineral that has been produced in the soil probably by anaerobic bacterial processes (such as sulphate reduction by sulphate reducing bacteria) cements these silt grains at their points of contacts. Fig. 3-5d shows a calcite/dolomite concentration (the circled aggregate), which can be

identified from its rugged surface. EDX analysis indicated a calcium/magnesium carbonate nature of this particle. In addition, the EDX area scan confirmed the results of previous chemical examinations, performed by the authors, indicating the presence of almost 4% calcite and 2% dolomite in this Ottawa clay specimen. Calcium carbonate has also been mentioned frequently by previous researchers as the possible cause of cementation in Leda clays (Townsend, 1965; Loiselle et al., 1971; Sangrey, 1972; Boone and Lutenegeger, 1997).

If destructured, Ottawa clay will exhibit a fairly dispersed fabric (Fig. 3-6). A clear lack of structure is observed in the reconstituted soil. However, since the reconstituted specimen has been freeze-dried shortly after being mixed at a high moisture content, a large amount of pores exists in the soil despite its dispersed structure. The presence of small particles of platy morphology and their importance in the formation of the fabric can be recognized in Fig. 3-6, as well. However, unlike the undisturbed clay, for the reconstituted specimen, the platy silt particles lie parallel to each other, rather than at different orientations.

Micrographs of treated Ottawa clay with 3.1 and 6.4% cement contents are presented in Fig. 3-7 and Fig. 3-8 at different magnifications. Comparing the reconstituted specimen (Fig. 3-6) with those treated with Portland cement, it can be seen that cementation has resulted in an agglomerated, open structure in the clay and has produced Ettringite needles that are scattered throughout the cemented samples in an uneven fashion. As expected, the higher the cement content, the higher the produced volume of Ettringite in the soil. Moreover, in cemented Ottawa clay we can see needle-shaped crystals as long as 12  $\mu\text{m}$ , which is much longer than the maximum values

detected in cemented Nanticoke clay. However, the Ettringite crystals produced in the two clays seem to have similar diameters. Since most of the components needed for Ettringite formation are supplied by the soil, the mineralogy will affect the size and total volume of the Ettringite produced during artificial cementation.

We can see in Fig. 3-7a and b that silt-sized particles of quartz or feldspar origin (according to the results of EDX analysis) have been coated with very small crystals that are probably the products of artificial cementation. In the sample with 3.1% cement, the clay particles have formed aggregates that are connected to each other by cementitious bonds. Comparing Fig. 3-6 with Fig. 3-7, it can be seen that the new cementitious crystals that have been produced in the cemented sample have a “popcorn-like” morphology (Fig. 3-7b, c, and d). Fig. 3-8 better illustrates the two-phase structure of the artificially cemented clay, i.e. one phase consists of clay aggregates formed when particles were bonded to each other firstly by charge forces and then by the cementitious material, and the second phase is the very porous matrix of cementitious matter filling the gaps between the aggregates and locking them in place. The formation of a reticular texture is evident in this figure. The highly flocculated structure of the clay treated with 6.4% cement is due to the availability of more  $\text{Ca}^{2+}$  cations and the higher pH of the pore fluid. Unlike the Nanticoke clay, the produced cementitious material in the Ottawa clay seems to be gelatinous and poorly crystalline and has coated the clay aggregates. The different morphologies of the cemented soil and precipitated products of Nanticoke and Ottawa clays confirm the importance of soil mineralogy in the resulting artificial cementation.

To investigate the effect of cementation by gypsum on clay structure, samples of EPK kaolin cemented by either Portland cement alone or by a combination of Portland

cement and gypsum were analyzed using the scanning electron microscopy (Fig. 3-9 and Fig. 3-10). The same patterns as those observed in cemented Nanticoke and Ottawa clays exist in the cemented kaolin clay; however, the degree of flocculation and the amount and size of needle-like crystals is less in the case of kaolin (Fig. 3-9), than for the other two clays. Having a higher magnification level than other figures, Fig. 3-9c reveals the presence of cementitious bridges (marked by circles) between clay aggregates and also the existence of particles with fibrous textures in the material. Using both cement and gypsum as cementing agents has resulted in a more compact fabric of the particles, with some very small openings and cracks in the material (Fig. 3-10). This could be due to the volume expansion that follows the hydration of calcined gypsum. The gypsum swelling, which is attributed to the growth of the crystal lattice, fills the larger pores and creates the observed packed structure. Fig. 3-10b, c, and d show a minute hole containing many needle-like crystals, a tiny crack with smooth surfaces on both sides, and an isolated crystal of gypsum, respectively. As can be seen in these images, compared to the kaolin sample with only Portland cement, the gypsum specimen has a lesser amount of Ettringite crystals. Moreover, the same fibrous textures are observed in the gypsum treated material (Fig. 3-10e and f). From these images, we can infer that the addition of gypsum has reduced the homogeneity of the cemented material, resulting in a potential increase in permeability of the soil.

#### **3.4.2 Pore size distribution: the effect of artificial cementation by Portland cement and gypsum**

Mercury intrusion porosimetry was conducted on the same cement treated and reconstituted clay specimens to study the effect of artificial cementation on the pore size

distribution of the clay. Most of the experiments were performed on freeze-dried samples; however, a few tests were also conducted on air-dried specimens to investigate the shrinkage properties of the cemented clays. Washburn's equation (Washburn, 1921), which is derived for capillary flow of a liquid in a cylindrical tube, was employed to calculate pore diameter based on the applied mercury pressure:

$$r = \frac{-2\gamma \cos \theta}{P} \quad (3.1)$$

Where  $r$  is the pore radius,  $P$  is the applied mercury pressure,  $\gamma$  is the surface tension of mercury, and  $\theta$  is the solid-liquid contact angle. Based on the recommendation by Diamond (1970) for kaolinite and illite, a mercury contact angle of  $147^\circ$  and also a surface tension of 485 dynes/cm were used in the calculations. If the calculated pore diameters are successively numbered, cumulative and log-differential pore volumes can be obtained for each calculated diameter,  $D_i$ , as follows:

$$V_{cumulative} = \sum_i \Delta V_i \quad (3.2)$$

$$V_{\log-differential} = \frac{-\Delta V_i}{\Delta \log D_i} \quad (3.3)$$

Where  $V_i$  is the measured total intruded pore volume corresponding to the diameter,  $D_i$ . Logarithmic differential distribution, which provides a qualitative measurement of the distribution of the pores, is used instead of the incremental distribution to eliminate the experimental point spacing effect that usually makes the latter curve uneven.

Fig. 3-11 shows pore size distributions of cemented samples of Nanticoke clay with a moisture content of 98% (LI=3) and with cement contents ranging from 0 to 19%.



The distribution is shown for a diameter range of 3 nm to 0.1 mm. Since all cumulative curves (Fig. 3-11a) become flat at diameters less than 10 nm, we can assume that regardless of the moisture content of the specimens, almost all of the pores in the specimens have a diameter larger than 3 nm. Thus, the cumulative volume reading at a diameter of 3 nm represents the total pore volume of the sample. All cemented specimens were cured for 28 days before being freeze-dried. However, despite being left for 28 days to cure under water, all specimens treated with Portland cement had a final moisture content similar to their initial one, because the flocculation happening shortly after the addition of cement prevented self-weight driven settlement of the particles. This is confirmed by the observation that all cumulative curves in Fig. 3-11a converge at very small pore diameters, indicating that the total pore volume of all cemented specimens is the same (about 0.85 ml/g).

As can be seen in Fig. 3-11b, a local minimum exists in all of the distribution curves at an approximate diameter of 7 microns (7000nm). This is an artefact due to the point of switchover from the low to the high pressure stages (Giesche, 2006) and should be neglected in the analysis. Hence, without this minimum, the actual pore size distributions (in log-differential graphs) will become either bimodal or unimodal.

Although the total pore volumes of all of the samples are equal (Fig. 3-11a), the distribution of the pores is highly variable depending on the cement content of the specimen (Fig. 3-11b). Two distinct patterns can be recognized; samples with 0.5, 1, and 2% cement contents have a pore size distribution very similar to that of the reconstituted specimen ( $c=0\%$ ), i.e. a bimodal pattern with a first peak between 70,000 and 400 nm and a second peak between 300 and 10 nm. We can associate the first peak with the free

water existing between soil aggregates (inter-aggregate pores) and the second one with the water that is trapped within the aggregates and on the surface of clay particles (intra-aggregate pores). Hence, a dispersed structure in which clay aggregates are separate from one another exists in these specimens. On the other hand, samples with cement contents higher than 2% display a unimodal pore size distribution with only one peak in the range of 3000 to 10 nm, indicating the existence of a flocculated structure in the specimens. It can also be seen that an increase in cement content substantially reduces the amount of large pores (with a diameter higher than 4000 nm), because the products of cement hydration fill the gaps between soil aggregates and divide each large pore into a number of smaller ones. Again, this reduction in inter-aggregate pore volume is significant when cement content is increased from 2% to 4%. Hence, we can conclude that at cement contents higher than 2%, a fundamental structural change from dispersed to flocculated takes place in the specimens. The specimen with 2% cement content seems to be in transition from a dispersed to a flocculated structure. In addition, the results show that in samples with a unimodal pore size distribution ( $c > 2\%$ ), a further increase in cement content widens the peak and slightly shifts it towards larger diameters (i.e. the right side of the figure). For example, the peak for specimens with 4.2 and 8.7% cement contents is at 250 nm, while the one corresponding to samples with 13.6 and 19% cement contents is at 380 nm. This implies that the degree of flocculation keeps increasing with a further increase in cement content.

Fig. 3-12 and Fig. 3-13 show the pore size distribution of samples of Ottawa clay and EPK kaolin, respectively. As these figures show, the arguments made for reconstituted and cemented Naticoke clay are also true for the other two clays. However,

comparing the behaviour of the three soils, the important effect of clay mineralogy on pore size distribution is noticeable. Ottawa clay, for example, at a relatively low cement content of 6.4% displays a very high degree of flocculation, which is identified by its very wide unimodal pore size distribution that extends into pore sizes with very low diameters (Fig. 3-12b) and has a peak at 197 nm. The reticular texture observed before, for the cemented Ottawa clay in Fig. 3-8, supports the wide range of pore sizes and small dominant pore diameters. EPK kaolin treated with 6.4% cement, on the other hand, displays a lower degree of flocculation and partly retains its bimodal structure.

The intact Ottawa clay specimen shown in Fig. 3-12 also exhibits a flocculated structure, explaining the soil sensitivity and its high *in-situ* moisture content. However, having semi-bimodal pore size distributions (i.e. a local peak at an approximate diameter of 100 nm followed by the main peak at a greater diameter), both undisturbed and 3.1% cement treated Ottawa clay specimens seem to have been in transition from a dispersed to a flocculated structure. This may explain why the dominant peak for cemented Ottawa clay moves significantly towards smaller diameters as the cement content increases from 3.1 to 6.4%. Reconstituted Ottawa clay, in contrast, has a discernible bimodal pore size distribution with a first dominant peak between 100,000 and 800 nm and a second one between 700 and 10 nm.

In addition, as shown in Fig. 3-13b for EPK kaolin, the peaks for specimens with 6.4% cement content become less intense and wider as the moisture content increases, indicating that a more porous, card-house structure is formed in cemented samples with a higher liquidity index. Nevertheless, at a constant cement content, an increase in moisture content does not seem to make a drastic change in the dominant pore diameter. For

instance, in EPK specimens with 6.4% cement content, the peak moves slightly from 80 nm to 120 nm as the moisture content increases from 61 to 86%.

For all of the three clays, we can see that with the addition of cement the total pore volume remains constant, while the inter-aggregate pores seem to disappear. This finding is contrary to the suggestion of Kamruzzaman et al. (2009) that at a certain initial moisture content, both inter-aggregate and total pore volumes significantly increase with a rise in cement content. The main reason for this fundamental disagreement is explained later in the paper. Based on the results, we can conclude that artificial cementation only increases the volume of the micropores by sacrificing that of the macropores. This is in accord with Choquette et al. (1987), who also reported the disappearance of the inter-aggregate large pores and the replacement of the bimodal pore distribution of reconstituted samples by a unimodal flocculated distribution in 4% lime treated clay. They also reported that cementation of clay by lime does not change the total pore volume of the soil. They attributed the reduction in macropores to the production of cementitious material in inter-aggregate pores, partitioning each larger pore into a number of smaller ones. Hence, a common factor seems to govern the pore size distribution of clays treated with both lime and Portland cement. This factor is probably the presence of  $\text{Ca}^{2+}$  cations in both cases. The flocculated distribution, which is formed immediately after the addition of lime or cement, stays as the cementing bonds form and solidify the material.

If left to dry at the room temperature, a soft clay specimen will shrink until it reaches the shrinkage limit, after which the clay will dry without further volume changes. Substantial particle rearrangements within the clayey material during the air-drying

process will change the pore size distributions and total pore volume of a soft clay specimen (Gillott 1970). Comparison of pore size distributions and total pore volumes of two originally identical specimens, one air-dried and one freeze-dried, can therefore provide us with useful information about microstructural changes in soil, and in cemented clay in particular, due to atmospheric drying. Results of the MIP analysis on both air-dried and freeze-dried specimens of Nanticoke clay are presented in Fig. 3-14. Except for the air-dried undisturbed Nanticoke clay, which had an *in-situ* moisture content of 28% (LI=0.2), all of the Nanticoke samples plotted in Fig. 3-14 were cement treated and had an initial moisture content of 98% (LI=3). Having similar moisture contents, all freeze-dried Nanticoke samples have the same total pore volume. In comparison, the total pore volume of the air-dried specimens changes depending on their cement content. The air-dried undisturbed Nanticoke sample and the ones with 0.5 and 1% cement all have a similar pore size distribution with the majority of the pores having a diameter less than 160 nm. The total pore volume remaining in these samples (residual pore volume) will be related to the shrinkage limit of the material. Conversely, Nanticoke samples with 2.0, 4.2, and 8.7% cement contents still have large pores left and also have a residual total pore volume greater than that of untreated and lightly cemented specimens, perhaps due to the presence of cementitious bonds that resist excessive shrinkage and particle rearrangement. The higher the cement content, the lower the shrinkage due to air-drying. Specimens with 8.7, 4.2 and 2.0% cement contents have lost 26, 31, and 52% of their total pore volume due to bulk shrinkage, respectively. Both samples with cement contents less than 2% have lost 75% of their total pore volume. Therefore, according to the results presented in Fig. 3-14, an effective cementation (one assumed to yield a considerable

strength gain in the soil) is not produced in Nanticoke specimens with less than 2% cement content. Moreover, the fact that even the sample with 8.7% cement content has gone through 26% bulk shrinkage, suggests that some structural damage may be caused by drying of artificially cemented clays. This structural damage could have negative effects such as a loss of strength in cemented materials in an arid environment. The resemblance between the results presented here for air-dried cemented Nanticoke clay and those of Kamruzzaman et al. (2009) obtained for cemented Singapore Marine clay suggests that the critical-point-drying method employed by Kamruzzaman et al. (2009) may not have been successful and has resulted in substantial shrinkage and fabric change in the material. In addition, Fig. 3-14 shows that the residual pore volume of air-dried undisturbed Nanticoke clay is similar to that of remoulded clay at low cement contents. Hence, being highly overconsolidated, undisturbed Nanticoke clay should have had limited structure due to bonding between the particles.

The effects of the addition of a second binder, gypsum, on the pore size distribution of soil-cement mixtures were studied by comparing MIP results for uncemented, cement treated, and cement/gypsum treated samples of EPK kaolin (Fig. 3-15). As the figure shows, addition of 25% gypsum almost completely eliminates all of the pores with a diameter higher than 4000 nm (4 microns). This is because the hydration of calcined gypsum is accompanied by a significant volumetric expansion and because the hydrated gypsum crystals fill the gaps between soil aggregates (inter-aggregate pores). Although it eliminates all of the large pores, gypsum treatment shifts the position of the dominant pore size towards larger diameters and makes the peaks wider. At 61% moisture content, the peak moves from 80 nm to 220 nm, and at 86% moisture content, it

shifts from 120 nm to 520 nm. This more flocculated structure of gypsum treated clays can be attributed to the presence of high amounts of  $\text{Ca}^{2+}$  cations in the soil. The crystal growth of gypsum, which is accompanied by swelling, could also produce larger pores within the material. We can also see that at similar cement and gypsum contents, the specimens with higher moisture content have a slightly less intense, wider peak, indicating higher degree of flocculation.

### **3.4.3 The effects of the developed microstructure on the mechanical behaviour of artificially cemented clays**

To further evaluate the micro-structural results for the cemented slurried clays, hydraulic conductivity and undrained shear strength were measured for the clays and cement contents described previously. Permeabilities, obtained by performing oedometer tests on undisturbed, reconstituted, and cemented samples of Nanticoke and Ottawa clays, are plotted in Fig. 3-16. For Nanticoke clay (Fig. 3-16a), the permeability of the specimen with 2% cement is close to that of the uncemented samples. This is in agreement with the observed resemblance between the pore size distributions of reconstituted Nanticoke and the 2% cement treated specimen (Fig. 3-11) and indicates that the dispersed structure observed in both samples governs their permeability behaviour. In contrast, as cement content increases to 4.2 and 8.7%, there is a considerable reduction in the permeability of the cemented Nanticoke clay. As observed in Fig. 3-11, artificial cementation of more than 2% creates a flocculated unimodal pore structure in Nanticoke clay and appreciably reduces the amount of inter-connected pores (with a diameter higher than 4000 nm) that exist between the soil aggregates. The cementitious material produced by cement hydration most likely blocks some of these water-channels, hence reducing the

permeability of the clay. A similar pattern exists in Fig. 3-16b for the Ottawa clay specimens. The results are in agreement with the suggestion by Garcia-Bengochea et al. (1979) that permeability is predominantly related to magnitude and frequency of macropores rather than micropores. These observations are also in accord with those of Locat et al. (1996), who reported an order of magnitude reduction in the permeability of a clay specimen treated with 10% lime.

It was shown earlier in the paper that unlike cement content, moisture content does not significantly affect the pore size distribution pattern of cemented EPK kaolin. Similarly, as Fig. 3-16 shows, the cement content has a more important effect than the moisture content on the permeability of Ottawa clay. Despite having different total pore volumes, the two specimens with a similar 6.4% cement content, but with different moisture contents, have almost the same permeability. Hence, the flocculated structure produced in these samples due to cementation should play a vital role in their pore size distribution and permeability behaviour. Furthermore, the important effect of mineralogy and activity on the behaviour of cement treated clay is again illustrated in Fig. 3-16; the addition of cement reduces permeability in Ottawa clay more than it does for Nanticoke clay. On average, the permeability of reconstituted Ottawa clay is 65 times that of the same clay treated with 6.4% cement. However, this ratio reduces to 30 when reconstituted Nanticoke is compared to 8.7% cement treated sample of Nanticoke clay.

The laboratory shear vane was employed to measure the undrained shear strength and sensitivity of the cement treated clays (Fig. 3-17). Focusing on the behaviour of the Nanticoke specimens, we can find correspondance between MIP and shear vane test results. Fig. 3-11 showed that at 98% moisture content, Nanticoke samples with less than



2% cement have a bimodal pore size distribution, similar to that of reconstituted material. Moreover, Fig. 3-14 suggests that almost no effective bonding is developed in samples with 1% cement content, since when they are air dried, they have shrunk to the same total pore volume as that of the reconstituted material. These findings are in agreement with the observation in Fig. 3-17 that the Naticoke specimens with 1% cement content have not gained any measurable strength. In addition, as illustrated before by SEM and MIP results, samples with higher cement contents have a more flocculated structure and a larger dominant pore diameter, explaining their brittle behaviour and higher sensitivity.

Fig. 3-17 also shows the important connection between the clay mineralogy and activity, and the effectiveness of artificial cementation. At a certain cement content and after 28 days of curing, Ottawa clay samples gain much higher strength,  $c_{u, 28 \text{ days}}$ , and sensitivity,  $s_{t, 28 \text{ days}}$ , than do samples of Naticoke clay or EPK kaolin. This is in agreement with the highly flocculated structure observed by the SEM and MIP analysis in cemented Ottawa clay. Compared to those of Naticoke clay or EPK kaolin, Ottawa clay particles appear to have more chemical interactions with the added cement. Some researchers have mentioned the presence of amorphous iron, silica, and alumina oxides as a reason for the high sensitivity of Champlain/Leda clays (Bentley and Smalley, 1978; Yong et al., 1979; Quigley, 1980; Locat et al., 1984; Locat et al., 1985). The presence of such minerals could explain the higher strength of the cemented Ottawa clay. Besides silica and alumina dissolved from clay surfaces, the amorphous sesquioxides previously present in Ottawa clay react more readily with the produced lime and create more secondary cementitious bonds within the material (Wissa et al., 1965). Townsend (1985) also suggested that the presence of amorphous silica produces higher pozzolanic strengths

in cemented clays. Choquette et al. (1987) postulated that a more significant change in volume distribution due to cementation is also accompanied by a higher strength gain of lime treated clays. We can see that for Ottawa clay, a unimodal pore distribution has formed with a much wider peak than that of the other two clays. In addition, SEM results showed that more significant structural changes occur to cemented Ottawa clay, when compared to cemented Nanticoke or EPK material. The higher strength gain of cemented Ottawa clay, therefore, can be attributed to the more significant structural modifications that occur for this soil after the addition of cement.

Pore size analysis of the cemented clays showed that after a certain cement content (for example 2% for Nanticoke clay), when a flocculated structure is formed in the material, further addition of cement does not significantly change the pore size distribution pattern (Fig. 3-11 and Fig. 3-13). However, the permeability and strength continue to change with more cement being added to the soil. Although it does not change the pore size distribution pattern, the addition of more cement partitions and eliminates the remaining macropores by forming cementitious bridges, further reducing the permeability of the material. Moreover, further addition of cement to the flocculated soil creates more and stronger cementitious bonds in inter-particle contacts, as well as inter-aggregate pore spaces, increasing the strength of the crystal lattice formed within the material. On the other hand, more cementation appears not to change the size of the micropores significantly. These intra-aggregate pore sizes should depend on particle size distribution, activity, and clay mineralogy rather than cementation.

### 3.5 Summary and Conclusions

Using mercury intrusion porosimetry and scanning electron microscopy, the effects of artificial cementation, by Portland cement or gypsum, on the fabric of Kaolin and two other Canadian clays with high moisture contents were studied. Results of oedometer and laboratory shear vane tests were also utilised to examine changes in the permeability, undrained shear strength and sensitivity of the material, and to find connections between the developed microstructure and the mechanical behaviour. The study produced the following main conclusions:

- From comparison of the SEM and MIP analyses for the clays, a bimodal distribution of the pore sizes was linked with dispersed soil fabrics. Conversely, a unimodal distribution was assumed to be an indication of a flocculated structure, in which a card house fabric exists and aggregates are connected to each other via cementitious bonding.
- Little identifiable structure was observed in micrographs of highly overconsolidated undisturbed Nanticoke clay. However, an openly structured fabric was identified in undisturbed sensitive Ottawa clay. The existence in undisturbed Ottawa clay of calcium carbonate, along with rotund quartz and feldspar particles, was recognised as a probable cause of the observed structure.
- SEM images of the reconstituted clay displayed an unstructured, dispersed fabric, while micrographs of cement treated clays indicated the presence of a reticulated matrix within the material. As the cement content increased, the structure of the remoulded materials gradually transformed from dispersed into flocculated states. It was also observed that the produced cementitious products were affixed to the

particles, coated particle surfaces, and formed matrices that filled the gaps between the clay aggregates.

- Links were observed between the structural changes due to artificial cementation and the mechanical properties such as permeability, shear strength, and sensitivity. Specimens undergoing higher structural alterations also experienced more significant changes in their mechanical behaviour.
- Although there is no change in the total pore volume of the clay, increasing the cement content results in a significant reduction in the volume of the macro-pores, as the cementation products fills the gaps between soil aggregates. This is also accompanied by a reduction in the permeability of the material.
- MIP results also showed that although an increase in the moisture content increases the total pore volume, it does not significantly change the pore size distribution of the cemented soil. The permeability analysis confirmed that cement content rather than moisture content controls the pore size distribution and permeability of cement treated clays.
- MIP and SEM results indicated that soil mineralogy and activity greatly affect the pore size distribution of cement treated clays. For the three clays used in this study, artificially cemented Ottawa clay and EPK kaolin attained the highest and lowest degree of flocculation, respectively. Moreover, cemented samples of Ottawa clay, which displayed a highly flocculated structure and a reticular texture in MIP and SEM analysis, gained higher strength and sensitivity and underwent more permeability reduction than the other two clays.

- The existence of needle-like Ettringite crystals in the artificially cemented specimens indicates that the clays experience some degree of sulphate attack. Inspection of the micrographs of the cement-treated clays showed that the size and amount of the produced Ettringite depend on the mineralogy and activity of the host clay.
- The addition of gypsum to cemented clay eliminated all of the macro-pores with a diameter greater than 4 microns, but increased the dominant pore diameter of the composite material. Both these effects are explained by gypsum crystal growth, which is accompanied by volumetric expansion.

### **3.6 Acknowledgments**

The authors would like to express their gratitude to the Natural Sciences and Engineering Research Council of Canada, NSERC, and The University of Western Ontario for providing financial support for this work.

### **3.7 References**

- Amaratunga, L.M. (1995). "Cold-bond agglomeration of reactive pyrrhotite tailings for backfill using low cost binders: Gypsum  $\beta$ -hemihydrate and cement." *Minerals Engineering*, 8(12), 1455–1465.
- Bentley, S.P., and Smalley, I.J. (1978). "Inter-particle cementation in Canadian post-glacial clays and the problem of high sensitivity ( $St > 50$ ).” *Sedimentology*, 25, 297–302.

- Bergado, D.T., Anderson, L.R., Miura, N., and Balasubramaniam, A.S. (1996). "Soft ground improvement in lowland and other environments." American Society of Civil Engineers (ASCE) Press, New York, U.S.A.
- Bhattacharja, S., Bhattya, J. I., and Todres, H. A. (2003). "Stabilization of clay soils by Portland cement or lime - A critical review of literature." PCA R&D Serial No. 2066, Portland Cement Association, Skokie, Illinois USA.
- Boone, S.J., and Lutenegeger, A.J. (1997). "Carbonates and cementation of glacially derived cohesive soils in New York State and southern Ontario." *Canadian Geotechnical Journal*, 34, 534–550.
- Chew, S.H., Kamruzzaman, A.H.M., and Lee, F.H. (2004). "Physicochemical and Engineering Behavior of Cement Treated Clays." *Journal of Geotechnical and Geoenvironmental Engineering*, 130(7), 696–706.
- Choquette, M., Marc-André Bérubé, and Locat, J. (1987). "Mineralogical and microtextural changes associated with lime stabilization of marine clays from eastern Canada." *Applied Clay Science*, 2(3), 215–232.
- Croft, J.B. (1967a). "The influence of soil mineralogical composition on cement stabilization." *Geotechnique*, 17, 119–135.
- Croft, J.B. (1967b). "The structures of soils stabilized with cementitious agents." *Engineering Geology*, 2(2), 63–80.
- Delage P., and Lefebvre, G. (1984). "Study of the structure of a sensitive Champlain clay and of its evolution during consolidation." *Canadian Geotechnical Journal*, 21, 21–35.

- Delage, P., Audiguier, M., Cui, Y.-J., and Howat, M.D. (1996). "Microstructure of a compacted silt." *Canadian Geotechnical Journal*, 33(1), 150–158.
- Diamond, S. (1970). "Pore size distribution in clays." *Clays and Clay Minerals*, 18, 7–23.
- Fischer, K.P., Anderson, K.H., and Moum, J. (1978). "Properties of an artificially cemented clay." *Canadian Geotechnical Journal*, 15, 322–331.
- Garcia-Bengochea, I., Lovell, C.W., and Altschaeffl, A.G., (1979). "Pore distribution and permeability of silty clays." *Journal of the Geotechnical Engineering Division (ASCE)*, 105(7), 839–856.
- Gartner, E.M., Tang, F.J., and Weiss, S.J. (1985). "Saturation factors for calcium hydroxide and calcium sulfates in fresh Portland cement pastes." *Journal of the American Ceramic Society*, 68 (12), 667–673.
- Giesche, H. (2006). "Mercury porosimetry: A general (practical) overview." *Particle & Particle Systems Characterization*, 23, 9–19.
- Gillott, J.E. (1970). "Fabric of Leda clay investigated by optical, electron-optical, and X-ray diffraction methods." *Engineering Geology*, 4(2), 133–153.
- Gillott, J.E. (1979). "Fabric, composition and properties of sensitive soils from Canada, Alaska and Norway." *Engineering Geology*, 14(2-3), 149–172.
- Graham, J., Man, A., Alfaro, M., Blatz, J.A., and Van Gulck, J. (2005). "Gypsum cementation and yielding in plastic clay." *Proceedings of the 16th International Conference on Soil Mechanics and Geotechnical Engineering*, Osaka, Japan, 507–512.

- Head, K.H. (1982). "Manual of laboratory testing; Volume 2: permeability, shear strength, and compressibility tests." ELE. International Ltd., Pentech Press, London.
- Herrin, M., and Mitchell, H. (1961). "Lime-soil mixtures". Highway research board, bulletin 304, Washington, D.C., 99-138.
- Herzog, A., and Mitchell, J.K. (1963). "Reactions accompanying the stabilization of clay with cement." *Highway Research Board Record*, 36, 146–171.
- Horpibulsuk, S., Rachan, R., Chinkulkijniwat, A., Raksachon, Y., and Suddeepong, A. (2010). "Analysis of strength development in cement-stabilized silty clay from microstructural considerations." *Journal of Construction and Building Materials*, 24, 2011–2021.
- Huang, J.T. and Airey, D.W. (1998) "Properties of artificially cemented carbonate sand". *Journal of Geotechnical and Geoenvironmental Engineering*, 124(6), 492–499.
- Ismail, M.A., Joer, H.A., Randolph, M.F., and Meritt, A. (2002a). "Cementation of porous materials using calcite." *Geotechnique*, 52(5), 313–324.
- Ismail, M.A., Joer, H.A., Sim, W.H., and Randolph, M.F. (2002b). "Effect of cement type on shear behavior of cemented calcareous soil." *Journal of Geotechnical and Geoenvironmental Engineering*, 128(6), 520–529.
- Kamruzzaman, A.H.M., Chew, S.H., and Lee, F.H. (2009). "Structuration and destructuration behavior of cement-treated Singapore Marine Clay." *Journal of Geotechnical and Geoenvironmental Engineering*, 135(4), 573–589.



- Koliji, A., Vulliet, L., and Laloui, L. (2010). "Structural characterization of unsaturated aggregated soil." *Canadian Geotechnical Journal*, 47(3), 297–311.
- Krinsley, D.H., and Smalley, I.J. (1973). "Shape and nature of small sedimentary quartz particles." *Science*, 180, 1277–1279.
- Lapierre, C., Leroueil, S., and Locat, J., (1990). "Mercury intrusion and permeability of Louisville clay." *Canadian Geotechnical Journal*, 27, 761–773.
- Lo, S.R., and Wardani, S.P.R. (2002). "Strength and dilatancy of a silt stabilized by a cement and fly ash mixture." *Canadian Geotechnical Journal*, 39(1), 77–89.
- Locat, J., Lefebvre, G., and Ballivy, G. (1984). "Mineralogy, chemistry, and physical properties interrelationships of some sensitive clays from Eastern Canada." *Canadian Geotechnical Journal*, 21, 530–540.
- Locat, J., Berube, M.-A., Chagnon, J.-Y., and Gelinias, P. (1985). "The mineralogy of sensitive clays in relation to some engineering geology problems — An overview." *Applied Clay Science*, 1(1-2), 193–205.
- Locat, J., Tremblay, H., and Leroueil, S. (1996). "Mechanical and hydraulic behaviour of a soft inorganic clay treated with lime." *Canadian Geotechnical Journal*, 33(4), 654–669.
- Loiselle, A., Massiera, M., and Sainani, U.R. (1971). "A study of the cementation bonds of the sensitive clays of the Outardes river region." *Canadian Geotechnical Journal*, 8, 479–498.
- MacKay, M. and Emery, J. (1992). "Stabilization/solidification of contaminated soils and sludges using cementitious systems". *Proceedings of the First International*

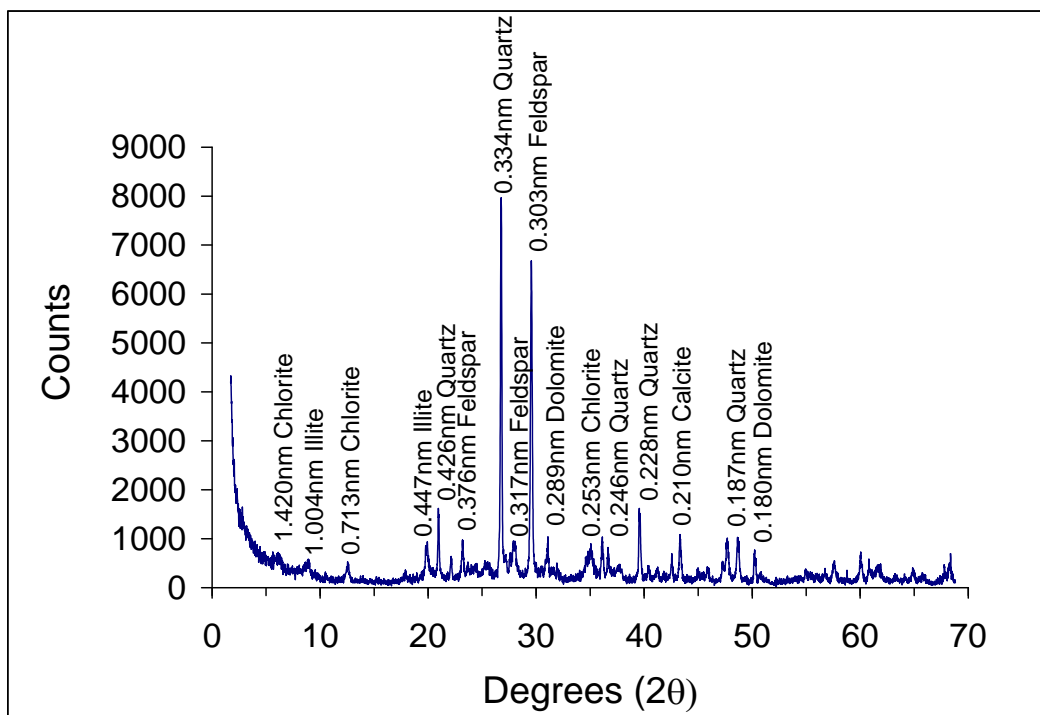
- Symposium, Cement Industry Solutions to Waste Management, Canadian Portland Cement Association, Toronto, Ontario, Canada, 135–151.*
- Mitchell J. K. (1986). “Practical problems from surprising soil behaviour.” *Journal of Geotechnical Engineering (ASCE)*, 112(3), 259–289.
- Mitchell, J.K., and Soga, K. (2005). “Fundamentals of soil behavior, 3rd Ed.” John Wiley & Sons, Hoboken, New Jersey.
- Ninjarav, E., Chung, S.-G., Jang, W.-Y., and Ryu, C.-K. (2007). “Pore size distribution of pusan clay measured by mercury intrusion porosimetry.” *Journal of Civil Engineering (KSCE)*, 11(3), 133–139.
- Noble, D.F., and Plaster, R.W. (1970). “Reactions in Portland cement – clay mixtures.” Final report, Virginia Highway Research Council, Charlottesville.
- Osula, D.O.A. (1996). “A comparative evaluation of cement and lime modification of laterite.” *Engineering Geology*, 42, 71–81.
- Quigley, R.M. (1980). “Geology, mineralogy, and geochemistry of Canadian soft soils: a geotechnical perspective.” *Canadian Geotechnical Journal*, 17(2), 261–285.
- Quigley, R.M., Haynes, J.E., Bohdanowicz, A., and Gwyn, Q.H.J. (1981). “Geology, geotechnique, mineralogy and geochemistry, Leda clay from deep boreholes, Hawkesbury, Ontario.” Ontario Geological Survey, Toronto, Ont. Open File Report 5357.
- Romero, E. and Simms, P.H. (2008). “Microstructure investigation in unsaturated soils: A review with special attention to contribution of mercury intrusion porosimetry and

- environmental scanning electron microscopy.” *Geotechnical and Geological Engineering*, 26, 705–727.
- Rowe, T.W. (1960). “The theory and practice of freeze-drying.” *Annals of the New York Academy of Science*, 85, 641–679.
- Sangrey, D.A. (1972). “Naturally cemented sensitive soils.” *Geotechnique*, 22(1), 139–152.
- Sereda, J., Feldman, R. F., and Ramachandran, V. S. (1965). “Hydration of gypsum plaster by the compact technique.” *The American Ceramic Society Bulletin*, 44(2), 151–155.
- Smalley, I. J., Cabrera, J.G., and Hammond, G. (1973). “Particle nature in sensitive soils and its relation to soil structure and geotechnical properties.” *Proceedings of the International Symposium on Soil Structure*, Gothenburg, Sweden, 184–193.
- Townsend, D.L. (1965). Discussion on “Geotechnical properties of three Ontario clays” by L.G. Soderman and R.M. Quigley, *Canadian Geotechnical Journal*, 2, 190–193.
- Townsend, F.C. (1985) “Geotechnical characteristics of residual soils.” *Journal of Geotechnical Engineering, ACSE*, 111(1), 77–94.
- Tremblay, H., Leroueil, S., and Locat, J. (2001). “Mechanical improvement and vertical yield stress prediction of clayey soils from eastern Canada treated with lime or cement.” *Canadian Geotechnical Journal*. 38, 567–579.

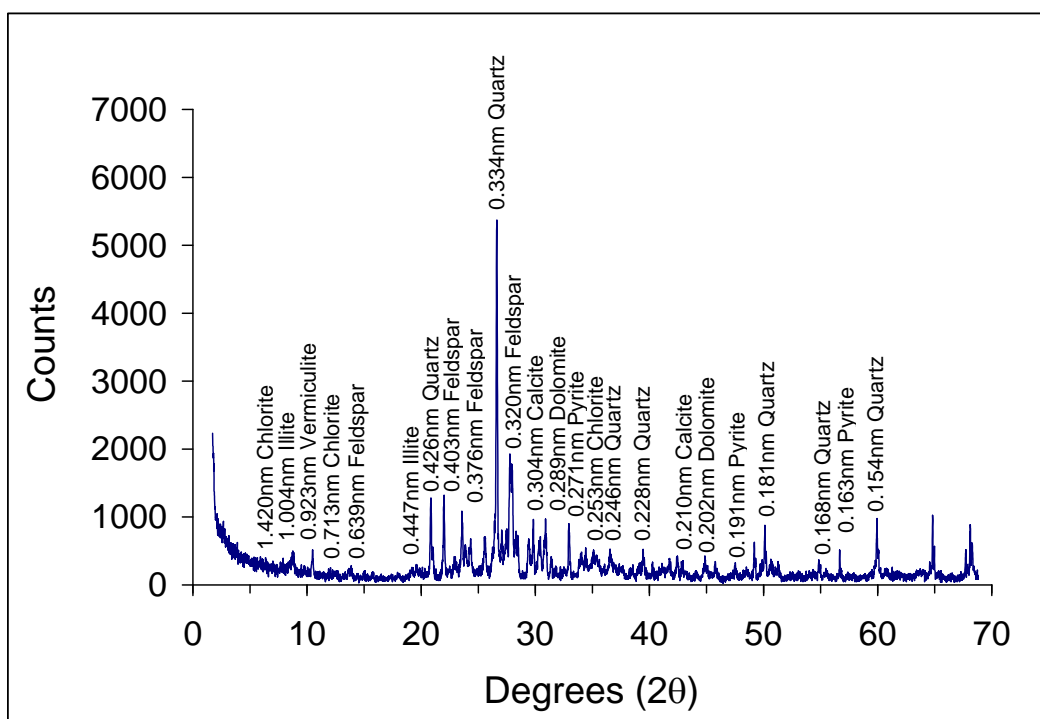
- Uddin, K., Balasubramaniam, A.S., and Bergado, D.T. (1997). "Engineering behavior of cement-treated Bangkok soft clay." *Geotechnical Engineering Journal*, 28(1), 89–119.
- Wang, L. (2002). "Cementitious stabilization of soils in the presence of sulfate." Doctoral Thesis, Louisiana State University, Baton Rouge, LA, U.S.A.
- Wang, L., Roy, A., Seals, R.K., and Byerly, Z. (2005). "Suppression of sulfate attack on a stabilized soil." *Journal of the American Ceramic Society*, 88(6), 1600–1606.
- Wareham, D.G., and Mackechnie, J.R. (2006). "Solidification of New Zealand harbor sediments using cementitious materials." *Journal of Materials in Civil Engineering*, 18(2), 311–315.
- Washburn, E.W. (1921). "Note on a method of determining the distribution of pore sizes in a porous material." *Proceedings of the National Academy of Sciences, USA*, 7(4), 115–116.
- Wissa, A.E.Z., Ladd, C.C., and Lambe, T.W. (1965). "Effective stress strength parameters of stabilized soils." *6th Int. Conf. on Soil Mechanics and Foundation Engineering, Montréal*, 1, 412–416.
- Yong, R.N., Sethi, A.J., and Larochelle, P. (1979). "Significance of amorphous material relative to sensitivity in some Champlain clays." *Canadian Geotechnical Journal*, 16, 511–520.

**Table 3-1.** Basic geotechnical properties of the three types of clay used in this study

Soil Characteristic	Ottawa clay	Nanticoke clay	EPK kaolin
Liquid limit, LL (%)	52	48	61
Plastic limit, PL (%)	24	23	36
Plasticity Index, PI (%)	28	25	25
Specific Gravity, $G_s$	2.82	2.73	2.61
Clay fraction (<2 $\mu\text{m}$ , %)	43	48	53
Activity, A	0.65	0.52	0.47



(a)



(b)

**Fig. 3-1.** X-ray diffraction analysis of (a) Nanticoke clay; (b) Ottawa clay

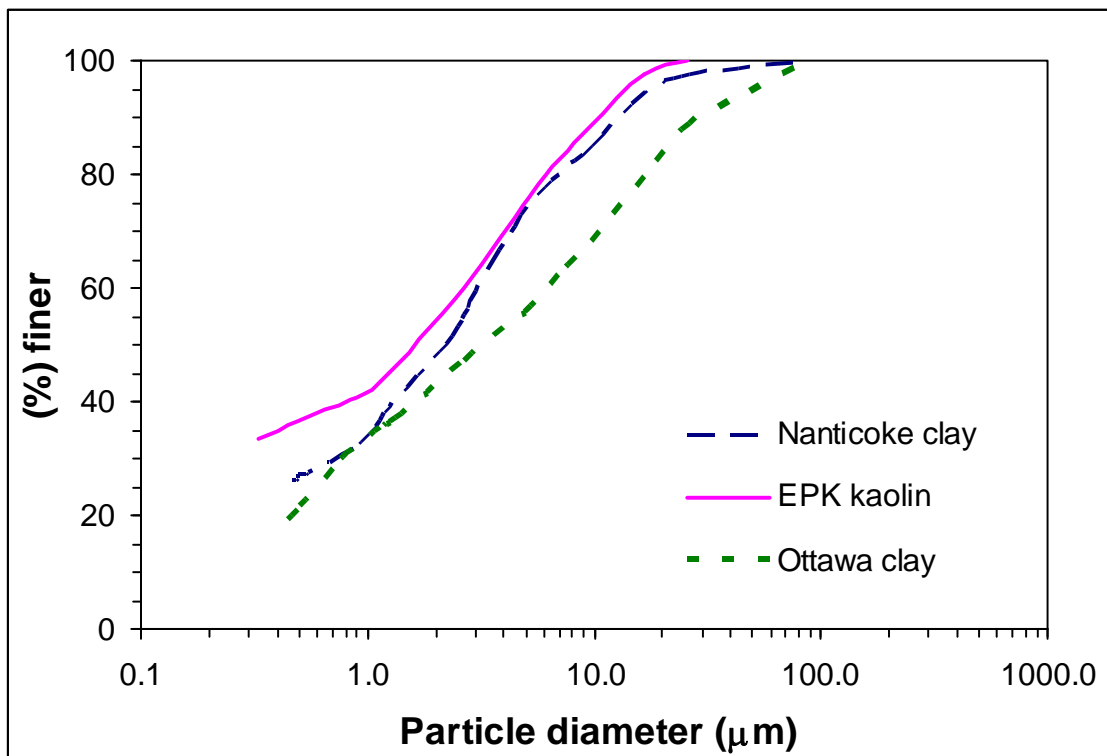


**Fig. 3-2.** Particle size distribution of the three clays used in this study

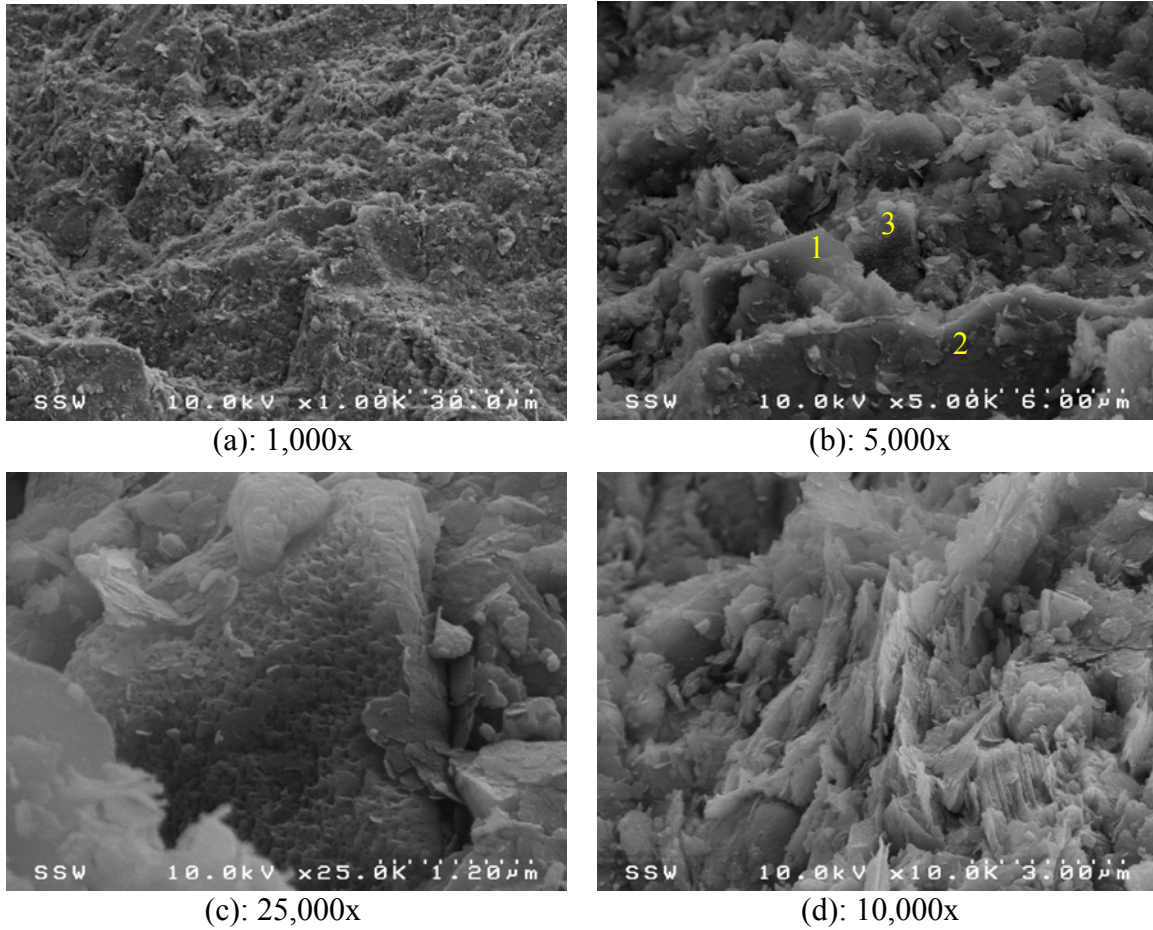


**Fig. 3-3.** Scanning electron micrographs of *undisturbed* Naticoke clay,  $w = 28\%$ ,  $LI = 0.2$  (the numbers in figure b mark the explained minerals)



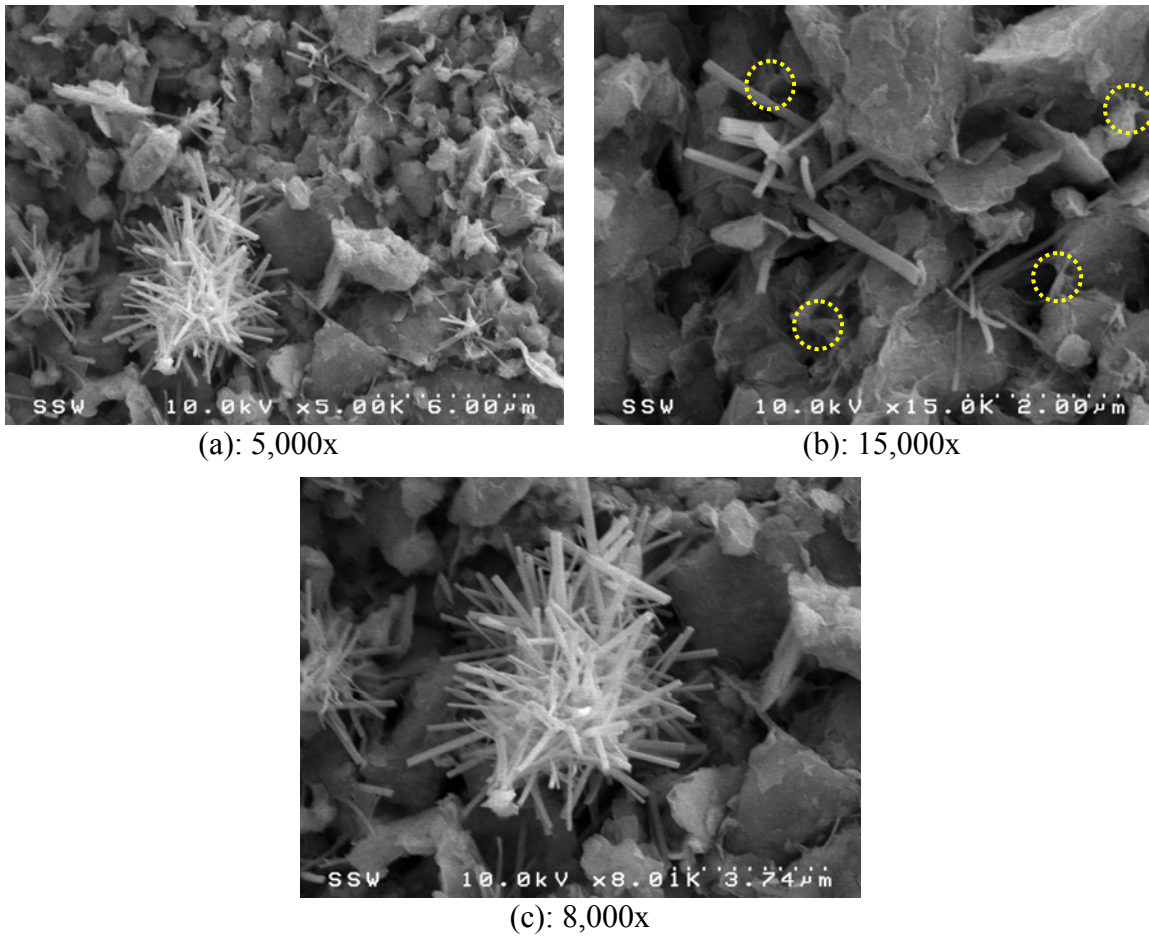


**Fig. 3-4.** Scanning electron micrographs of Nanticoke clay treated with 8.7% Portland cement,  $w = 98\%$ ,  $LI = 3$  (the circles in figure b mark some of the bonded contacts)

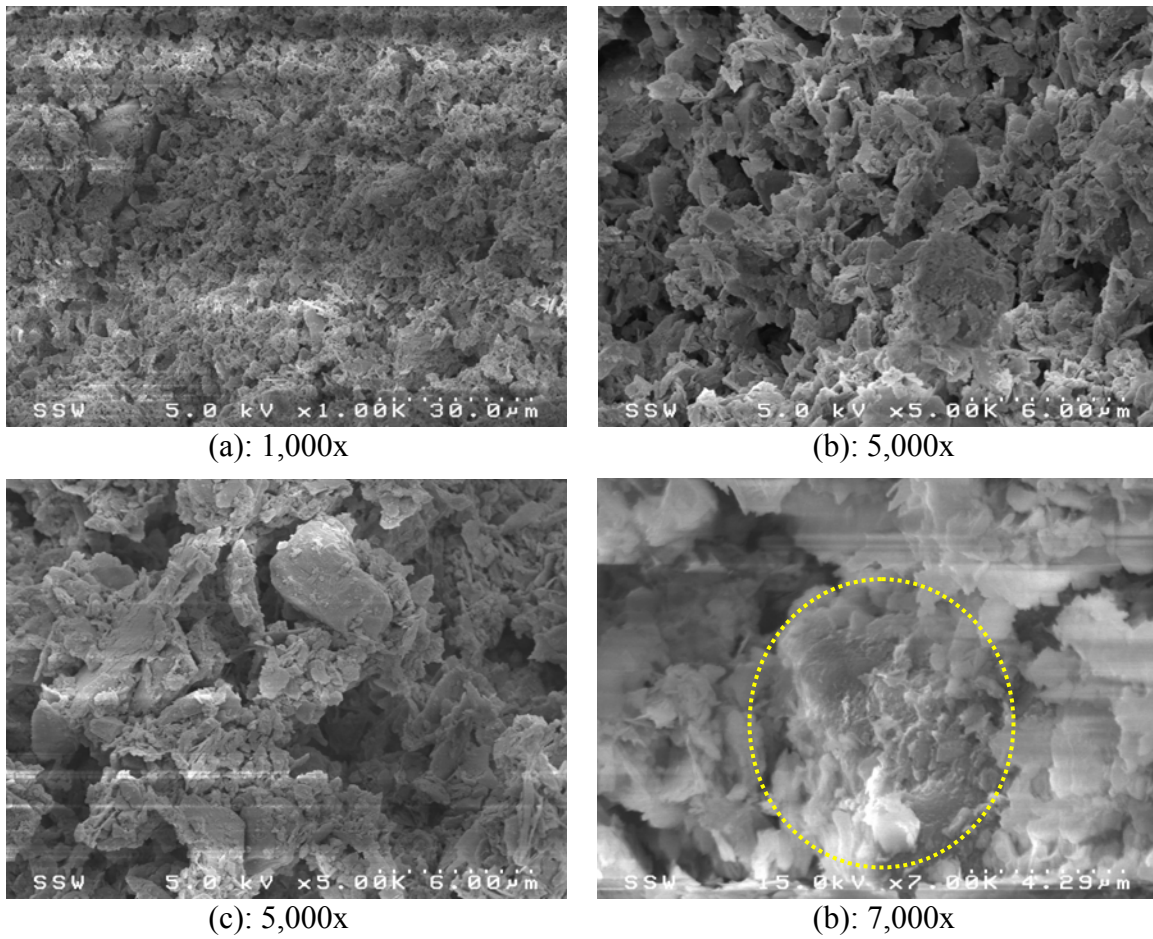


**Fig. 3-5.** Scanning electron micrographs of *undisturbed* Ottawa clay,  $w = 80\%$ ,  $LI = 2$   
(the circle in figure d marks a clast of calcium carbonate)

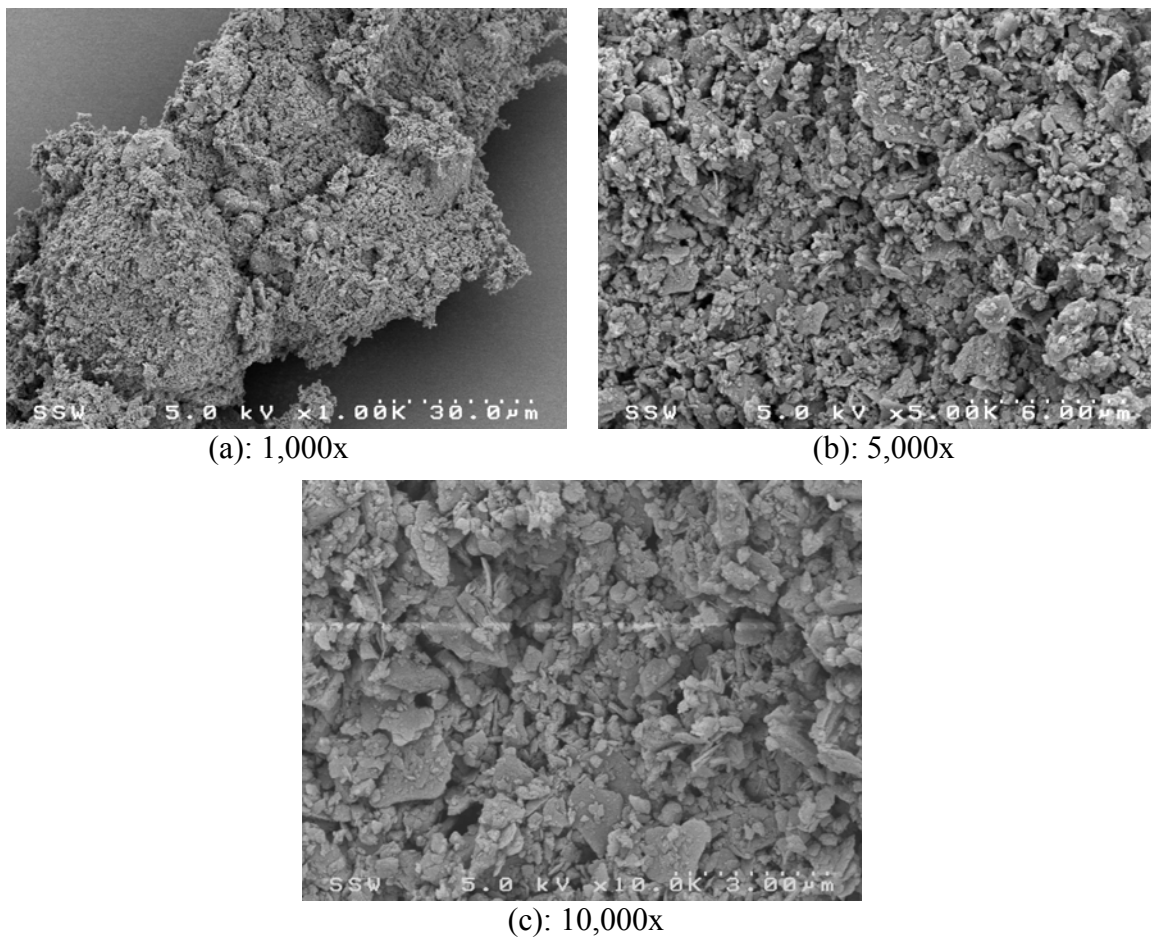


**Fig. 3-6.** Scanning electron micrographs of reconstituted specimens of Ottawa clay,  $w = 80\%$ ,  $LI = 2$

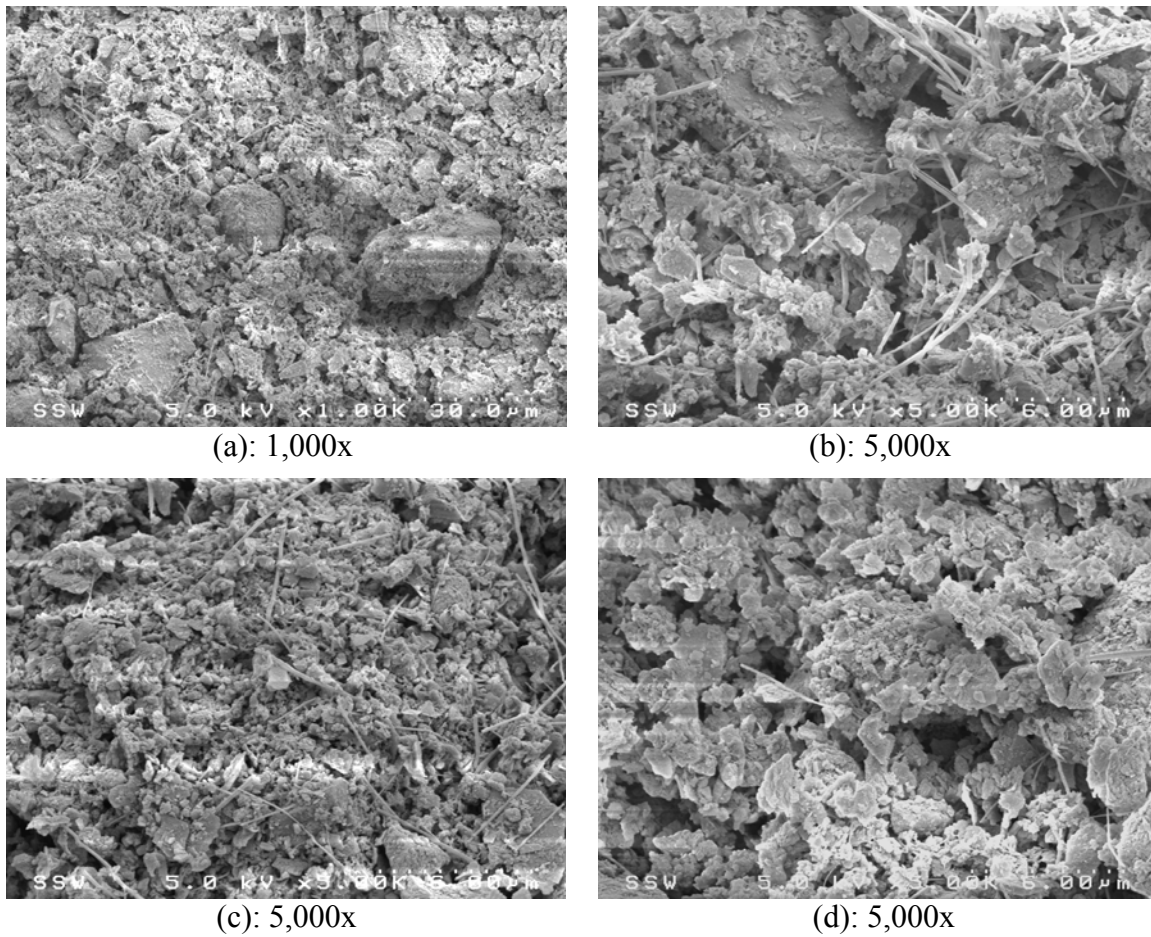
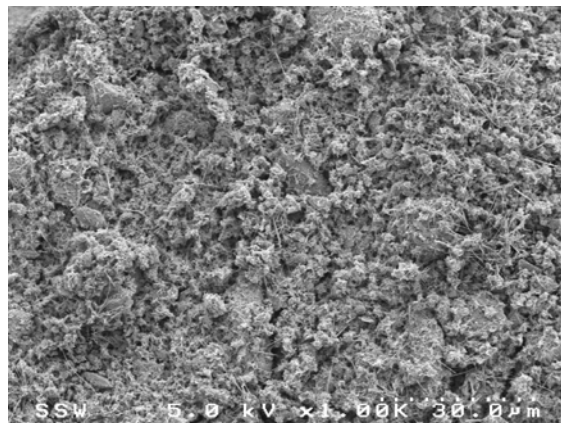
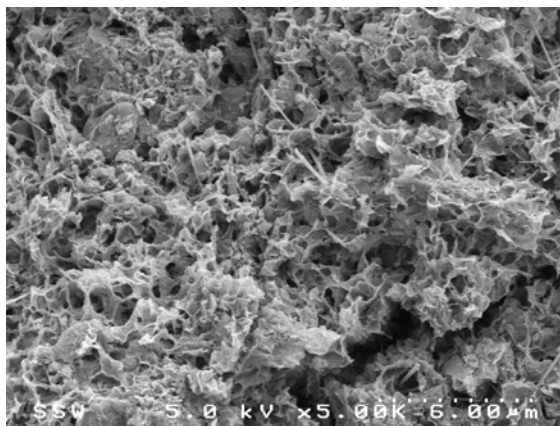


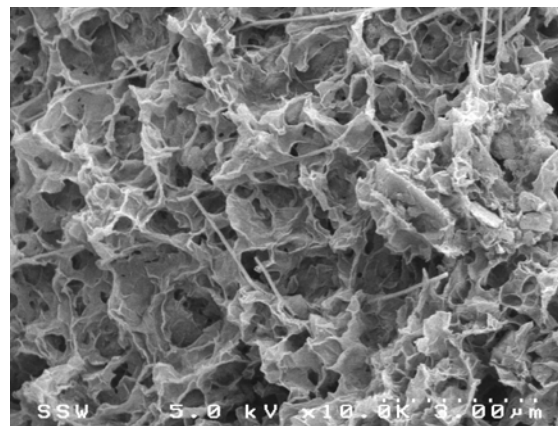
**Fig. 3-7.** Scanning electron micrographs of Ottawa clay treated with 3.1% Portland cement,  $w = 80\%$ ,  $LI = 2$



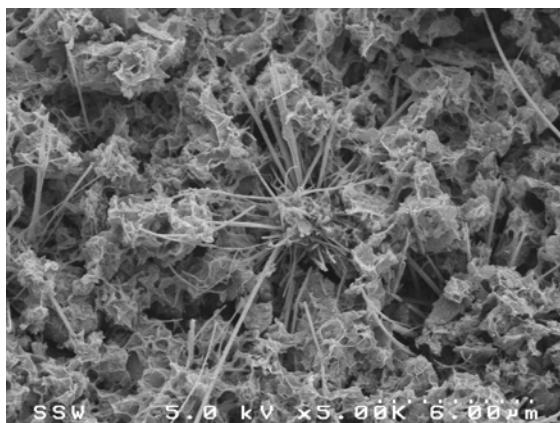
(a): 1,000x



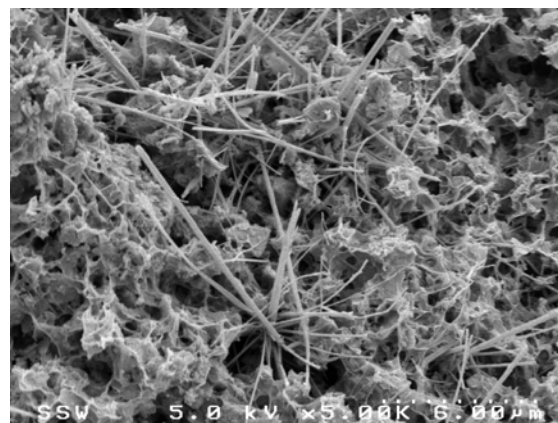
(b): 5,000x



(c): 10,000x



(d): 5,000x



(e): 5,000x

**Fig. 3-8.** Scanning electron micrographs of Ottawa clay treated with 6.4% Portland cement,  $w = 80\%$ ,  $LI = 2$



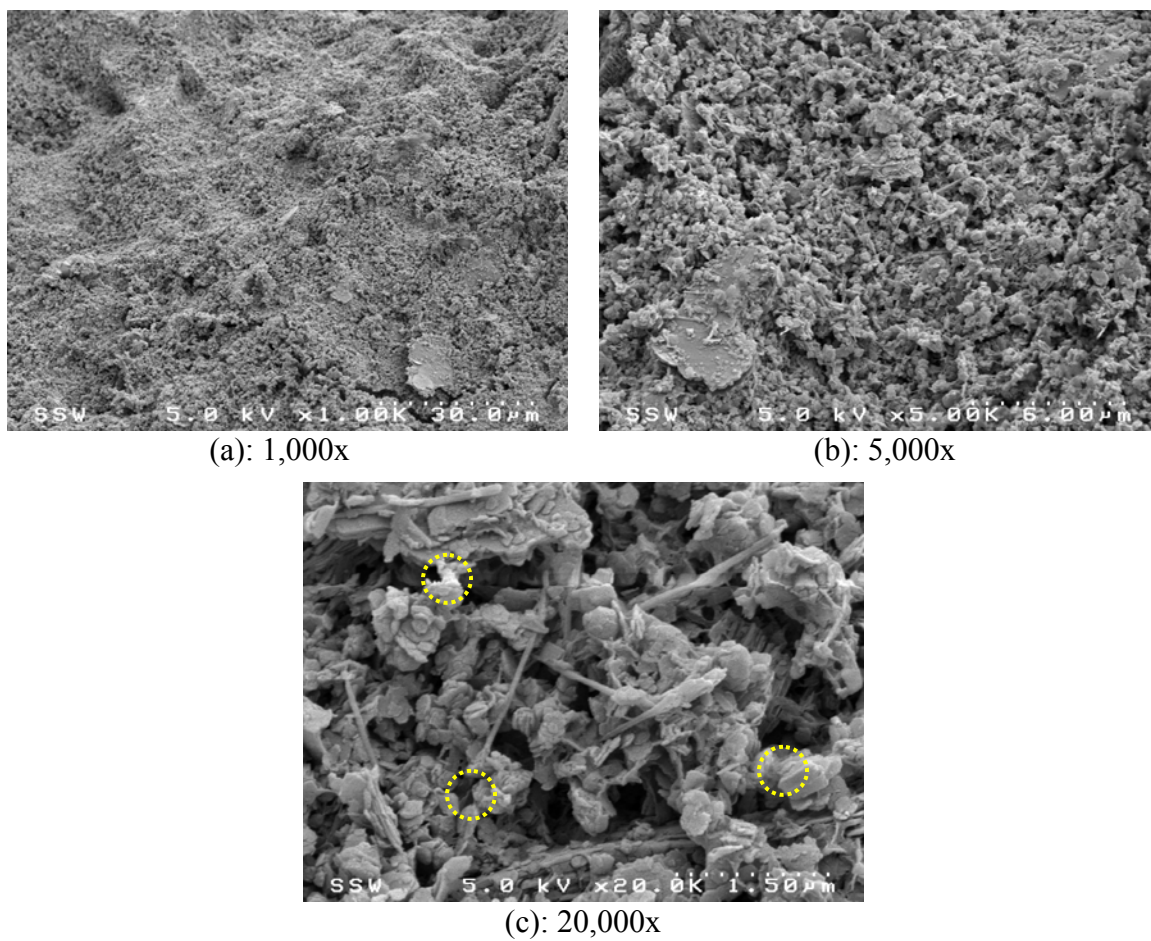


**Fig. 3-9.** Scanning electron micrographs of EPK Kaolin treated with 6.4% Portland cement,  $w = 61\%$ ,  $LI = 1$  (the circles in figure c mark some of the bonded contacts)

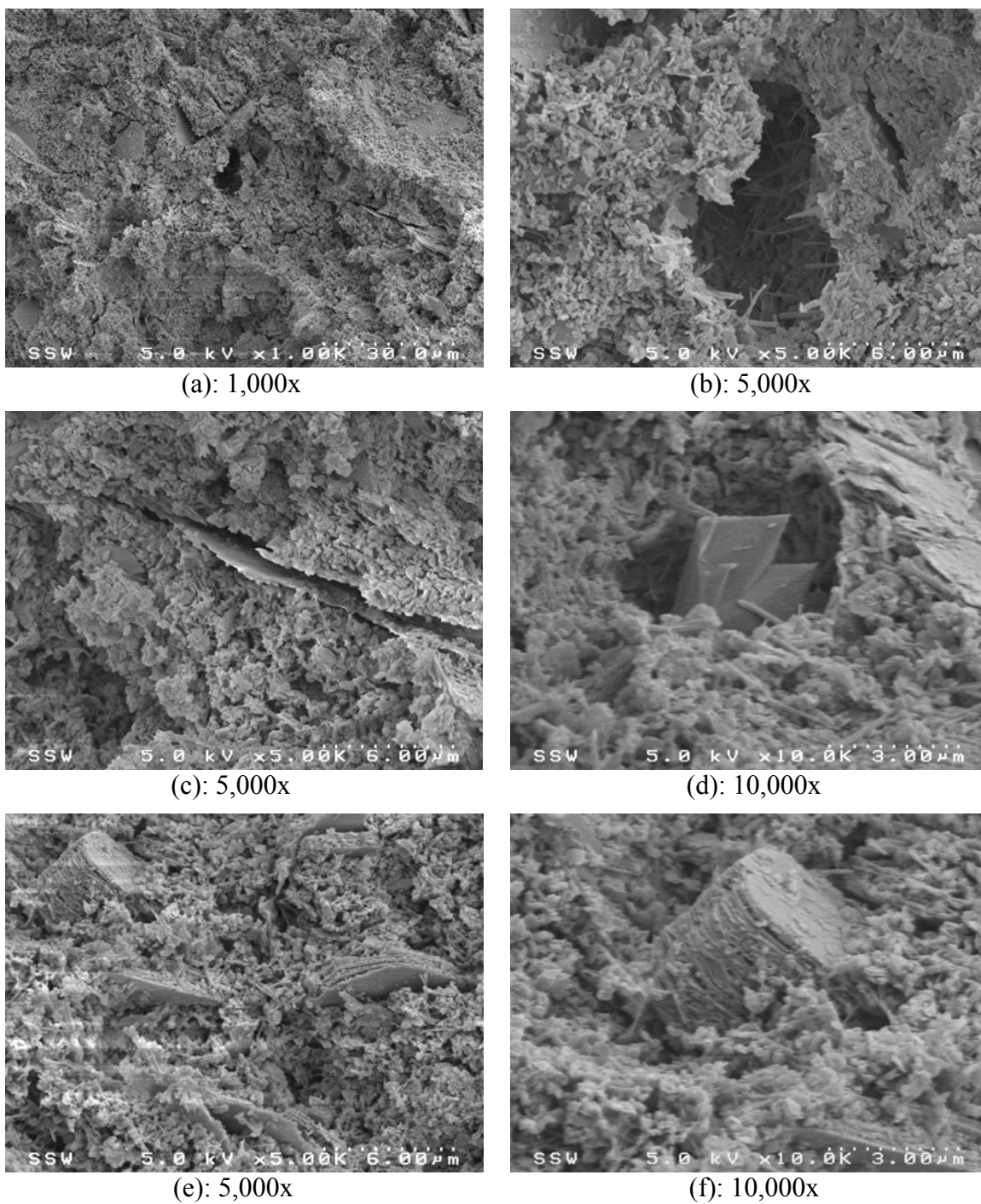
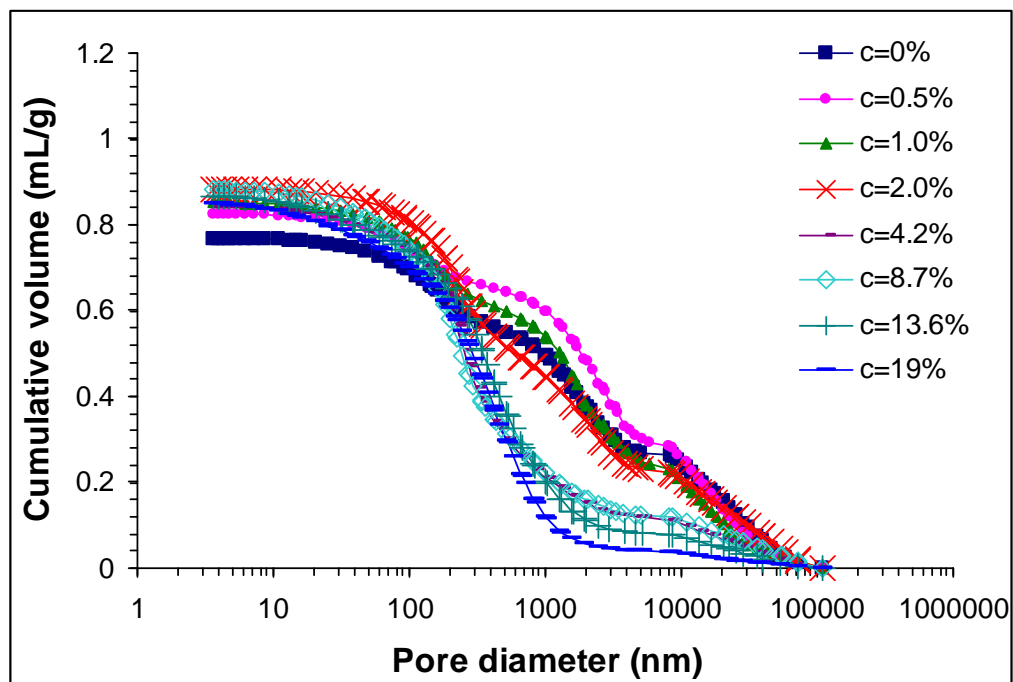
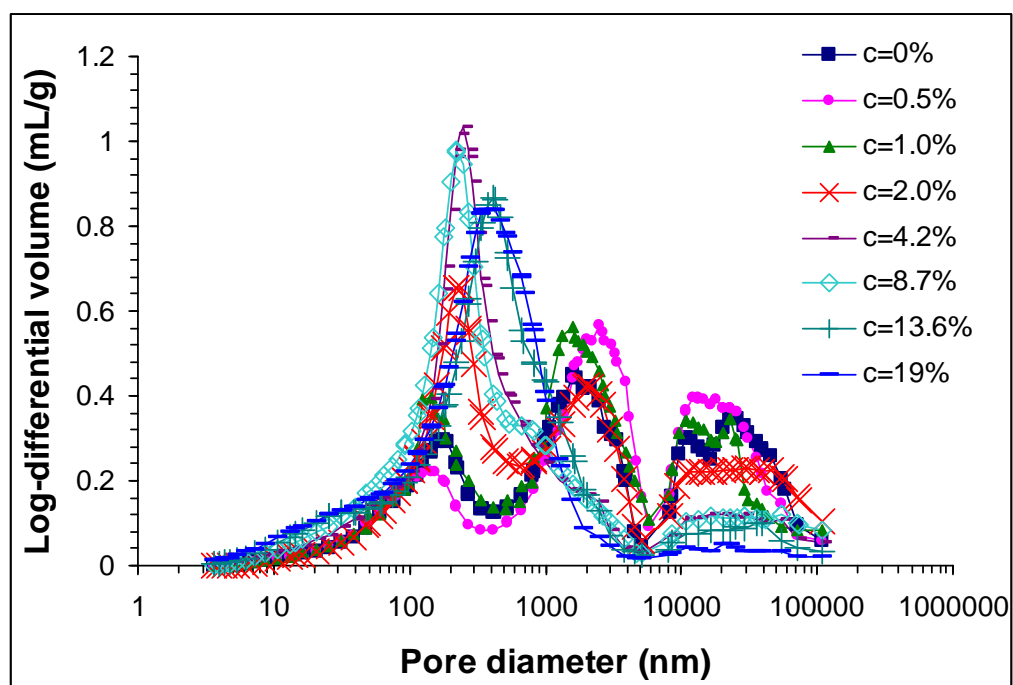


**Fig. 3-10.** Scanning electron micrographs of EPK Kaolin treated with 6.4% Portland cement and 25% gypsum,  $w = 61\%$ ,  $LI = 1$



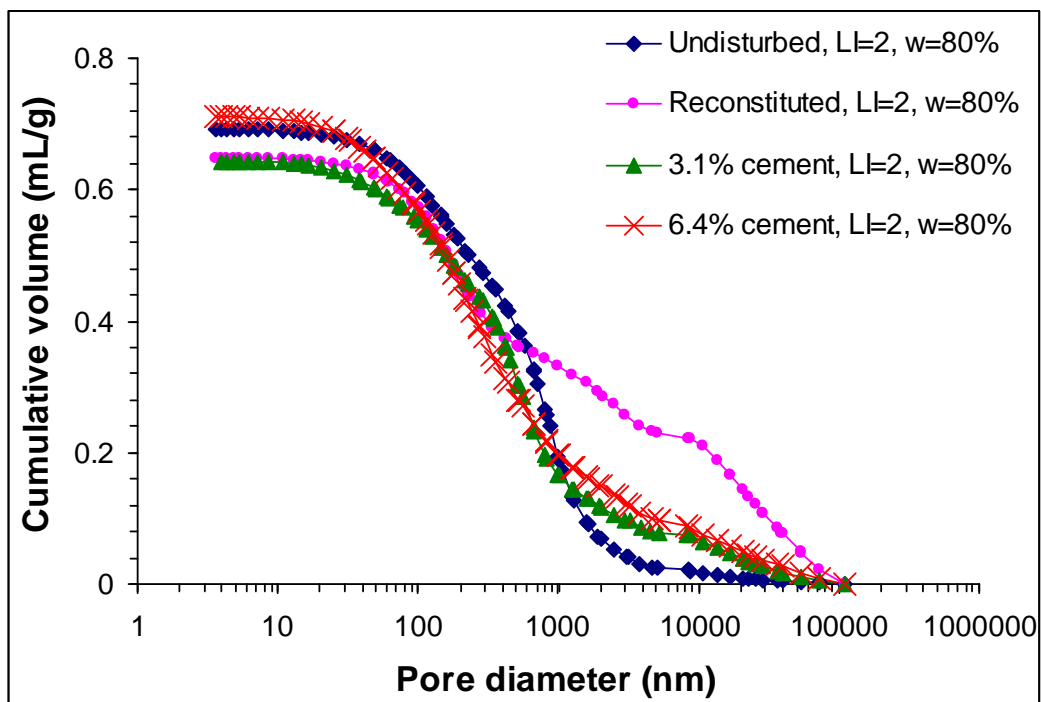
(a)



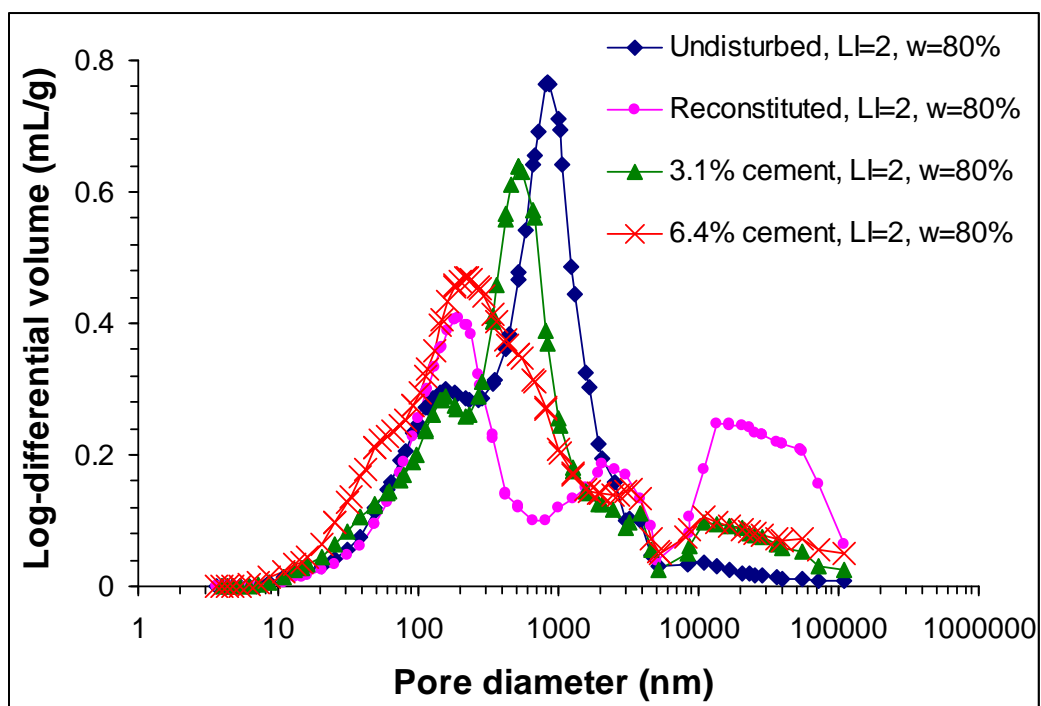
(b)

**Fig. 3-11.** Pore size distribution of cement treated Nanticoke clay specimens with LI=3 (w=98%) at different cement contents: (a) cumulative distribution; (b) log-differential distribution



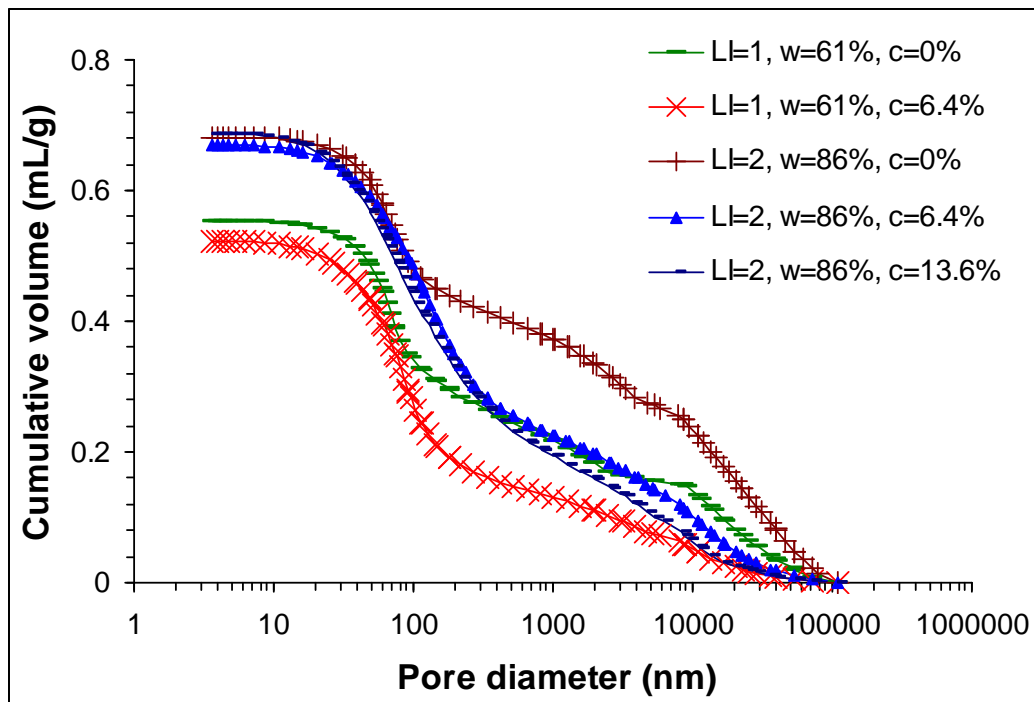


(a)

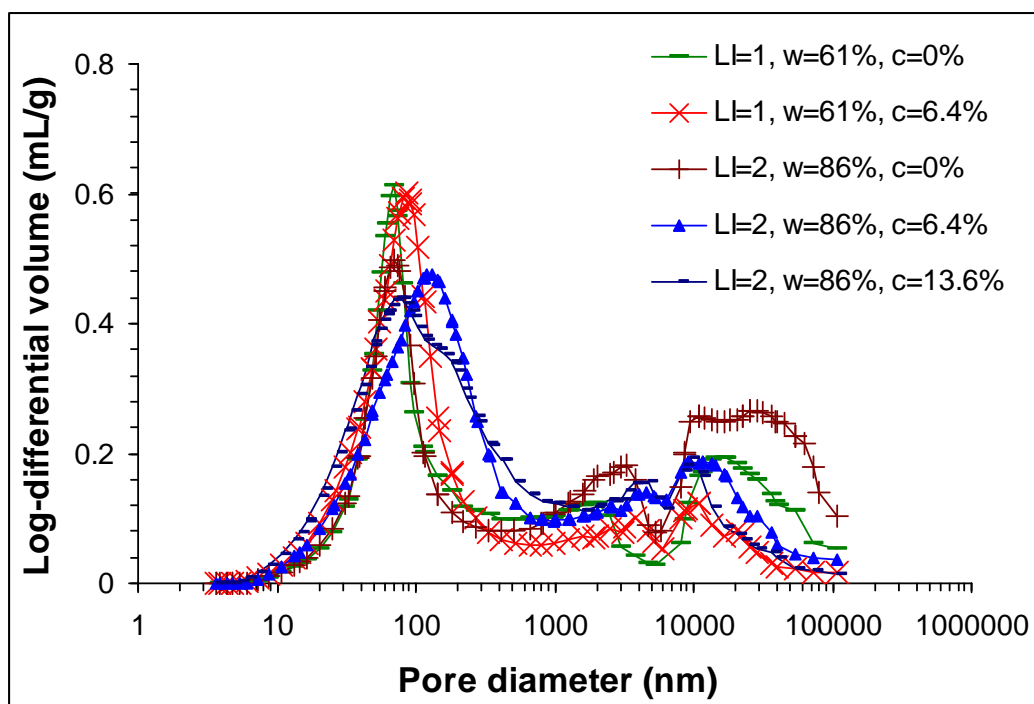


(b)

**Fig. 3-12.** Pore size distribution of undisturbed, reconstituted, and cement treated Ottawa clay specimens: (a) cumulative distribution; (b) log-differential distribution

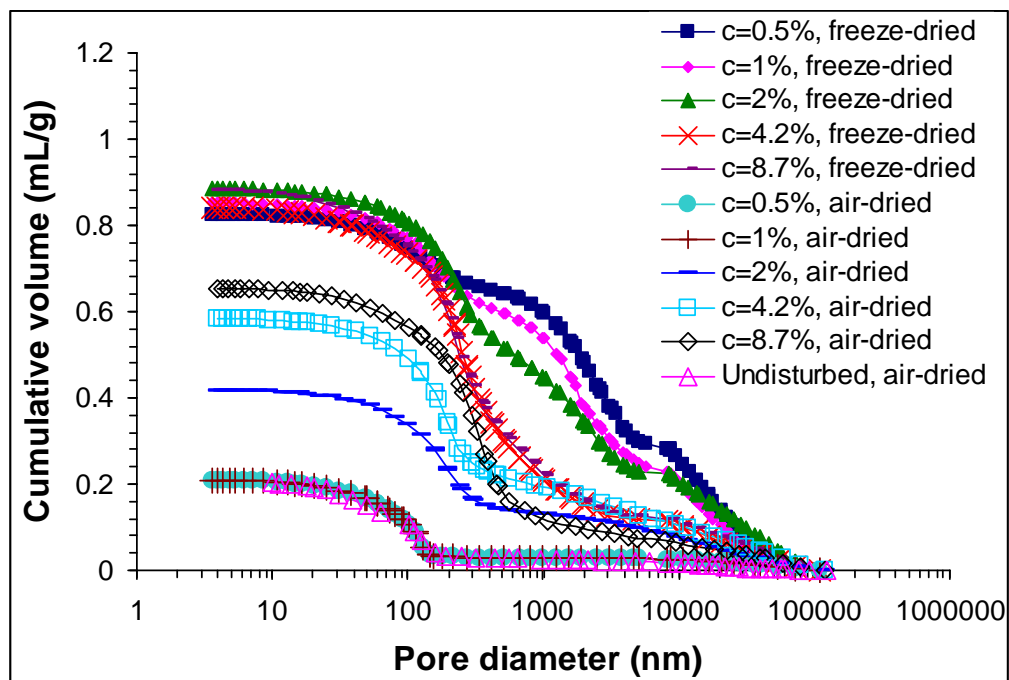


(a)

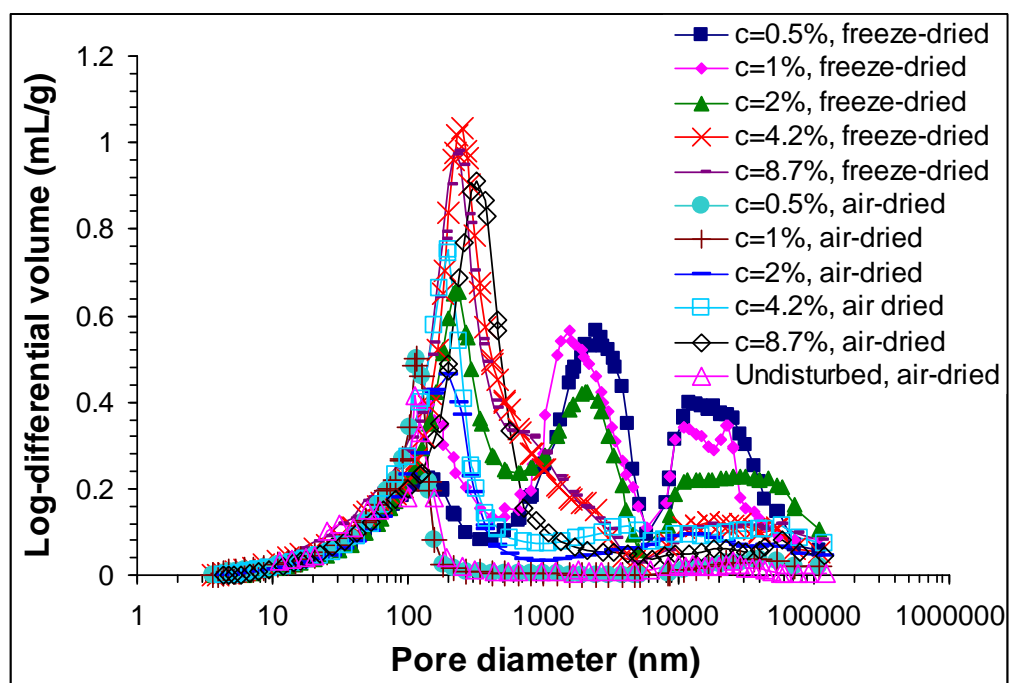


(b)

**Fig. 3-13.** Pore size distribution of reconstituted and cement treated EPK kaolin: (a) cumulative distribution; (b) log-differential distribution

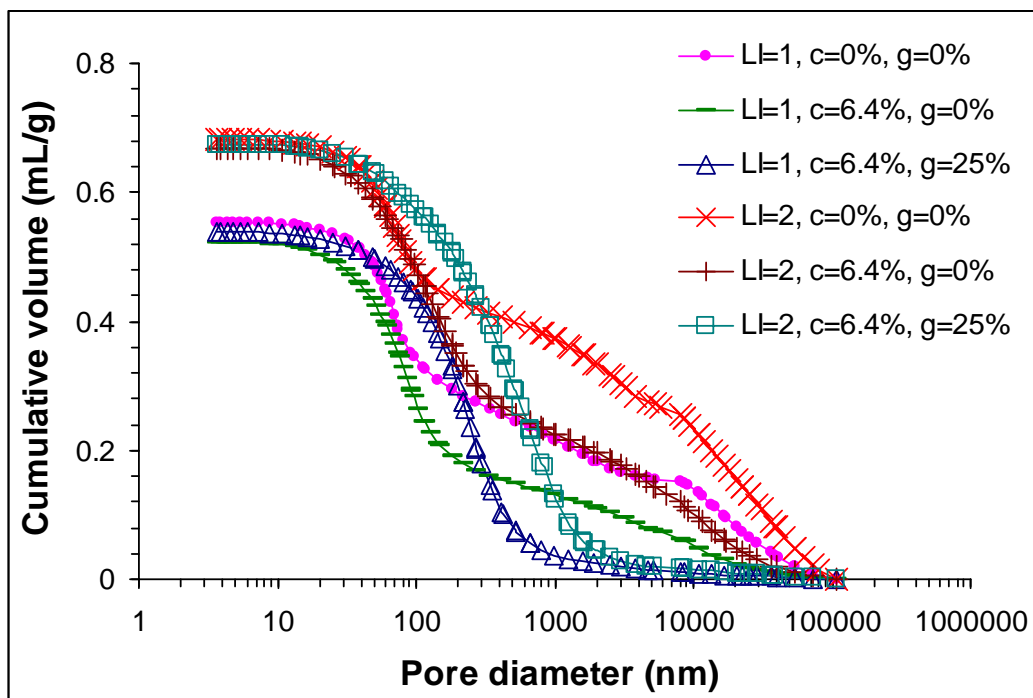


(a)

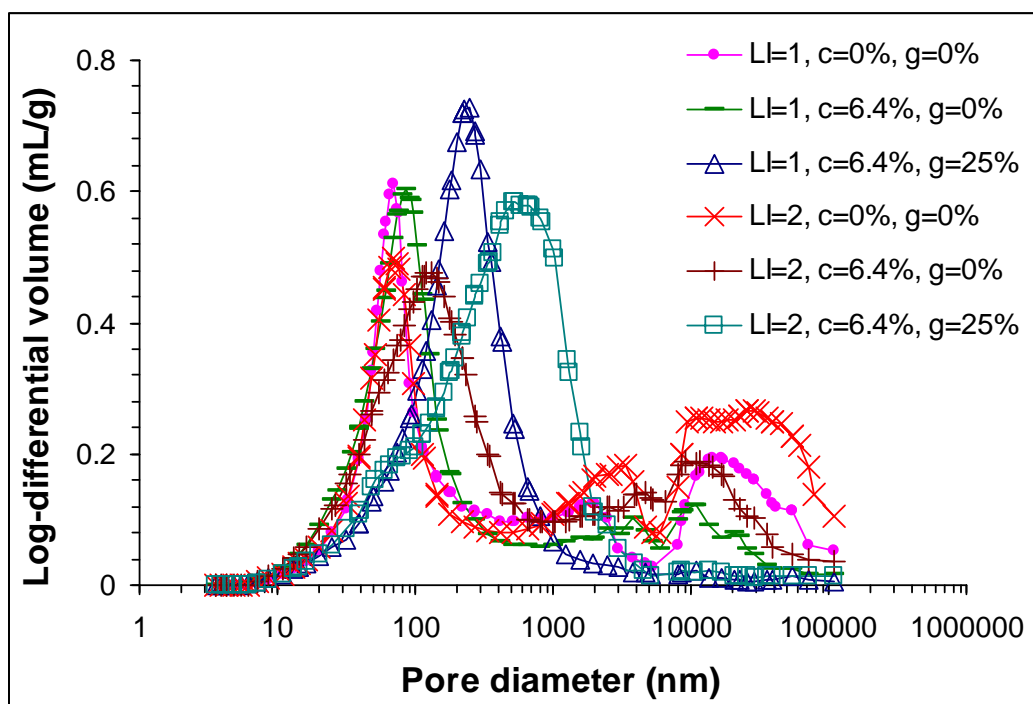


(b)

**Fig. 3-14.** Pore size distribution of freeze-dried and air-dried cement treated Nanticoke clay specimens with LI=3 ( $w=98\%$ ) at different cement contents: (a) cumulative distribution; (b) log-differential distribution

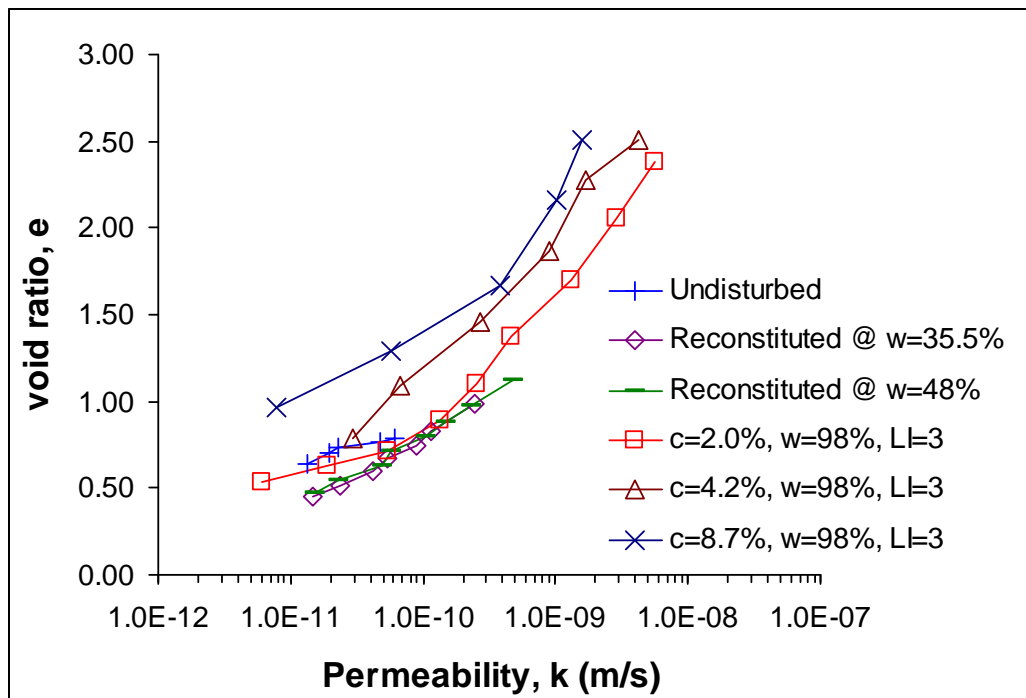


(a)

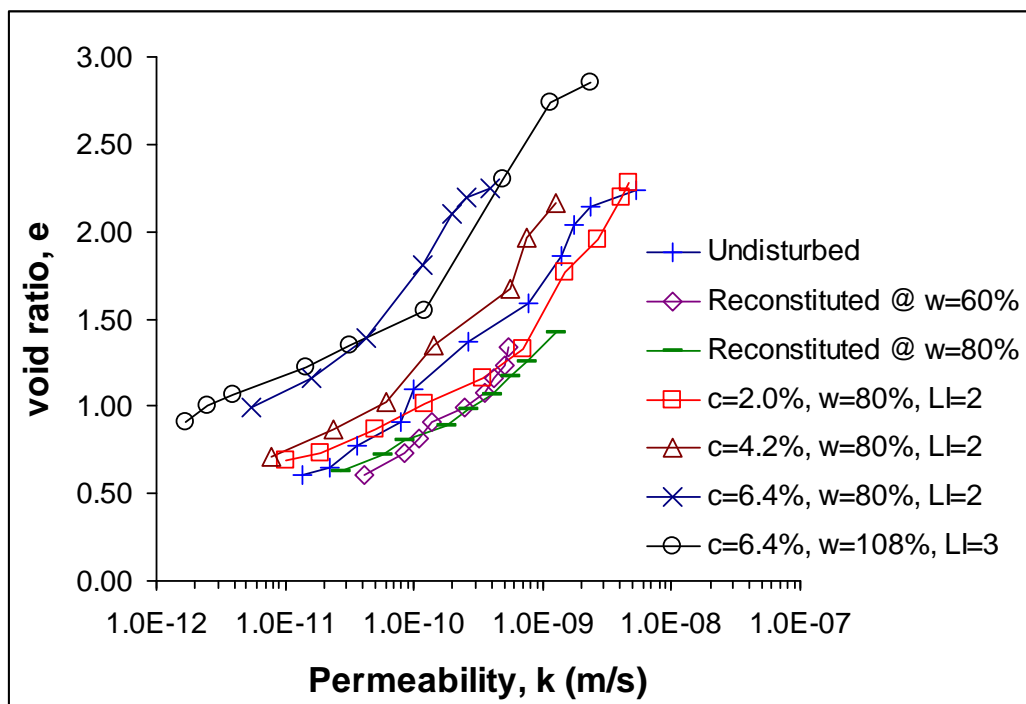


(b)

**Fig. 3-15.** Pore size distribution of cement and gypsum treated EPK kaolin: (a) cumulative distribution; (b) log-differential distribution



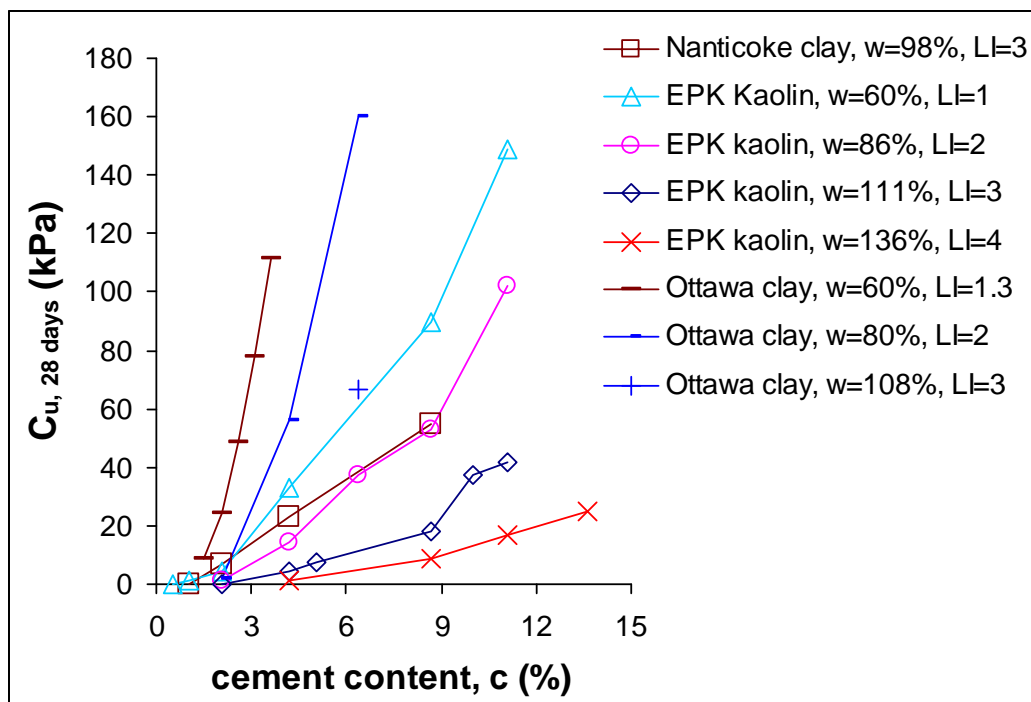
(a)



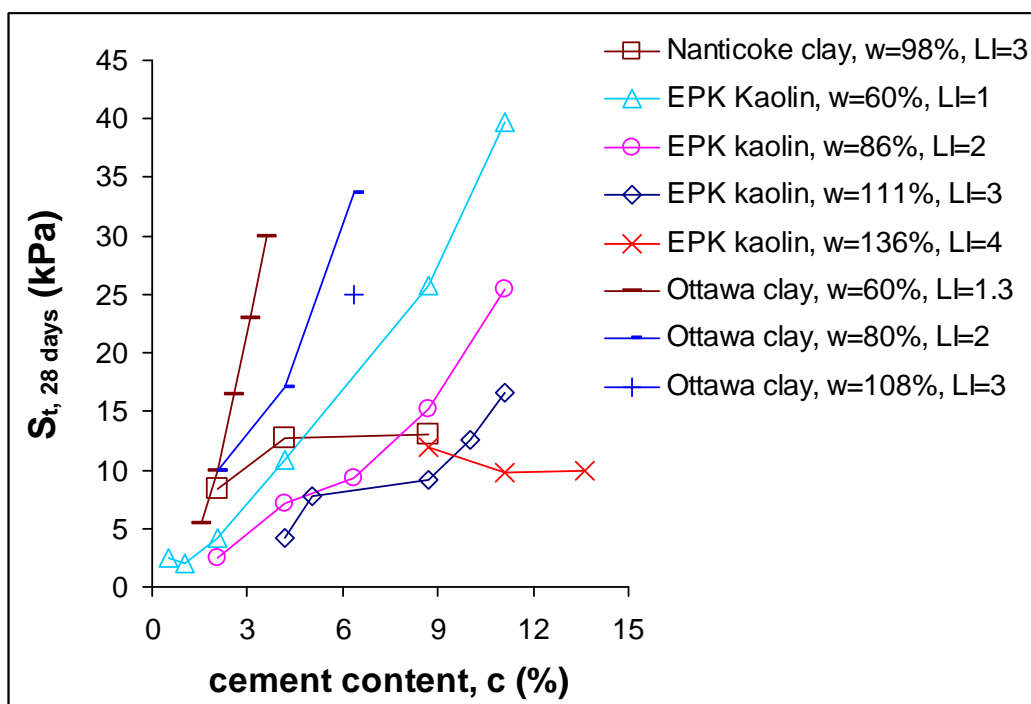
(b)

**Fig. 3-16.** Permeability of undisturbed, reconstituted, and cement treated specimens of (a)

Nanticoke clay; (b) Ottawa clay



(a)



(b)

**Fig. 3-17.** The effect of cement content on (a) undrained shear strength, and (b) sensitivity of Nenticoke, EPK, and Ottawa clay specimens with different moisture contents

## **4 BASIC PARAMETERS GOVERNING THE BEHAVIOUR OF CEMENT-TREATED CLAYS**

### **4.1 Introduction**

Soft clays cover large areas of our built environment, including many important coastal and low-land regions, where major urban and industrial areas are located, and are often encountered in land reclamation projects. These clays can have high *in situ* water contents and are considered to be potentially problematic soils, because of their low strength and susceptibility to large settlements. Although accelerated consolidation of these clays using various drainage techniques (e.g. wick drains) is common, it is not preferable in many cases, due to time constraints and expense. An alternative approach for increasing the stiffness and strength of soft ground is to create cementitious bonds within the soil material by adding cementing agents (e.g. Nagaraj and Miura, 2001).

Depending on the specific needs of different projects, various cement stabilization techniques, such as shallow soil mixing, deep mixing, and jet grouting, have been developed and are now routinely applied (e.g. Bergado et al., 1996; Nagaraj and Miura, 2001). Many of these treatments are used to provide soft soil underlying roads and railways with higher stiffness and bearing capacity. Deep mixed cement columns are also utilized as an alternative to piles to stabilize slopes, trenches and deep excavations in soft ground (Bergado et al., 1996). These chemical stabilization methods differ in their approaches for creating soil bonding, but they all utilise at least one form of bonding agent (usually Portland cement, lime, or fly ash). Due to common availability and

effectiveness, Portland cement is currently the most widely used cementing agent for ground improvement projects.

Although the changes in mechanical behaviour of many different clays stabilized by cement have been studied before by various researchers, limited attempts have been made to correlate the data from different soils and to introduce unified approaches describing the effect of clay mineralogy. Such a framework would assist engineers in preliminary design studies and minimize the number of trials needed to determine the required cement content and curing period. The significant volumes of data that have been reported recently by several researchers on the mechanical properties of cement-treated clays at high water contents have made these aims more feasible. The primary objective of this study was to combine data available in the literature, with further results from the authors, and to identify pertinent parameters for predicting the strength, stiffness, sensitivity, and other important geotechnical characteristics of soft clays cemented with Portland cement.

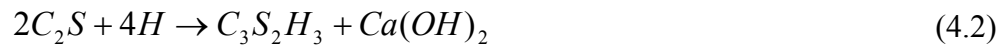
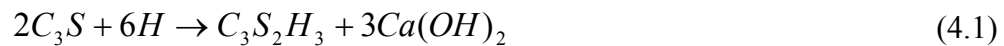
## **4.2 Literature Review**

Many researchers (e.g. Uddin et al., 1997; Yin and Lai, 1998; Tremblay et al., 2001; Tan et al., 2002; Rotta et al., 2003; Horpibulsuk et al., 2003; Horpibulsuk et al., 2004a; Lorenzo and Bergado, 2004; Chew et al., 2004; Lee et al., 2005; Xiao and Lee, 2008; Kamruzzaman et al., 2009) have investigated the effect of artificial cementation by Portland cement on the mechanical behaviour of clay and have reported increases in strength, stiffness, and brittleness of the soil. Increases in the peak strength and stiffness of the material occur due to the formation of a cementitious structure within the soil



skeleton. In soils with high water contents, this cemented structure may be responsible for a significant proportion of the mechanical behaviour of the soil.

Adding Portland cement to a soil body results in a primary hydration reaction in the cement, followed by a secondary pozzolanic reaction. The former happens in any mixture of cement and water, but the latter only occurs in the vicinity of soil crystals between calcium hydroxide supplied by the cement, and silica and alumina from the soil (Herzog and Mitchell, 1963; Croft, 1967a; Bergado et al., 1996; Bhattacharja et al., 2003). The primary hydration reactions are (Bergado et al., 1996; Bhattacharja et al., 2003):



Where the following symbols represent short forms of the compounds: H = H<sub>2</sub>O, C = CaO, and S = SiO<sub>2</sub>. The subsequent secondary reactions occur as soon as calcium hydroxide is produced in the mixture (Bergado et al., 1996; Bhattacharja et al., 2003):



Where A = Al<sub>2</sub>O<sub>3</sub>. Due to the purity and fineness of the calcium hydroxide produced during the hydration reactions, it reacts more strongly than ordinary lime with the soil minerals (Herzog and Mitchell, 1963; Bhattacharja et al., 2003). Both hydration and pozzolanic reactions lead to the creation of gelatinous and amorphous materials, which later crystallize to form inter-aggregate and inter-particle bonds (Croft, 1967a). The production of cementitious bonds between soil mineral substances creates a matrix

that encloses the unbonded particles and aggregates and results in an apparent cohesion in the soil material, making its engineering behaviour more complex (Kasama et al., 2000).

Bonding, composition, and fabric are often identified as important elements that contribute to the overall structure of a clay (Mitchell and Soga, 2005). For artificially cemented soils, these factors depend on cement and water chemistry, type, grain size distribution, and plasticity of clay, and the process of mixing and curing. Although soil properties can greatly influence the cementation process, few researchers have investigated the effect of soil mineralogy on artificial cementation. Early works on the hardening of soil-cement mixtures considered the soil material to be relatively inert (Croft, 1967b). Croft (1967a) investigated the effect of mineralogical composition of clay on cement stabilization by analyzing the behaviour of seven types of clay mixed with Portland cement. He suggested that although most clay minerals eventually consume the lime produced in the hydration process, more expansive clay minerals, such as montmorillonite, are much quicker to react with lime than less active minerals, such as kaolinite and illite. Noble and Plaster (1970) investigated the chemical reactions in Portland cement-clay mixtures and reported that the rate of cement hydration in most clays mixed with cement was slower than normal. Their results also showed that the reaction of calcium hydroxide with the soil minerals (secondary reactions) was related to the magnitude of the clay size fraction and that soil mineralogy and size distribution controlled the strength development. Woo (1971) suggested that an increase in clay content or plasticity index would make artificial cementation by Portland cement less effective. Tremblay et al. (2001) investigated the effect of organic content on artificial cementation of clays from eastern Canada and concluded that the presence organic matter

can negatively affect the efficiency of artificial cementation, especially if the organic content is higher than 3 to 4 %.

A new parameter to characterise the behaviour of artificially cemented clays has been introduced during the past decade. Miura et al. (2001) suggested that Abrams' law (Abrams, 1918), which is commonly used in concrete technology, can also be applied to cemented soils. They proposed w/c (clay-water/cement ratio) as a parameter for studying the engineering behaviour of cemented clays with high liquidity indices. For any given clay, Miura et al. (2001) showed that lower values of w/c result in higher strength and that two mixtures with different cement and water contents will have a similar strength level if their w/c ratios are the same. However, they also noted that at low w/c ratios (for example w/c = 7.5), soil fabric has a bigger influence on the behaviour of cemented clays and using w/c ratio alone is not sufficient to predict the soil behaviour.

Horpibulsuk et al. (2003) provided empirical equations correlating the w/c ratio with unconfined compressive strength for Ariake and Bangkok clays. They proposed different coefficients in their equation for each clay type and curing period. They also provided a logarithmic equation for predicting strength development with curing time based on the results of experiments performed on different types of clay, up to 180 days after curing. Horpibulsuk et al. (2005), Lee et al. (2005), and Lorenzo and Bergado (2005) also confirmed that shear strength can be expressed as a function of w/c ratio for Ariake, Singapore, and Bangkok clays.

## **4.3 Description of Laboratory Studies and Data Analysis**

### **4.3.1 Experimental work**

To investigate the effect of mineralogy, laboratory studies were conducted by the authors on cement-treated specimens of three different clays, i.e. EPK kaolin, Nanticoke clay, and Ottawa clay. Portland cement (type I according to ASTM C150) was chosen for this study, since it is one of the most commonly added cementing agents (Bergado et al., 1996; Nagaraj and Miura, 2001; Bhattacharja et al., 2003). Most ground improvement projects involving artificial cementation occur in zones with a high water table; hence, the specimens used in this study were covered with water, so that their moisture content did not drop significantly due to cement hydration. The effect of curing time on the strength and sensitivity of the cemented material was investigated by performing laboratory shear vane tests on the cement-treated samples at various time intervals after curing. In addition, the results of oedometer and triaxial tests were used to obtain relationships between soil/cement parameters and the mechanical properties of the artificially cemented clays. The results of these laboratory studies were added to those found in the literature and described in Section 4.3.3 below.

### **4.3.2 Specimen preparation and testing procedures**

EPK Kaolin is already available in a powdered form. To make the powdered Nanticoke and Ottawa clays, the soil was cut into small pieces, dried at room temperature, and then finely pulverized into a powder (100% passing Sieve No. 40), using a rubber hammer to avoid crushing the soil particles. Clay powders were mixed with distilled, deionised water to form a slurry with a water content close to the desired

value. The slurry was mixed until a uniform paste was achieved. Next, the required amount of cement mixed with water was added to the mixture to increase the water content to the desired level. The slurry was mixed again for a maximum of 15 minutes, so that the mixing process did not disturb the produced bonds. The mixture was then poured into plastic cups 70 mm in diameter and 120 mm in height. Trapped air bubbles were removed from the samples by gently tapping on the walls of each cup, and some water was added on top of the slurry in every cup to provide it with moisture throughout the curing period. The cups were then covered by plastic wraps and placed in a temperature controlled room to be cured at a constant temperature of 25°C. Cemented samples were prepared with different moisture contents,  $w(\%)$ , and cement contents,  $c(\%)$ , where cement content is defined as the ratio of mass of cement to the mass of dry soil in terms of percentage. A few oedometer tests were also performed on undisturbed and reconstituted specimens of Ottawa clay. The reconstituted specimens were prepared at water contents of 1.2 and 1.5 times the liquid limit to obtain the intrinsic compression line (ICL) for the material (Burland, 1990).

Since the undrained shear strength of a large number of cemented specimens were to be measured, the laboratory shear vane was chosen as the primary testing method. The vane had a diameter and height of 19 and 28 mm, respectively. The vane tests were carried out at a rate of one complete revolution per minute (Serota and Jangle, 1972; Kogure et al., 1988). Although it is generally recognised that due to the different modes of failure, undrained shear strengths measured with the shear vane apparatus vary from those measured with other test methods (Kogure et al., 1988), the manufacturer of the shear vane calibrated the device using UU triaxial tests on clay specimens (Serota and

Jangle, 1972). Accordingly, the calibration factor obtained based on this approach was used herein, allowing for the comparison of the vane results to those obtained from unconfined compression or quick triaxial tests shown later in the paper. A similar apparatus was used by Kirwan (2003) and Kainourgiaki (2004) to measure the shear strengths of cemented Speswhite kaolin specimens. In addition to the shear vane, a number of oedometer and CIU triaxial tests were also performed to obtain further parameters. The oedometer and CIU triaxial tests were conducted according to ASTM D2435 and ASTM D4767, respectively. For testing, the samples were taken out of the plastic cups and were cut with a thin wire trimmer to the required size.

#### **4.3.3 Additional database compilation**

In addition to the experimental studies, a detailed literature survey and analysis of the data was conducted by the authors. To ensure as diverse a collection of data as possible, the results of laboratory shear vane, unconfined compression, undrained triaxial, and oedometer tests performed by different researchers on different types of clay treated with Portland cement were included in the analysis. The database covers twenty-three studies published from 1967 to 2010. For the parametric studies, information on the following cement-treated clays were gathered from the literature: *Speswhite Kaolin* (Ritchie, 2004; Kainourgiaki, 2004; Kirwan, 2003;); *Ariake clay* (Miura et al., 2001; Horpibulsuk et al., 2003; Horpibulsuk et al., 2004a; Horpibulsuk et al., 2004b; Horpibulsuk et al., 2005); *Bangkok clay* (Uddin, 1994; Uddin et al., 1997; Bergado et al., 1999; Lorenzo and Bergado, 2004; Horpibulsuk et al., 2004b); *Singapore marine clay* (Tan et al., 2002; Chew et al., 2004; Lee et al., 2005; Xiao and Lee, 2008; Kamruzzaman et al., 2009); *Hong Kong clay* (Yin and Lai, 1998); *Brown, Black cotton, and Red earth*

*Indian clays* (Nagaraj et al., 1996; Narendra et al., 2006); *Illite* (Nagaraj et al., 1996); *Home Rule Kaolin* (Croft, 1967a); *Louiseville clay* (Tremblay et al., 2001); *Bothkennar clay* (Kirwan, 2003; Kainourgiaki, 2004); *Rotoclay Kaolin* (Flores et al., 2010).

#### **4.3.4 Material properties**

Analysis was performed on laboratory test results conducted by the authors for artificially cemented specimens of two commercially produced kaolin clays: EPK and Speswhite, and two naturally occurring Canadian clays: Nanticoke and Ottawa clays. EPK is a pulverized kaolin clay from Georgia, U.S., and Speswhite china clay is produced from deposits in the southwest of England. Air dried clay powders were also obtained from block samples of a stiff fissured clay with a glacio-lacustrine origin taken from 3 m depth in a test pit in Nanticoke, Ontario, and from samples of a sensitive Leda/Champlain clay (St~20), also taken from 3 m depth in a borehole in Ottawa, Ontario. X-ray diffraction analysis showed that the primary clay minerals of both soils are illite and chlorite, with traces of vermiculite found in the Ottawa clay. The engineering properties of these four clays are summarized in Table 4-1.

In addition to the aforementioned clay tests, the laboratory results from other researchers on clayey soils listed in Section 4.3.3 were used in the overall analysis. Some basic properties of these soils are given in Table 4-2 and Table 4-3. The liquid limit (LL) plastic limit (PL), plasticity index (PI), and activity number (A) of these clays range from 38 to 125, 15 to 60, 20 to 65, and 0.47 to 1.18, respectively. It should be noted that except for Bothkennar clay and Rotoclay Kaolin, which are from the U.K, and Home Rule Kaolin, which is from Australia, the remaining clays are from East and Southeast Asia or Canada.

## 4.4 Analysis of the Data

### 4.4.1 Hardening of cemented clays with time

Fig. 4-1 shows the results of typical laboratory shear vane tests on artificially cemented samples of Nanticoke clay prepared at a moisture content of 98% (liquidity index,  $LI=3$ ). The tests were conducted on cemented samples cured up to forty months. Four cement percentages were used, namely 1, 2, 4.2, and 8.7%. Samples with 1% cement did not produce any measurable strength, even after long curing periods, so the results for these samples are not plotted in the figure. Likewise, the strength of the sample with 8.7% cement after forty months of curing could not be measured, since it exceeded the maximum capacity of the shear vane device. As expected, the shear strength increases with curing time and cement content, since both contribute to the production of more cementing bonds within the soil body, and this confirms the previous findings of many other researchers (e.g. Nagaraj et al., 1996; Uddin et al., 1997; Bergado et al., 1999; Horpibulsuk et al., 2003; Kamruzzaman et al., 2009). However, an interesting observation is that the cemented samples kept gaining significant amounts of strength, long after the start of curing, as the curves in Fig. 4-1 have considerable slope even after one thousand days. It is typically assumed that the hydration rate of ordinary Portland cement drops significantly with time after curing. This trend of increasing strength is not typical for cement based construction materials, such as concrete, and may be attributed to the slower secondary reactions that happen between clay minerals and cementation products. Further explanation of this behaviour is provided in the discussion section.



The values plotted in Fig. 4-1 are peak undrained shear strengths measured with the laboratory shear vane device. If these peak strengths are normalised by the peak strength of the same sample after 28 days of curing ( $c_{u, 28 \text{ days}}$ ), all three curves in Fig. 4-1 plot on the same curve (Fig. 4-2), indicating that the hardening trend is independent of the amount of cement added to the soil. Fig. 4-2 better illustrates the continuation of the rate of increase of peak shear strength; the peak strength after 400 and 1200 days of curing is 2 and 3 times that after 28 days, respectively. As reported by Tan et al. (2002), the results of unconfined compression tests on cemented specimens of Singapore marine clay suggest the same independence of hardening trend from cement and water contents. Horpibulsuk et al. (2003) have also shown the same independence for Bangkok, Ariake, and Indian clays.

The data plotted in Fig. 4-2 were obtained for one type of clay, with a single value of moisture content and variations in the cement content. To investigate whether a unique relationship occurs for a number of clays, where the hardening trend is independent from mineralogy and moisture content (as well as from the cement content), unconfined compression tests results collected from the literature for the different soils described in Section 4.3.3 have been plotted, along with the results for Nanticoke clay, in Fig. 4-3. It can be seen that all data follow a similar trend, yielding the following relationship:

$$\frac{c_u}{c_{u,28\text{days}}} = 0.96 \times \left( \frac{t}{t_{28\text{days}}} \right)^{0.31} \quad (4.5)$$

Where “ $c_u$ ” is the undrained shear strength after “ $t$ ” days of curing. More than 440 data points for 12 different clays, with a wide range of liquidity indices ( $LI \sim 0.4$  to  $3.0$ ) and cement contents ( $c \sim 1$  to  $100\%$ ) were used to derive Eq. (4.5). Table 4-2 summarizes

soil properties of the samples plotted in this figure. The dashed line in Fig. 4-3 is calculated from the logarithmic equation that was suggested earlier by Horpibulsuk et al. (2003) for soils with a liquidity index of 1.0 to 2.5. It should be noted that the proposed equation has been obtained for curing times in the range of 1 to 1250 days and may not provide a good prediction particularly for curing times less than 1 day.

In addition to the peak strengths, residual vane shear strengths of three of the clays were also measured by the authors. Since the cementation process changes the mechanical behaviour and the mineralogy of the soil, the measured residual strengths of the cemented soils are much higher than those expected for a soil with such a high moisture content. It was observed that samples with higher cement content and curing time have higher residual strengths. For example, the residual strengths of the samples with 2% cement and 1 and 600 days of curing were 0.5 and 1.5 kPa, while those of the samples with 8.7% cement were 2 and 6 kPa, respectively. The residual strength appeared to be mobilized due to friction rather than bonding; the stronger samples also formed a thinner shear band after failure. In addition, the changes in the mineralogy of the soil due to pozzolanic reactions, which produce cementitious bonds within the soil aggregates, could increase the residual strength of the material. However, the residual strength does not increase at the same rate as the peak strength. As a result, the brittleness and sensitivity of the soil also increase with cement content and curing time. Fig. 4-4 shows the development of sensitivity in cemented samples of Nanticoke clay with three different cement contents; the sensitivity number of the specimen with 8.7% cement has reached up to 13 and 24, after 28 and 600 days of curing, respectively.

The sensitivity values of Nanticoke clay samples are plotted along with those for samples of EPK and Speswhite kaolin in Fig. 4-5. Similar to the previous analysis, the value measured after 28 days of curing,  $S_{t, 28 \text{ days}}$ , is used as a normalizing parameter. The sensitivity is seen to increase with curing time in a logarithmic fashion according to:

$$\frac{S_t}{S_{t, 28 \text{ days}}} = 0.14 \times \ln\left(\frac{t}{t_{28 \text{ days}}}\right) + 1.03 \quad (4.6)$$

Where “ $S_t$ ” is the sensitivity after “ $t$ ” days of curing. Comparison of Fig. 4-3 and Fig. 4-5 shows that while both peak strength and sensitivity initially increase linearly with time in logarithmic space, after almost 100 days of curing, the peak strength begins to increase with a faster rate than the sensitivity. Since the pozzolanic reactions, which occur more slowly than the hydration reactions and continue for a longer time, mainly strengthen the soil aggregates, they lead to more frictional soil resistance and continue to increase the residual strength for a long time after the addition of Portland cement to the soil.

#### 4.4.2 Shear strength of artificially cemented clays: state parameters

In addition to curing time and cement content, other parameters, such as water content and liquidity index, plasticity index, clay content, curing temperature, and soil mineralogy, affect the behaviour of artificially cemented clays (Croft, 1967a; Croft, 1967b; Woo, 1971; Broms, 1986; Bergado et al., 1996; Uddin et al., 1997; Miura et al., 2001). To further investigate the parameters that have a significant effect on the strength of cemented clays, the results of the laboratory shear vane tests on samples made of different clays with varying moisture and cement contents were studied. Fig. 4-6 shows the relationship between liquidity index and undrained shear strength after 28 days,  $c_{u, 28}$

days, for EPK and Speswhite Kaolins and Ottawa clay. As expected, a reduction in liquidity index (LI) is followed by an increase in the shear strength. A bilinear relationship seems to exist. As the liquidity index reduces from 4 to 1, the rate of increase in the strength is initially low but increases after a threshold in the curves is reached. For kaolin clays with 4.2 and 8.7% cement, this threshold is at  $LI=3$ . The figure also shows that at LI values higher than 4, the addition of 11.1% cement does not result in a substantial strength gain for EPK kaolin. Considering only EPK and Speswhite kaolin clays, we can see that at a certain liquidity index, shear strength increases with an increase in the cement content, i.e. the two types of kaolin clay gain almost the same amount of shear strength due to cementation bonding, if they are mixed at a similar cement content and liquidity index. However, this is not necessarily true for all types of clays mixed with Portland cement. As can be seen in Fig. 4-6, at a similar liquidity index, Ottawa clay samples with 6.4% cement gain much higher strengths than samples of kaolin with 11.1% cement. Fig. 4-7 better illustrates this phenomenon; Ottawa and Nanticoke clays, which are both predominantly illitic, gain significantly higher strengths than does kaolin clay, when mixed with cement at a similar cement content and a similar liquidity index or water content. This again illustrates the importance of soil mineralogical composition in cement stabilization. It can be seen in Fig. 4-7 that a threshold exists for cemented EPK kaolin clay at  $c=8.7\%$ ; as the cement content exceeds this value, the strength starts to increase with a greater rate.

Miura et al. (2001) introduced clay-water/cement ratio,  $w/c$ , as a key parameter in understanding the behaviour of soft clays admixed with Portland cement. Horpibulsuk et al. (2003) and Horpibulsuk et al. (2005) further discussed the importance of this

parameter and proposed an expression for calculating the amount of added cement to stabilize soft clays based on in-situ water content of the soil. The results of this study corroborate the previous findings regarding the importance of clay-water/cement ratio. To better illustrate the results, cement-moisture ratio,  $c/w$ , which is the ratio of cement content (%) to initial moisture content of the clay (%), is used instead of water-cement ratio,  $w/c$ . The cement-moisture ratios of the samples tested with laboratory shear vane have been plotted against 28-days undrained shear strength and sensitivity in Fig. 4-8 and Fig. 4-9, respectively. Similar trends are observed in both graphs as the undrained shear strength and sensitivity are closely related. In both figures, a trend can be detected for each type of clay, i.e. the shear strength and sensitivity increase with an increase in  $c/w$ . Moreover, the increase in the strength with an increase in  $c/w$  ratio is non-linear; the rate of increase in strength and sensitivity with  $c/w$  ratio increases as the  $c/w$  ratio gets larger. However, due to their mineralogical variations, different clay types follow different paths, and the overall data are rather scattered. To create an expression that may be used to predict the behaviour of cemented clays accounting for clay mineralogy, an additional parameter that takes into account the effect of clay type is introduced.

On inspection of Fig. 4-8 and Fig. 4-9, it can be seen that at similar cement-moisture ratios, the highest and lowest strength and sensitivity belong to samples of Ottawa clay and EPK kaolin, respectively. For Ottawa clay, a cement-moisture ratio of 8 results in a shear strength of 160 kPa, while for EPK kaolin, a cement-moisture ratio as high as 18.5 only gives a shear strength of 149 kPa. Further comparison between the activity numbers from Table 4-1 and the results presented in Fig. 4-8 and Fig. 4-9 confirms that the higher the activity number ( $A$ ) of the soil, the higher its strength and

sensitivity at a given cement-moisture ratio. Plotting the undrained strength and sensitivity against cement-moisture ratio multiplied by  $A^{2.7}$  is found to eliminate the effect of variations in the type of clay and results in a unique curve for all four clays (Fig. 4-10 and Fig. 4-11). Again, this relationship is non-linear; the strength and sensitivity increase with an increase in  $(A^{2.7})*(c/w)$ , indicating that higher soil activity leads the cementing agent producing more and/or stronger bonds.

#### **4.4.3 Predicting the behaviour of artificially cemented clays**

##### *4.4.3.1 Undrained shear strength: Unconfined compression*

The data presented in Fig. 4-10 and Fig. 4-11 only cover a small range of clay types and cement and moisture contents, due to the limitations of using the laboratory shear vane device; cement contents for ground improvement applications are typically higher. Unlike laboratory shear vane, unconfined compression tests can be performed on samples with much higher undrained shear strengths. Several researchers have performed such experiments on various types of artificially cemented clay. Their results, in terms of undrained shear strength, are also plotted versus the  $c/w$  ratio of the specimens in Fig. 4-12 along with the results presented in the previous figures. The kaolinite data include those for EPK, Speswhite, and Rotoclay kaolins. Although some scatter exists within the data for each clay type, a clear pattern of increase in strength with  $c/w$  ratio is shown. Ariake clay, which has an activity number of 1.18, gains much higher strengths than Hong Kong, Bangkok, or Singapore clays the activity of which is 0.91, 0.87, and 0.76, respectively, confirming the importance of soil activity in the gained strength. Based on this concept, a relationship between activity,  $c/w$  ratio and undrained shear strength was defined using the parameter  $\beta$  below:

$$\beta = A^{3.2} \times \frac{c}{w} \quad (4.7)$$

Fig. 4-13 shows the values of undrained shear strength normalised by the atmospheric pressure,  $P_a$  (=101.3 kPa), plotted against this new  $\beta$  parameter. The relationship can be satisfactorily modelled by the following polynomial function:

$$\frac{c_{u,28days}}{P_a} = 128.36\beta^2 + 6.49\beta + 0.42 \quad (4.8)$$

This correlation enables an estimate of the shear strength of a cemented soil based on  $c/w$  ratio and activity. It should be noted that Eq. (4.8) has been derived for  $\beta$  values less than 0.4 and may not be applicable to cemented clays with  $\beta > 0.4$ . During the analysis, it was also noticed that in some cases,  $w/c$  ratios lower than 3 ( $c/w$  values higher than 0.33) resulted in lower than expected undrained shear strength especially for Bangkok and Singapore clays. This indicates that the addition of high amounts of cement to certain soils might also reduce the efficiency of the soil improvement process.

#### 4.4.3.2 Undrained shear strength: Triaxial

In addition to data from unconfined compression tests, the results of several undrained triaxial test studies on artificially cemented clays were used in the analysis. All of these cemented specimens had been isotropically consolidated to 25, 50, or 100 kPa before undrained shearing, but in all cases, the consolidation pressure had been considerably lower than the yield stress of the specimens, indicating that the cementitious bonds had remained relatively intact. Fig. 4-14 shows the undrained shear strengths measured with triaxial tests for confined specimens, consolidated below the yield stress, versus those measured for unconfined specimens with unconfined compression or shear

vane tests. As it shows, the slope of the line fitting the data is very close to unity and indicates only 4% of increase in strength due to confinement. Hence, Eq. (4.8), which is obtained based on the results of unconfined compression tests, should be able to predict undrained shear strengths obtained from triaxial experiments, as long as the yield consolidation pressure is not exceeded. It can also be concluded that if the isotropic loading phase does not cause the soil to yield, confinement does not have any significant effect on the undrained shear strength of cemented clays. This indicates that cemented clay pre-yield behaviour is predominantly dependent on the cementitious bonds, rather than friction. Fig. 4-15 shows the peak undrained shear strengths, obtained from triaxial experiments, versus the  $\beta$  parameter. It can be seen that the same trend observed in Fig. 4-13 also exists for the triaxial specimens. The dashed line, which represents Eq. (4.8), can also provide a reasonable match for the results of this specific form of undrained triaxial test.

#### 4.4.3.3 *Compressibility and vertical yield stress: Oedometer*

Since they usually have high moisture contents and void ratios, cemented clays are often meta-stable and undergo a significant amount of compression after the yield point is passed. Thus, accurate prediction of the yield stress can be very important in the design of cement-clay mixtures for settlement problems. Analysis was conducted on the results of oedometer experiments performed for this study, along with those found in the literature. Fig. 4-16 shows the relationship between  $\sigma'_y$ , which is the vertical yield stress obtained from oedometer tests, and undrained shear strength,  $c_u$ , for the cemented specimens. All of the  $\sigma'_y$  values have been calculated based on Casagrande method (ASTM D2435). The results support the suggestion by Horpibulsuk et al. (2004b) that a linear relationship



exists between vertical yield stress and undrained shear strength of cement-admixed clays. Although there is significant scatter in the data, it can be seen that the  $c_u/\sigma'_y$  ratio is insensitive to the PI. An average value of  $c_u/\sigma'_y = 0.22$  is found, which is similar to those proposed by Mesri (1975) and re-evaluated by other researchers (Trak et al., 1980; Trak and Leroueil, 1983; Jamiolkowski et al., 1985; Mesri 1989) for normally consolidated and lightly overconsolidated clays. Horpibulsuk et al. (2004b) performed similar analysis on cemented Bangkok, Tokyo, and Ariake clays and suggested a range of 0.23 to 0.36 for  $c_u/\sigma'_y$  with a slightly higher average value of 0.29. The significant scatter in  $c_u/\sigma'_y$  ratios is better illustrated in Fig. 4-17. The variation in the data may originate in the effect of additional cementitious fines on the plasticity index, which has not been accounted for in the results.

Since vertical yield stress correlates with undrained shear strength and also represents the strength of the cemented material, we would expect it to correlate with the  $\beta$  parameter as well. Using Eq. (4.8) and assuming a  $c_u/\sigma'_y$  ratio of 0.22, the vertical yield stress of the cemented material can be approximated as follows:

$$\frac{\sigma'_{y,28days}}{P_a} = 583.45\beta^2 + 29.5\beta + 1.9 \quad (4.9)$$

This also enables the estimation of the yield stress based on cement-moisture ratio and the activity number. Fig. 4-18 gives the values of  $\sigma'_y$  versus the  $\beta$  parameter with Eq. (4.9) plotted as a dashed line. The solid line represents the relationship obtained by using a  $c_u/\sigma'_y$  ratio of 0.29, as suggested by Horpibulsuk et al. (2004b). As the figure shows, using a ratio of 0.22 provides a better approximation of the overall data.

Most naturally structured soft clays experience a relatively abrupt destructuration once the virgin yield stress is exceeded (e.g. Burland, 1990). In comparison, numerous consolidation test results on artificially cemented clays have confirmed that this type of structured material undergoes a more gradual breakage of the bonds and has an approximately linear post-yield compression curve (e.g. Miura et al., 2001; Rotta et al., 2003; Lorenzo and Bergado, 2004; Xiao and Lee, 2008; Kamruzzaman et al., 2009). In common with other structured soils, however, this compression line still converges with the intrinsic compression line (ICL) of the material at high pressures (Burland, 1990; Liu and Carter, 2002; Rotta et al., 2003). Fig. 4-19 illustrates an example of the different compression behaviours of naturally structured and artificially cemented clays. Naturally structured Ottawa clay undergoes higher amount of pre-yield compression followed by an abrupt post-yield destructuration, while the artificially cemented material displays a stiffer pre-yield response and a more gradual post-yield breakage of the cementitious bonds. Even though artificially cemented clays have been previously treated as “structured soils”, they may be better represented in  $e : \sigma'_v$  space using two limiting relationships (Horpibulsuk et al., 2004b); one a near horizontal pre-yield line followed by a pseudo-normal compression line (Fig. 4-20). This pseudo-normal compression line (so called since it may represent a family of changing gradient lines with destructuration) can be represented by the following equation:

$$e = e_{\lambda} - C_c \cdot \log(\sigma'_v) \quad (4.10)$$

Where  $e_{\lambda}$  is the void ratio at  $\sigma'_v = 1$  kPa, and  $C_c$  is the “average” slope of the compression line. As Fig. 4-20 indicates, steeper compression lines (i.e. greater values of

$C_c$ ) are expected to be accompanied by higher interception values ( $e_\lambda$ ) for a specific type of clay.

A number of researchers have previously proposed normalised such relationships for predicting the generalized compression behaviour of reconstituted or artificially cemented clays (e.g. Nagaraj and Srinivasa Murthy, 1986; Burland, 1990; Nagaraj et al., 1993; Nagaraj et al., 1994; Horpibulsuk et al., 2004b). These relationships are often written in the following form:

$$\frac{e}{e_n} = a - b \cdot \log(\sigma'_v) \quad (4.11)$$

Where  $a$  and  $b$  are normalized parameters usually obtained from experimental data, and  $e_n$  is a normalizing void ratio. The void ratio at the liquid limit ( $e_L$ ) has been commonly used as the normalizing void ratio for reconstituted clays (e.g. Burland, 1990; Nagaraj et al., 1994). However,  $e_{100}$  (the void ratio at  $\sigma'_v = 100$  kPa) was used also by Horpibulsuk et al. (2004b) to normalize the compression behaviour of both cemented and uncemented material. At a void ratio equal to  $e_L$ , reconstituted clays have an undrained shear strength ( $c_u$ ) of approximately 1.7 kPa (Wood, 1990), corresponding to a vertical effective stress ( $\sigma'_v$ ) of 7.7 kPa (based on the relationship suggested by Mesri, 1975). Likewise,  $e_\lambda$  (the void ratio at  $\sigma'_v = 1$  kPa) can also be used as another pressure based, normalizing reference volume. Since  $e_L$  is a reference state associated with remoulded soil states, it is essentially arbitrary with respect to cemented and structured soils. In such cases,  $e_\lambda$  is preferred since it is a fixed and known reference volume for an effective stress of 1 kPa, without the uncertainty associated with the determination of liquid limit states. Therefore, Eq. (4.11) can be rewritten as:

$$\frac{e}{e_{\lambda}} = 1 - \frac{b}{a} \cdot \log(\sigma'_v) \quad (4.12)$$

Here the ratio  $b/a$  is equal to  $C_c/e_{\lambda}$  (Eq. 4.10). An examination of relationships with a similar form to Eq. (4.11) that are available in the literature reveals that the  $b/a$  ratio ( $\sim C_c/e_{\lambda}$  ratio) has a very narrow range (between 0.21 and 0.23) and appears to be independent of the value of the  $a$  and  $b$  parameters (e.g. Nagaraj and Srinivasa Murthy, 1986; Nagaraj et al., 1993; Nagaraj et al., 1994; Horpibulsuk et al., 2004b). Interestingly, assuming that the vertical yield stress at the liquid limit is approximately 7.7 kPa, the relationship proposed by Burland (1990) between  $C_c^*$  (for reconstituted clay) and  $e_L$  also gives a  $C_c^*/e_{\lambda}$  ratio of approximately 0.21.

The average  $e_{\lambda}$  and  $C_c$  parameters were also obtained for the cemented clays studied herein. The results again suggest that a linear relationship exists between the two parameters (Fig. 4-21):

$$C_c = 0.23e_{\lambda} \quad (4.13)$$

Hence, as was previously suggested by Horpibulsuk et al. (2004b), the same relationship (Eq. 4.13) governs both the destructuration/compression of artificially cemented clays and the compression of reconstituted material. This resemblance in behaviour could be related to the more gradual breakage of the bonds within the artificially cemented clay; although the bond breakage is brittle, it appears to be sufficiently disseminated to lead to elasto-plastic frictional behaviour of the cemented material. It should be noted that the data used to find Eq. (4.13) were obtained by oedometer tests for a vertical effective stress ( $\sigma'_v$ ) range of 5 to 8000 kPa and initial void ratios ( $e_0$ ) less than 5.5.

Combining Eqs. (4.12) and (4.13) gives:

$$\frac{e}{e_{\lambda}} = 1 - 0.23 \log(\sigma'_v) \quad (4.14)$$

Thus, Eq. (4.14) produces a number of discrete lines in the  $e - \log(\sigma'_v)$  space, restricting the pseudo-normal compression lines to only moving on certain paths. Therefore, having the value of  $e_0$  for a particular cemented clay and estimating  $\sigma'_y$  from Eq. (4.9), we can utilize Eq. (4.14) to calculate the values of  $e_{\lambda}$  and  $C_c$  for a specific cemented clay.

A further parametric study was completed to provide a deeper understanding and enable the prediction of  $e_{\lambda}$  and  $C_c$  directly from the basic geotechnical properties of the cemented material. As illustrated in Fig. 4-22, for a given vertical yield stress ( $\sigma'_y$ ), a higher post-curing void ratio ( $e_0$ ) will increase the post-yield destructuration rate of the material and will thus be accompanied by an increase in  $e_{\lambda}$  and  $C_c$ . Similarly, for a given initial void ratio, a higher yield stress results in greater  $e_{\lambda}$  and  $C_c$  values. Based on the information available in the literature it seems reasonable that there are links between form of cementation, post-curing void ratio, yield stress, and clay mineralogy. Horpibulsuk et al. (2004b) suggested that the slope of the compression line ( $C_c$ ) only depends on the cement content and clay type and is independent of the moisture content. However, the results of this study indicate that the water content can also affect the compressibility of a cemented clay. Since a number of researchers have previously correlated the slope of the compression line of remoulded clays with the plasticity index or liquid limit (Burland, 1990; Wood, 1990), the liquidity index was used in calculations

to incorporate the effect of index properties with water content. After analyzing the oedometer data, it was found that the post-yield compressibility of the cemented clays is related to the liquidity index (LI), cement content (c), and activity number (A). Hence, a new parameter,  $\alpha$ , was defined as follows:

$$\alpha = LI.c.A^{3.2} \quad (4.15)$$

The calculated  $C_c$  values are plotted versus the new  $\alpha$  parameter in Fig. 4-23 for different cemented clays. A clear trend can be detected in the results, providing the following relationship:

$$C_c = 0.85\alpha^{0.32} \quad (4.16)$$

Similarly, a relationship for estimating the representative  $e_\lambda$  values based on the  $\alpha$  parameter can be obtained (Fig. 4-24):

$$e_\lambda = 3.70\alpha^{0.32} \quad (4.17)$$

Substitution of Eq. (4.16) and Eq. (4.17) into Eq. (4.10) provides:

$$e = 3.7\alpha^{0.32} [1 - 0.23 \log(\sigma'_v)] \quad (4.18)$$

Previous works have shown that addition of Portland cement reduces the swelling potential of the improved clay (Bhattacharja et al., 2003). Based on the available data, the slope of the swelling line,  $C_s$ , of a specific clay seems to be essentially constant and independent from the cement content. However, for a certain type of clay, cemented samples with higher  $\beta$  parameters tend to have slightly lower swelling indices (Fig. 4-25). Although a clear relationship cannot be obtained due to the scatter that exists in the data, this suggests that higher cementation does indeed reduce the tendency of the soil to rebound due to unloading.

It should be noted that the equations presented in this section are derived based on the available data for a number of clays with a certain range of water content, cement content, and activity number; the properties of these clays, along with the type of experiments performed on each soil, are given in Table 4-3.

## 4.5 Discussion

Two interesting observations emerge from the results presented herein. First, the strength of artificially cemented clays continues to increase with curing time even beyond three years. Second, the gained strength appears to be a function of the activity number of the soil, as well as the w/c ratio. Both of these phenomena can be further understood by taking into account the importance of the secondary pozzolanic reactions.

The hydration reaction is primarily responsible for the short-term gain in strength, since it produces the primary bonds and reduces the moisture content of the mixture. In contrast, the pozzolanic reactions commence when adequate concentration of hydroxide ions is produced and a certain level of alkalinity is reached in the pore fluid (Herzog and Mitchell, 1963; Xia and Lee, 2008). The secondary reactions are considerably slower than the hydration reaction and can continue for months, or even years after mixing (Bergado et al., 1996), but only if there is sufficient calcium available in the matrix and the pH continues to be elevated. According to Stocker (1975), the first layer of secondary reaction products covers the particle surfaces and impedes further reactions. For the reactions to continue,  $\text{Ca(OH)}_2$  must diffuse through the first layer of reaction products (Stocker, 1975; Croft, 1967b; Bhattacharja et al., 2003). This process of diffused cementation occurs at a much slower rate than the hydration reaction of the cement.

Furthermore, clay minerals are much more chemically reactive than concrete aggregates, so the pozzolanic reaction is more pronounced in artificially cemented clays than it would be in concrete or other granular pastes. Thus the continuation of strength gain, which differentiates the hardening response of a cemented clay from that of concrete, could be attributed to the secondary pozzolanic reactions between the clay minerals and cement hydration products.

As stated by Bergado et al. (1996), if cured and mixed under similar conditions, soils with higher pozzolanic reactivity obtain greater strengths, compared to those with lower reactivity. Most physicochemical phenomena that happen in the soil material are affected by the available surface area (Bhattacharja et al., 2003). Croft (1967a) suggested that expansive minerals, which have high surface areas and activity numbers, consume the lime released during the cement hydration more rapidly. Therefore, secondary reactions commence sooner and are of higher intensity in active clays. This could result in higher gained strength in such soils, compared to those of soils with lower activity number. In addition, based on the work of Wissa et al. (1965), the amount of cementitious material produced during the pozzolanic reaction depends on the amount of clay fraction as well as that of amorphous silica and alumina that exist in the soil; having a high surface area and therefore a high activity, poorly crystallized minerals react more readily with calcium hydroxide and produce more cement. Hence, the activity number of the clay is an important parameter in determining the gained strength, as it represents the ability of the material to be involved in the pozzolanic reactions.

Although the results of this work imply that secondary reactions, which are often deemed to be lower in significance compared to the hydration reactions, play an



important role in providing the cemented clay with strength, further elucidation from a micro-structural point of view is needed to understand the mechanisms by which these reactions affect the cemented soil behaviour.

Soil aggregates or clusters are the fundamental components controlling soil behaviour. They can act almost as single particles and interact to generate the strength and stiffness in clays (Mitchell and Soga, 2005). Even if the soil-cement mixture is thoroughly blended, clay particles will form aggregates enclosed by the cement slurry (Croft, 1967b; Bergado et al., 1996). As a result, during the curing period, hydration reactions form hardened cement bodies, which connect to develop a matrix within the soil mass (also called skeletal cementation by Bhattacharja et al., 2003). On the other hand, since pozzolanic reactions take place between clay minerals and cement hydration products and hence happen near particle surfaces, they form cementitious material on or near the surface of clay particles. Stocker (1975) suggests that these reactions take place exclusively at particle edges. The produced cement pastes the flocculated particles together at points of contact, developing hardened soil bodies and increasing the strength of soil aggregates (Herzog and Mitchell, 1963). The strength of the improved soil will depend on the strength of the hardened cement and soil skeleton (Bergado et al., 1996). However, because the cementitious bonds produced by pozzolanic reactions (CSH and CAH) have a lower strength compared to those created by the hydration reactions [mainly  $C_3S_2H_3$ ] (Bergado et al., 1996), the strength of the whole cemented soil mass should mainly depend on the strength of the hardened aggregates, rather than that of hydrated cement bodies. This is consistent with the findings of Saitoh et al. (1985), who suggested that the lower the pozzolanic reactivity of the soil, the higher its strength dependence on

the properties of hardened soil bodies. Thus, the strength of the cemented material is greatly dependent on the degree and intensity of the secondary reactions.

Nonetheless, it should be borne in mind that the results presented here are only for soils with low to medium values of activity number (less than 1.2). Very high activity numbers, which are usually encountered in smectitic clays, may have a negative effect on the strength of cement treated soil (Bergado et al., 1996), as the high affinity of these clays for lime depletes the soil-cement mixture from calcium hydroxide and reduces the pH of the aqueous phase (Croft, 1967a), decreasing the solubility of silicates and aluminates and bringing the secondary reactions to a halt (Herzog and Mitchell, 1963; Bergado et al., 1996). This is further evidenced by the works of Croft (1967), Noble and Plaster (1970), Ingles and Metcalf (1972), and Osula (1996), who suggested that Portland cement treatment does not develop much strength in highly active clays, such as montmorillonite, and recommended that it be replaced by lime stabilization, so that there would be enough lime available in the mix to keep the pH at a high level.

Other factors could also be contributing to the observed behaviour of the artificially cemented clays. Noble and Plaster (1970), who examined the chemical reactions in mixtures made by the addition of Portland cement to various types of clay, suggested that the hydration reaction takes place at a slower rate in clays than concrete. This is in accord with the statement made by Bergado et al. (1996) that cemented soil is better improved if type III Portland cement, which provides relatively high early strengths, is used rather than type I. Therefore, one reason why the rate of increase in the strength of cemented clays is lower than that of concrete could be the slower hydration reaction due to the presence of clay minerals.

Additionally, to better understand the importance of the activity number compared to that of water-cement ratio, we can further deliberate on Abrams' law. This law states that the strength of concrete only depends on the ratio of "free" water content to the cement content in the mix (Abrams, 1918). To successfully apply Abrams' law, which was originally intended for concrete material, to artificially cemented clays, we should address the main difference between concrete and clay constituents. Unlike concrete, clayey materials tend to absorb significant amounts of water. The extent of this absorption depends on the specific surface area, which can be represented by the activity number of the soil. The amount of adsorbed water increases in more active clays, which usually have higher surface area and charge deficiency (Mitchell and Soga, 2005). Hence, there will be less "free" water available in the paste for cement hydration. This adsorbed water is not taken into account when water-cement ratio ( $w/c$ ) is calculated. Consequently, comparing two different clays that have been artificially cemented and have similar clay water-cement ratios, the one having a higher activity would probably gain higher strength, since the actual  $w/c$  ratio is lower than the nominal value.

A few researchers have tried to correlate the mechanical behaviour of cemented clays with the index properties (e.g. Woo, 1971). Using the activity number for modelling the behaviour of cemented soil appears to have an advantage over using other soil parameters such as plasticity index, liquid limit, or clay content. As postulated by Skempton (1953), since the plasticity of a soil depends on both the type and amount of clay existing in that soil, the activity number is constant for a certain type of material, regardless of its index properties. This eliminates the variability observed in index

properties of different samples taken from the same site and makes possible further interpretations based on the activity number.

Analysis of the available data in the literature has shown that at very low water-cement ratios ( $w/c < 3$ ), the strength gained by the mixture after 28 days is in some cases lower than the expected value. In almost all of these cases, this low  $w/c$  ratio was accompanied by a very high cement content ( $c > 25\%$ ) and a relatively low liquidity index ( $LI < 1.5$ ). According to Abrams' law, lower water cement ratios should result in higher strength. However, there seems to be a threshold for water cement ratio of cemented clays, after which the cementation process will not be as efficient as expected. It is known in concrete technology that for every 4 portions of cement, 1 portion of water is needed to fully complete the hydration reaction ( $w/c = 0.25$ ). However, concrete mixtures obtained by using this minimum ratio are often considered too dry, because some of the water is absorbed by the sand and gravel grains and is not available to participate in the hydration reaction. The same phenomenon appears to happen to a greater extent in clays. At low liquidity indices, the soil still has a "plastic state". Hence, inter-aggregate free water, which is not absorbed to the clay surface, will not be available to complete the hydration reaction of cement. Croft (1967b) reported that the development of cementitious material consumes the free moisture existing in interconnected voids, and unless additional water is added, a strong pattern of intersecting cracks will develop in the cemented soil, reducing the strength and stiffness of the material. Horpibulsuk et al. (2003) also showed that cement contents higher than 40% ( $w/c < 4.5$ ) resulted in lower than expected undrained shear strength in cement-treated high water content Ariake clay. In addition, Horpibulsuk et al. (2010) illustrated for a

compacted silty clay that at cement contents higher than 11% ( $w/c < 2.4$ ), the addition of cement did not noticeably increase the strength, and that at cement contents higher than 30% ( $w/c < 0.9$ ), the strength reduced even further with addition of cement to the mixture. Therefore, due to the high surface area of the clayey material, the minimum  $w/c$  ratio required for clay-cement mixtures is much higher than that of concrete. Thus,  $w/c$  ratio higher than 3 appears to produce more efficiency for the cementation process.

In addition to soil activity and the  $w/c$  ratio, the presence of organics in the soil could also significantly affect the cementation process and its outcome. High organic contents hinder the development of strength in soils improved by Portland cement or lime (Tremblay et al., 2001). Miura et al. (1986) suggest that cement rather than lime should be used in the stabilization of organic clays to achieve better results. None of the clays described in this study contain amounts of organic material large enough to affect the cementation process. Thus, caution should also be exercised should the equations provided herein be used for organic clays.

## **4.6 Summary and Conclusions**

To study the effect of soil mineralogy and activity on the properties of cemented clays and to find important parameters governing cement-treated clay mechanical behaviour, the results of laboratory shear vane, unconfined compression, undrained triaxial, and oedometer tests on many different types of clays treated with Portland cement have been examined. The results indicate that:

- Although the hydration rate of ordinary Portland cement used to stabilize clay drops significantly with curing time, cemented clays continue to gain significant

amount of strength long after the curing has started. This behaviour, which is not typical of cement-based construction materials can be attributed to slower pozzolanic reactions that happen between clay minerals and cementation products.

- The hardening trend of artificially cemented clays is independent of the water and cement contents, and the clay type and can be modelled by a power function.
- The residual shear strength of the cemented soil increases with increasing curing time or cement content. This has been attributed to the changes in the frictional properties of the destructured soil and therefore the secondary reactions, which produce cementitious bonds within the soil aggregates. However, the residual strength increases with a slower rate than does the peak strength. Consequently, the sensitivity and brittleness of the material increases with curing time and cement content.
- Undrained shear strength of cemented clays is dependent on their mineralogical composition. The strength of the cement-treated material is also closely related to its cement-water ratio,  $c/w$ . However, this ratio alone is not enough to predict the behaviour of cemented clays. The activity of the soil, which represents its mineralogy and its ability to be involved in chemical reactions, should also be considered. The higher the activity number, the higher the strength of the clay at a given cement-moisture ratio.

- Using the empirical  $\beta$  and  $\alpha$  parameters has enabled the prediction of the undrained shear strength, vertical yield stress, and the slope of the compression line for artificially cemented clays.
- Undrained shear strength of cemented clays is independent of the confining pressure of the soil, unless the yield stress has been exceeded. Therefore, the pre-yield behaviour of cement-treated clays is predominantly dependent on cementation bonds, rather than friction.
- Pozzolanic reactions are believed to be responsible for the observed behaviour of cemented clays. A matrix of hardened material is formed in the soil body due to hydration of cement. However, the hydration process does not necessarily produce bonds between the particles. Since they form cementing bonds between the soil particles and within the aggregates, the pozzolanic reactions are responsible for the overall strength of the cement-cluster network.
- Due to the slow rate of the pozzolanic reactions, the hardening of cemented clay takes much longer than that of concrete. In addition, more active clays, which react more rapidly and intensely with the hydration products and therefore produce more cementing bonds, gain higher amount of strength due to artificial cementation.
- Water/cement ratios less than 3 may hinder the cementation process and reduce its efficiency.

## 4.7 Acknowledgements

The authors would like to express their gratitude to the Natural Sciences and Engineering Research Council of Canada, NSERC, and The University of Western Ontario for providing financial support for this work.

## 4.8 References

- Abrams, D.A. (1918). "Design of concrete mixtures." Bulletin 1, Structural Materials Research Laboratory, Lewis Institute, Chicago.
- Bergado, D.T., Anderson, L.R., Miura, N., and Balasubramaniam, A.S. (1996). "Soft ground improvement in lowland and other environments." American Society of Civil Engineers (ASCE) Press, New York, U.S.A.
- Bergado, D.T., Ruenkairergsa, T., Taeisiri, Y., and Balasubramaniam, A.S. (1999). "Deep soil mixing used to reduce embankment." *Ground Improvement*, 3, 141–162.
- Bhattacharja, S., Bhatta, J. I., and Todres, H. A. (2003). "Stabilization of Clay Soils by Portland Cement or Lime - A Critical Review of Literature." PCA R&D Serial No. 2066, Portland Cement Association, Skokie, Illinois USA.
- Broms, B.B. (1986). "Stabilization of soft clay with lime and cement columns in Southeast Asia." Applied Research Project RP10/83, Nanyang Technical Institute, Singapore.
- Burland, J.B. (1990). "On the compressibility and shear strength of natural clays." *Geotechnique*, 40(3): 329–378.



- Chew, S.H., Kamruzzaman, A.H.M., and Lee, F.H. (2004). "Physicochemical and Engineering Behavior of Cement Treated Clays." *Journal of Geotechnical and Geoenvironmental Engineering*, 130(7), 696–706.
- Croft, J.B. (1967a). "The influence of soil mineralogical composition on cement stabilization." *Geotechnique*, 17, 119–135.
- Croft, J.B. (1967b). "The structures of soils stabilized with cementitious agents." *Engineering Geology*, 2(2), 63–80.
- Flores, R.D.V., Di Emidio, G., and Van Impe, W.F. (2010). "Small-Strain Shear Modulus and Strength Increase of Cement-Treated Clay". *Geotechnical Testing Journal*, 33(1), 62–71.
- Herzog, A., and Mitchell, J.K. (1963). "Reactions accompanying the stabilization of clay with cement." *Highway Research Board Record*, 36, 146–171.
- Horpibulsuk, S., Miura, N., and Nagaraj, T.S. (2003). "Assessment of strength development in cement-admixed high water content clays with Abrams' law as a basis." *Geotechnique*, 53(4), 439–444.
- Horpibulsuk, S., Miura, N., and Bergado, D.T. (2004a). "Undrained shear behavior of cement admixed clay at high water content." *Journal of Geotechnical and Geoenvironmental Engineering*, 130(10), 1096–1105.
- Horpibulsuk, S., Bergado, D.T., and Lorenzo, G.A. (2004b). Compressibility of cement-admixed clays at high water content. *Geotechnique*, 54(2), 151–154.

- Horpibulsuk, S., Miura, N., and Nagaraj, T.S. (2005). "Clay-water/cement ratio identity for cement admixed soft clays." *Journal of Geotechnical and Geoenvironmental Engineering*, 131(2), 187–192.
- Horpibulsuk, S., Rachan, R., Chinkulkijniwat, A., Raksachon, Y., and Suddeepong, A. (2010). "Analysis of strength development in cement-stabilized silty clay from microstructural considerations." *Journal of Construction and Building Materials*, 24, 2011–2021.
- Ingles, O.G., and Metcalf, J.B. (1972). "Soil stabilization: principles and practice." Butterworths, Sydney, N.S.W.
- Jamiolkowski, M., Ladd, C.C., Germaine, J.T., and Lancelotta, R. (1985). "New developments in field and laboratory testing of soils." *Proceedings of the 11th International Conference on Soil Mechanics and Foundation Engineering*, A.A. Balkema, San Francisco, CA, 57–153.
- Kainourgiaki, G. (2004). "Development of artificial structure in clays." M.Sc. Thesis, Division of Civil Engineering, University of Dundee, Dundee, UK.
- Kamruzzaman, A.H.M., Chew, S.H., and Lee, F.H. (2009). "Structuration and Destructuration Behavior of Cement-Treated Singapore Marine Clay Cement-Treated Singapore Marine Clay." *Journal of Geotechnical and Geoenvironmental Engineering*, 135(4), 573–589.
- Kasama, K., Ochiai, H., and Yasufuku, N. (2000). "On the stress-strain behaviour of lightly cemented clay based on an extended critical state concept." *Soils and foundations*, 40(5): 37–47.

- Kirwan, K. (2003). "The collapse behaviour of clayey soil." Honours Year Project, Division of Civil Engineering, University of Dundee, Dundee, UK.
- Kogure, K., Yamaguchi, H., and Ohira Y. (1988). "Comparison of strength and soil thrust characteristics among different soil shear tests." *Journal of Terramechanics*, 25(3), 201–221.
- Lee, F.H., Lee, Y., Chew, S.H., and Yong, K.W. (2005). "Strength and modulus of marine clay – cement mixes." *Journal of Geotechnical and Geoenvironmental Engineering*, 131(2), 178–186.
- Liu, M.D., and Carter, J.P. (2002). "A Structured Cam Clay model." *Canadian Geotechnical Journal*, 39(6), 1313–1332.
- Lorenzo, G.A., and Bergado, D.T. (2004). Fundamental parameters of cement-admixed clay – New approach." *Journal of Geotechnical and Geoenvironmental Engineering*, 130(10), 1042–1050.
- Mesri, G. (1975). "New design procedure for stability of soft clays: Discussion." *Journal of the Geotechnical Engineering Division, ASCE*, 101(GT4), 409–412.
- Mesri, G. (1989). "A reevaluation of  $s_{u(mob)}=0.22\sigma'_p$  using laboratory shear tests". *Canadian Geotechnical Journal*, 26(1), 162–164.
- Mitchell, J.K., and Soga, K. (2005). "Fundamentals of Soil Behavior, 3rd Ed." John Wiley & Sons, Hoboken, New Jersey.
- Miura, N., Koga, Y., and Nishida, K. (1986). "Application of a deep mixing method with quicklime for the Ariake clay ground." *Journal of Japan Society of Soil Mechanics and Foundation Engineering*, 34(4), 5–11.

- Miura, N., Horpibulsuk, S., and Nagaraj, T.S. (2001). "Engineering behavior of cement stabilized clay at high water content." *Soils and Foundations*, 41(5), 33–45.
- Nagaraj, T. S., and Srinivasa Murthy, B. R. (1986). "A critical reappraisal of compression index equations." *Geotechnique*, 36(1), 27–32.
- Nagaraj, T.S., Pandian, N.S., and Narasimha Raju, P.S.R. (1993). "Stress state-permeability relationships for fine-grained soils" *Geotechnique*, 43(2), 333–336.
- Nagaraj, T. S., Pandian, N. S., Narasimha Raju, P. S. R. (1994). "Stress-state-permeability relations for overconsolidated clays. *Geotechnique*, 44(2), 349–352.
- Nagaraj, T.S., Miura, N., Yaligar, P., and Yamadera, A. (1996). "Predicting strength development by cement admixture based on water content." *Proc. IS-Tokyo 96, 2<sup>nd</sup> Int. Conf. on Ground Improvement Geosystems, Grouting, and Deep mixing, Tokyo*, 1, 431–436.
- Nagaraj, T.S., and Miura, N. (2001). "Soft clay behaviour – analysis and assessment." A.A. Balkema, Rotterdam, The Netherlands.
- Narendra, B.S., Sivapullaiah, P.V., Suresh, S. and Omkar, S.N. (2006). "Prediction of unconfined compressive strength of soft grounds using computational intelligence techniques: A comparative study." *Computers and Geotechnics*, 33, 196–208.
- Noble, D.F., and Plaster, R.W. (1970). "Reactions in Portland cement – clay mixtures." Final report, Virginia Highway Research Council, Charlottesville.
- Osula, D.O.A. (1996). "A comparative evaluation of cement and lime modification of laterite." *Engineering Geology*, 42, 71–81.

- Ritchie, S. (2004). "A study of the collapse of structured clay." Honours Year Project, Division of Civil Engineering, University of Dundee, Dundee, UK.
- Rotta, G.V., Consoli, N.C., Prietto, P.D.M., Coop, M.R., and Grahams, J. (2003). "Isotropic yielding in an artificially cemented soil cured under stress." *Geotechnique*, 53(5), 493–501.
- Saitoh, S., Suzuki, Y., and Shirai, K. (1985). "Hardening of soil improved by deep mixing method." *Proc. 11<sup>th</sup> Intl. Conf. Soil Mech. and Found. Eng'g, Helsinki, Finland*, 947–950.
- Serota, S., and Jangle, A. (1972). "A direct-reading pocket shear vane." *Civil Engineering, ASCE*, 42(1), 73–74.
- Skempton, A.W. (1953). "The colloidal activity of clays". *Proceedings of 3rd international conference on soil mechanics and foundation engineering, Zurich, Switzerland*, 1, 57–61.
- Stocker, P.T. (1975). "Diffusion and Diffuse Cementation in Lime- and Cement-Stabilized Clayey Soils - Chemical Aspects." *Australian Road Research, Vermont South, Victoria, Australia*, 5(9), 6–47.
- Tan, T.S., Goh, T.L., and Yong, K.Y. (2002). "Properties of Singapore marine clays improved by cement mixing." *Geotechnical Testing Journal*, 25(4), 1–12.
- Trak, B., and Leroueil, S. (1983). "New stability method for embankments on clay foundations: Discussion." *Canadian Geotechnical Journal*, 20(2), 366–366.

- Trak, B., La Rochelle, P., Tavenas, F., Leroueil, S., and Roy, M. (1980). "A new approach to the stability analysis of embankments on sensitive clays." *Canadian Geotechnical Journal*, 17(4), 526–544.
- Tremblay, H., Leroueil, S., and Locat, J. (2001). "Mechanical improvement and vertical yield stress prediction of clayey soils from eastern Canada treated with lime or cement." *Canadian Geotechnical Journal*. 38, 567–579.
- Uddin , K. (1994). "Strength and deformation behaviour of cement treated Bangkok clay." Doctoral Thesis, Asian Institute of Technology, Bangkok, Thailand.
- Uddin, K., Balasubramaniam, A.S., and Bergado, D.T. (1997). "Engineering behavior of cement-treated Bangkok soft clay." *Geotechnical Engineering Journal*, 28(1), 89–119.
- Wissa, A.E.Z., Ladd, C.C., and Lambe, T.W. (1965). "Effective stress strength parameters of stabilized soils." *6th Int. Conf. on Soil Mechanics and Foundation Engineering, Montréal*, 1, 412–416.
- Woo, S.M. (1971). "Cement and Lime stabilization of selected lateritic soils." M. Eng. Thesis No. 409, Asian Institute of Technology, Bangkok, Thailand.
- Wood, D.M. (1990). "Soil behaviour and critical state soil mechanics." Cambridge University Press, Cambridge.
- Xiao, H.W., and Lee, F.H. (2008). Curing Time Effect on Behavior of Cement Treated Marine Clay. *Proceedings of world academy of science, engineering and technology*, 33, 71–78.

Yin, J.H., and Lai, C.K. (1998). "Strength and stiffness of Hong Kong marine deposits mixed with cement." *Geotechnical Engineering Journal*, 29(1), 29–44.

**Table 4-1.** Geotechnical properties of the four types of clay tested by the authors

Soil Characteristic	Ottawa clay	Nanticoke clay	EPK kaolin	Speswhite kaolin
Liquid limit, LL (%)	52	48	61	64
Plastic limit, PL (%)	24	23	36	34
Plasticity Index, PI (%)	28	25	25	30
Specific Gravity, $G_s$	2.82	2.73	2.61	2.62
Clay fraction (<2 $\mu\text{m}$ , %)	43	48	53	61
Activity, A	0.65	0.52	0.47	0.49



**Table 4-2.** Properties of the cemented soil samples from the literature used in the time analysis (Fig. 4-3)

Soil	Plastic limit, PL (%)	Liquid limit, LL (%)	Plasticity index, PI (%)	Clay content (%)	Activity, A	Water content, w (%)	Liquidity index, LI	Cement content, c(%)	Reference
Home Rule kaolin	33	64	31	88	0.35	45	0.4	1, 5, 10, 20	Croft (1967a)
Rotoclay kaolin	30	58	28	40	0.70	115	3.0	10, 20	Flores et al. (2010)
Singapore marine clay	35	87	52	68	0.76	120	1.6	5, 10, 20, 30, 40, 50, 60	Kamruzzaman et al. (2009)
	25	90	65	a	a	100	1.2	10, 15, 20	Xia and Lee (2008)
						133	1.7	50	
						150	1.9	77, 100	
32	72	40			90, 120, 150	1.5, 2.2, 3	10, 20, 30	Tan et al. (2002)	
Bangkok clay	43	103	60	69	0.87	86, 106, 136, 166	0.7, 1, 1.5, 2	10	Lorenzo and Bergado (2004)
						80	1.3	5, 7.5, 10, 12.5, 15, 20, 25, 30, 35, 40	Uddin et al. (1997); Uddin (1994); Bergado et al. (1999)
Ariake clay	60	125	65	55	1.18	106	0.7	10, 20	Horpibulsuk et al. (2003)
						130	2.0	10, 15, 20	
						160	2.5	15, 20	
Illite	a	a	a	a	a	118	a	10, 20	Nagaraj et al. (1996)
Brown Indian clay	23	60	37	46	0.80	60, 90, 120	1, 1.8, 2.6	3 - 24 <sup>b</sup>	Narendra et al. (2006)
Brown Indian clay	a	a	a	a	a	62	a	10, 20	Nagaraj et al. (1996)
Black cotton Indian clay	35	97	62	61	1.02	97, 145, 194	1, 1.8, 2.6	5 - 19.5 <sup>b</sup>	Narendra et al. (2006)
Black cotton Indian clay	a	a	a	a	a	72	a	10, 20	Nagaraj et al. (1996)
Black cotton Indian clay	a	a	a	a	a	86	a	20	Nagaraj et al. (1996)
Red earth Indian clay	15	38	23	32	0.72	38, 57, 76	1, 1.8, 2.7	4 - 15 <sup>b</sup>	Narendra et al. (2006)

a: no data available, b: data ranging between the two values

**Table 4-3.** Properties of the cemented soil samples from the literature used in the parametric study

Soil	Activity, A	Water content, w (%)	Cement content, c (%)	Type of test	Reference
Rotoclay kaolin	0.70	115	10, 20	UC	Flores et al. (2010)
Singapore marine clay	0.76	90 - 150 <sup>b</sup>	5 - 77 <sup>b</sup>	UC, CIU, Oed.	Kamruzzaman et al. (2009); Xiao and Lee (2008); Tan et al. (2002); Chew et al. (2004); Lee et al. (2005)
Bangkok clay	0.87	80 - 209 <sup>b</sup>	3 - 35 <sup>b</sup>	UC, CIU, Oed.	Lorenzo and Bergado (2004); Uddin et al. (1997); Uddin (1994); Horpibulsuk et al. (2004b)
Ariake clay	1.18	106 - 250 <sup>b</sup>	6 - 33 <sup>b</sup>	UC, CIU, Oed.	Miura et a. (2001); Horpibulsuk et al. (2003); Horpibulsuk et al. (2004a); Horpibulsuk et al. (2004b); Horpibulsuk et al. (2005)
Hong Kong clay	0.91	60 - 100 <sup>b</sup>	5 - 20 <sup>b</sup>	UC, CIU	Yin and Lai (1998)
Brown Indian clay	0.80	60 - 120 <sup>b</sup>	3 - 24 <sup>b</sup>	UC	Narendra et al. (2006)
Black cotton Indian clay	1.02	97 - 194 <sup>b</sup>	5 - 19.5 <sup>b</sup>	UC	Narendra et al. (2006)
Red earth Indian clay	0.72	38 - 76 <sup>b</sup>	4 - 15 <sup>b</sup>	UC	Narendra et al. (2006)
Louiseville clay	0.56	122	5.3	Oed.	Tremblay et al. (2001)
Bothkennar clay	0.50	60	4.2	CIU, Oed.	Kirwan 2003; Kainourgiaki (2004)

b: data ranging between the two values

UC: unconfined compression test

CIU: conventional undrained triaxial test

Oed: oedometer test

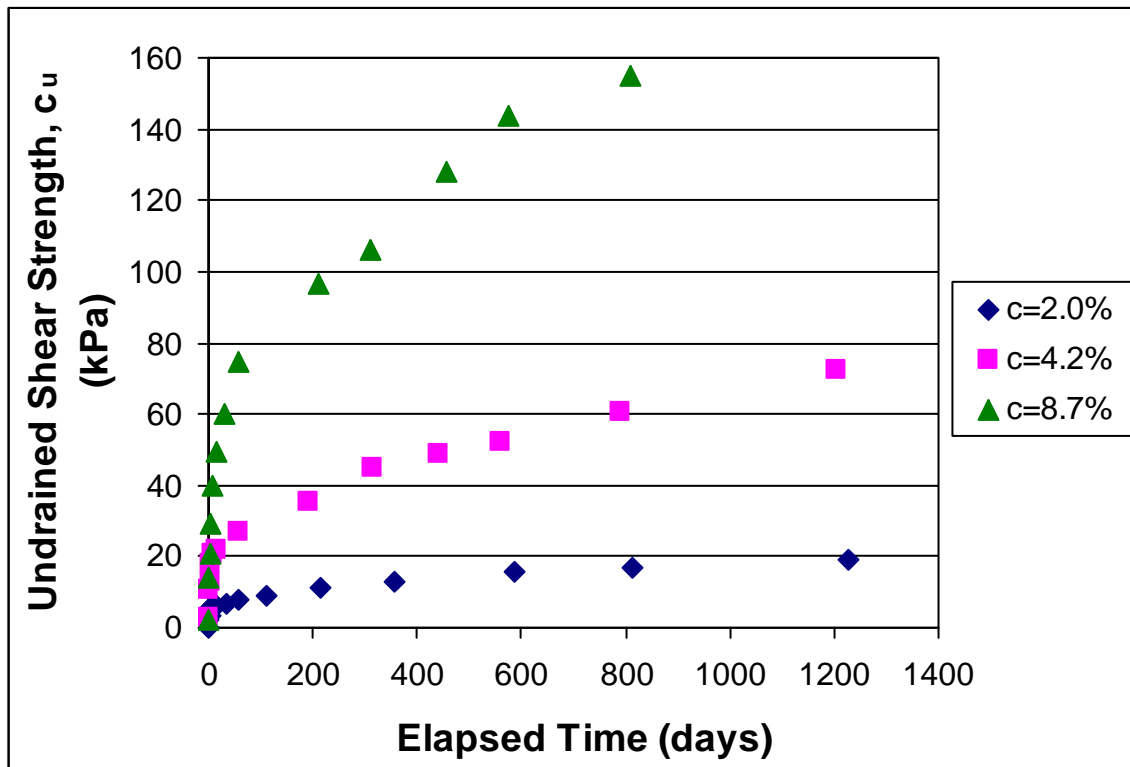


**Fig. 4-1.** Shear strength of artificially cemented Nanticoke clay (LI=3, w=98%) with curing time

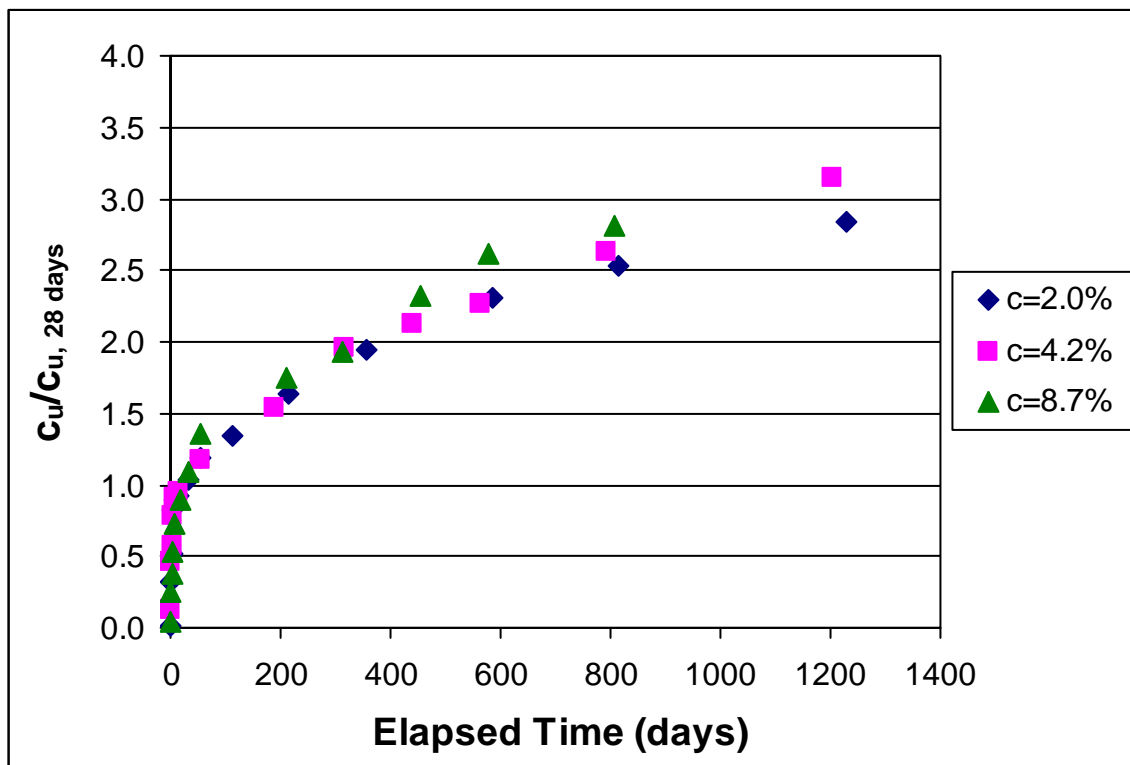


**Fig. 4-2.** Normalized undrained shear strength of cemented Nanticoke clay (LI=3, w=98%) versus curing time

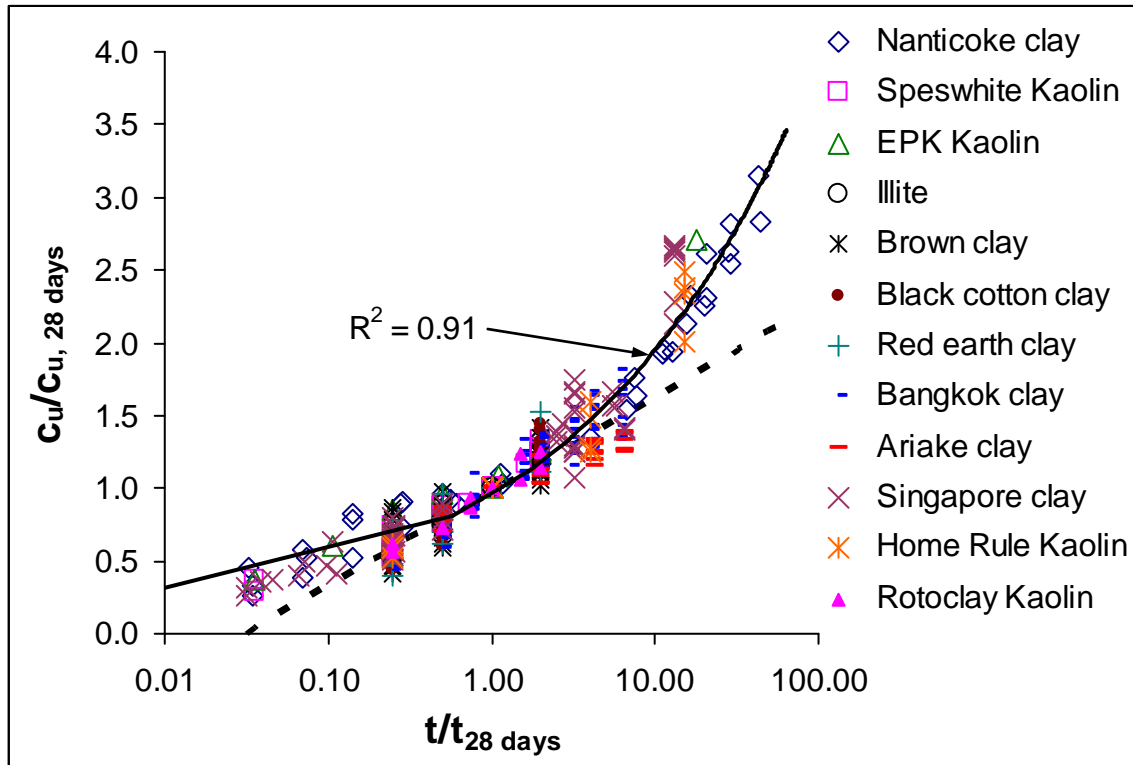


**Fig. 4-3.** Normalized undrained shear strength of various clays cemented with Portland cement versus curing time

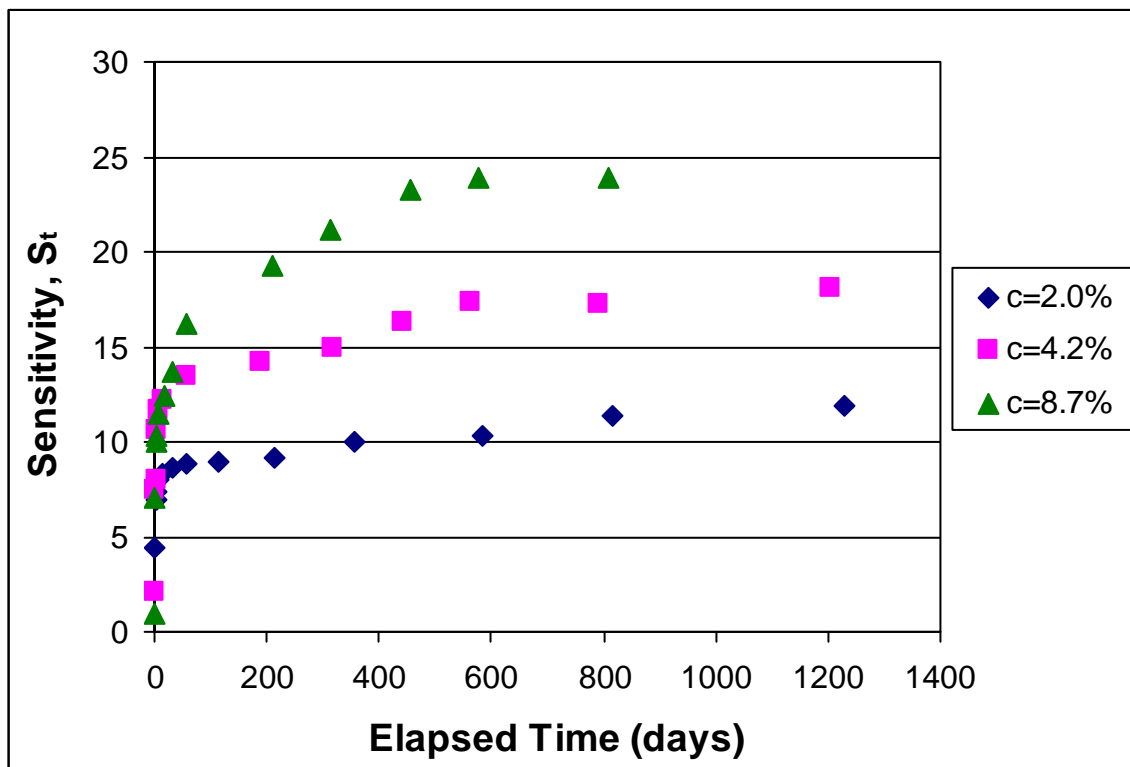


**Fig. 4-4.** Sensitivity of artificially cemented Naticoke clay (LI=3, w=98%) with curing time

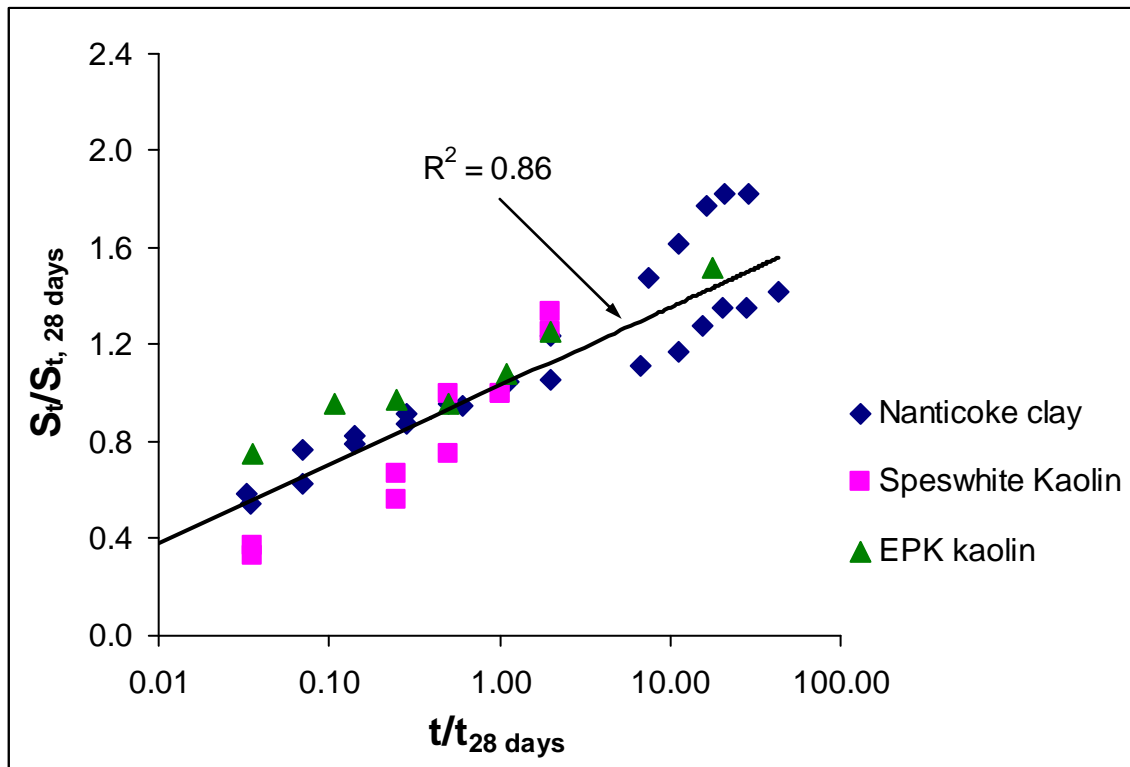


**Fig. 4-5.** Normalized sensitivity of three cemented clays versus curing time

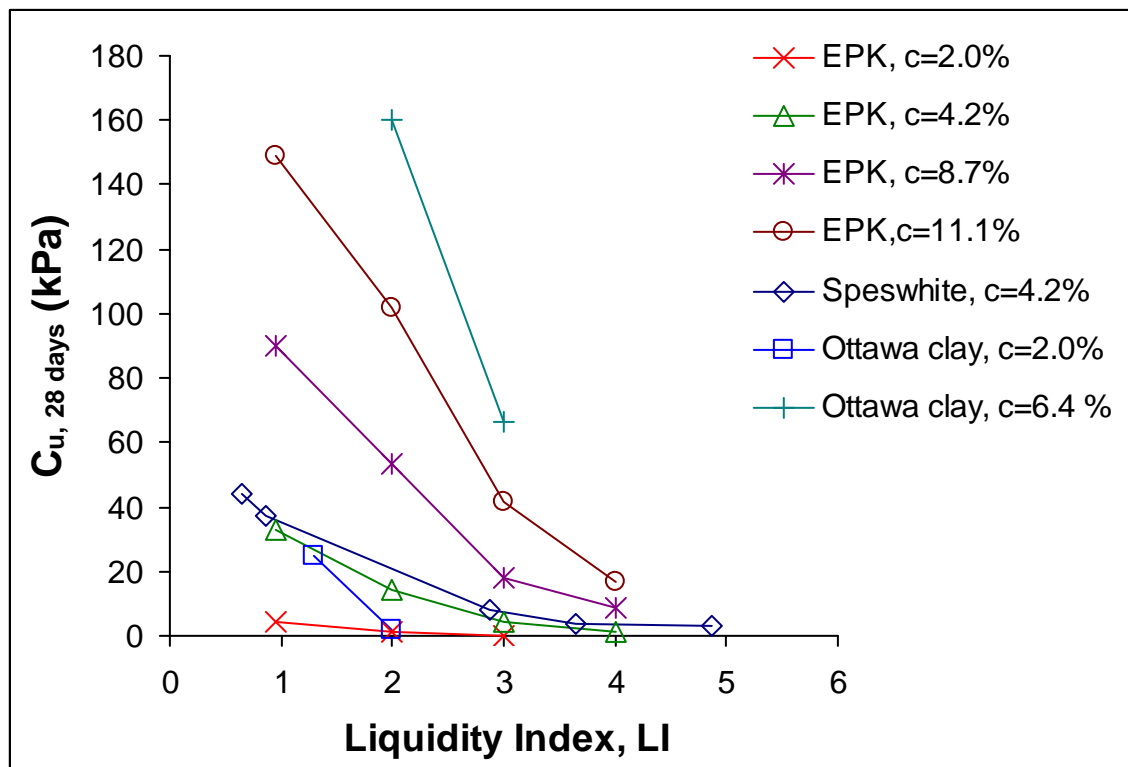


**Fig. 4-6.** The relationship between liquidity index and undrained shear strength for soils with different cement contents



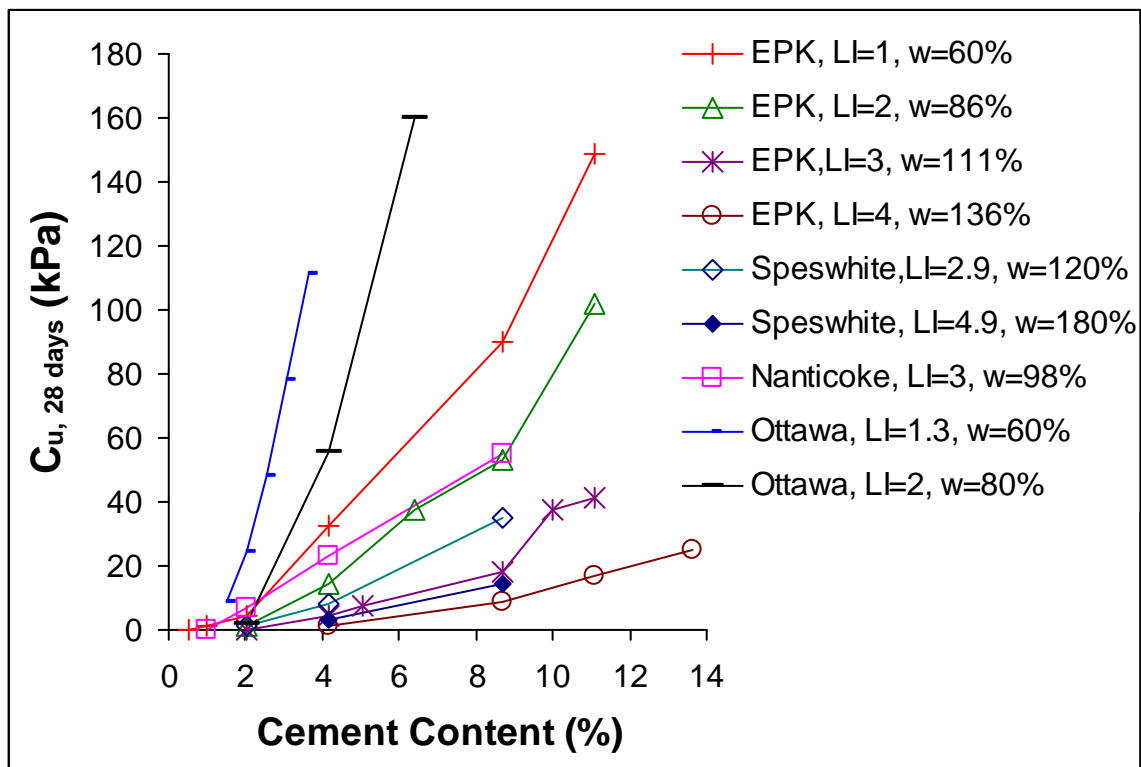


**Fig. 4-7.** The relationship between cement content and undrained shear strength for soils with different liquidity indices

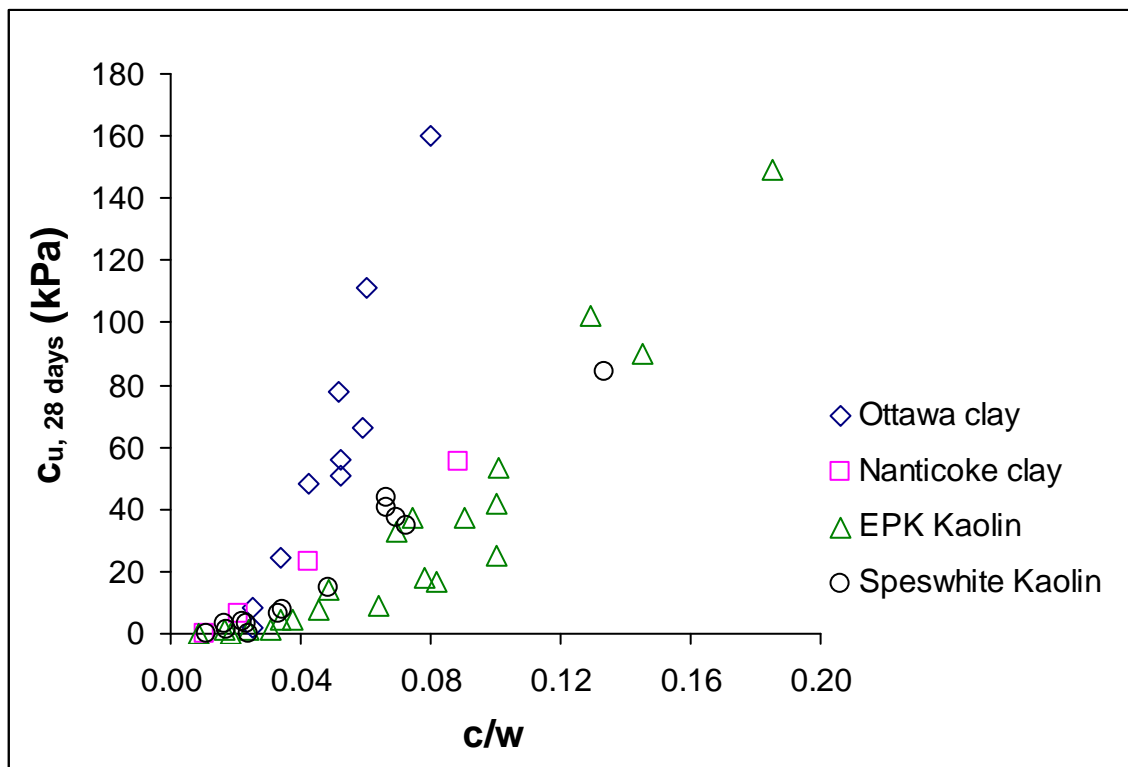


**Fig. 4-8.** Variations in undrained shear strength with cement-moisture ratio (c/w)

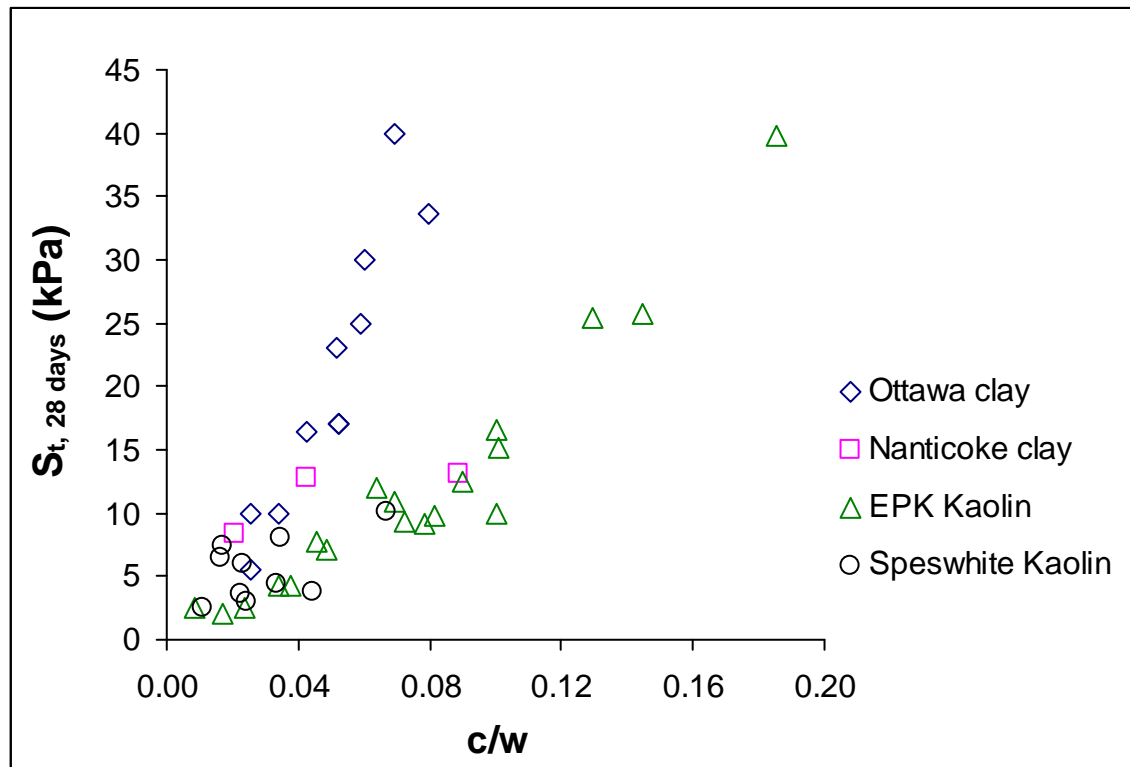


**Fig. 4-9.** Variations in sensitivity with cement-moisture ratio ( $c/w$ )

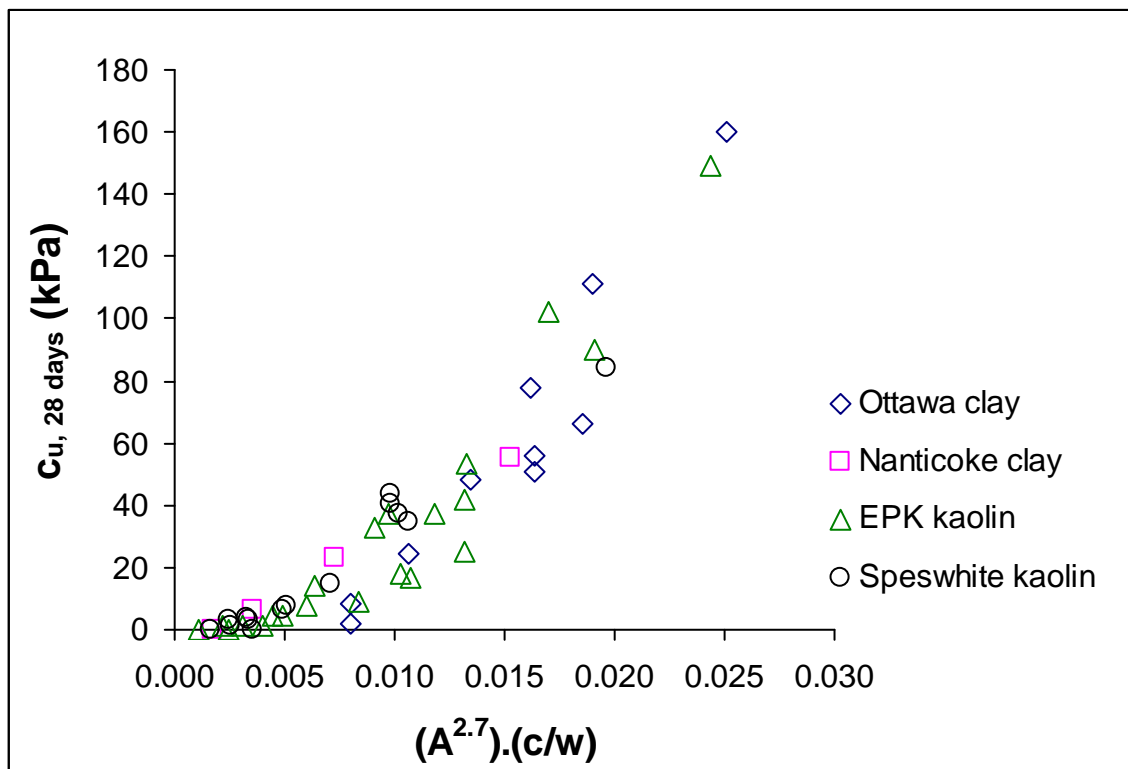


**Fig. 4-10.** The effect of cement-moisture ratio ( $c/w$ ) and activity number ( $A$ ) on undrained shear strength

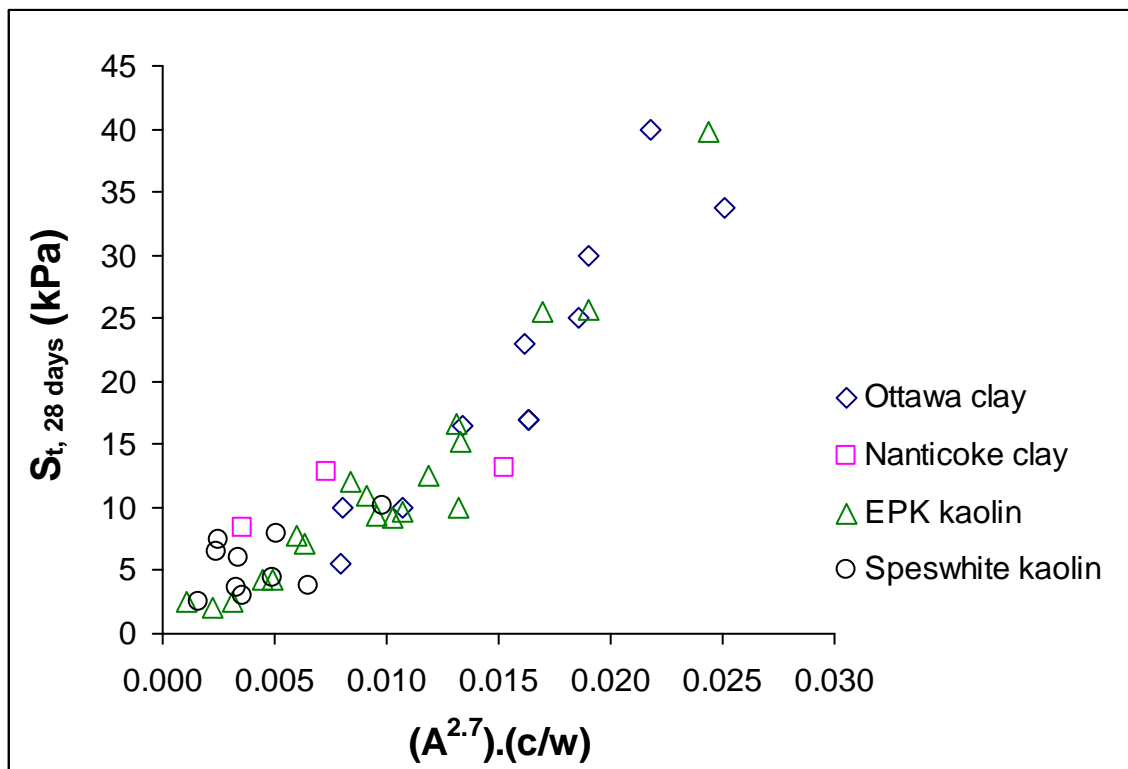


**Fig. 4-11.** The effect of cement-moisture ratio ( $c/w$ ) and activity number ( $A$ ) on sensitivity

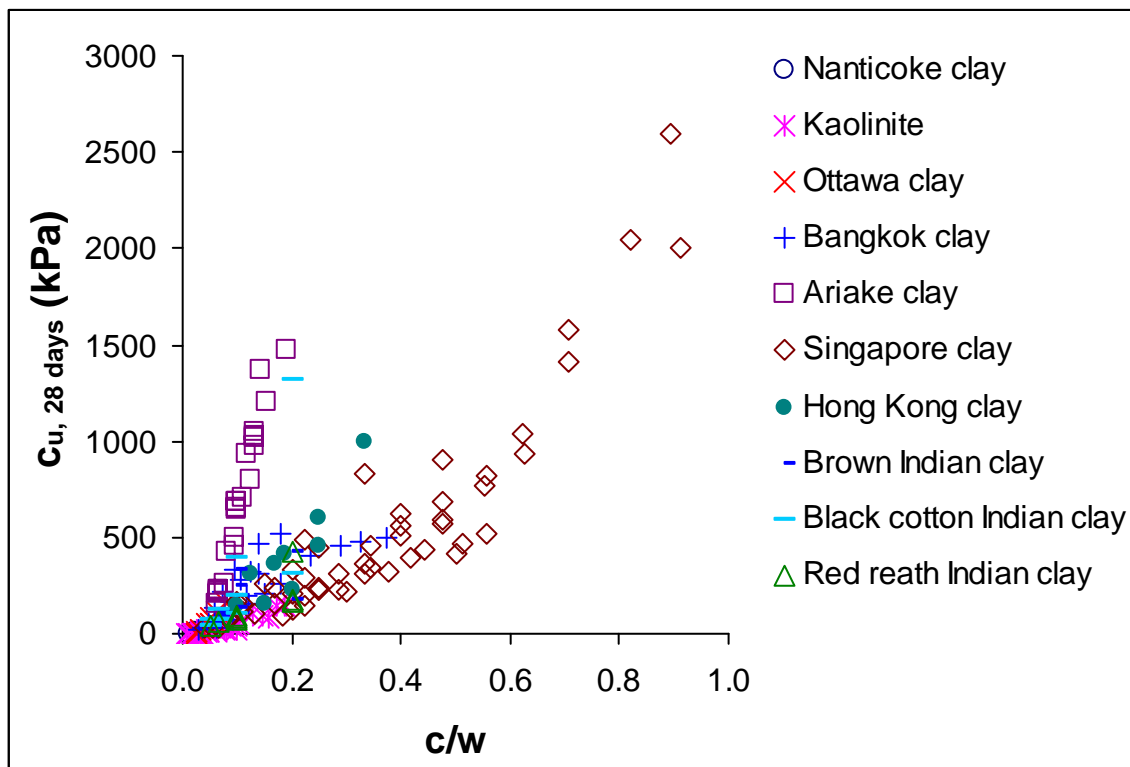


**Fig. 4-12.** Undrained shear strength of various cemented clays versus cement-moisture ratio

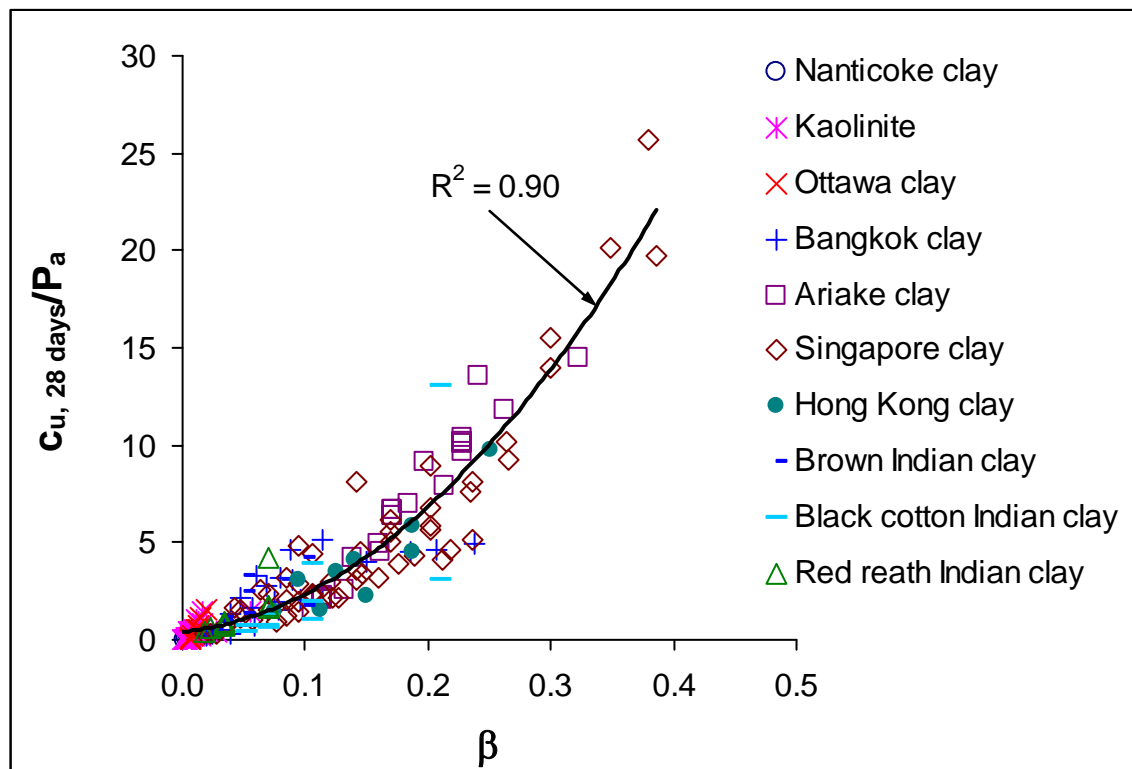


**Fig. 4-13.** Undrained shear strength of various clays versus the  $\beta$  parameter

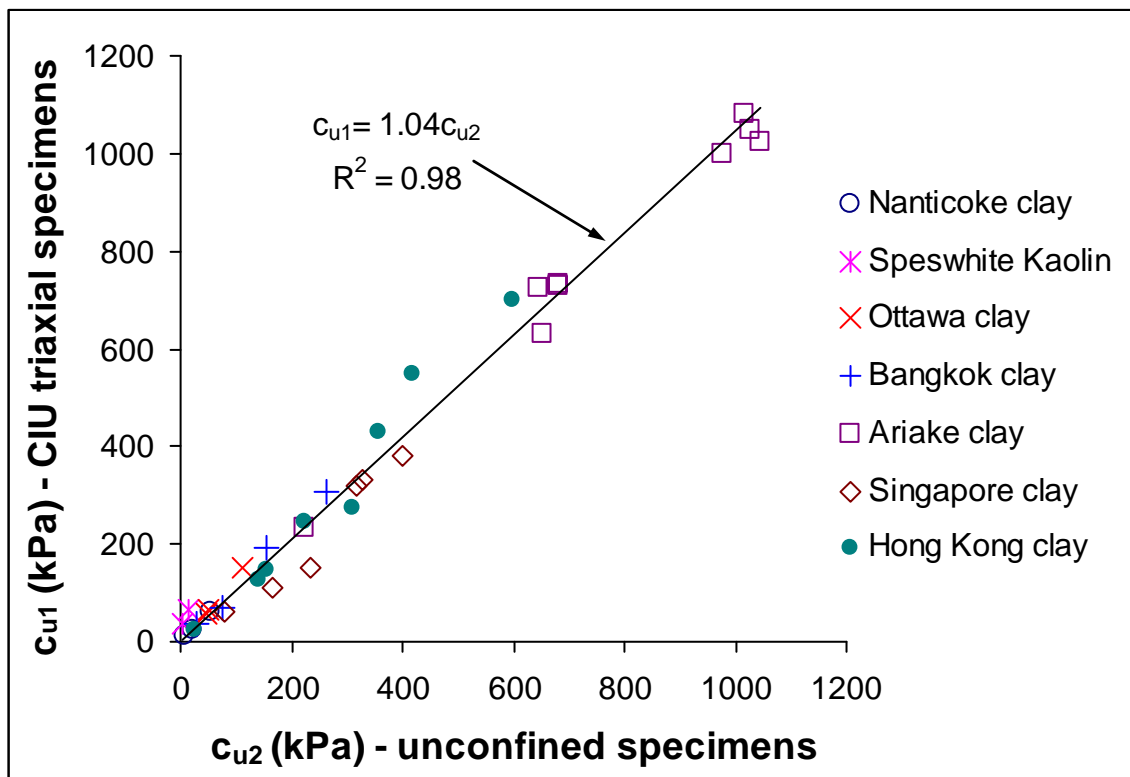
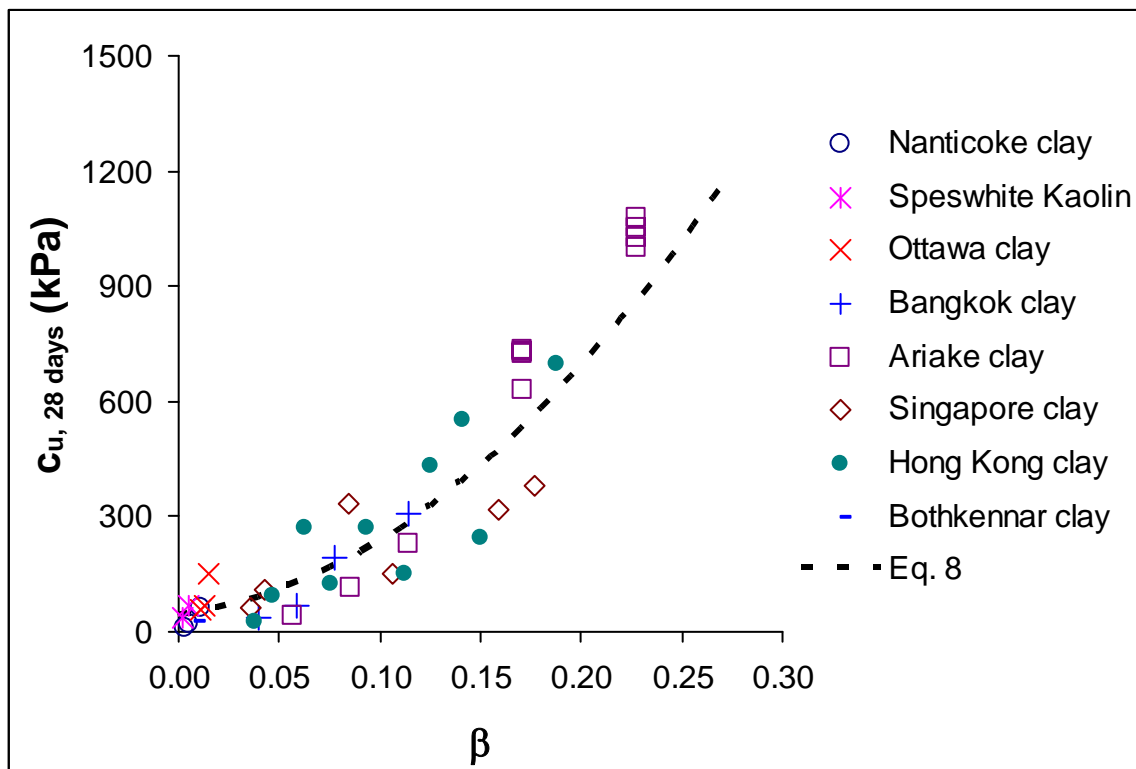


Fig. 4-14. Comparison between undrained shear strengths obtained for consolidated triaxial specimens and those obtained for unconfined specimens





**Fig. 4-15.** Undrained shear strength from CIU triaxial tests versus the  $\beta$  parameter

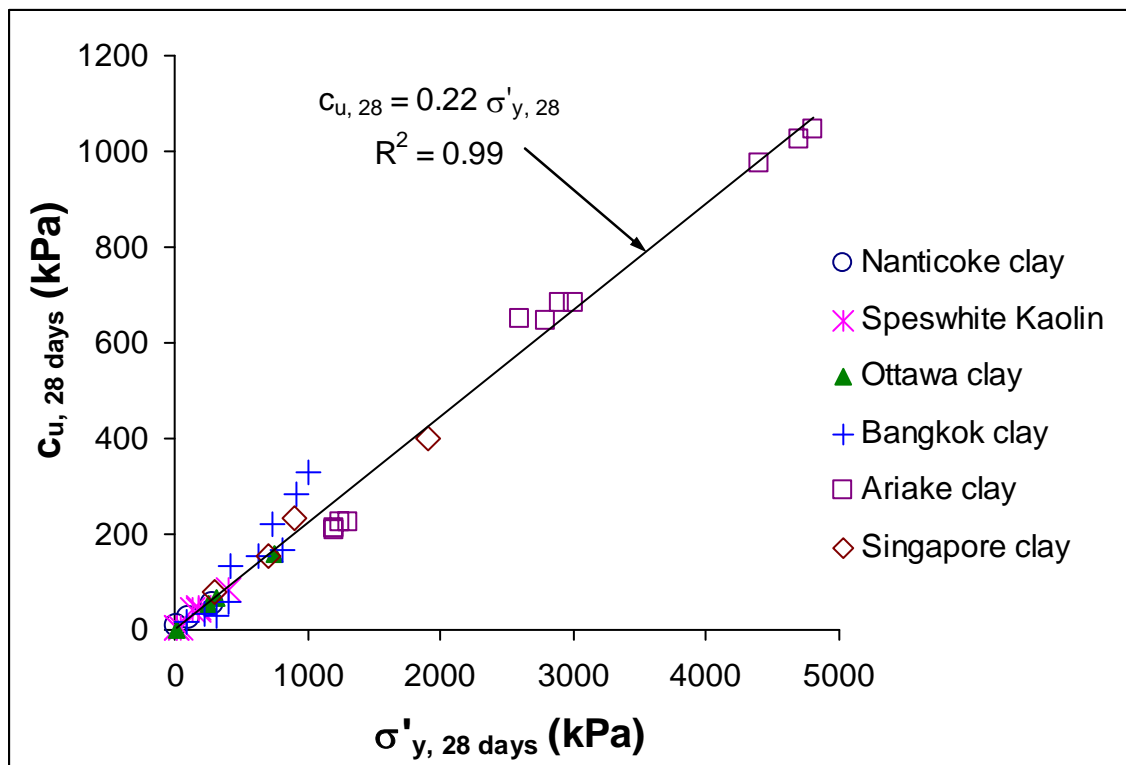
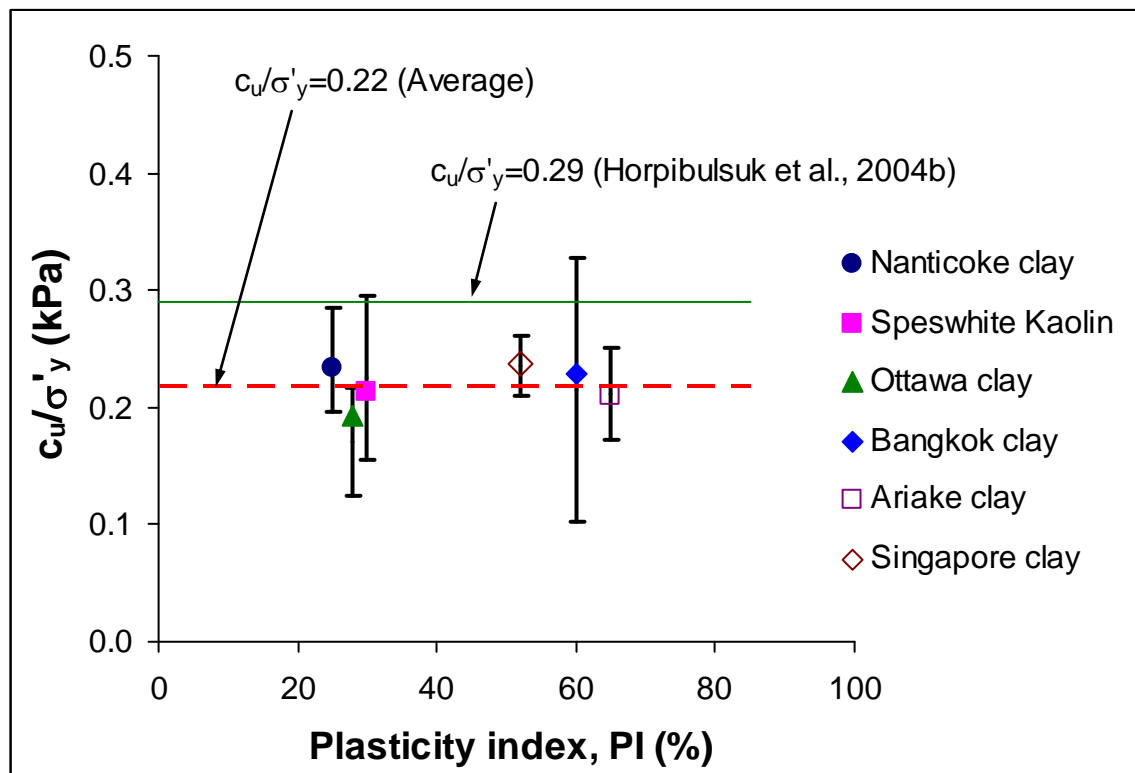
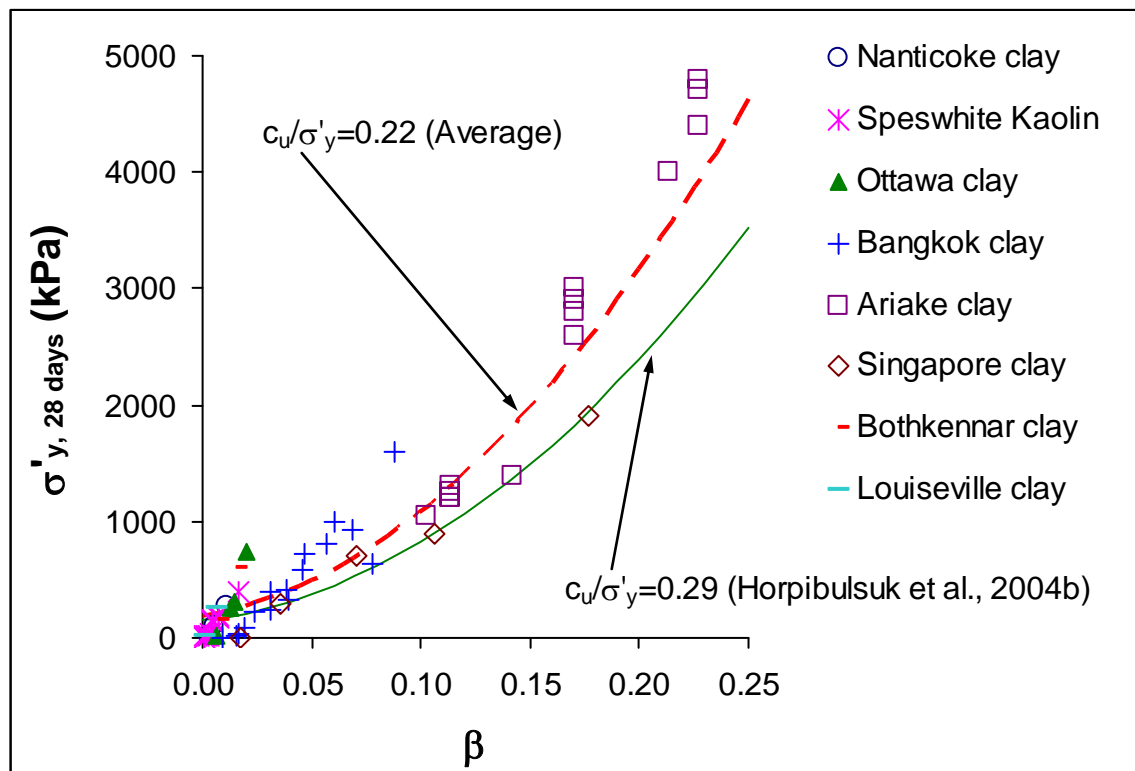


Fig. 4-16. Vertical yield stress versus undrained shear strength



**Fig. 4-17.** The relationship between the plasticity index and the  $c_u/\sigma'_y$  ratio



**Fig. 4-18.** The relationship between vertical yield stress and  $\beta$

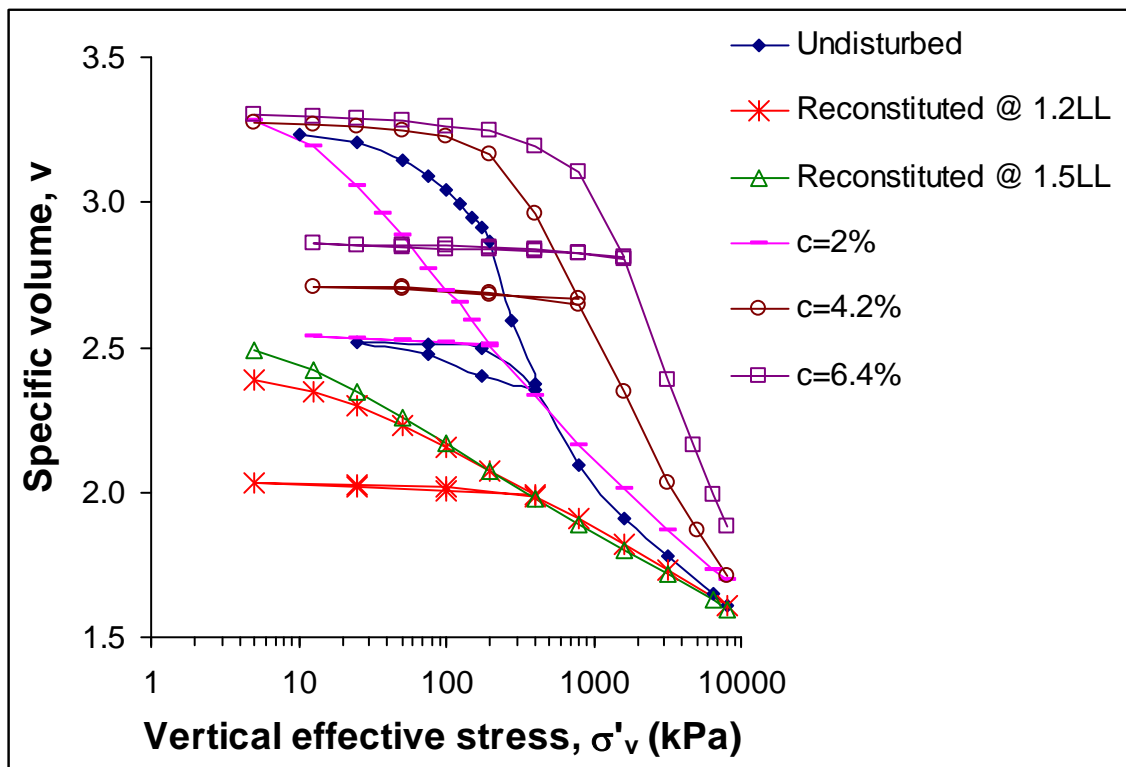


**Fig. 4-19.** One dimensional compression curves for undisturbed, artificially cemented, and reconstituted Ottawa clay.

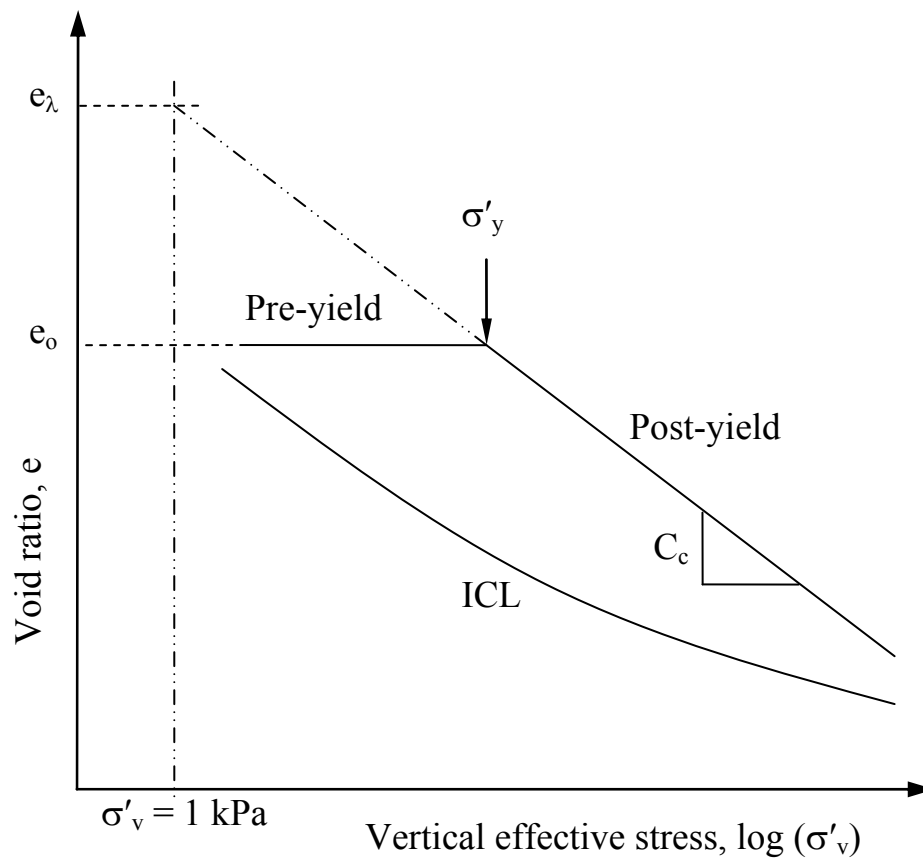


**Fig. 4-20.** Idealized compression behaviour of artificially cemented clays (after Horpibulsuk et al., 2004b)

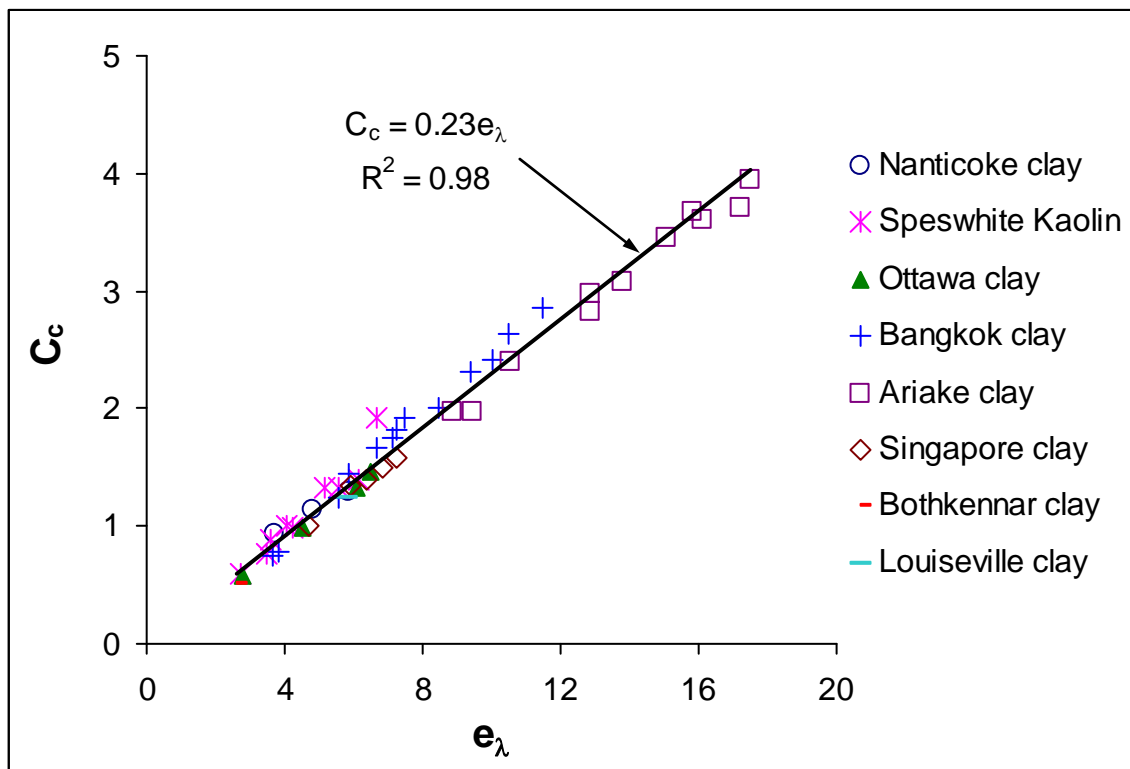
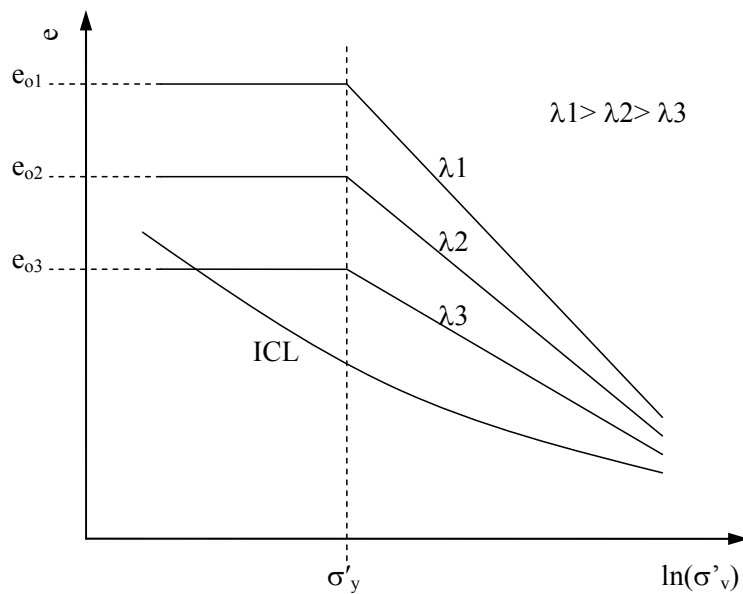
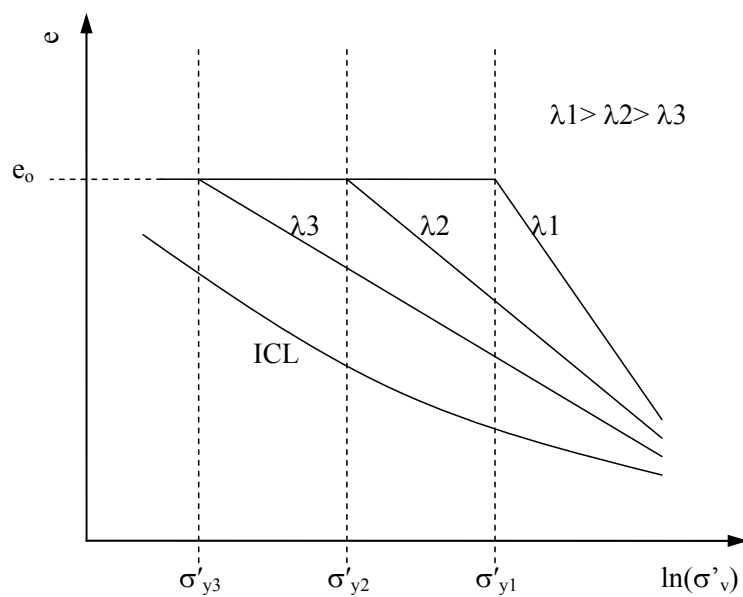


**Fig. 4-21.** The relationship between  $C_c$  (the slope of the compression line) and  $e_\lambda$  (void ratio at  $\sigma'_v = 1$  kPa)



(a)



(b)

**Fig. 4-22.** The effect of variations in (a) initial void ratio; and (b) vertical effective yield stress, on the slope of the pseudo-normal compression line



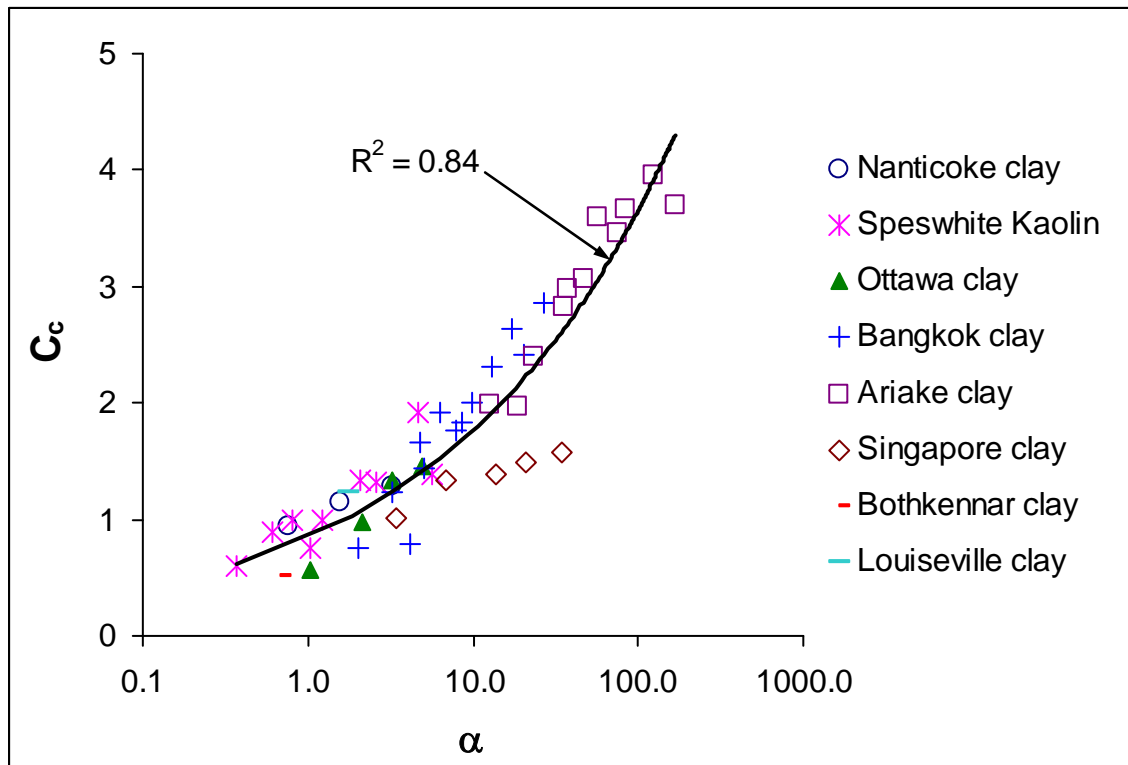


**Fig. 4-23.** The relationship between the slope of the compression line,  $C_c$ , and  $\alpha$

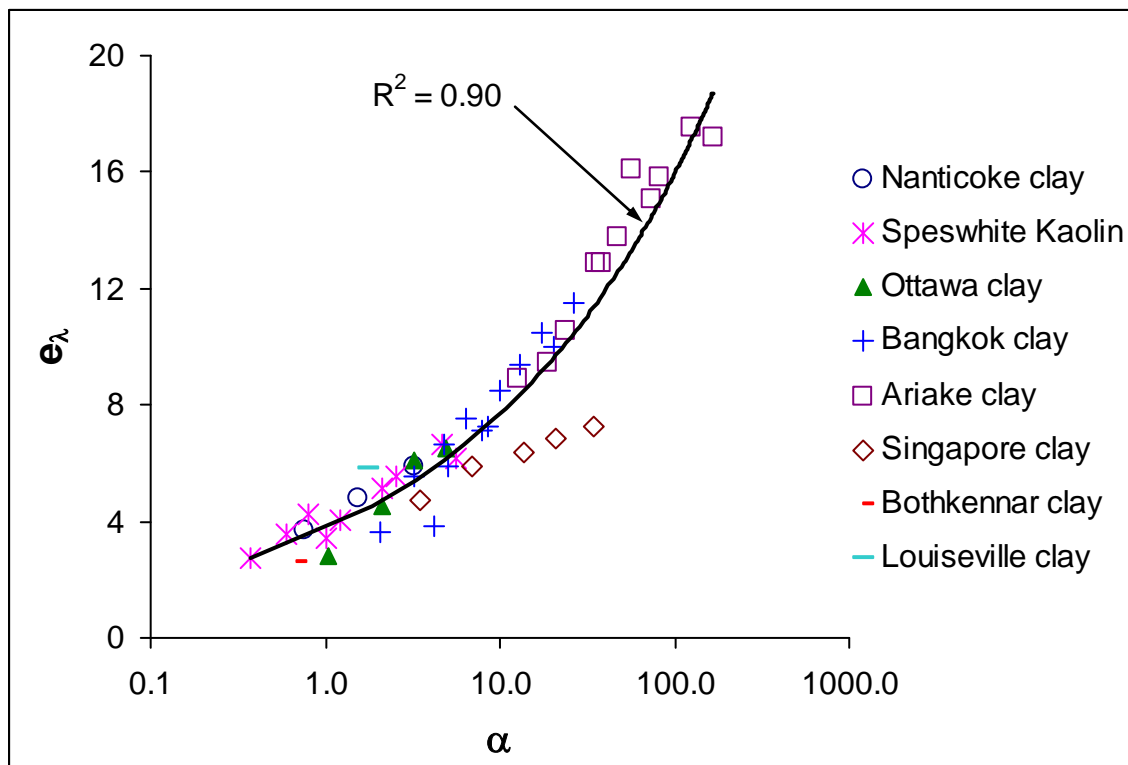


**Fig. 4-24.** The relationship between  $e_\lambda$  (void ratio at  $\sigma'_v=1$ ) and  $\alpha$

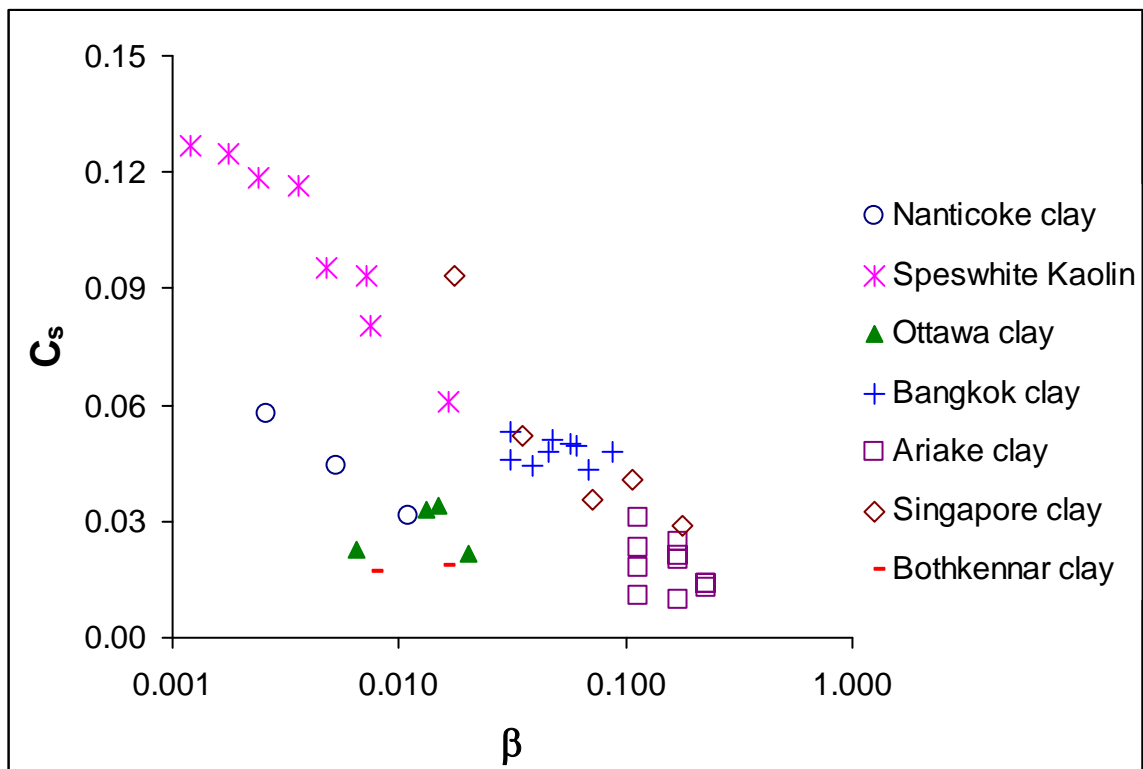


**Fig. 4-25.** The relationship between the slope of the swelling line,  $C_s$ , and  $\beta$

## **5 A FRAMEWORK FOR YIELDING AND STRESS-STRAIN BEHAVIOUR OF ARTIFICIALLY CEMENTED CLAYS**

### **5.1 Introduction**

Artificial cementation is used in civil engineering practice as an effective method for the stabilization of soft ground. Both shallow and deep stabilization techniques have been developed over the past few decades to enhance engineering properties, such as strength and compressibility, and to solidify soft and slurried clays (e.g. Bergado et al., 1996; Nagaraj and Miura, 2001). Deep mixed cementitious soil columns, for instance, are employed to stabilize trenches and deep excavations and to increase the bearing capacity of lightly loaded structures. Lime has been a commonly used cementing agent in ground improvement projects. However, Portland cement is becoming more preferable in recent years due to its lower cost, easier storage, and higher effectiveness (Bergado et al., 1996).

Several researchers have experimentally studied the yielding behaviour of natural structured soft clays, and a number of models have been developed for predicting the shearing and compression behaviour of such material (e.g. Mitchell, 1970; Wong and Mitchell, 1975; Graham et al., 1983b; Clausen et al., 1984; Folks and Crookes, 1985). Natural sensitive cemented clays tend to exist in a meta-stable state; once the apparent “preconsolidation pressure” caused by the natural cementation is exceeded, rupture of the particle bonds results in an abrupt increase in compressibility (e.g. Mitchell, 1970). Since the material forms an anisotropic structure prior to cementation, evidence of this fabric is apparent in the mechanical response of the soil (e.g. Lo and Morin, 1972; Tavenas and Leroueil, 1977). In contrast, many artificial cementation techniques involve significant

remoulding of the *in-situ* material, replacing the meta-stable fabric of the soil with an almost uniform isotropic matrix of bonded particles and aggregates (Nagaraj and Miura, 2001). Although this material has been previously described as “structured” and modelled accordingly (e.g. Horpibulsuk et al., 2010), the yielding and plastic flow of artificially cemented clays appears to be fundamentally different from that of naturally cemented clayey soil. Thus far, little implementation of these forms of constitutive model into finite element software has occurred (e.g. Helinski et al., 2007), but it is important that suitable approaches are developed for accurate prediction of complex boundary value problems.

Although significant work has been published on the compression and undrained/drained shearing behaviour of artificially cemented clays from standard triaxial and oedometer tests, very limited data concerning the yielding and plastic flow of this material, when subjected to complex stress paths in triaxial space, is available. Such information would aid researchers to develop more realistic constitutive models, resulting in improved predictions of the soil behaviour and better models for geotechnical systems. The main objective of this study was to experimentally investigate the yielding and stress-strain behaviour of an artificially cemented clay enhanced with Portland cement and to propose a constitutive framework to describe the observed behaviour.

## **5.2 Literature Review**

Yielding and compression behaviour of remoulded and naturally structured clays has been well studied and documented. Mitchell (1970) performed a number of conventional, constant  $p'$ , and constant  $\eta$  (stress ratio) triaxial experiments to study the yielding and mechanical strength of Ottawa clay. Depending on the type of experiments,

yield points were established using plots of either void ratio ( $e$ ) versus mean effective stress ( $p'$ ) or axial strain ( $\epsilon$ ) versus deviatoric stress ( $q$ ), forming an approximately unique curve in the  $p'$ - $q$  plane. The obtained yield surface confirmed the anisotropic elastoplastic behaviour of the material. Three different modes of failure were observed, depending on the value of the mean normal stress at failure. In addition, yielding and plastic flow of sensitive Ottawa clay was further investigated by Wong and Mitchell (1975). They suggested that the pre-yield behaviour of the sensitive clay can be considered to be quasi-elastic and isotropic. They also proposed an experimentally defined flow rule, correlating the plastic strain increments with the stress ratio ( $\eta$ ), to derive a plasticity theory describing the post-yield behaviour of sensitive cemented clays.

Tavenas et al. (1979) performed stress path-controlled triaxial experiments on four different sensitive Champlain clays and used strain energy as a criterion to define the yield surface of the material. They proposed that unlike other criteria, strain energy can be used to acceptably define the limit state stress condition of the material along any selected stress path. Graham et al. (1983b) used the same concept along with a newly defined parameter, i.e. the length of the stress vector (LSSV), to study the yield states of naturally cemented Winnipeg clay. They also found the plastic strain increment vectors for the material, assuming a pre-yield cross-anisotropic pseudo-elastic behaviour for the material. They showed that specimens with different preconsolidation pressures produced a well-defined normalized yield locus and that the plastic strain increment vectors were approximately perpendicular to the proposed yield envelope. However, systematic deviations from normality were observed along certain stress paths, suggesting a counter-clockwise average deviation.

Graham and Li (1985) compared the behaviour of remoulded and natural Winnipeg clay and concluded that many of the important conceptual principles of critical state soil mechanics equally apply to both remoulded and natural clay. They also showed that the normal consolidation lines (NCL) and critical state lines (CSL) obtained for remoulded and natural clays were approximately parallel. Clausen et al. (1984) used measurements of pore pressures and deformations obtained by instrumentation of a circular test fill embankment built on a quick clay at Mastemyr, Norway to determine the occurrence of yielding within the material. They coupled their analysis with the results of laboratory tests on high quality specimens to produce a simple elastic-plastic model for the clay. They explained the slight discrepancy observed between the field and laboratory test results in terms of underestimation of the apparent preconsolidation ratio of the soil. More recently, Smith et al. (1992) studied the yielding behaviour of undisturbed Bothkennar clay by performing a number of drained probing and undrained shearing triaxial tests and confirmed the previous hypothesis that the behaviour of the soil at small strains can be explained by two kinematic sub-yield envelopes that exist within the primary bounding surface, which marks the onset of large-strain yielding. Although accurately mapping the first small elastic zone was difficult, the second zone was successfully located by undrained cyclic and drained probing triaxial experiments.

In addition to naturally structured material, artificially cemented clays have been subjected to a number of investigations mostly during the past decade. Uddin et al. (1997) conducted a comprehensive study of the engineering behaviour of cement-treated soft Bangkok clay. Results of conventional undrained triaxial experiments indicated that the stress paths in the  $p'$ - $q$  plane were initially perpendicular to the  $p'$  axis, followed by an

abrupt change in the curvature of the stress paths at higher deviator stresses. This phase transformation was utilized to obtain a family of curved loci for the material.

Tremblay et al. (2001) experimentally investigated one-dimensional compression behaviour of a number of clays from eastern Canada treated with lime or cement. Based on the experimental data, they developed a general compressibility model, estimating the resistance to compression for a given soil treated with a particular additive, by defining relationships between initial void ratio, additive content, and vertical effective yield stress. Horpibulsuk et al. (2004) studied the undrained shear behaviour of cement admixed Ariake clay at high water content and suggested that cementitious bonds play a dominant role on the strength characteristics of the material, if particularly sheared at confining pressures less lower than the mean effective yield stress. They also found that even if the specimens are sheared at confining pressures higher than the mean effective yield stress, cementation bonding still had a marked effect on the shear resistance of the material. Artificial cementation was also shown to increase the friction angle of the material, as well as its cohesion intercept. Although addition of a slight amount of cement significantly increased the friction angle of the material, further addition of cement did not significantly change the friction angle.

Kamruzzaman et al. (2009) studied the mechanical behaviour of cement-treated Singapore marine clay by performing a number of oedometer and conventional undrained triaxial experiments and reported that cementation resulted in a significant increase in the apparent preconsolidation pressure and a decrease in the swelling index of the clay. They also observed progressive post-yield destructuration of the cemented clay and attributed it to the gradual breakage of the cementitious bonds. The effect of cementation on the



shearing behaviour was observed even in specimens consolidated well beyond the yield stress. However, specimens sheared at low confining stresses exhibited a more brittle failure followed by strain softening of the material.

A number of constitutive models have also been proposed to predict the yielding and compression behaviour of structured clayey material. Rouainia and Muir Wood (2000) adopted a bubble model to extend the modified Cam Clay, to improve the estimates of small strain stiffness and degradation of stiffness with strain. The bubble was chosen to have the same elliptical shape, and the elastic behaviour was assumed to be isotropic. The suggested model could effectively reproduce the shearing and compression responses of a Swedish natural structured clay. Vatsala et al. (2001) proposed a framework considering the behaviour of a structured soil to be due to the coupled response of the soil skeleton and cementation bonding. The two components were represented separately; modified Cam Clay was used to represent the behaviour of uncemented soil skeleton, and a new elasto-plastic model was proposed for the bond component. At every strain level, the stresses produced due to each component were calculated and added to generate the overall response. Therefore, the model was described to be appropriate only if the microstructure of the material was not changed due to cementation. The proposed framework could successfully approximate the compression behaviour of a number of natural soils ranging from highly soft to very stiff clayey and non-clayey material.

Baudet and Stallebrass (2004) proposed a constitutive framework for structured clays that used sensitivity of the material as a single parameter to represent the structure. They defined a damage strain as a function of plastic volumetric and shear strains and

postulated that sensitivity decreases exponentially with the damage strain. They also suggested that natural soil structure is composed of meta-stable and stable elements. The stable components were considered not to degrade with straining and were simulated by allowing the limit value of sensitivity to be greater than unity. In an attempt to produce a structured Cam-clay model, Liu and Carter (2002) assumed the void ratio of a structured material at any state of stresses to be the sum of the void ratio for the corresponding reconstituted soil plus the additional void ratio due to structure. They proposed a formulation to find the additional void ratio based on the mean yield effective stress and a “b” parameter called the destructuration index, which should be obtained for a specific soil based on experimental data. They incorporated this framework into modified Cam Clay and used the resulting “structured Cam Clay” framework to predict the compression and shearing behaviour of five naturally structured soils.

Most of the aforementioned frameworks are mainly designed to predict the behaviour of naturally structured clays. Further work (although limited) has been done to develop models representing the behaviour of artificially cemented material. Yasufuku et al. (1997) proposed a generalized dissipated energy equation to find a yield function for lightly cemented clays. They took the effect of artificial cementation into account by shifting the critical state line in the  $p'$ - $q$  plane, so that its intercept with the  $q$  axis was not zero. The model assumed that the intercept of the critical state line with the  $p'$  axis ( $P'_r$ ) is constant, and used a parameter,  $c$ , as a soil constant characterizing the shape of the yield surface. The produced framework could moderately predict the behaviour of Ariake clay, reconstituted at twice the liquid limit and mixed with cement at 1 and 3% cement contents. Kasama et al. (2000) further developed and modified the model proposed earlier

by Yasufuku et al. (1997) and used the produced framework to predict the results of undrained triaxial experiments on a lightly cemented clay. Horpibulsuk et al. (2010) later adopted the model proposed by Liu and Carter (2002) to artificially cemented clays, assuming a critical state behaviour similar in concept to that suggested by Yasufuku et al. (1997), i.e. the yield surface was shifted to the left in the  $p'$ - $q$  plan, so that its intercept with the  $q$  axis was not zero. The model, which tied the behaviour of the cemented material to that of reconstituted clay using a few characterizing parameters, could reasonably predict the shearing behaviour of a number of artificially cemented soils.

The term “structured” has often been used in the literature to describe both naturally and artificially cemented clays, and the aforementioned models have been developed to predict the behaviour of both types of material. However, there appears to be significant differences in the behaviour of the natural and artificial structure, which are not fully understood and addressed. In addition, most of the experimental works conducted on artificially cemented clays are mainly concerned with the effect of parameters such as cement content, water content, and curing time on the mechanical behaviour, and to date no significant study has been performed to investigate the yielding and stress-strain properties of this type of material. Therefore, this study has investigated the mechanical response of artificial and natural clay soils, when subjected to complex stress path tests. A comparison of the behaviour of the two types of structure (natural and artificial) is made and a new framework for predicting the behaviour of the artificially cemented material is presented.

## 5.3 Experimental Design

### 5.3.1 Material properties

Clay specimens were obtained for use in this study from a site in the Ottawa valley. The samples were collected from 3 m deep boreholes. Given the high sensitivity of the material, specially designed Shelby tubes with a 15 cm diameter were used to obtain specimens for minimal disturbance to the *in-situ* structure of the clay. The soil is a sensitive Champlain clay ( $S_{t \sim 20}$ ) with a specific gravity ( $G_s$ ) of 2.82 and can be classified as a highly plastic clay (CH), according to the Unified Soil Classification System (ASTM D2487). The liquid (LL) and plastic (PL) limits are 52 and 24%, respectively, and the pH of the pore water is about 8.3. The grain size distribution is 43% clay ( $D < 0.002$  mm), 55% silt ( $0.002$  mm  $< D < 0.06$  mm), and only 2% sand ( $D > 0.06$ ). X-ray diffraction analysis of the soil showed that the primary clay minerals are illite and chlorite, while traces of vermiculite are also found in the material. The primary non-clay minerals are quartz, feldspar, calcite, dolomite, and pyrite. At the time of sampling, the groundwater table was located at 1.2 m depth below the ground surface, and the natural moisture content of the sampled material was close to 80%, indicating a liquidity index (LI) of 2. The bulk density of the soil was almost  $15 \text{ kN/m}^3$  and the *in-situ* vertical overburden pressure was 27 kPa, indicating an apparent over-consolidation ratio (OCR) of 7.4. Ordinary Portland cement (type I according to ASTM C150) was used to produce the cementitious bonding in the reconstituted material, due to its common usage as a cementing agent in ground improvement projects (e.g. Bergado et al., 1996; Nagaraj and Miura, 2001; Bhattacharja et al., 2003).

### 5.3.2 Specimen preparation

Undisturbed specimens of Ottawa clay were extruded from the Shelby tubes, carefully trimmed to size, and tested. Artificially cemented and reconstituted specimens, in contrast, were obtained from powdered material. To prepare the powdered clay, the soil was cut into small pieces and dried at room temperature. Then, it was finely pulverized into a powder (100% passing Sieve No. 40), using a rubber hammer to avoid crushing any soil particles.

To make the artificially cemented samples, clay powder was added to de-ionised water to form a slurry with a water content close to the desired value. The slurry was then mixed in a commercial food blender until it was uniform. Next, the required amount of cement and water was added to the mixture to increase the water content to the target level. The slurry was then gently mixed for a maximum of 15 minutes, to ensure that the mixing process would not break any produced bonds. Next, the mixture was poured into plastic cups, 70 mm in diameter and 120 mm in height. Trapped air bubbles were removed from the specimens by gently tapping on the walls of each cup, and some water was added above the slurry surface in every cup, to provide it with moisture throughout the curing period. The cups were then covered by plastic wrap and placed in a temperature controlled room to be cured at a constant temperature of 25°C. All cemented samples were cured for a period of 28 days before being used for testing. To be comparable to the natural soil, all of the artificially cemented specimens were prepared at a moisture content equal to 80%. In addition, the majority of the samples were mixed at one of the three cement contents: 3.1, 4.2, or 6.4%, where cement content,  $c$  (%), is defined as the ratio of mass of cement to the mass of dry soil.

For the preparation of the reconstituted samples, powdered clay was added to the amount of water needed to reach the target moisture content. The resulting mixture was blended for a few minutes and was left to soak for at least 24 hours in a sealed container, before being mixed again and used for testing. The moisture content of a portion of the specimen was measured prior to performing experiments to ensure that the target moisture content was reached.

### **5.3.3 Testing programme**

The experimental study programme involved a number of oedometer and triaxial experiments on undisturbed and artificially cemented Ottawa clay specimens. Since both undisturbed and artificially cemented samples had a relatively high sensitivity, extra care was taken to preserve the structure of the material during the preparation of the specimens for the oedometer and triaxial testing, and a lubricated thin wire trimmer was used to cut all of the specimens to the required size. The oedometer tests were performed in accordance with ASTM D2435, using oedometer rings 15 and 50 mm in height and diameter, respectively. Two oedometer experiments were also performed on reconstituted Ottawa clay at water contents of 1.2 and 1.5 times the liquid limit to obtain the intrinsic compression line (ICL) for the material (Burland, 1990). The triaxial tests were conducted in a GDS microcomputer controlled triaxial system with hydraulic controllers, enabling the execution of complex stress path controlled experiments. All of the triaxial samples had a height and diameter of 100 and 50 mm, respectively. A back pressure of at least 200 kPa was used in all of the experiments, and B-value checks were carried out after the saturation phases to ensure proper saturation of the samples. Seven undrained triaxial tests were carried out on undisturbed Ottawa clay, isotropically consolidated to

25, 45, 75, 150, 300, 400, and 600 kPa before undrained shearing with constant cell pressure. The isotropic compression of these samples was conducted by applying consecutive increments of stress. To minimize any effects of rate sensitivity of the undisturbed sensitive Leda clays (e.g. Lo and Morin, 1972; Graham et al., 1983a), the undrained shearing phase of each test was conducted at a standardized slow rate of 0.006 %/min. In addition, twenty eight drained and undrained triaxial experiments were performed on artificially cemented specimens, with an initial moisture content of 80% (similar to that of undisturbed material) at three different cement contents. After saturation, the samples were isotropically consolidated to initial stresses, presented as  $p'_i$  in Table 5-1. A number of the experiments included unloading-reloading stages after the initial shearing phase to monitor the changes with yielding in the size and shape of the yield surface. Isotropic loading was carried out at a constant slow rate of 4 kPa/h, and drained and undrained shearing was conducted at rates of 0.003 and 0.006 %/min, respectively. The aforementioned rates were determined based on the methods suggested by Head (1986). The “Cambridge” form of invariants has been used herein to describe the stress and strain state of the material (Schofield and Wroth, 1968):

$$q = \sigma'_a - \sigma'_r \quad (5.1)$$

$$p' = \frac{\sigma'_a + 2\sigma'_r}{3} \quad (5.2)$$

$$\varepsilon_q = \frac{2(\varepsilon_a - \varepsilon_r)}{3} \quad (5.3)$$

$$\varepsilon_p = \varepsilon_a + 2\varepsilon_r \quad (5.4)$$

Where  $q$  and  $p'$  are deviatoric and mean effective stresses, and  $\varepsilon_q$  and  $\varepsilon_p$  are shear and volumetric strains, respectively. The subscripts  $a$  and  $r$  denote axial and radial directions in triaxial space. Table 5-1 summarizes the laboratory triaxial tests performed on the artificially cemented samples. Unless stated otherwise, the tests listed in the table have been conducted in compression. For experiments that have been carried out with multiple stages, the sequence is also detailed in the test stage descriptions. To define the yield curve, a number of drained triaxial tests have been performed with a constant incremental stress ratio of  $\zeta = \delta q / \delta p'$ . Note that this has been used to differentiate from the more commonly used stress ratio,  $\eta$ , which is usually defined as:  $\eta = q/p'$ . Fig. 5-1 shows the schematic direction of the different probing tests performed on specimens with 4.2% cement content. A number of these probing tests were followed by drained unloading-reloading or undrained shearing, so that the specimens would undergo failure and reach the critical state condition (Table 5-1). As illustrated in the figure, the direction of each probing vector can also be shown with an angle ( $\theta$ ), which ranges from  $0^\circ$  to  $180^\circ$  and  $180^\circ$  to  $360^\circ$  for compression and extension tests, respectively.

## 5.4 Results and Analysis

### 5.4.1 General volumetric behaviour and hardening

1-D compression of reconstituted, undisturbed, and artificially cemented Ottawa clay was studied by performing a number of oedometer and triaxial experiments (Fig. 5-2). The dashed lines represent the paths obtained by performing  $K_0$  compression tests using the triaxial equipment. These triaxial tests were performed by volumetric



measurements rather than direct measurement of the diameter of the specimen and based on the assumption that the cylindrical shape of the triaxial specimen is maintained during  $K_0$  compression. The figure confirms the relative accuracy of this assumption, as the test paths obtained by triaxial experiments for a certain sample are close to those found with the oedometer tests. In addition, the compression curves for the two reconstituted specimens, which were prepared at different initial moisture contents, essentially follow a similar path at effective vertical pressures higher than 50 kPa. This unified curve can be assumed to be the intrinsic compression line (ICL) of this material. The solid line in Fig. 5-2 represents the empirical equation proposed by Burland (1990) to estimate the ICL of a clay based on its void ratio at the liquid limit,  $e_L$ . It can be seen that this equation is unable to estimate the ICL for the Ottawa clay, perhaps due to the relatively high silt content of the material.

As the figure shows, both natural structure and artificial cementation result in yield stresses that are significantly higher than the yield stress of an uncemented reconstituted specimen at the same void ratio, enabling the structured material to endure relatively high stresses at high void ratios. However, the results show that important distinctions exist between the behaviour of naturally structured and artificially cemented Ottawa clays. Unlike the undisturbed clay, which undergoes higher pre-yield deformations and has a steeper unloading-reloading line, the artificially cemented specimens exhibit a relatively stiff pre-yield behaviour and lesser elastic rebound due to unloading (Table 5-3). In addition, after the yield point is passed, undisturbed Ottawa clay experiences a more sudden structural collapse as its compression curve rapidly approaches the intrinsic compression line of the material, demonstrating the highly meta-

stable condition of the naturally structured Ottawa clay. In contrast, the artificially cemented specimens undergo a more gradual destructuration displayed by an approximately linear post-yield compression response that steadily approaches the ICL line. Many other researchers have also reported an approximately linear compression of clays treated with lime or cement (e.g. Locat et al., 1996; Miura et al., 2001; Rotta et al., 2003; Kamruzzaman et al., 2009). This steady destructuration can be attributed to the relatively uniform matrix of cementitious bonds that are formed within the artificially cemented material. As a result of this inter-connected texture, the cementitious bonds do not rupture simultaneously but rather break gradually until the post-yield compression line merges into the intrinsic compression line (ICL).

As expected, the yield stress increases in the artificially cemented clay with an increase in the cement content. Hence, higher cementation results in a higher destructuration rate and increases the slope of the post-yield compression line. The same trends are also observed in Fig. 5-3, which shows the isotropic compression and swelling paths of undisturbed and artificially cemented Ottawa clay. Both figures indicate that the unloading-reloading lines of artificially cemented specimens with different cement contents have approximately the same inclinations ( $C_s \sim 0.022$ ), which are also close to the slope of the pre-yield compression lines of the samples. The results of the oedometer tests (Fig. 5-2) also show that the swelling index ( $C_s$ ) of the undisturbed Ottawa clay ( $\sim 0.135$ ) is approximately five times that of the reconstituted ( $\sim 0.025$ ) or cement-treated ( $\sim 0.022$ ) clays, indicating a less elastic nature of the artificially produced compared to the natural bonds.

Two important observations were made herein for artificially cemented Ottawa clay: the isotropic and  $K_o$  post-yield compression curves are linear, and the isotropic and  $K_o$  unloading-reloading lines are parallel to the pre-yield compression lines. The same phenomena were also observed in compression or loading-unloading tests conducted along other stress paths (e.g. Fig. 5-4). Therefore, assuming that the yielding of the material during any compression path occurs at a mean effective stress equal to  $p'_y$ , the linear post-yield compression of the artificially cemented clay can be represented by the following equation (Wood, 1990):

$$v = v_{\lambda} - \lambda \ln p' \quad (5.5)$$

Moreover, both pre-yield compression and loading-unloading lines can be modelled by (Wood, 1990):

$$v = v_{\kappa} - \kappa \ln p' \quad (5.6)$$

In these equations,  $v_{\lambda}$  and  $v_{\kappa}$  are specific volumes corresponding to  $p'=1$ , and  $\lambda$  and  $\kappa$  are the slopes of the compression and unloading-reloading lines, respectively. Among these parameters,  $\kappa$  is almost constant for a certain cement content while  $\lambda$  and  $v_{\lambda}$  may change depending on the stress path followed during compression, and  $v_{\kappa}$  varies depending on the current size of the yield locus.

However, as Fig. 5-3 indicates, Eq. (5.5) does not give a good representation of the post-yield compression of the naturally structured clay; other more appropriate models, such as the one proposed by Liu and Carter (2000), can be used to represent the collapse behaviour of the material. In contrast, employing this linear model to represent the volumetric behaviour and hardening of artificially cemented clays has several advantages over employing the model proposed by Liu and Carter (2000) for the

destruction of clays during virgin compression. Although that model can also predict the behaviour of structured material undergoing linear gradual destructure, applying it to artificially cemented clays adds unnecessary complexity to the mathematical calculations needed to find the virgin compression line. Moreover, the model proposed by Liu and Carter (2000) couples the virgin compression line to the intrinsic compression line of the material and hence requires an accurate prediction of the ICL. However, as illustrated in Fig. 5-2, the available empirical equations may not provide an acceptable prediction of the ICL, giving rise to the need for additional experimentation to find the actual ICL for a particular material. Even the experimental ICL may not be unique for soils with different cement contents, perhaps due to the additional granular fins that are released into the soil matrix during destructure.

Using equations (5.5) and (5.6), the volumetric behaviour of the artificially cemented material during compression and shear can be modelled. Fig. 5-5 shows the experimentally obtained volumetric paths, along with the lines that can replace these paths to represent the elastic and plastic volumetric response of the cemented clay. In addition, using the limit specific volume and mean effective stress of the specimens sheared to high strains, the projection of the critical state line on the volumetric plane is plotted in Fig. 5-5. As the figure shows, the three lines representing isotropic and  $k_o$  compression and the critical state are almost parallel in samples with 4.2 and 6.4% cement contents, while the critical state line of the specimen with 3% cement content is relatively steeper than the other two lines. Table 5-2 and Table 5-3 summarize the  $\lambda$ ,  $\kappa$ ,  $v_\lambda$  and  $v_\kappa$  values obtained for the dashed lines plotted in Fig. 5-5, along with the volumetric parameters of the natural clay. Table 5-2 shows that the parameters corresponding to the

presumed isotropic compression line for the natural clay (Fig. 5-3) are close to those obtained for the specimen with 4.2% cement content. Moreover, the tables indicate that the values of  $\lambda$  and  $\kappa$  can be assumed to be constant for each cement content. Although the individual cementitious bonds have a brittle response, since they are disseminated through the material and break gradually, the overall response of the cemented clay is elasto-plastic and follows the critical state concept. Therefore, the critical state theory can be applied, and these two parameters can be used to separate the elastic and plastic volumetric responses of the cemented material.

#### **5.4.2 Yielding and critical state**

The undrained and drained shearing stages were continued to axial strains of about 15 and 20%, respectively. In the majority of the compression tests, a relatively well-defined critical state, where no significant changes were observed in the deviator stress ( $q$ ), mean effective stress ( $p'$ ), and specific volume ( $v$ ), was reached. However, two of the four extension tests did not reach the critical state; this may be due to the limitations of the triaxial apparatus to shear the samples beyond the tension cut-off line. In addition, the other two extension tests did not reach a well-defined critical state, perhaps due to significant changes occurred to the sample geometry after failure. Fig. 5-6 shows the critical state lines obtained for the artificially cemented specimens along with that of natural Ottawa clay. A best fit to the experimental data obtained for the natural clay is plotted in the figure. As it shows, the CSL of the natural Ottawa clay is almost parallel to the one obtained for the specimen with 4.2% cement content (Table 5-2).

Fig. 5-7 shows the points representing the critical state condition of the undisturbed and artificially cemented Ottawa clay in the  $p'$ - $q$  plane. A number of observations can be made. The slope of the critical state line ( $M$ ) of the artificially cemented specimens only negligibly increases with an increase in the cement content and is around 1.9 for all three samples. This slope is significantly higher than the one obtained for the natural clay ( $M=1.3$ ). In addition, the slope of the critical state line ( $M$ ) is preserved in the artificially cemented specimens even at very high confining stresses, although it drops in the undisturbed specimen isotropically consolidated to a high pressure before shearing. This again suggests that during drained compression, the natural structure disappears more quickly than artificial cementation after the yield stress is passed. A good illustration of this significant difference between the natural and artificial structure is provided in Fig. 5-8. As it shows, a shear band is formed in the undisturbed sample sheared after isotropically consolidated to 25 kPa (close to the *in-situ* stresses), although the undisturbed specimen consolidated to 600 kPa experiences buckling with no single shear band formed in the sample. The isotropic yield pressure of this material is approximately  $p_o'=80$  kPa (Fig. 5-3), and further isotropic compression results in the collapse of the structure. At a  $p_i'=600$  kPa, limited structure is left in the material (in Fig. 5-3 the specific volume is reduced to 2.07 at  $p_i'=600$  kPa), and the shear behaviour is mostly frictional. In contrast, although it yields at a low isotropic pressure of  $p_o'=35$  kPa, the artificially cemented specimen ( $c=3.1\%$ ) preserves a portion of its structure up to high stresses (in Fig. 5-3 the specific volume is reduced to 2.33 at  $p_i'=600$  kPa). Therefore, it experiences a brittle failure with the deformations after failure being concentrated along a shear band rather than being spread throughout the specimen (Fig. 5-8c).

Unlike many construction materials, such as steel or concrete, soil does not usually have a precisely defined yield surface, as it undergoes a gradual transition from elastic to plastic behaviour and rarely exhibits a linear, purely elastic pre-yield response (Wong and Mitchell, 1975). Hence, the method of extrapolation introduced by Taylor and Quinney (1931) is usually employed to estimate the yield point for a particular stress path. Moreover, different loading paths in soils induce different straining modes. Therefore, on each particular stress path, certain strain variables may provide a more sensitive indication of the yield point (Wood, 1990), and some other variables, which stay constant during the test, would not give any sign of where yielding takes place. One approach to locating the yield point is to use as many different plots as possible and take the average to have a maximum number of independent estimates of the position of the yield. Alternatively, a single plot containing all different stress and strain variables can be utilized (Wood, 1990); defining the yield point using such variables would be possible for all different stress paths. This is achievable by plotting the cumulative work done in straining the sample,  $W$ , against the length of the stress vector,  $s$ , which is a scalar quantity introduced by Graham et al. (1983b):

$$W = \Sigma(p' \delta \varepsilon_p + q \delta \varepsilon_q) \quad (5.7)$$

$$s = \sqrt{\Delta p'^2 + \Delta q^2} \quad (5.8)$$

In these equations,  $\Delta$  represents the total change in a variable, while  $\delta$  represents an incremental variation.

Plots of  $W$  and  $s$  were utilized to find the position of the yield points for artificially cemented specimens of Ottawa clay tested along different stress paths. Fig. 5-9 illustrates the method that was used to define yield states along different stress paths.

The obtained yield states for different cement contents normalised against the isotropic yield stress ( $p'_o$ ) of the material are plotted in Fig. 5-10. It can be seen that all of the data fall on a relatively well defined envelope. This is in agreement with the previous observation that the slope of the critical state line for the three different cement contents is approximately the same ( $M \sim 1.9$ ). In addition, due to the effect of cementitious bonds, the obtained yield locus is vertically well-extended in the  $p'$ - $q$  plane. This vertical elongation of the yield locus is even more pronounced than is usually observed in naturally structured clays (e.g. Mitchell, 1970; Wong and Mitchell, 1975). As expected, the behaviour of the artificially cemented material seems to be isotropic, since the yield surface meets the hydrostatic line at its maximum mean effective stress ( $p'$ ). Furthermore, a significant number of the specimens did not fail until their stress paths reached the tension cut-off line. This happened in a number of drained tests along with all of the CIU tests performed at  $p'_i < p'_o$  and is in agreement with the results of a recent literature review conducted by the authors indicating that the undrained shear strengths obtained for artificially cemented clays by CIU triaxial tests performed at  $p'_i \ll p'_o$  are similar to those obtained for the same specimens with unconfined compression experiments (Sasanian and Newson, 2010).

A total of 16 compression and 4 extension tests were performed on the specimens with a 4.2% cement content. Fig. 5-11a shows the resulting yield points in the  $p'$ - $q$  plane along with the critical state lines in compression and extension. As the data indicate, the yield locus is bounded by the tension cut-off lines in both compression and extension ( $\eta_c = 3$  in compression and  $\eta_e = -1.5$  in extension). A combination of two elliptical models was adopted to match the obtained data: the elliptical cap (Chen and Mizuno, 1990) for



$M_c \leq \eta \leq M_c$  and the modified Cam-Clay (Wood, 1990) for  $M_c \leq \eta \leq \eta_c$  and  $\eta_e \leq \eta \leq M_e$ . Fig. 5-11b shows the parameters used to define the yield locus. For  $\eta > 0$  (compression) the equation of the yield locus can be written as:

$$\text{For } 0 \leq \eta \leq M_c: \quad f = q - M_c l_c \sqrt{1 - \left( \frac{p' - l_c}{p'_o - l_c} \right)^2} = 0 \quad (5.9)$$

$$\text{For } M_c \leq \eta \leq \eta_c: \quad f = q - M_c \sqrt{p'(2l_c - p')} = 0 \quad (5.10)$$

Where  $p'_o$  is the isotropic yield stress, and  $l_c$  is the mean effective stress corresponding to the critical state in compression. Using Eqs. (5.9) and (5.10) to define the yield surface increases the flexibility to find a good match with the experimental data while limiting the number of variables required to define the yielding of a cemented material. The mean effective stress equivalent to  $\eta=3$  can be defined as:

$$p'_i = \frac{2M_c^2 l_c}{M_c^2 + \eta_c^2} \quad (5.11)$$

Similar equations can be used to define the yield locus in extension by only replacing  $M_c$ ,  $l_c$ , and  $\eta_c$  with  $M_e$ ,  $l_e$ , and  $\eta_e$ , where  $l_e$  is the mean effective stress corresponding to the critical state in extension.

Fig. 5-12 shows the compression test results for the specimens with 3.1 and 6.4% cement contents, along with the yield loci obtained from Eqs. (5.9) and (5.10). Using the proposed model requires the estimation of three parameters:  $p'_o$ ,  $M$ , and  $l$ . For convenience in mathematical calculations,  $l$  and  $p'_o$  can be related with introducing the following parameter:

$$R = \frac{p'_o - l}{M \cdot l} \quad (5.12)$$

The parameters used to plot the yield loci shown in Fig. 5-11a and Fig. 5-12 are summarized in Table 5-4. The values of  $p'_o$  and  $M$  (in compression) have been obtained from the data plotted in Fig. 5-5 and Fig. 5-7, respectively. The values of  $l$  and  $R$  were chosen so that the yield loci provided the best estimate of the experimental data. As mentioned previously, the relatively high  $M_e$  obtained herein for the specimen with 4.2% cement content is possibly in error, since it was found from the results of only two experiments and the samples did not reach a well-defined critical state due to significant changes in their geometry. Allman and Atkinson (1992) also reported difficulties with finding the slope of the critical state line from the results of extension tests on reconstituted Bothkennar clay.

The size of the proposed yield surface can be directly determined by finding the isotropic yield pressure,  $p'_o$ , of the material. Alternatively, the effective vertical yield stress,  $\sigma'_y$ , obtained from oedometer tests can be utilized to determine the size of the yield locus for an artificially cemented clay. This can be achieved by finding the intersection of the following line representing  $\sigma'_a = \sigma'_y$  in  $p'$ - $q$  plane (Wood, 1990) with the elliptical cap model (Eq. 5.9):

$$p' + \frac{2q}{3} = \sigma'_y \quad (5.13)$$

Fig. 5-13 shows the experimentally obtained yield loci along with the lines obtained from Eq. (5.13) using the oedometer test data (Fig. 5-2). Since no oedometer test was performed on the specimen with 3.1% cement content, the results of  $K_o$  compression

test in the triaxial apparatus were used to find  $\sigma'_y$  of the specimen. The results show that the one dimensional compression tests can acceptably define the size of the yield envelope for cemented material. The intersection points are also close to the yielding points obtained for the  $K_o$  stress paths. By using this method, it is possible to find the yield envelope without performing an isotropic compression test on the material. This can be very beneficial as artificially cemented clays with high cement contents, usually used in practice, have  $p'_o$  values that are too high to be directly measured in a conventional triaxial apparatus.

Among the parameters listed in Table 5-4, the values of  $p'_o$  and  $M$  can be found for any type of artificially cemented clay with performing a number of conventional triaxial and oedometer experiments. The value of  $R$  (and  $l$ ) can also be estimated using the critical state concept. Doing so requires the determination of the isotropic compression and critical state lines in the volumetric plane. Assuming that the slope of the two lines in  $v$ - $\ln p'$  space is equal to  $\lambda$  (e.g. the average of the values experimentally found and reported in Table 5-2), and using  $N$  and  $\Gamma$  to represent  $v_\lambda$  of the isotropic compression and critical state lines (in Eq. 5.5), respectively, we can find the specific volume at the critical state as follows (Wood, 1990):

$$v_{cs} = N - \lambda \ln p'_o + \kappa \ln \frac{p'_o}{l} \quad (5.14)$$

Where  $\kappa$  is the slope of the unloading-reloading lines and can be estimated by finding the slope of the initial elastic compression line (refer to Fig. 5-5 and Table 5-3).

In addition, we know that:

$$v_{cs} = \Gamma - \lambda \ln l \quad (5.15)$$

Combining these two equations with Eq. (5.12) yields:

$$R = 1/M \left[ \exp\left(\frac{N - \Gamma}{\lambda - \kappa}\right) - 1 \right] \quad (5.16)$$

This equation was used to estimate R based on the obtained critical state parameters for each cement content (Table 5-4). As the table shows, the R values calculated from Eq. (5.16) for the compression tests are relatively close to the values found from the yield loci. However, there is a significant difference between the  $R_e$  obtained from the yield locus and the one calculated based on the critical state concept for the specimen with 4.2% cement content. This again supports the viewpoint that the  $M_e$  value used in Eq.(5.16) to find  $R_e$  is not accurate; a lower  $M_e$  would provide a yield locus that is still well fit to the yield data while giving a more reasonable  $R_e$  value.

As mentioned earlier, the yield states shown in Fig. 5-11a and Fig. 5-12 have been obtained using the energy method, which considers a significant shift in the slope of the energy curve as an indication of yielding. However, the amount of work required to cause yielding was not equal in all of the tests, but rather depended on the stress path. Fig. 5-14 shows the measured yielding energy versus the direction of the drained probing tests, performed on specimens with 4.2% cement content and started at  $p'_i=75$  kPa (Fig. 5-1). The angle  $\theta$  represents the direction of the stress path and is calculated clockwise, assuming that the angle of the vector on the isotopic line connecting  $p'_i=75$ kPa to the origin is equal to zero (Fig. 5-1). The volumetric ( $\epsilon_{p,y}$ ) and shear ( $\epsilon_{q,y}$ ) strains at yield are also given for each test direction. As the figure shows, the work required to cause yielding in experiments with  $\theta$  values lower than  $90^\circ$  or higher than  $270^\circ$  is minimal. This is in agreement with the stiff pre-yield behaviour observed in experiments failed “dry” of

the CSL. In contrast, high energy levels are required to cause yielding, when specimens yield “wet” of the CSL. Moreover, as implied by the bimodal pattern of the representative curve, a relatively lower amount of work is needed to yield the specimen along the isotropic stress path ( $\theta=180^\circ$ ). The two maxima, which indicate the stress paths inducing the greatest ductile response, occur at angles close to  $120^\circ$  and  $240^\circ$ . These results are in accordance with those obtained by Smith et al. (1992) for undisturbed Bothkennar clay.

To avoid the complexities involving changes in the shape of the yield surface due to volumetric compression, it is typically assumed that the shape remains the same irrespective of the stress path causing hardening in the material, i.e. isotropic hardening occurs (Wood, 1990). To check the validity of this assumption for artificially cemented clays, a number of loading-unloading-reloading tests were conducted along different stress paths on specimens with 4.2% cement content (Fig. 5-15). Although loaded along different stress paths, all of the specimens were unloaded after reaching the same unloading-reloading line corresponding to  $v_k=2.80$ . Hence, the specimens can be assumed to be all on the same sized yield locus just before the commencement of the unloading stage. After being unloaded to very low stresses (refer to Fig. 5-15 and Table 5-1), the reloading stage was conducted to find the position of the yield along a different stress path. Three of the reloading tests (AC5, AC15, and AC15) were drained stress path controlled, while one (AC16) was conventional undrained starting at a  $p'_i=25$  kPa, after being isotropically unloaded from a  $p'_o=600$  kPa. Since both loading and reloading yielding points fall close to the proposed yield surface, the above-mentioned assumption can be considered to be acceptable for the artificially cemented material. Comparison of AC13 and AC16, which both have undergone conventional drained shear at  $p'_i=25$  kPa

and have failed on the unconfined compression path, shows that AC13 with a  $p'_o$  equal to 168 kPa fails at a  $p'_f=43$  kPa, and AC16 with a  $p'_o$  expanded to 600 kPa fails at a  $p'_f=176$  kPa, indicating an almost similar  $p'_o/p'_f$  ratio for both specimens.

Fig. 5-16 shows the changes in the work input (W) due to load reversals of the artificially cemented specimens with 4.2% cement content versus the length of the stress path (s). The “s” values have been calculated from a point on the isotropic line with a  $p'$  corresponding to the start of the experiment ( $p'_i$  values in Table 5-1). The figure also shows the starting points of each stage for one of the experiments (AC5). This figure indicates the relatively linear elastic unloading-reloading of the material within the yield surface for AC14, AC15, and AC16. However, despite moving inside the yield surface, the unloading of the specimen in AC5 has been accompanied by some plastic deformations. This is perhaps because the specimen has been unloaded from the  $K_o$  path to  $p'=500$  kPa on the isotropic line (Table 5-1), which is very close to the  $p'_o=600$  kPa, and is an indicator of the elasto-plastic response of the material.

To obtain the state boundary surface for the artificially cemented specimens, the stresses in the  $p'$ - $q$  plane were divided by the equivalent pressure,  $p'_e$ . By definition, the equivalent pressure is the mean effective stress on the isotropic compression line corresponding to the specific volume at any stage of a triaxial test (e.g. Atkinson and Bransby, 1978). Therefore, for a particular specific volume ( $v$ ) during the test,  $p'_e$  can be obtained from (e.g. Atkinson and Bransby, 1978):

$$p'_e = \exp\left(\frac{N - v}{\lambda}\right) \quad (5.17)$$

As shown in Fig. 5-17, being normalized by the equivalent pressure, both drained and undrained stress paths fall inside a single bounding surface. The figure also shows that this state boundary surface can be satisfactorily represented by the proposed yield locus, plotted in the normalised space (the bounding curves in Fig. 5-17) using the linear hardening model. At any mean effective stress ( $p'$ ) on or inside a current yield locus of size  $p'_o$ , the equivalent pressure ( $p'_e$ ) can be related to  $p'$  using the following equation (Wood, 1990):

$$\frac{p'}{p'_e} = \left( \frac{p'}{p'_o} \right)^{\left( \frac{\lambda - \kappa}{\lambda} \right)} \quad (5.18)$$

Using this equation for the points on the yield surface, along with Eq. (5.17), defines a surface in  $p'$ - $q$ - $v$  space corresponding to the proposed yield locus. The  $p'/p'_o$  ratio for the suggested yield locus can be obtained as follows:

$$\text{For } 0 \leq \eta \leq M: \quad \frac{p'}{p'_o} = \frac{1 - M^2 R^2}{(1 - R \sqrt{M^2 - \eta^2 + M^2 \eta^2 R^2})(1 + MR)} \quad (5.19)$$

$$\text{For } M \leq \eta \leq 3: \quad \frac{p'}{p'_o} = \frac{2M^2}{(M^2 + \eta^2)(1 + MR)} \quad (5.20)$$

Combining Eq. (5.18) with Eqs. (5.19) and (5.20) yields the  $p'/p'_e$  ratios defining the state boundary surface for the proposed model. The  $q/p'_e$  ratio can then be simply found by multiplying  $p'/p'_e$  by  $\eta$ . At  $\eta=M$ , both of the obtained equations will be simplified to the following form:

$$\frac{q}{p'_e} = \frac{M \cdot p'}{p'_e} = M \cdot \left( \frac{1}{(1 + MR)} \right)^{\left( \frac{\lambda - \kappa}{\lambda} \right)} \quad (5.21)$$

Eq. (5.21) defines a point on the normalised space corresponding to the critical state line. Although all of the normalized stress paths shown in Fig. 5-17 fall inside the defined state boundary surface, most of them do not terminate on the point representing the theoretical critical state line according to Eq. (5.21). This is better illustrated in Fig. 5-18, which shows the points representing the critical state for each experiment along with the ones obtained by Eq. (5.21). The experimental values are stretched along a line with  $\eta \sim M$ , indicating that in most of the experiments, the experimental critical state has been reached at a equivalent pressure higher than the expected value. A closer examination of Fig. 5-17 shows that this deviation from the expected critical state point in the normalised space is more pronounced in the undrained experiments.

Since the post-yield compression of the undisturbed Ottawa clay is not linear, a unique state boundary surface, similar to the one defined for the artificially cemented material, cannot be found for the undisturbed clay (Fig. 5-19a). The hypothetical isotropic compression line shown in Fig. 5-3 underestimates the equivalent pressure ( $p'_e$ ) for undisturbed specimens sheared at low confining pressures ( $p'_i$ ). However, for comparison purposes, the stress paths obtained for the undisturbed clay can be normalised using the real isotropic yield stress of the material ( $p'_o$ ). Based on the isotropic compression behaviour of the undisturbed clay (Fig. 5-3),  $p'_o$  has been considered to be equal to 80 kPa for specimens sheared at  $p'_i < 80$  kPa and equal to  $p'_i$  for those sheared at  $p'_i > 80$  kPa. The results (Fig. 5-19b) show that the obtained pseudo-state boundary surface for the undisturbed material is not as vertically elongated as the one obtained for the artificially cemented clay. However, the presented normalised surface does not provide a



good indication of the shape of the yield envelop for the undisturbed clay due to possible anisotropic response of the material.

### 5.4.3 Stiffness and deformations

The relatively diverse types of triaxial experiment performed on the artificially cemented specimen with 4% cement content allow for the investigation of the failure mode based on the stress path and stress ratio ( $\eta$ ) at failure. In general, the specimens that failed wet of the critical state line in  $p'$ - $q$  plane underwent a gradual failure accompanied by volumetric compression, while the ones that failed dry of the CSL experienced a sudden, brittle failure accompanied by a slight volumetric expansion. Fig. 5-20 shows the normalised deviator stress and secant shear modulus obtained from a number of drained triaxial experiments in compression and extension. Among the experiments shown in this figure, AC2 and AC3 were conventional drained tests, AC4 and AC17 were sheared at a constant  $p'$ , and AC9 and AC18 were conducted with an almost similar incremental stress ratio ( $\zeta$ ). The presented secant moduli were calculated from (Wood, 1990):

$$G_{\text{sec}} = \frac{\delta q}{3\delta\epsilon_q} \quad (5.22)$$

As the figure shows, AC2, AC3, and AC18, which failed wet of the critical state line, have smoother transition from elastic to plastic behaviour, while the rest of the experiments exhibit an almost linearly elastic pre-yield response, followed by a brittle failure. Moreover, the post-yield reduction of the shear modulus is slower and less significant in the specimens experiencing a gradual yielding than in those undergoing a brittle failure.

Similar normalised graphs obtained by performing undrained triaxial tests on the artificially cemented and undisturbed Ottawa clays are shown in Fig. 5-21 and Fig. 5-22, respectively. Three of the undrained experiments shown in Fig. 5-21 (AC11, AC12 and AC13) were conducted at  $p'_i$  values less than the isotropic yield pressure of the material ( $p'_o$ ). These experiments have undergone a more abrupt failure, followed by a sudden loss of strength, while AC 1 and AC7, which had a  $p'_i > p'_o$ , exhibit a gradual post-yield strain softening. In addition, unlike in the other three tests, the normalised shear moduli obtained from AC1 and AC7 are approximately the same, indicating the more frictional response of the material. Considering the approximately linear pre-yield behaviour (Fig. 5-21a) and the almost vertical stress paths (Fig. 5-17b) observed in the undrained experiments performed inside the original yield locus, the  $G_u$  values shown in Fig. 5-21b for AC11, AC12 and AC13 can be considered to be equal to  $G'$  of the material. Rather similar observations can be also made for the undisturbed clay (Fig. 5-22). However, comparison of the two figures indicate that unlike the artificially cemented clay, the undisturbed material does not display any post-yield strain softening, if sheared at  $p'_i > p'_o$ . Moreover, the failure of the undisturbed specimens sheared at low confining pressures is not as brittle as those observed in the artificially cemented clays. These can be related to the faster rate of destructuration of the undisturbed clay due to post-yield isotropic compression, along with a more ductile failure of the natural bonds.

To predict the pseudo-elastic behaviour of any artificially cemented clay, there is a need to determine the Poisson's ratio ( $\nu'$ ) of the material. This can be achieved by obtaining the coefficient of earth pressure at rest,  $K_o$ , of the cemented clay. Assuming a purely elastic behaviour (Wood, 1990):

$$\varepsilon_r = 1/E' [\sigma'_r - \nu'(\sigma'_a + \sigma'_r)] \quad (5.23)$$

In  $K_o$  condition, the lateral strain ( $\varepsilon_r$ ) is equal to zero, and therefore:

$$\nu' = \frac{K_o}{1 + K_o} \quad (5.24)$$

In addition, the knowledge of the  $K_o$  coefficient is useful for predicting the at-rest stresses in ground improvement projects involving artificially cemented material and aids the interpretation of the results of oedometer tests performed on improved soil. The  $K_o$  compression experiments, performed herein by the triaxial apparatus, produced rather interesting results. Fig. 5-23 shows the stress paths followed during the  $K_o$  tests in samples with different cement contents. A bilinear behaviour is observed; the stress paths start with a significant slope until they reach the critical state line. At this point, they change direction and continue with a lesser slope until relatively high stresses. Interestingly, the yield points obtained by the method described in Section 5.4.2 fall exactly where the stress paths change direction. Therefore, the pre-yield  $K_o$  coefficient of the specimens can be approximated by the slope of the critical state lines. Although the one dimensional stress paths are bilinear, an average  $K_o$  can also be calculated for the material with an acceptable error, using the relationships shown in Fig. 5-23. Assuming that the slope of the representative lines shown in the figure is  $m$ , the average  $K_o$  of the material can be obtained as:

$$K_o = \frac{1 - \left(\frac{m}{3}\right)}{1 + \left(\frac{2m}{3}\right)} \quad (5.25)$$

The calculated average  $K_o$  coefficients and Poisson's ratios (using Eq. 5.24) are summarized in Table 5-5. The obtained Poisson's ratios are very similar to the values typically assumed (e.g. Lamond and Pielert, 2006) for the concrete material ( $\nu \sim 0.18$ ). Moreover, it can be seen that the  $K_o$  coefficients calculated for the three specimens are almost equal, indicating that the addition of more cement does not significantly change the Poisson's ratio of the material. Moreover, as Fig. 5-23 shows, unlike in naturally structured Champlain clays, which typically have an initially low  $K_o$  coefficient followed by a significantly higher post-yield value (e.g. Silvestri 1984), in the artificially cemented Ottawa clay, the slope of the  $K_o$  stress path in  $p'$ - $q$  plane does not significantly reduce ( $K_o$  does not increase) after the yield point is passed, confirming again the gradual post-yield destructuration of the artificially cemented clay. By calculating the friction angle,  $\phi'$ , from  $M$  values (in Table 5-4) based on the Mohr-Coulomb criterion and using Jaky's relationship (Jaky, 1948), similar  $K_o$  coefficients as those experimentally found herein are obtained for the material (Table 5-5).

The suggested yield locus can be also used to predict the magnitude of plastic volumetric and shear strains if associated flow is obeyed. To examine normality, the direction of the plastic increment vectors at yield for each experiment should be determined. The total measured strain is equal to the sum of plastic, non-recoverable and elastic, recoverable strains:

$$\delta \varepsilon_p = \delta \varepsilon_p^e + \delta \varepsilon_p^p \quad (5.26)$$

$$\delta \varepsilon_q = \delta \varepsilon_q^e + \delta \varepsilon_q^p \quad (5.27)$$

Where superscripts e and p refer to elastic and plastic components of strain, respectively. Therefore, to obtain the plastic components for each experiment, the elastic component was calculated and subtracted from the total measured strain. Assuming isotropic pseudo-elasticity of the artificially cemented material, the elastic shear and volumetric strains were obtained from (Wood, 1990):

$$\begin{bmatrix} \delta\varepsilon_p^e \\ \delta\varepsilon_q^e \end{bmatrix} = \begin{bmatrix} 1/K' & 0 \\ 0 & 1/(3G') \end{bmatrix} \begin{bmatrix} \delta p' \\ \delta q \end{bmatrix} \quad (5.28)$$

Where  $K'$  and  $G'$  are the bulk and shear moduli, respectively. The average pre-yield secant shear modulus was used to calculate the elastic shear strains. For the reasons mentioned earlier, the pre-yield undrained and drained shear moduli were assumed to be equal in the CIU triaxial experiments. Changing with the mean effective stress during the test, the bulk modulus at any stage of the experiment was calculated from (Wood, 1990):

$$K' = \frac{\nu p'}{\kappa} \quad (5.29)$$

For consistency, the plastic strains were all calculated for a range equivalent to  $0.2\Delta W_{\text{yield}}$ , where  $\Delta W_{\text{yield}}$  is the total work done since the beginning of the experiment up to the yielding point. Fig. 5-24 shows the yield loci, along with the obtained plastic strain increment vectors plotted in the  $p'$ - $q$  plane. In this figure, it is assumed that  $p'$  and  $\delta\varepsilon_p^p$ , and  $q$  and  $\delta\varepsilon_q^p$  are coaxial, respectively. The figure shows that the normality condition is generally followed at yielding points that are “wet” of the CSL. These are the experiments that displayed a gradual yielding accompanied by an elasto-plastic behaviour. In contrast, the associated flow rule appears not to be valid for the points that are “dry” of the CSL. As discussed earlier, these experiments underwent sudden failure

and exhibited a pseudo-elastic pre-yield behaviour. This brittle failure was accompanied by a relatively low amount of volumetric expansion, perhaps due to the already higher than normal void ratio of the material. Consequently, all of the increment vectors located at the left of the CSL are almost vertical.

The results can be better examined if the deviation from normality is measured and illustrated (Fig. 5-25). The normal directions to the yield locus were obtained by finding the derivation of the Eqs. (5.9) and (5.10) against  $p'$  and writing:

$$\frac{dq}{dp'} \cdot \frac{d\varepsilon_q^p}{d\varepsilon_p^p} = -1 \quad (5.30)$$

The deviation was then determined as the angular difference between the measured and calculated vectors. In the calculations, a clock-wise deviation was considered to be positive. As Fig. 5-25 shows, at  $\eta$  values less than 1.5, the deviation from normality ( $\theta_d$ ) is less than  $5^\circ$  in all of the tests and is usually negative. However, as  $\eta$  increases beyond 1.5, the deviation angle rapidly increases and reaches a value of  $37^\circ$  at  $\eta=3$ . In general, it can be concluded that the normality condition is generally met for  $\eta < M$  but is significantly violated at  $\eta > M$  values. All of the three points with  $\eta < M$  that have a high deviation from normality correspond to the  $K_o$  compression tests (for the three different cement contents). This could be related to the fact that unlike the remaining experiments, these tests were stress controlled, and as shown previously, the direction of the stress path changed in  $K_o$  tests exactly at the yielding state.

The proposed framework appears to successfully represent the yielding behaviour of the artificially cemented Ottawa clay. However, it was unable to precisely predict the direction of the plastic strain increment vectors for specimens failing “dry” of the CSL.

The brittle nature of the failure in such specimens induces shifts in the direction of the increment vectors, making more difficult accurate prediction of the plastic response of the material. In general, the results indicated that although the specimens failing “dry” of the CSL experience some volumetric expansion, the resulting negative volumetric strains are negligible in amount comparing to the experienced shear strains; thus the direction of the plastic strain increment vectors obtained for these specimens is close to 90°. Consequently, the proposed yield locus can be used only to predict the strains when specimens yield “wet” of the critical state line. In such cases ( $\eta < M$ ) in the compression plane, the slope of the plastic strain increment vectors can be determined as:

$$\frac{d\varepsilon_q^p}{d\varepsilon_p^p} = \frac{(p'_o - l)^2 \sqrt{1 - \left(\frac{p' - l}{p'_o - l}\right)^2}}{Ml(p' - l)} \quad (5.31)$$

In contrast, for specimens yielding “dry” of the CSL, the proposed yield locus does not coincide with the plastic potential surface of the material. Since the observed plastic strain increment vectors were almost perpendicular to the  $p'$  axis (in  $p'$ - $q$  plane), the plastic potential surface for ( $\eta > M$ ) in the compression plane can be approximated by a horizontal line with a constant deviator stress ( $q$ ) equal to:

$$q = Ml \quad (5.32)$$

By using this method, the small plastic volumetric expansions occurring after failure would be neglected.

## 5.5 Conclusions

In this study, the results of drained and undrained triaxial experiments on undisturbed and artificially cemented specimens of Ottawa clay were utilised to investigate the fundamental differences in the mechanical behaviour of naturally and artificially structured clays and to propose a new constitutive framework for the behaviour of the artificially cemented material. The following main conclusions can be made:

- It was observed that compression behaviour of the reconstituted Ottawa clay does not follow the general pattern reported for many other types of clay (Burland, 1990). This was attributed to the high silt content of the material.
- Whilst the naturally structured Ottawa clay existed in a meta-stable state and was highly collapsible, the artificially cemented Ottawa clay exhibited a more gradual degradation of the cementitious bonds. This was attributed to the approximately uniform dissemination of the cementitious bonds within the artificially cemented material. It was hypothesised that these brittle bonds do not break simultaneously in shearing or compression, but rather rupture gradually, resulting in an overall elasto-plastic response in accord with the critical state framework.
- Using estimates of dissipated plastic energy, the yield states were found for different stress ratios based on the experimental data for the artificially cemented clay. A mathematical formulation was employed to predict the observed yield states. The parameters defining the proposed formulation were also examined and alternative ways were proposed to obtain some of the required parameters.
- Expansion of the proposed yield envelop with plastic straining was studied by performing a number of unloading-reloading tests along different stress paths.



Isotropic hardening was confirmed since the shape of the yield locus was found to be unchanged due to plastic hardening. The energy variations during the unloading-reloading cycles showed that the deformations were recoverable only if the stress paths stayed well inside the current yield envelop.

- It was observed that the critical state line is preserved in the artificially cemented clay even at high confining pressures. Although cementation significantly increased the slope of the critical state line ( $M$ ), a further increase in the cement content was found to have a negligible effect on the slope of the CSL. In addition, the parameters required to define the proposed yield locus for the artificially cemented material were successfully predicted using the critical state concept.
- The proposed framework could predict a state boundary surface for the artificially cemented Ottawa clay. However, the attempt to apply the same concept to the natural clay was unsuccessful due to the non-linear post yield compression of the material.
- Two distinct modes of behaviour were observed in stress-strain curves for the artificially cemented clays. The specimens that failed “dry” of the CSL showed an approximately linear elastic pre-yield response followed by an abrupt failure. In contrast, the samples that yielded “wet” of the CSL exhibited an elasto-plastic gradual yielding. Work input data for different stress paths also indicated a brittle behaviour “dry” of the CSL and a ductile response “wet” of the critical state line.
- The test results showed that associated flow was obeyed in artificially cemented specimens failing “wet” of the CSL, while deviations from normality were observed in samples failing “dry” of the critical state line. A simple linear,

horizontal plastic potential surface was suggested to predict the plastic flow “dry” of the CSL.

## 5.6 Acknowledgements

The authors would like to express their gratitude to the Natural Sciences and Engineering Research Council of Canada, NSERC, and The University of Western Ontario for providing financial support for this work.

## 5.7 References

- Allman, M.A., and Atkinson, J.H. (1992). “Mechanical properties of reconstituted Bothkennar soil.” *Geotechnique*, 42(2),289–301.
- Atkinson, J.H., and Bransby, P.L. (1978). “The mechanics of soils: an introduction to critical state soil mechanics.” McGraw Hill, London, U.K.
- Baudet, B., and Stallebrass, S. (2004). “A constitutive model for structured clays.” *Geotechnique* , 54(4) , 269–278.
- Bergado, D.T., Anderson, L.R., Miura, N., and Balasubramaniam, A.S. (1996). “Soft ground improvement in lowland and other environments.” American Society of Civil Engineers (ASCE) Press, New York, U.S.A.
- Bhattacharja, S., Bhatta, J. I., and Todres, H. A. (2003). “Stabilization of Clay Soils by Portland Cement or Lime - A Critical Review of Literature.” PCA R&D Serial No. 2066, Portland Cement Association, Skokie, Illinois USA.

- Burland, J.B. (1990). "On the compressibility and shear strength of natural clays." *Geotechnique*, 40(3): 329–378.
- Chen, W.F., and Mizuno, E. (1990). "Nonlinear analysis in soil mechanics." Elsevier Science Publishers B.V., Amsterdam, The Netherlands.
- Clausen, C.-J.F., Graham, J., and Wood, D.M. (1984). "Yielding in soft clay at Mastemyr, Norway." *Geotechnique*, 34(4), 581–600.
- Folkes, D.J., and Crooks, J.H.A. (1985). "Effective stress paths and yielding in soft clays below embankments." *Canadian Geotechnical Journal*, 22(3), 357–374.
- Graham, J., Crooks, J.H.A., and Bell, A.L. (1983a). "Time effects on the stress-strain behaviour of natural soft clays." *Geotechnique*, 33(3), 327–340.
- Graham, J., Noonan, M. L., and Lew, K. V. (1983b). "Yield states and stress-strain relationships in a natural plastic clay." *Canadian Geotechnical Journal*, 20(3), 502–516.
- Graham, J., and Li, E.C.C. (1985). "Comparison of natural and remoulded plastic clay." *Journal of Geotechnical Engineering*, 111(7), 865–881.
- Head, K.H. (1986). "Manual of soil laboratory testing, Vol. 3: effective stress tests." Pentech Press Limited, London, England.
- Helinski, M., Fahey, M., and Fourie, A. (2007). "Numerical modeling of cemented mine backfill deposition." *Journal of Geotechnical and Geoenvironmental Engineering*, 133(10), 1308–1319.

- Horpibulsuk, S., Miura, N., and Bergado, D.T. (2004). "Undrained shear behavior of cement admixed clay at high water content." *Journal of Geotechnical and Geoenvironmental Engineering*, 130(10), 1096–1105.
- Horpibulsuk, S., Liu, M.D., Liyanapathirana, D.S., and Suebsuk, J. (2010). "Behaviour of cemented clay simulated via the theoretical framework of the Structured Cam Clay model." *Computers and Geotechnics*, 37(1-2), 1–9.
- Jaky, J. (1948). "Pressure in soils." *Proceedings of the 2nd ICSMFE, London*, (1), 103–107.
- Kamruzzaman, A.H.M., Chew, S.H., and Lee, F.H. (2009). "Structuration and Destructuration Behavior of Cement-Treated Singapore Marine Clay Cement-Treated Singapore Marine Clay." *Journal of Geotechnical and Geoenvironmental Engineering*, 135(4), 573–589.
- Kasama, K., Ochiai, H., and Yasufuku, N. (2000). "On the stress-strain behaviour of lightly cemented clay based on an extended critical state concept." *Soils and foundations*, 40(5): 37–47.
- Lamond, J.F., and Pielert, J.H. (2006). "Significance of tests and properties of concrete and concrete-making materials." ASTM International, Bridgeport, NJ, USA.
- Liu, M. D., and Carter, J. P. (2000). "Modelling the destructuring of soils during virgin compression." *Geotechnique*, 50(4), 479–483.
- Liu, M. D., and Carter, J. P. (2002). "A structured Cam Clay model." *Canadian Geotechnical Journal*, 39(6), 1313–1332.

- Lo, K.Y., and Morin, J.P. (1972). "Strength anisotropy and time effects of two sensitive clays." *Canadian Geotechnical Journal*, 9(3), 261–277.
- Locat, J., Tremblay, H., and Leroueil, S. (1996). "Mechanical and hydraulic behaviour of a soft inorganic clay treated with lime." *Canadian Geotechnical Journal*, 33(4), 654–669.
- Mitchell, R. J. (1970). "On the yielding and mechanical strength of Leda clays." *Canadian Geotechnical Journal*, 7, 297–312.
- Miura, N., Horpibulsuk, S., and Nagaraj, T.S. (2001). "Engineering behavior of cement stabilized clay at high water content." *Soils and Foundations*, 41(5), 33–45.
- Nagaraj, T.S., and Miura, N. (2001). "Soft clay behaviour – analysis and assessment." A.A. Balkema, Rotterdam, Netherlands.
- Rotta, G. V., Consoli, N. C., Prietto, P. D. M., and Graham, J. (2003). "Isotropic yielding in an artificially cemented soil cured under stress." *Geotechnique*, 53(5), 493–501.
- Rouainia, M., and Muir Wood, D. (2000). "A kinematic hardening constitutive model for natural clays with loss of structure." *Geotechnique*, 50(2), 153–164.
- Sasanian, S., and Newson, T.A. (2010). "Basic parameters governing the behaviour of cement-treated clays." To be submitted to *Soils and Foundations*.
- Schofield, A., and Wroth, P. (1968). "Critical state soil mechanics." McGraw Hill, Maidenhead, Berkshire, England.

- Silvestri, V. (1984). Discussion on “Preconsolidation pressure of Champlain clays. Part II. Laboratory determination” by Leroueil, S., Tavenas, F., Samson, L., and Morin, P., *Canadian Geotechnical Journal*, 21, 600–602.
- Smith, P.R., Jardine, R.J., and Hight, D.W. (1992). “The yielding of Bothkennar clay.” *Geotechnique*, 42(2), 257–274.
- Tavenas, F., and Leroueil, S. (1977). “Effects of stresses and time on yielding of clays.” *Proceedings of 9th International Conference on Soil Mechanics and Foundation Engineering*, Tokyo, 1,319–326.
- Tavenas, F., Des Rosiers, J.-P., Leroueil, S., La Rochelle, P., and Roy, M. (1979). “The use of strain energy as a yield and creep criterion for lightly overconsolidated clays.” *Geotechnique*, 29(3), 285–303.
- Taylor, G.I., and Quinney, H. (1931). “The plastic distortion of metals.” *The Philosophical Transaction of the Royal Society of London*, Series A, No. 230, 323–362.
- Tremblay, H., Leroueil, S., and Locat, J. (2001). “Mechanical improvement and vertical yield stress prediction of clayey soils from eastern Canada treated with lime or cement.” *Canadian Geotechnical Journal*. 38, 567–579.
- Uddin, K., Balasubramaniam, A.S., and Bergado, D.T. (1997). “Engineering behavior of cement-treated Bangkok soft clay.” *Geotechnical Engineering Journal*, 28(1), 89–119.

- Vatsala, A., Nova, R., and Srinivasa Murthy, B.R. (2001). "Elastoplastic model for cemented soils." *Journal of Geotechnical and Geoenvironmental Engineering*, 127(8): 679–687.
- Wong, P.K.K., and Mitchell, R.J. (1975). "Yielding and plastic flow of sensitive cemented clay." *Geotechnique*, 25, 763–782.
- Wood, D.M., (1990). "Soil Behaviour and critical state soil mechanics". Cambridge University Press, Cambridge, UK.
- Yasufuku, N., Ochiai, H., and Kasama, K. (1997). "The dissipated energy equation of lightly cemented clay in relation to the critical state model." *Proceedings of 9<sup>th</sup> International Conference on Computer Methods and Advances in Geomechanics*, Yuan, 2, 917–922.

**Table 5-1.** Summary of laboratory triaxial experiments performed on artificially cemented Ottawa clay

Test ID	c (%)	P <sub>i</sub> (kPa)	Test description
AC21	3.1	10	(i) Isotropic consolidation to p'=600 kPa, (ii) Undrained shear at constant cell pressure
AC22			(i) K <sub>o</sub> consolidation to p'=236 & q=307 kPa, (ii) Undrained shear at constant cell pressure
AC27			(i) Drained shear ( $\zeta = 3$ )
AC28			(i) Drained probing ( $\zeta = 0.5$ ) to p'=124 & q=60 kPa, (ii) Undrained shear at constant cell pressure
AC1	4.2	10	(i) Isotropic consolidation to p'=600 kPa, (ii) Undrained shear at constant cell pressure
AC16			(i) & (iii) Isotropic loading to p'=200 & 600 kPa, (ii) & (iv) Isotropic unloading to p'=25 kPa, (vi) Undrained shear
AC5	30	100	(i) K <sub>o</sub> consolidation to p'=500 & q=775 kPa, (ii) Unloading to p'=500 & q=0 kPa, (iii) Drained shear ( $\zeta=-3$ )
AC2			(i) Drained shear ( $\zeta = 3$ )
AC6			(i) Drained shear ( $\zeta = -3$ )
AC10	75	75	(i) Drained shear ( $\zeta = -4.7$ )
AC3			(i) Drained shear ( $\zeta = 3$ )
AC4			(i) Drained shear with constant p'
AC8			(i) Drained probing ( $\zeta = 1$ ) to p'=220 & q=149 kPa, (ii) Undrained shear at constant cell pressure
AC9	25	75	(i) Drained shear ( $\zeta = -3$ )
AC14			(i) Drained probing ( $\zeta=0.5$ ) to p'=606 & q=292 kPa, (ii) Unloading to p'=200 & q=0 kPa, (iii) Drained shear ( $\zeta=3$ )
AC15			(i) Drained probing ( $\zeta=1.6$ ) to p'=466 & q=630 kPa, (ii) Unloading to p'=200 & q=0 kPa, (iii) Drained shear ( $\zeta=3$ )
AC13			(i) Undrained shear at constant cell pressure
AC12			(i) Undrained shear at constant cell pressure
AC11	150	400	(i) Undrained shear at constant cell pressure
AC7			(i) Undrained shear at constant cell pressure
AC17	4.2	75	(i) Drained shear in extension with constant p'
AC18			(i) Drained shear in extension ( $\zeta = -2.5$ )
AC19			(i) Drained shear in extension ( $\zeta = 3$ )
AC20			(i) Undrained shear in extension at constant cell pressure
AC24	6.4	10	(i) Isotropic consolidation to p'=1000 kPa, (ii) Undrained shear at constant cell pressure
AC23			(i) K <sub>o</sub> consolidation to p'=855 & q=1360 kPa, (ii) Undrained shear at constant cell pressure
AC26			(i) Drained probing ( $\zeta = 0.58$ ) to p'=897 & q=378 kPa, (ii) Undrained shear at constant cell pressure
AC25			(i) Drained probing ( $\zeta = 1.73$ ) to p'=688 & q=765 kPa, (ii) Undrained shear at constant cell pressure



**Table 5-2.** Parameters defining the isotropic and  $K_0$  compression and the critical state line for the artificially cemented Ottawa clay

Soil parameter	Cement content, c (%)	Isotropic compression line	$K_0$ compression line	Critical state line (CSL)
$\lambda$	3.1	0.275	0.283	0.311
	4.2	0.345	0.348	0.358
	6.4	0.435	0.451	0.466
	Undisturbed	0.365		0.382
$v_\lambda$	3.1	4.09	4.06	4.01
	4.2	4.92	4.86	4.75
	6.4	5.93	5.85	5.67
	Undisturbed	4.36		4.24

**Table 5-3.** Parameters defining the elastic isotropic compression and unloading-reloading lines for the artificially cemented Ottawa clay

Soil parameter	Cement content, c (%)	Elastic compression line	Unloading-reloading line (1)	Unloading-reloading line (2)
$\kappa$	3.1	0.015		
	4.2	0.014	0.014	0.013
	6.4	0.011		
	Undisturbed	0.028		
$v_{\kappa}$	3.1	3.25		
	4.2	3.28	3.19	2.81
	6.4	3.28		
	Undisturbed	3.21		

**Table 5-4.** Parameters required to define the proposed yield loci for samples with different cement contents

Cement content, $c$ (%)	$P'_{o}$ (kPa)	$M$	$l$ (kPa)	$R_{\text{yield data}}$	$R_{\text{critical state}}$
3.1	32	1.86	23	0.21	0.18
4.2 (compression)	168	1.89	115	0.24	0.34
4.2 (extension)	168	-0.72	140	-0.28	-0.91
6.4	557	1.99	320	0.37	0.40

**Table 5-5.** The measured average  $K_o$  coefficients and calculated Poisson's ratios of the artificially cemented Ottawa clay

Cement content, c (%)	Coefficient of earth pressure at rest, $K_o$	Poisson's ratio, $\nu'$	$K_o$ (Jaky, 1948)
3.1	0.29	0.22	0.29
4.2	0.22	0.18	0.28
6.4	0.22	0.18	0.25

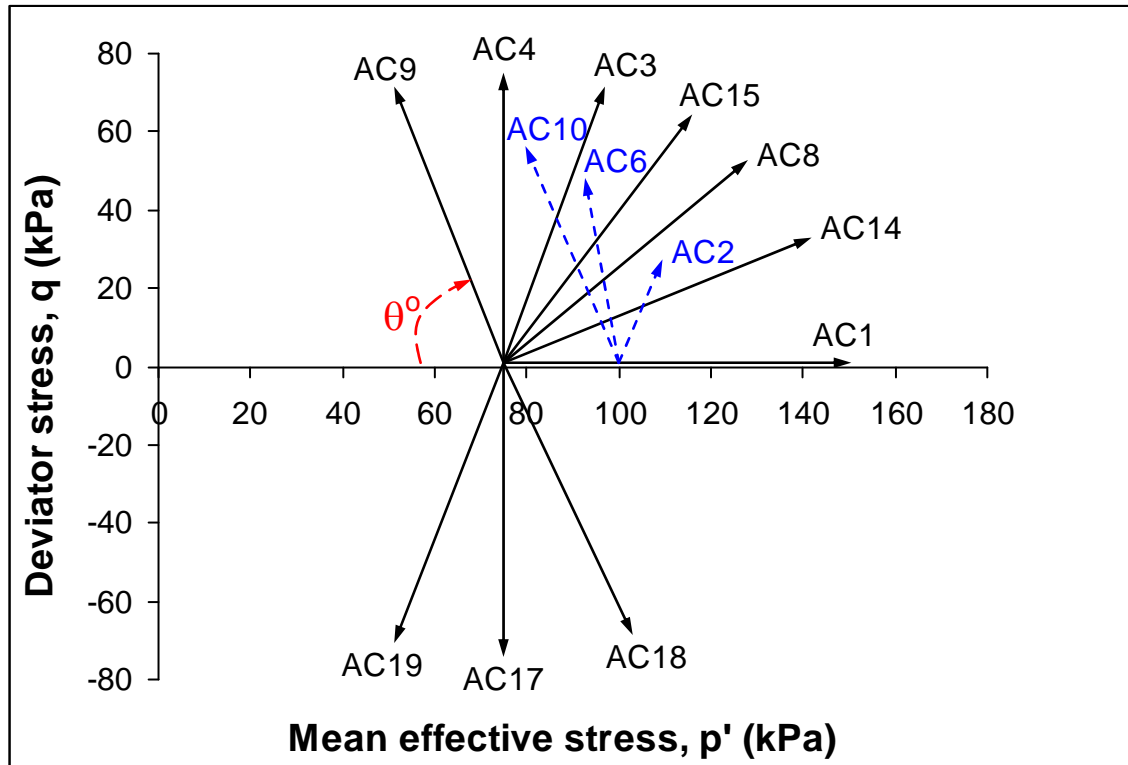


**Fig. 5-1.** The direction of the drained probing triaxial tests performed on specimens with 4.2% cement content

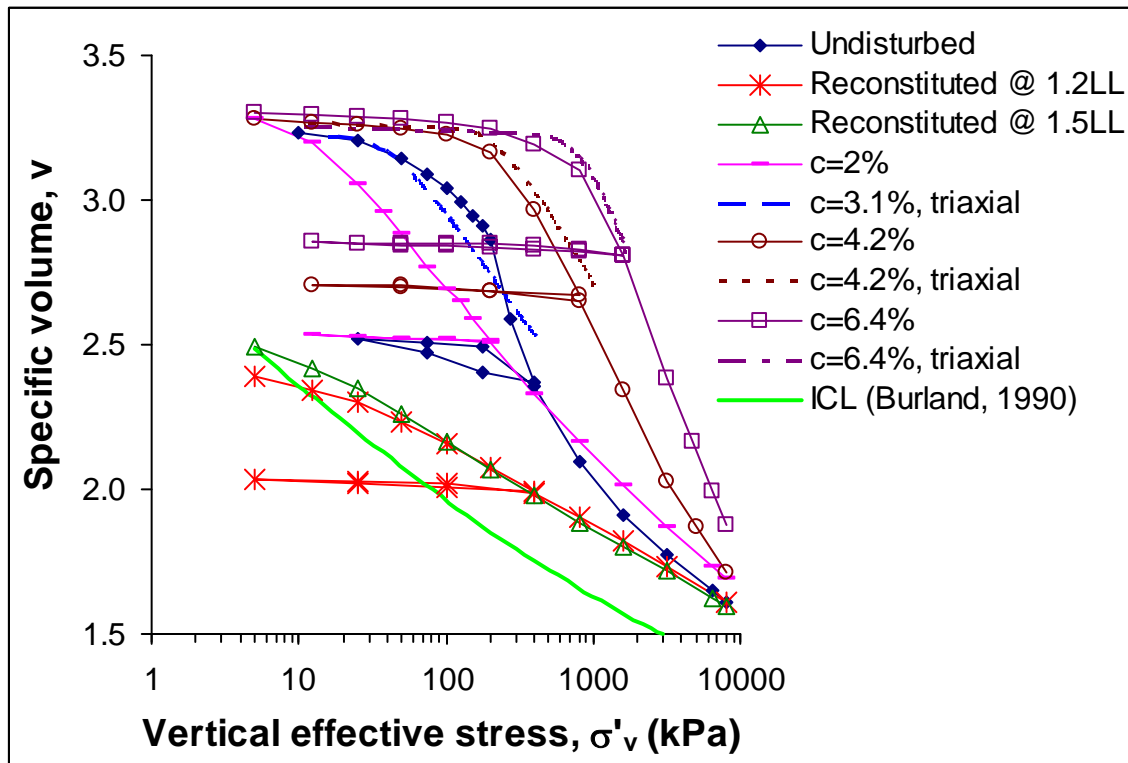


**Fig. 5-2.** One dimensional compression of undisturbed, reconstituted, and artificially cemented Ottawa clay

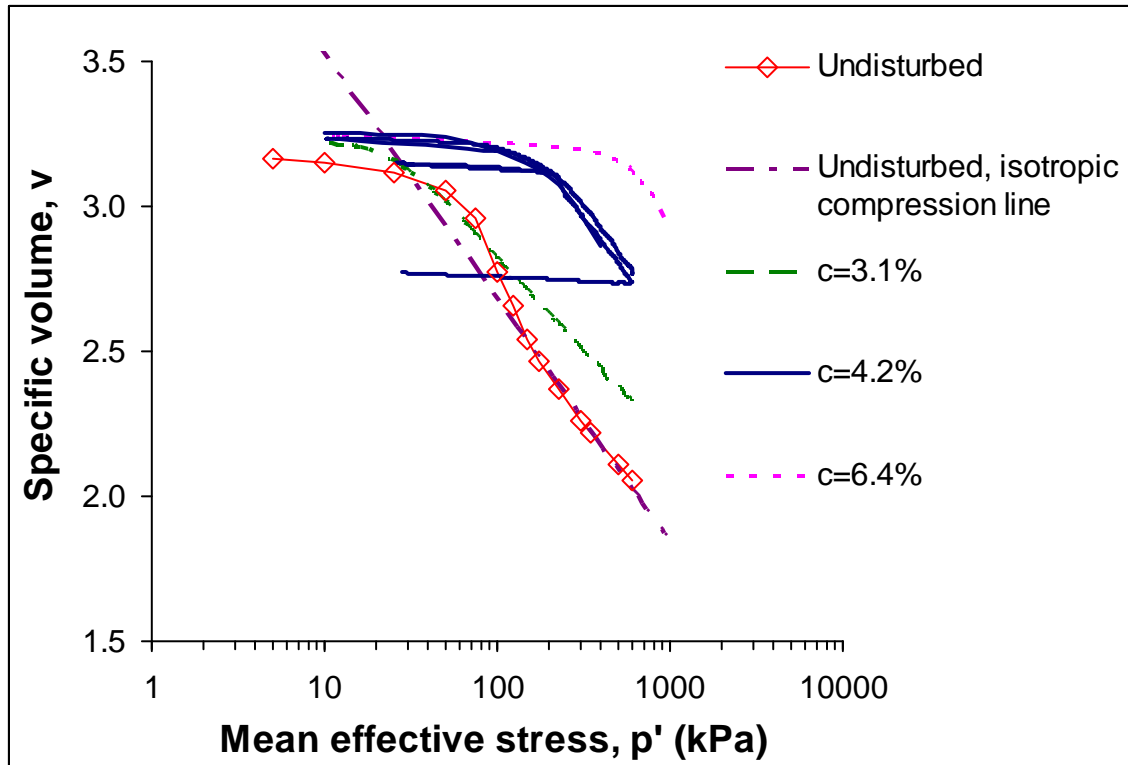


**Fig. 5-3.** Isotropic compression of undisturbed and artificially cemented Ottawa clay

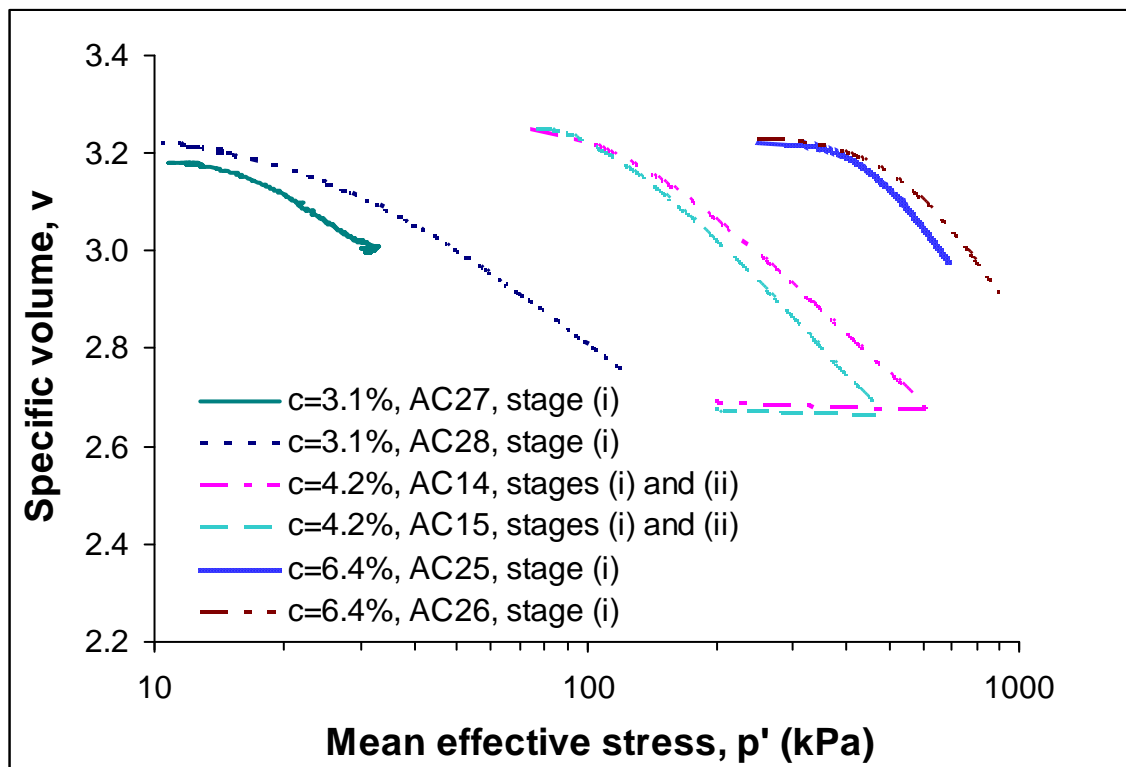
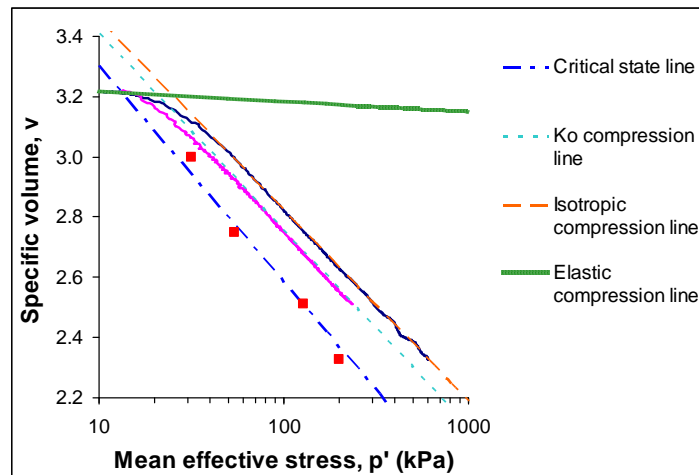
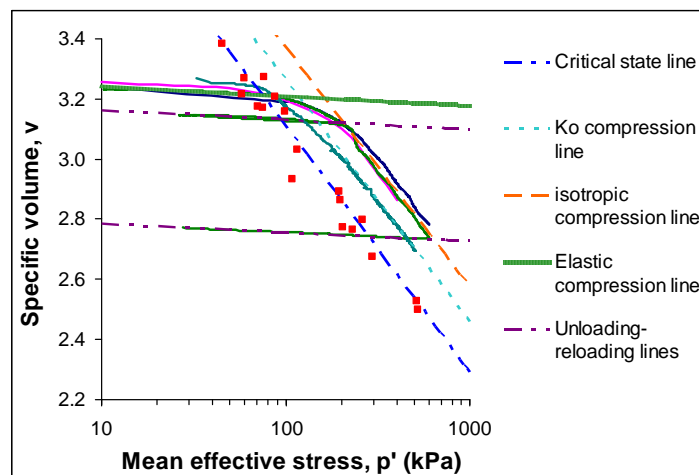


**Fig. 5-4.** Volumetric response of artificially cemented specimens due to loading and unloading in different stress paths

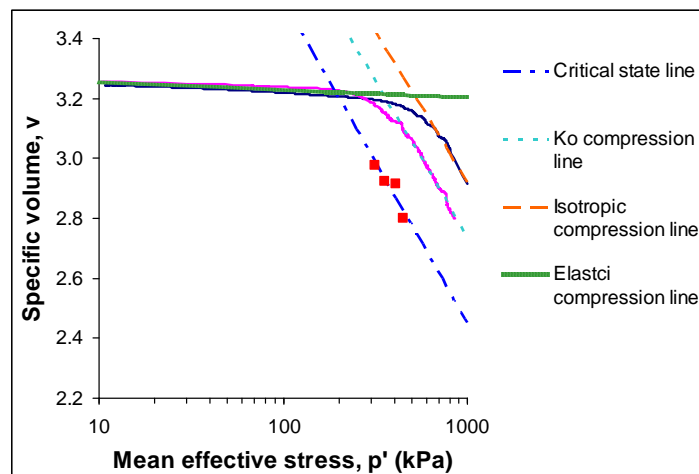




(a)



(b)



(c)

**Fig. 5-5.** Modeling of the volumetric behaviour with changes in the mean effective stress

( $p'$ ) of artificially cemented Ottawa clays: (a)  $c=3.1\%$ ; (b)  $c=4.2\%$ ; (c)  $c=6.4\%$

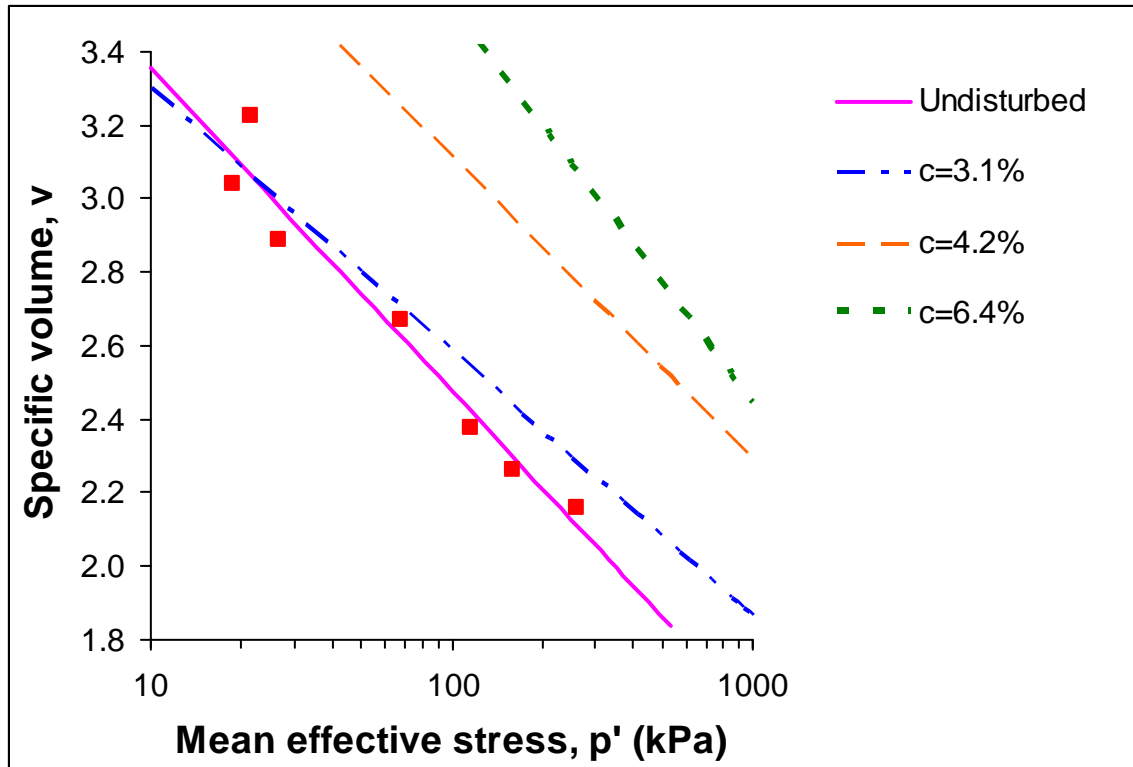


**Fig. 5-6.** The critical state lines on the volumetric plane of the naturally and artificially structured Ottawa clay

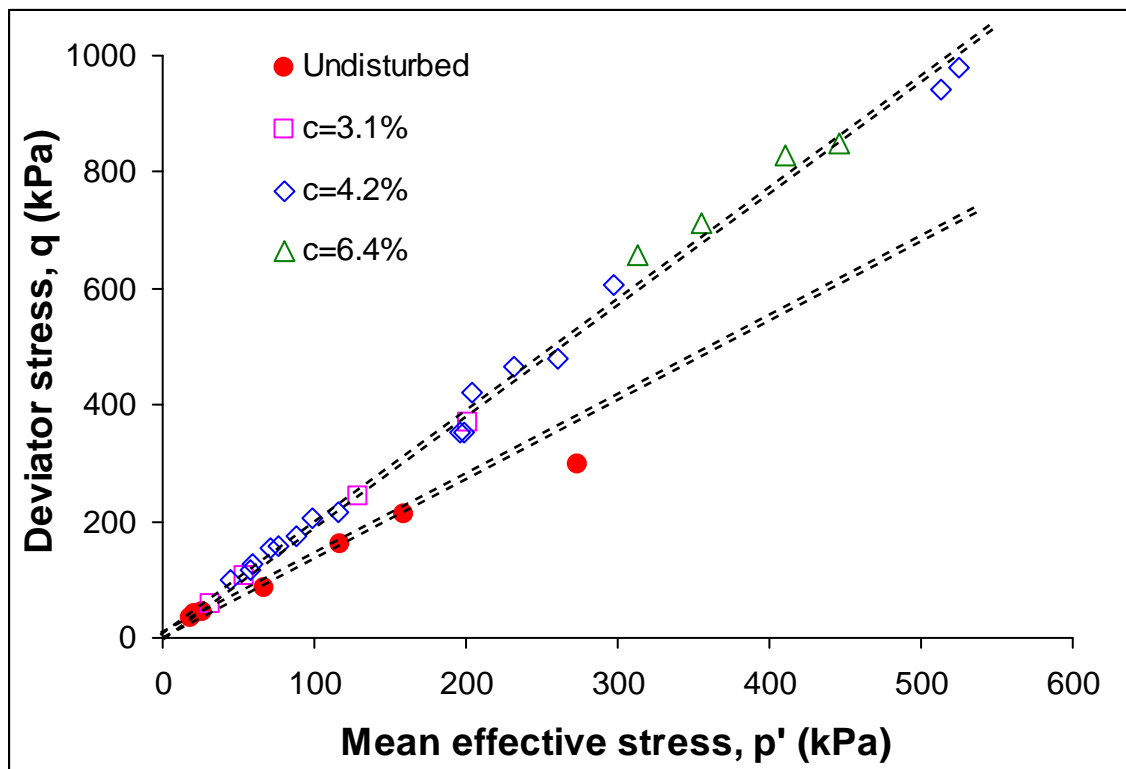


**Fig. 5-7.** The critical state lines on the  $p'$ - $q$  plane of the naturally and artificially structured Ottawa clay

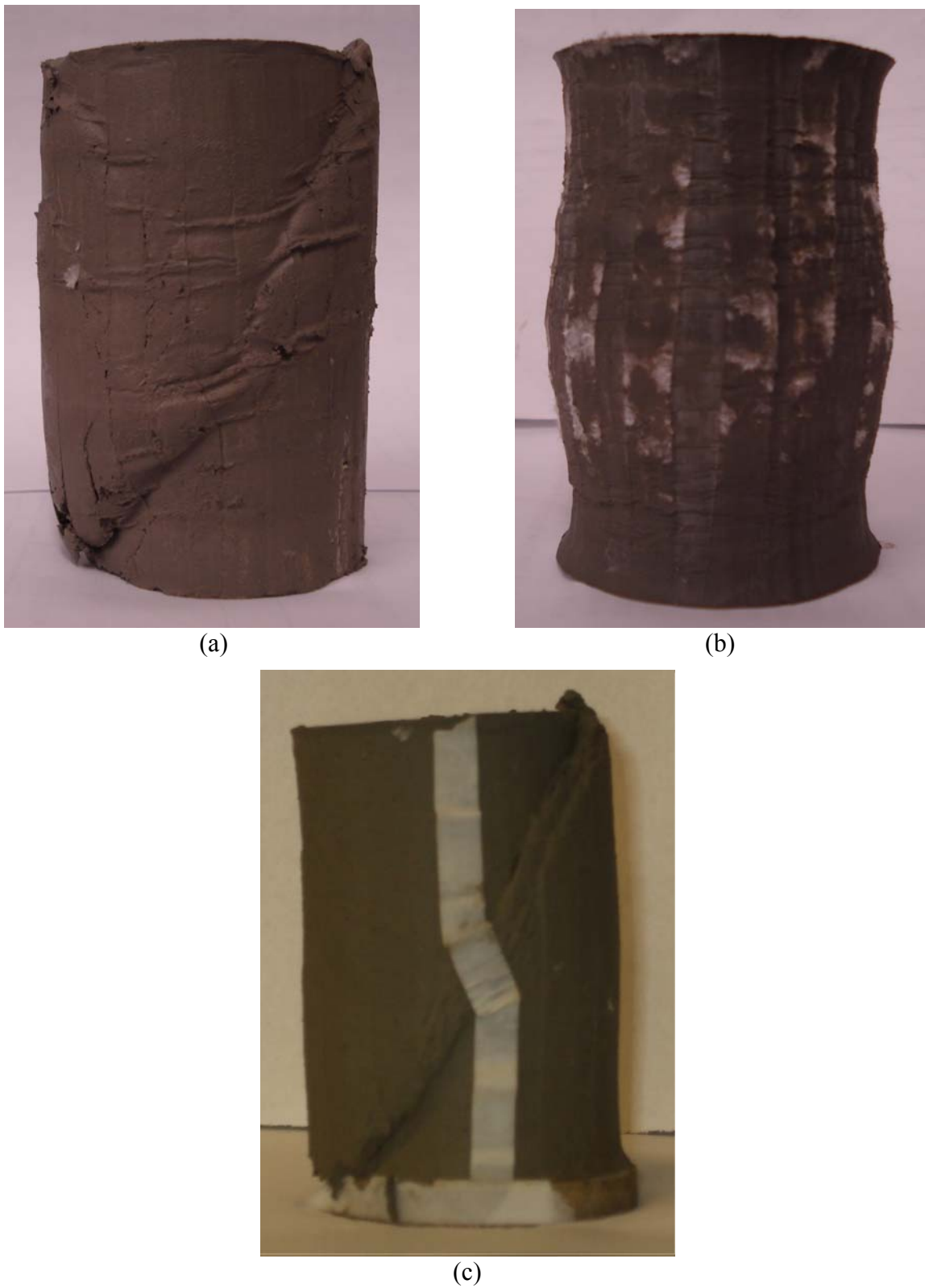


**Fig. 5-8.** Images of the sheared specimens: (a) Undisturbed,  $p'_i = 25$  kPa; (b) Undisturbed,  $p'_i = 600$  kPa; (c) artificially cemented ( $c = 3.1\%$ ),  $p'_i = 600$  kPa

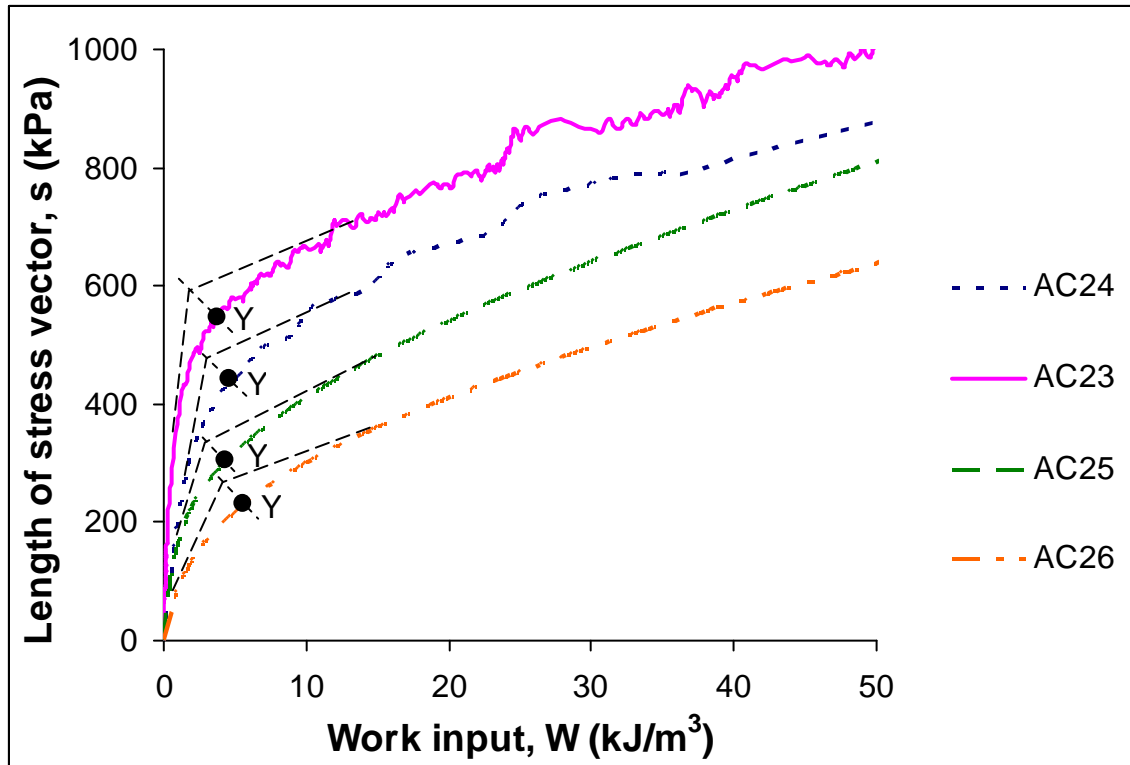


**Fig. 5-9.** The derivation of the yield states for tests performed along different stress paths

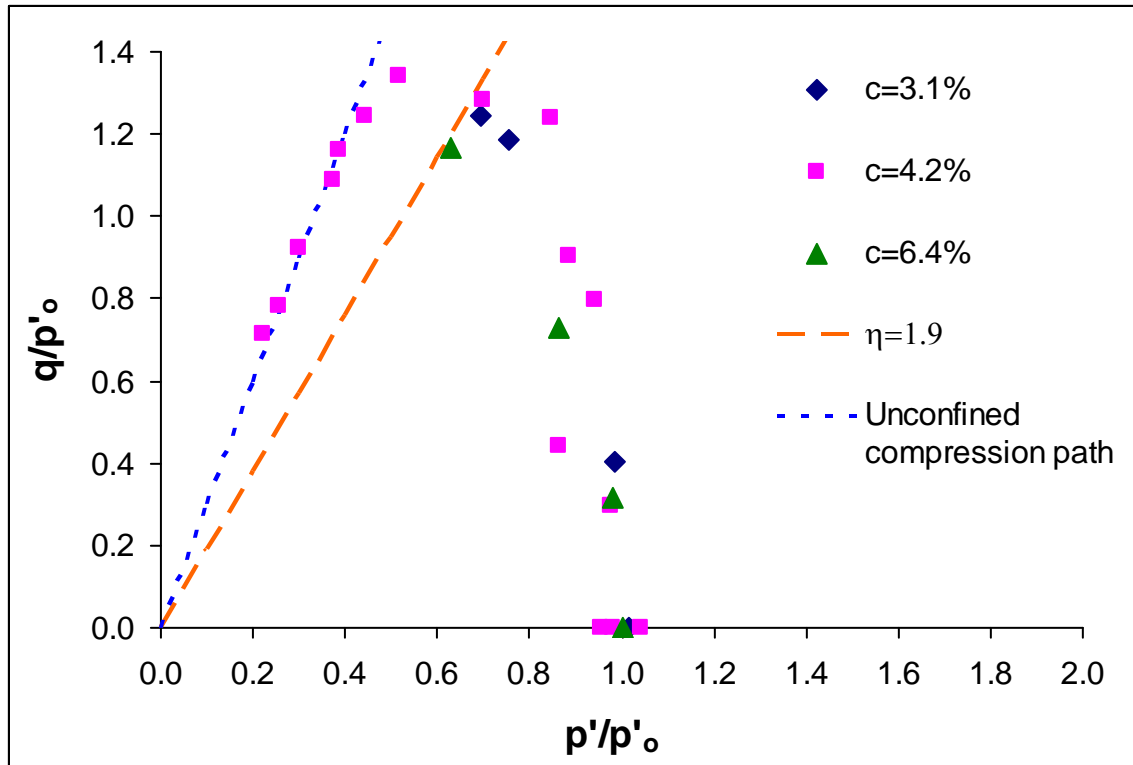
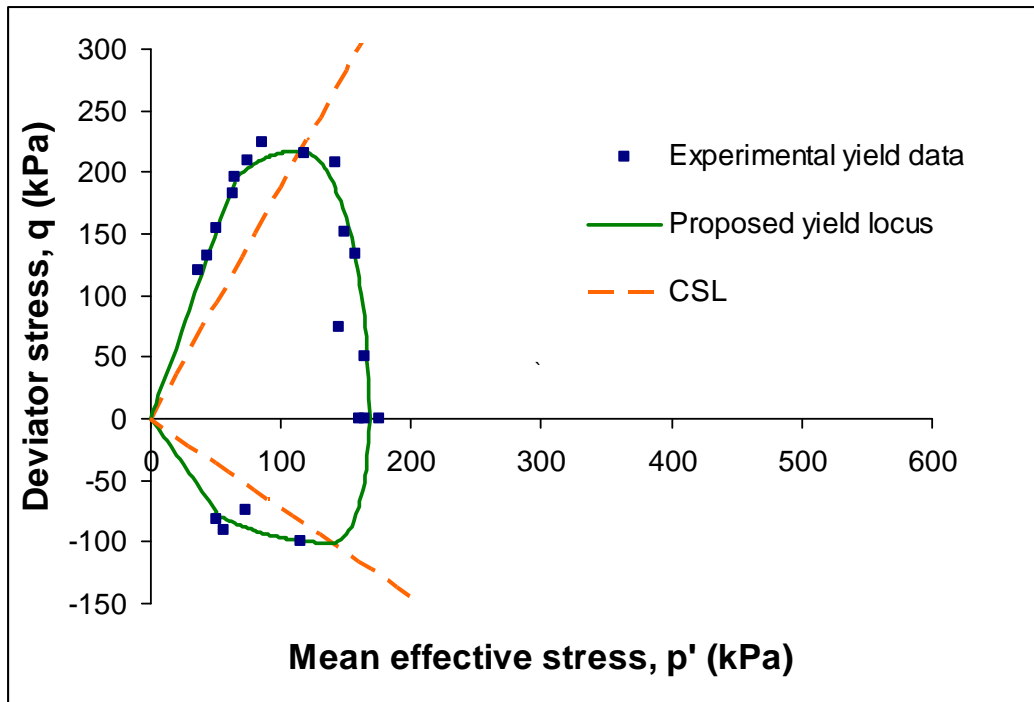
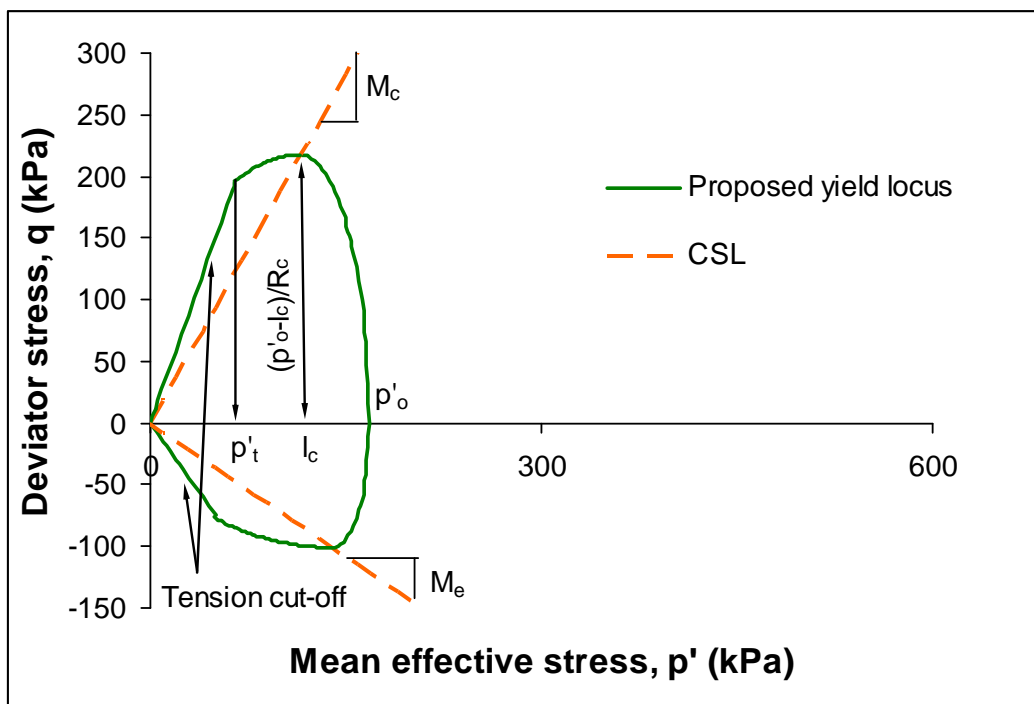


**Fig. 5-10.** Normalised yielding states of the artificially cemented specimens with different cement contents

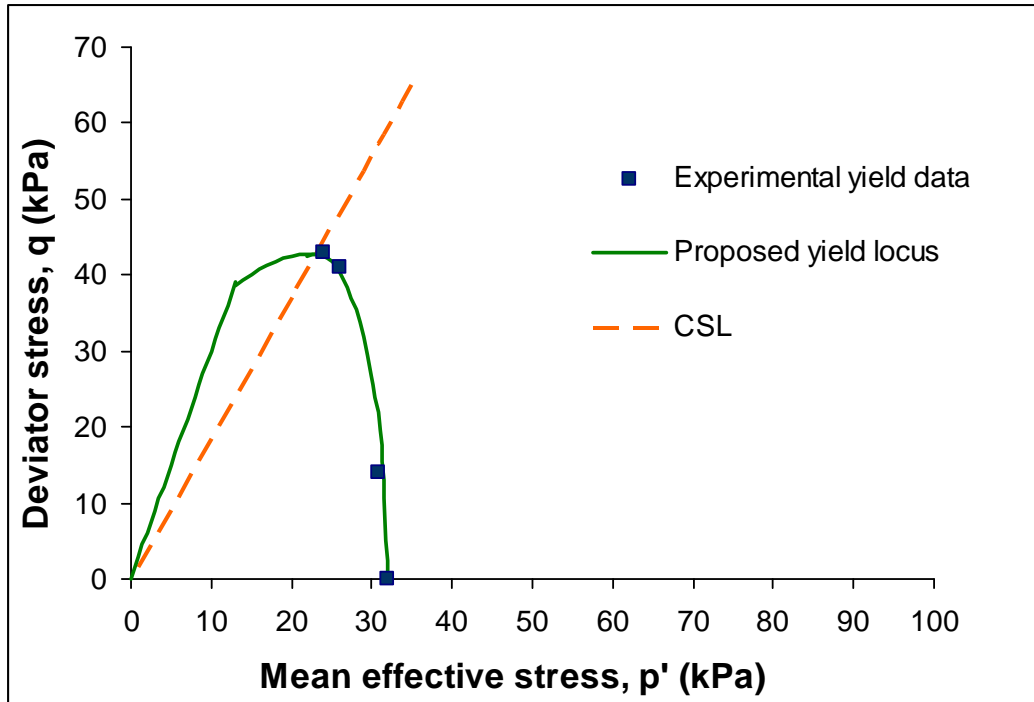


(a)

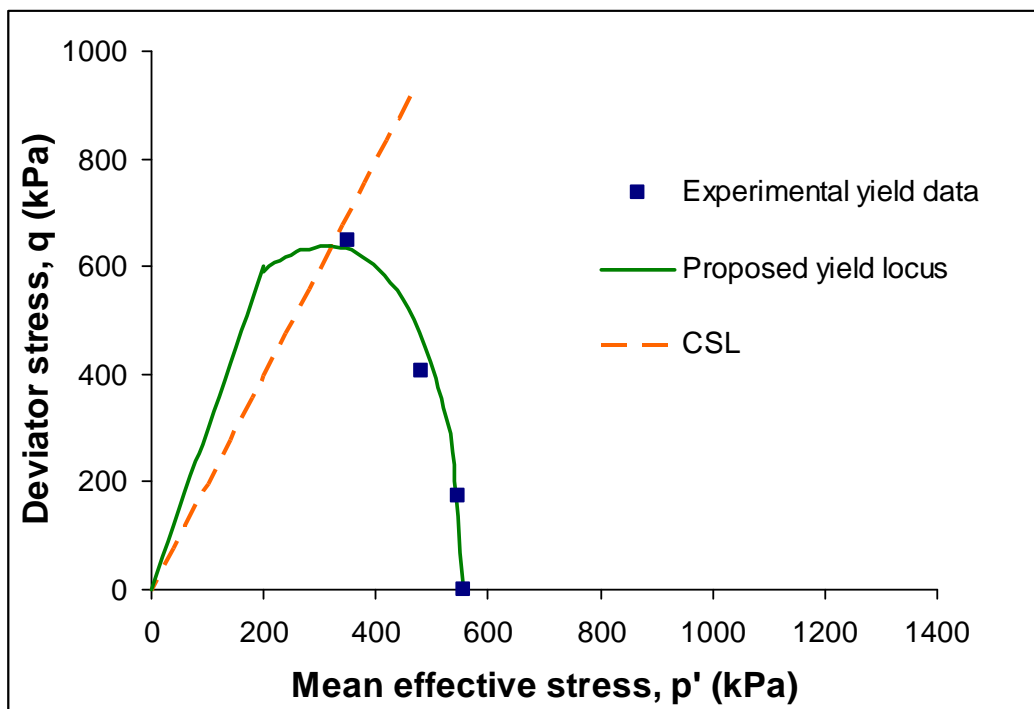


(b)

**Fig. 5-11.** (a) The experimental yielding states, and (b) the proposed model for the artificially cemented specimen with 4.2% cement content



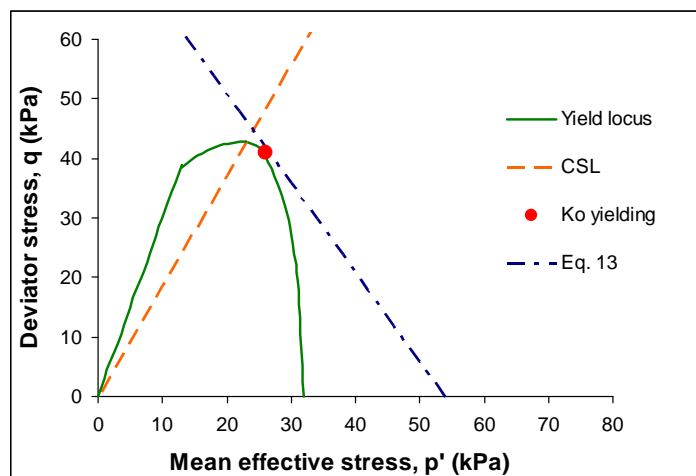
(a)



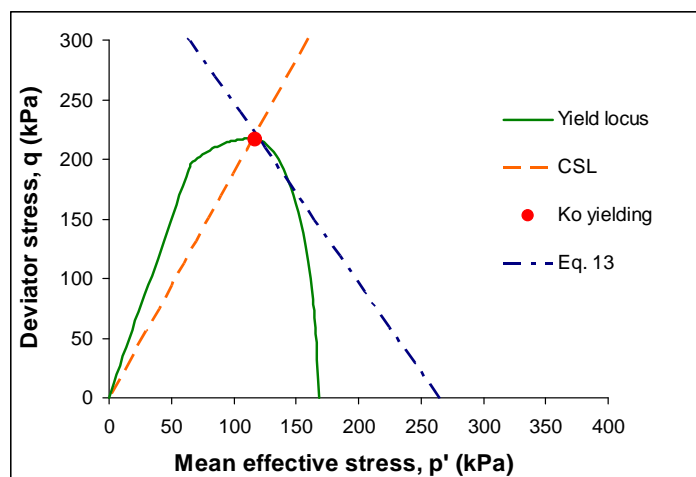
(b)

**Fig. 5-12.** The experimental yielding states and the proposed model for the artificially cemented specimen with: (a)  $c=3.1\%$ ; (b)  $c=6.4\%$

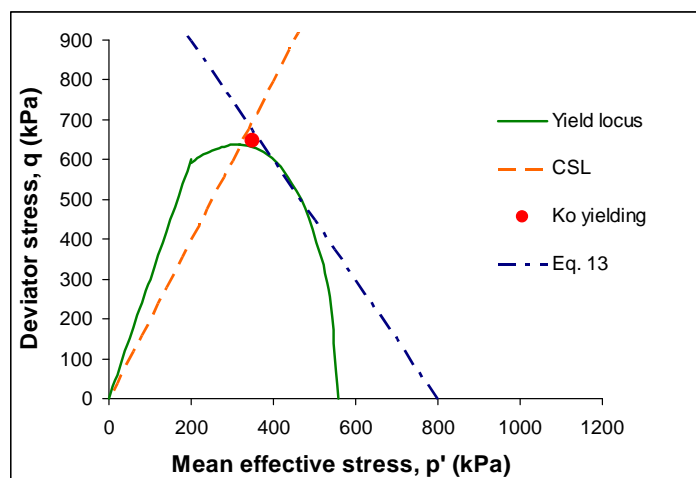




(a)



(b)



(c)

**Fig. 5-13.** The determination of the size of the yield locus using oedometer test results:

(a)  $c=3.1\%$ ; (b)  $c=4.2\%$ ; (c)  $c=6.4\%$

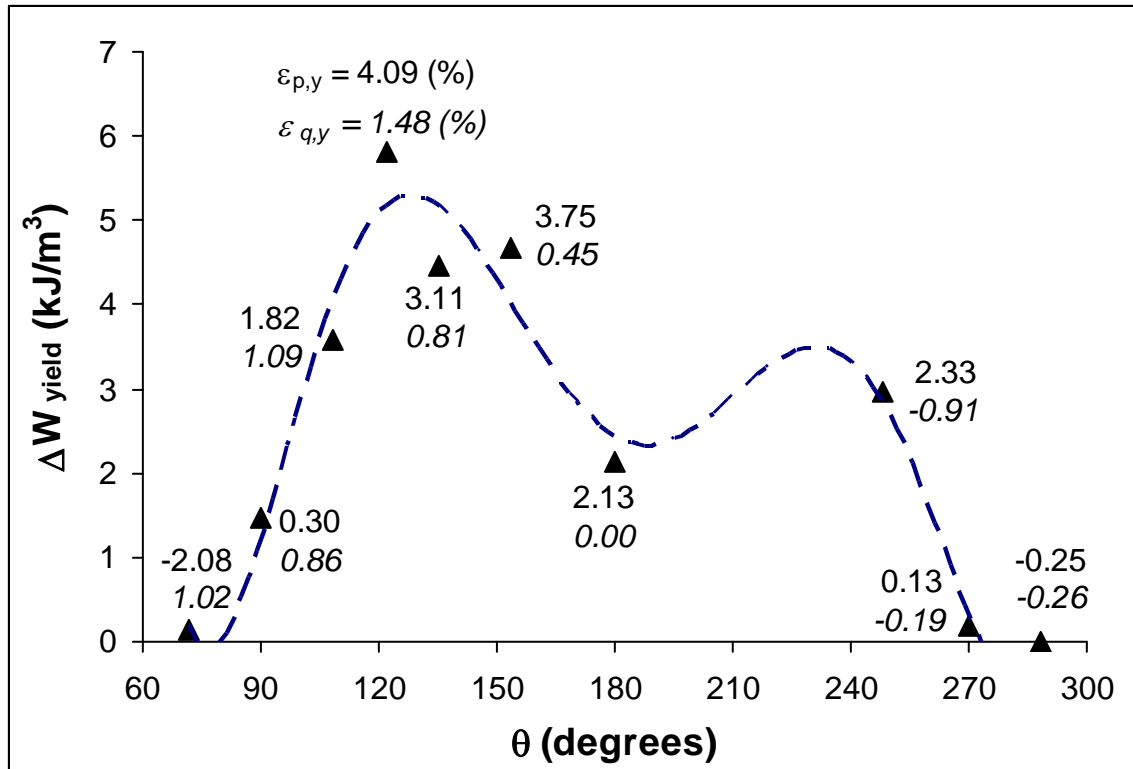


**Fig. 5-14.** The amount of work required to cause yielding in specimens with 4.2% cement content versus the direction of the drained probing tests (all started at  $p'_i=75\text{kPa}$ )

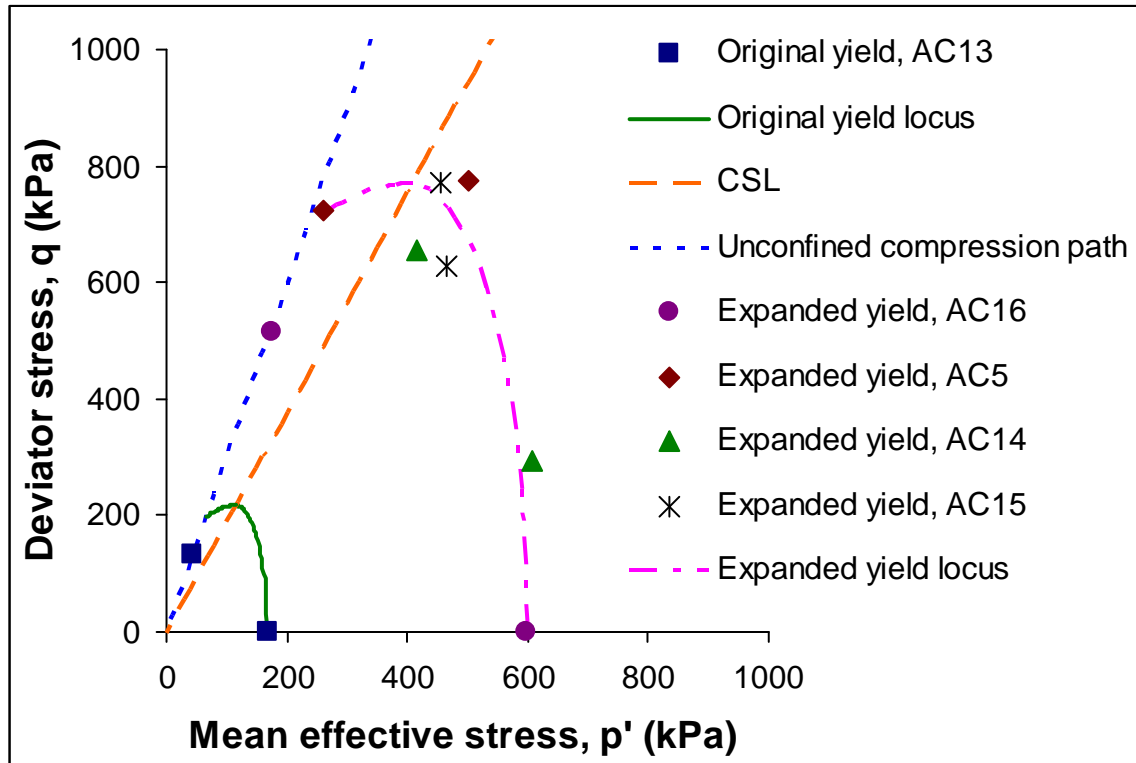


**Fig. 5-15.** The expansion of the yield surface along different stress paths in the artificially cemented specimen with 4.2% cement content

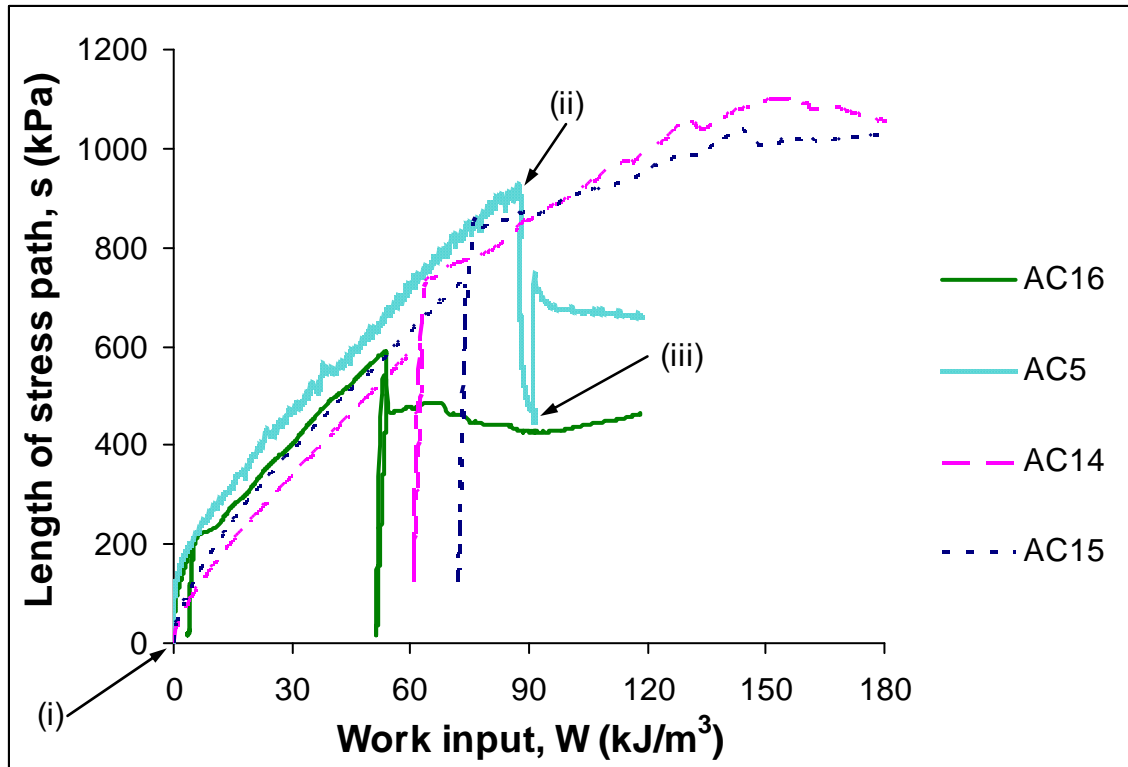
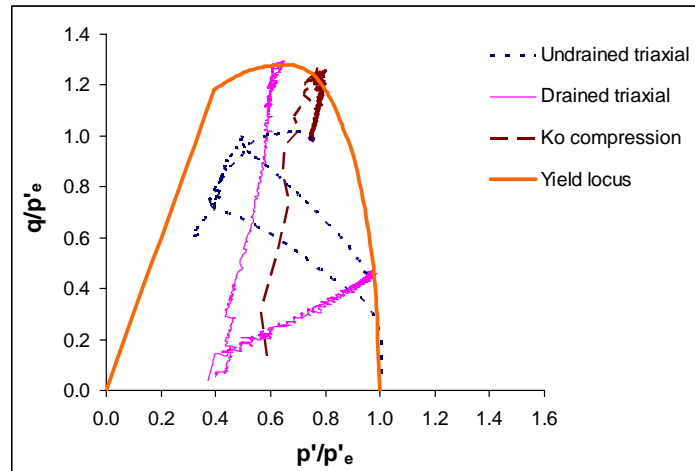
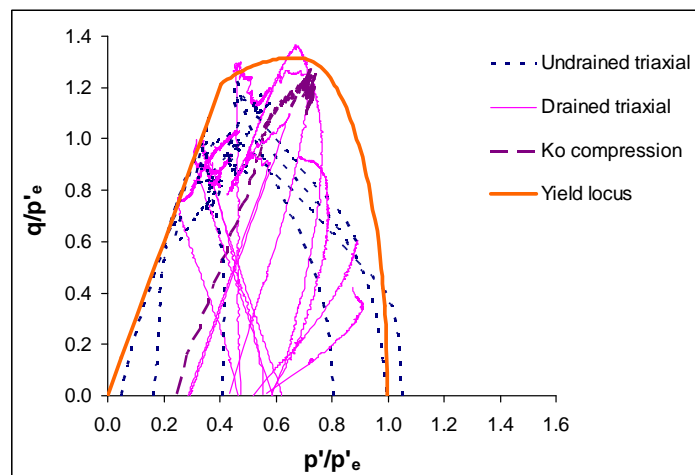


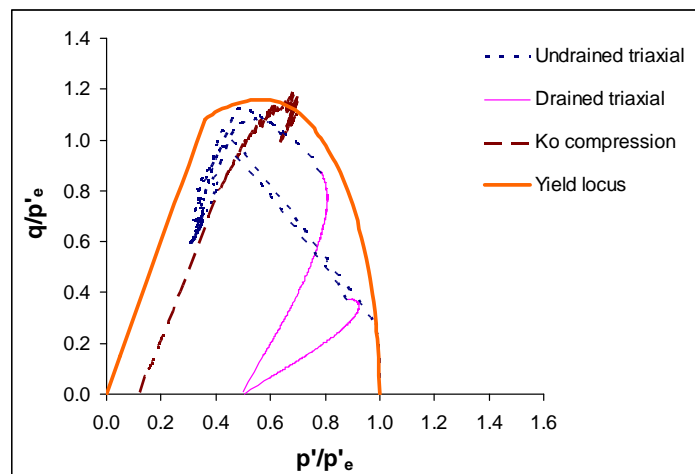
**Fig. 5-16.** The variations in the work input during the unloading-reloading of the specimens with 4.2% cement content along different stress paths



(a)



(b)



(c)

**Fig. 5-17.** The state boundary surface of artificially cemented specimens with: (a)

$c=3.1\%$ ; (b)  $c=4.2\%$ ; (c)  $c=6.4\%$

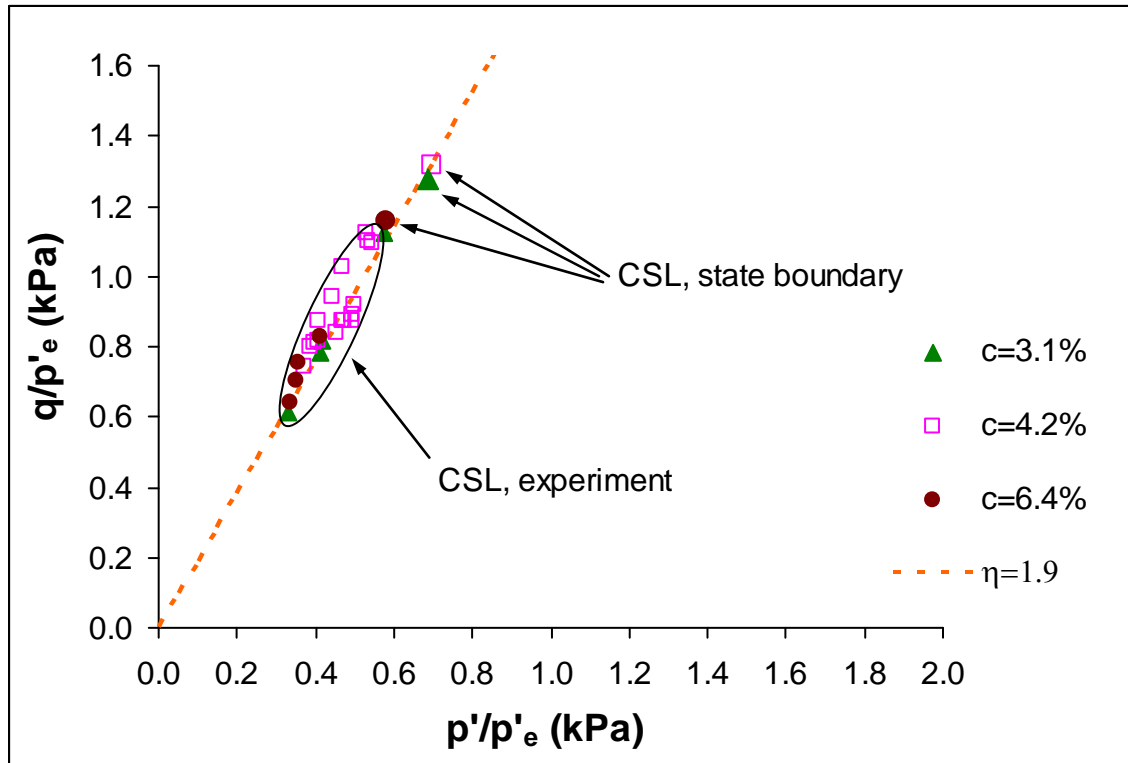
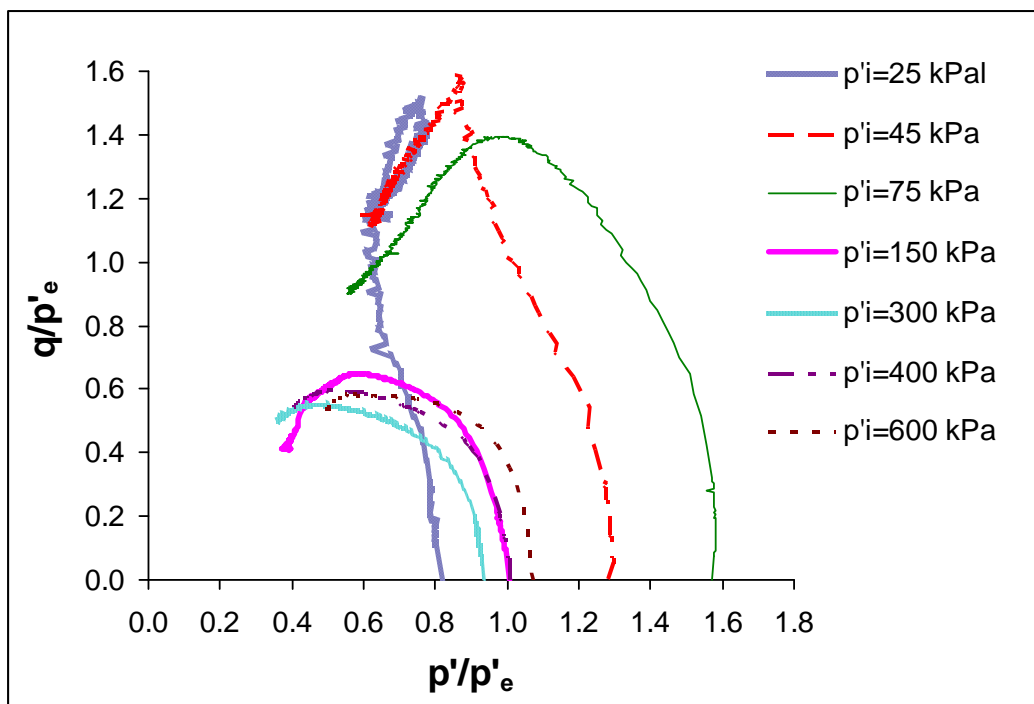
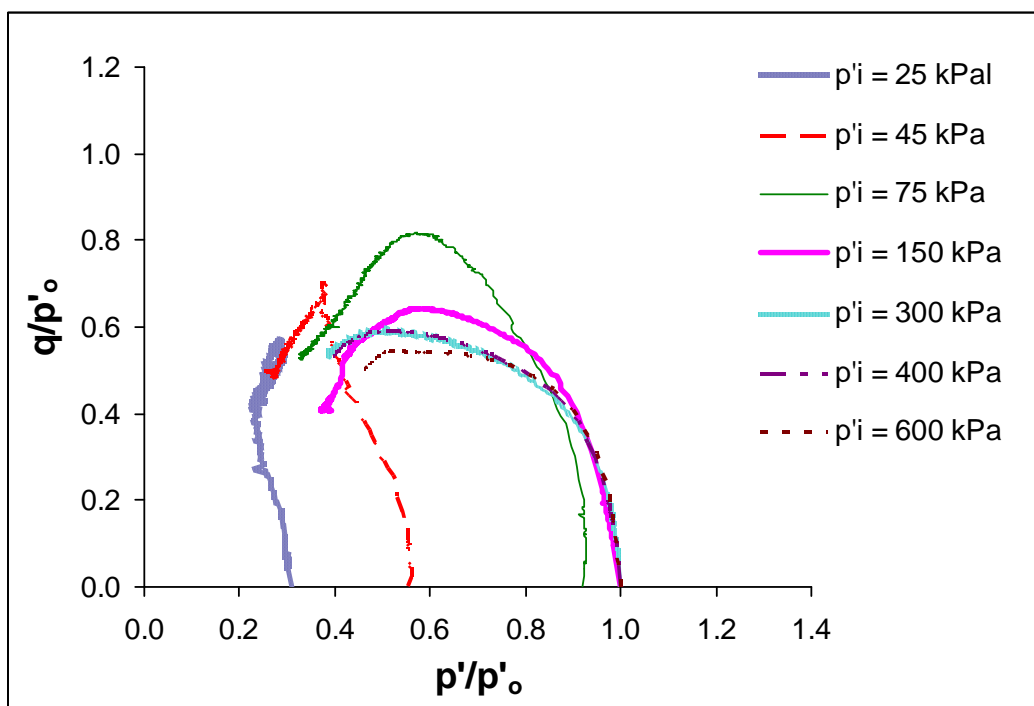


**Fig. 5-18.** Theoretical and experimental critical state lines in normalized stress space

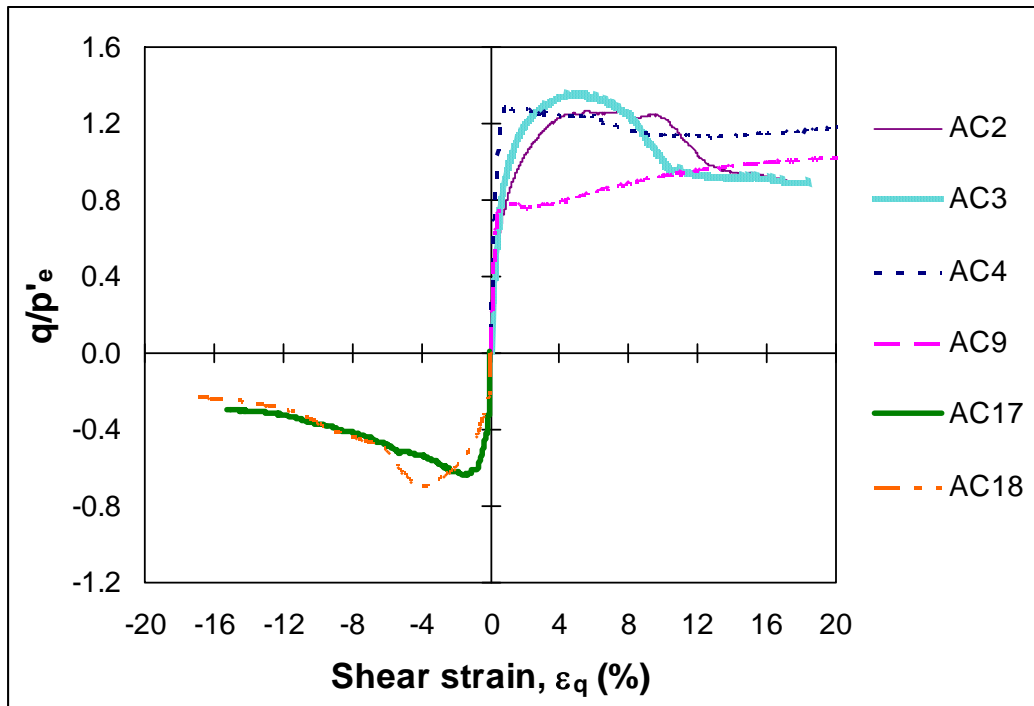


(a)

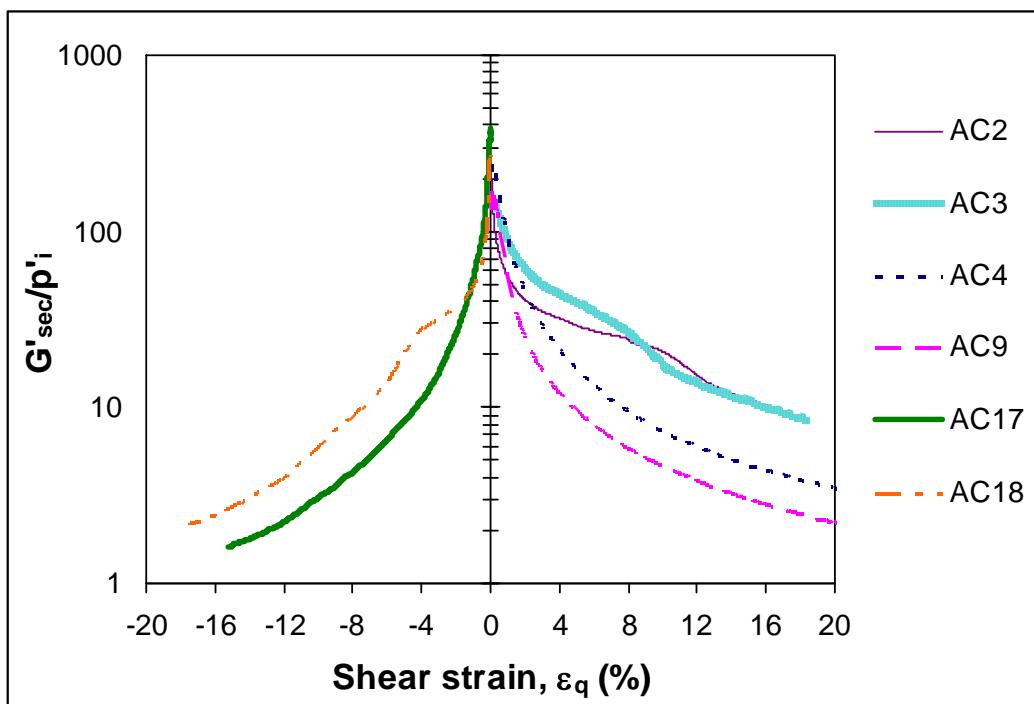


(b)

**Fig. 5-19.** Normalized stress paths obtained for undisturbed Ottawa clay: (a) using the equivalent pressure ( $p'_e$ ); (b) using the isotropic yield stress ( $p'_o$ )



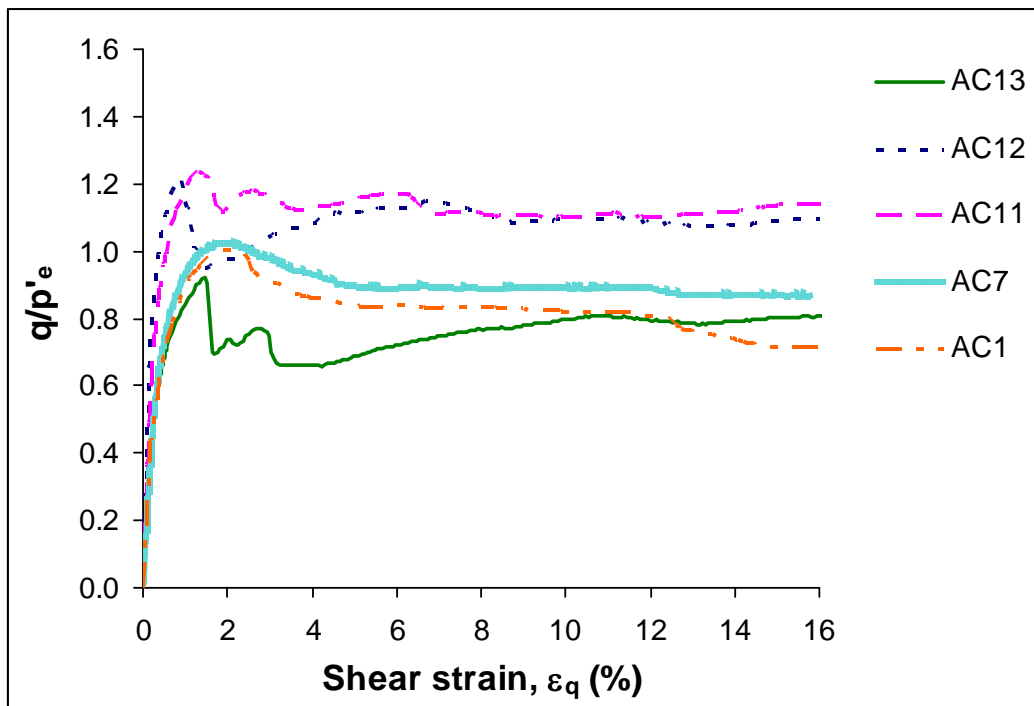
(a)



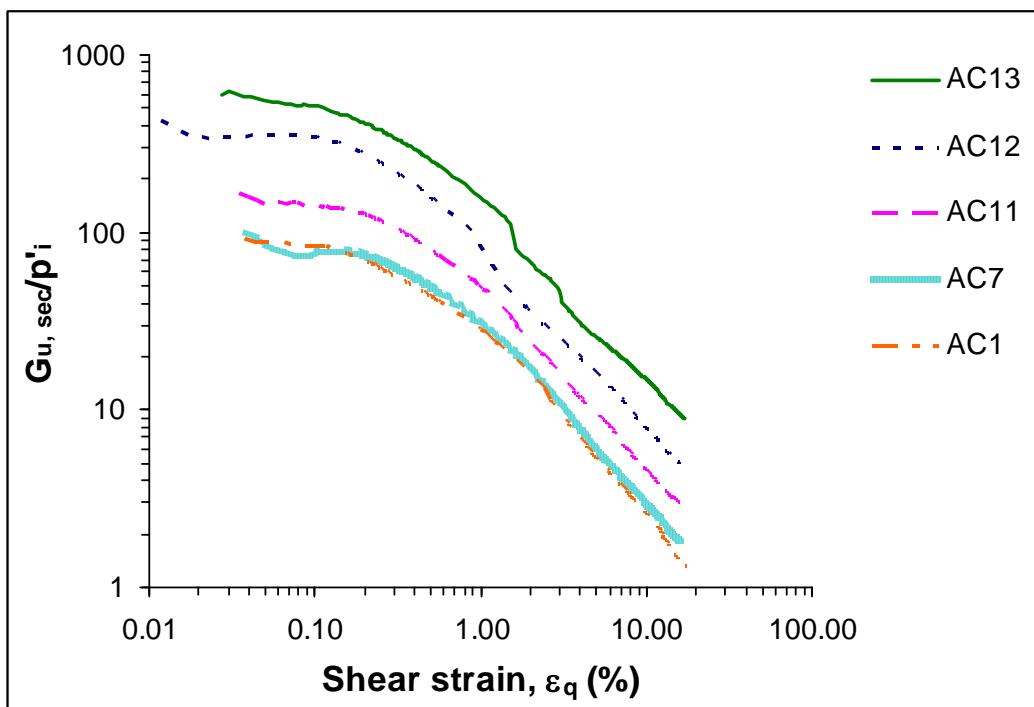
(b)

**Fig. 5-20.** Gradual versus brittle failure of artificially cemented clay ( $c=4.2\%$ ) in drained compression and extension: (a) normalized deviator stress versus shear strain; (b) normalized shear modulus versus shear strain





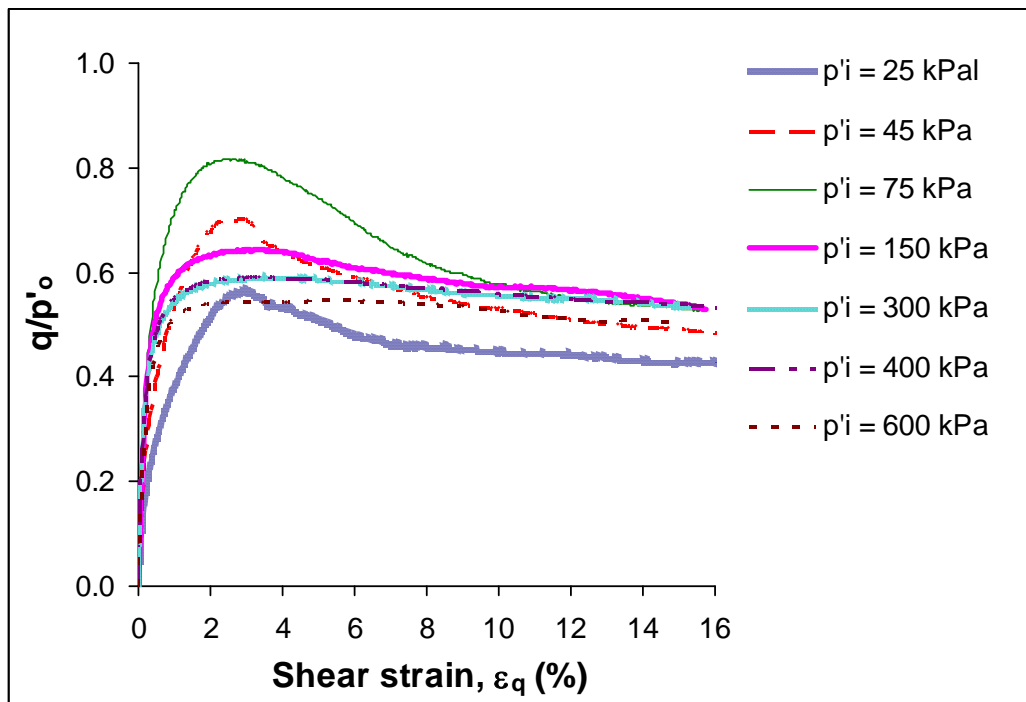
(a)



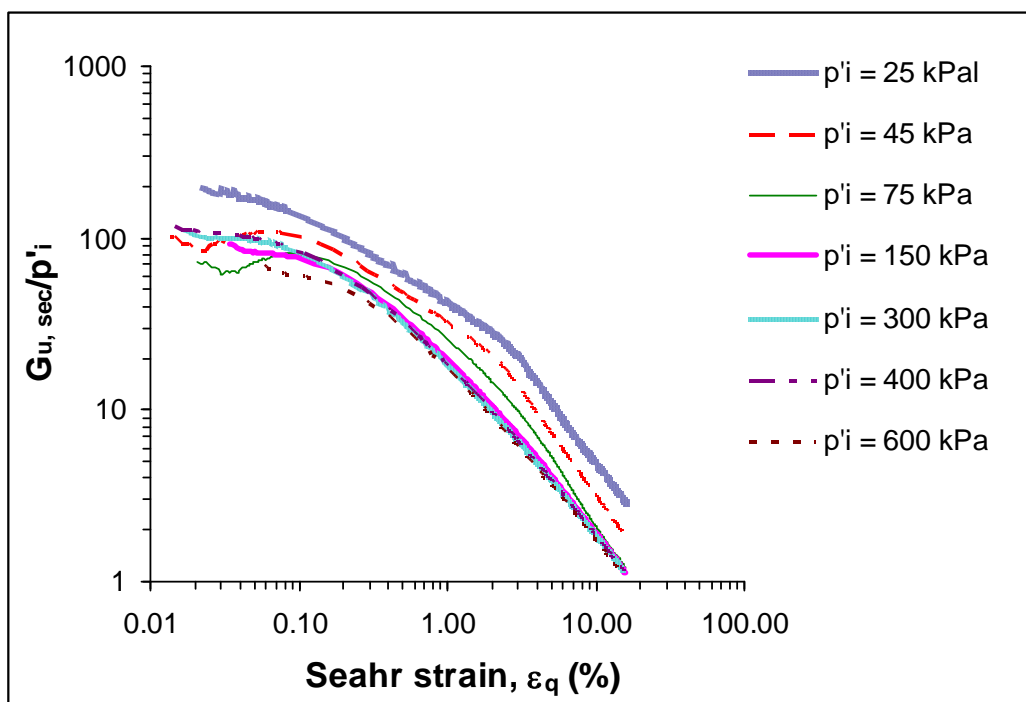
(b)

**Fig. 5-21.** Undrained shear behaviour of the artificially cemented Ottawa clay ( $c=4.2\%$ ):

(a) normalized deviator stress versus shear strain; (b) normalized shear modulus versus shear strain

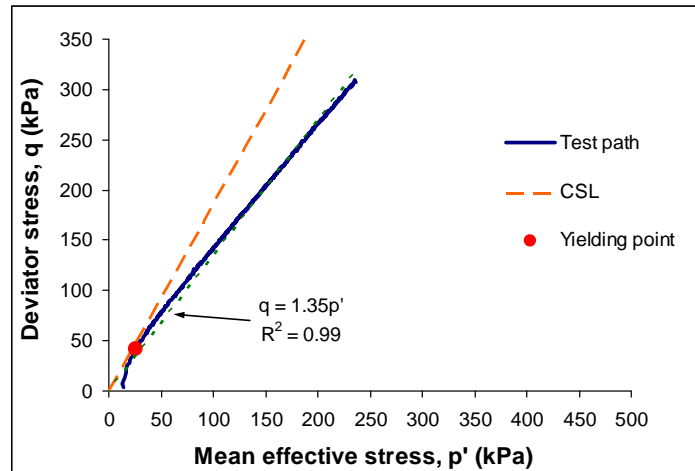


(a)

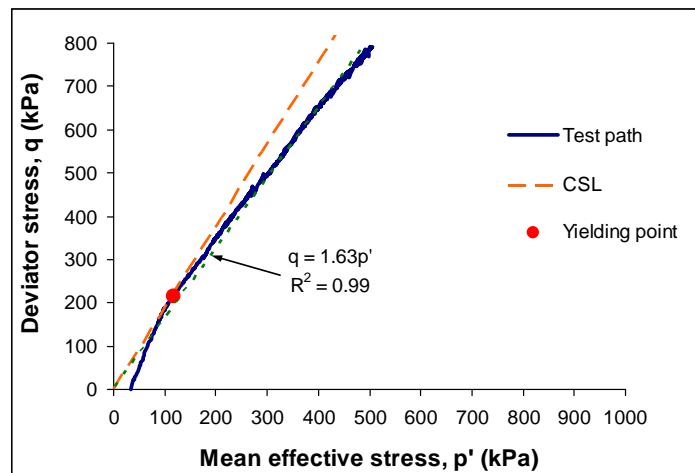


(b)

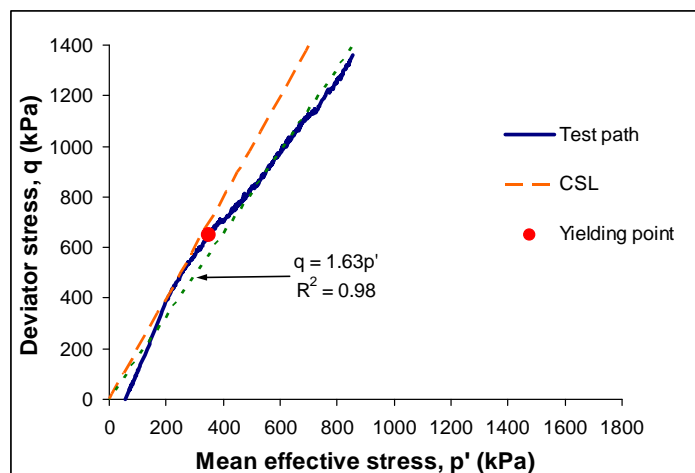
**Fig. 5-22.** Undrained shear behaviour of undisturbed Ottawa clay: (a) normalized deviator stress versus shear strain; (b) normalized shear modulus versus shear strain



(a)

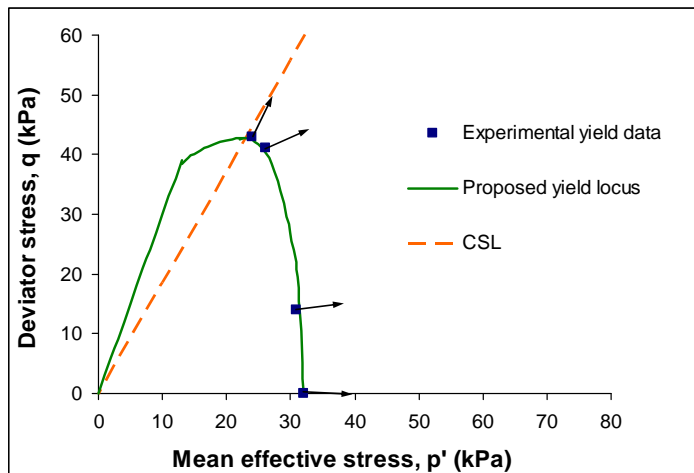


(b)

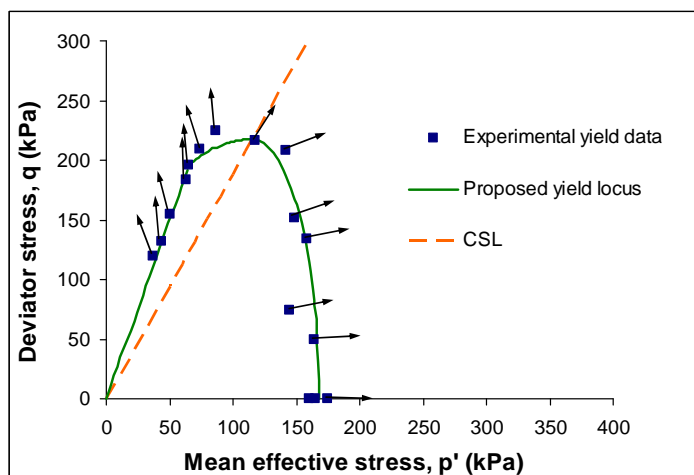


(c)

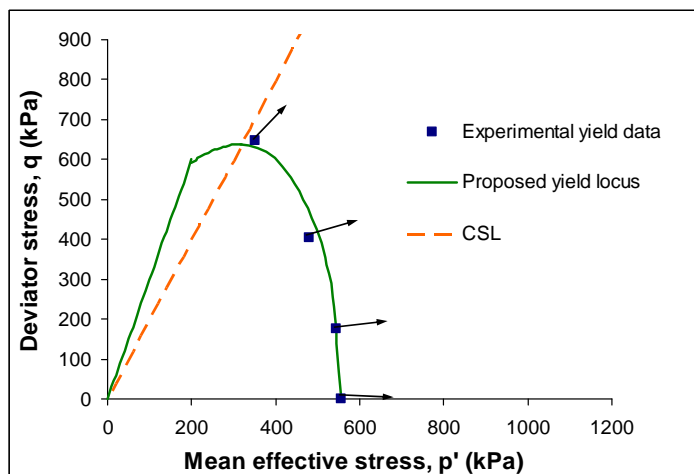
**Fig. 5-23.** Ko stress paths for artificially cemented specimens with: (a)  $c=3.1\%$ ; (b)  $c=4.2\%$ ; (c)  $c=6.4\%$



(a)



(b)



(c)

**Fig. 5-24.** Experimentally determined yield loci along with plastic strain increment

vectors: (a)  $c=3.1\%$ ; (b)  $c=4.2\%$ ; (c)  $c=6.4\%$

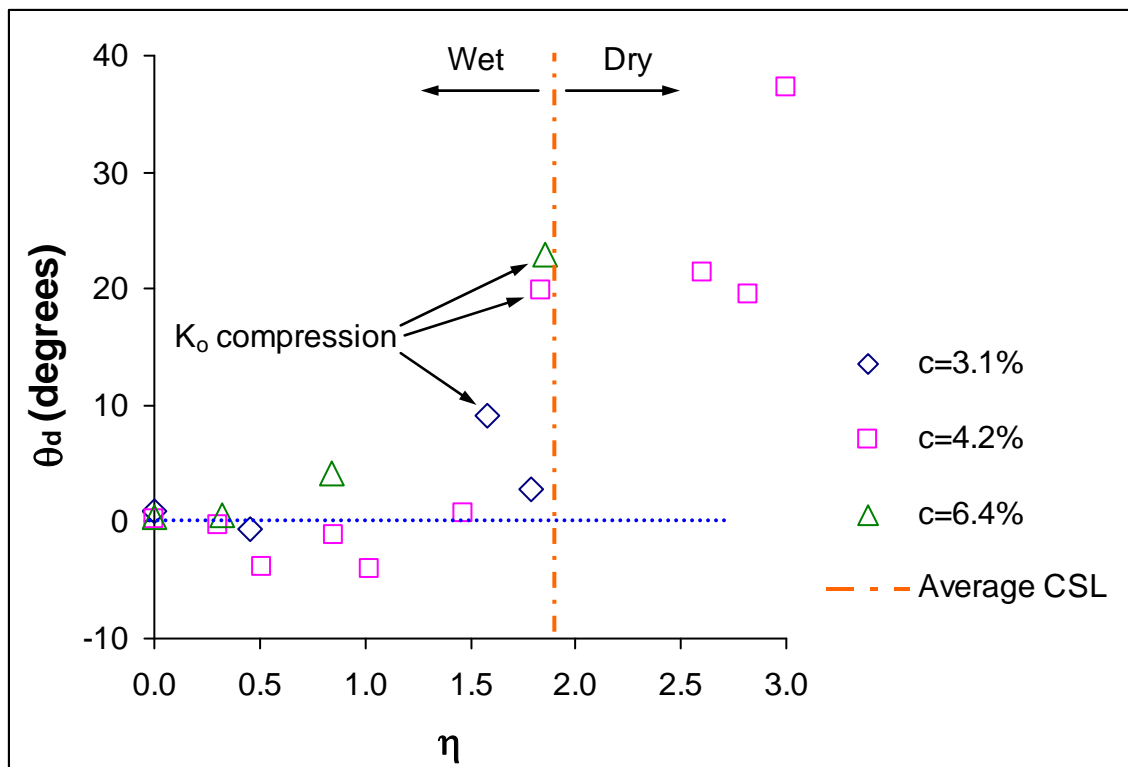


**Fig. 5-25.** The deviation from normality versus the stress ratio

## 6 CONCLUSIONS AND RECOMMENDATIONS

### 6.1 Summary and conclusions

The effects of artificial cementation on the structure and mechanical properties of clays were investigated. The research involved extensive laboratory testing, coupled with statistical and empirical formulation, and theoretical analysis and modelling. Various experiments were conducted on a number of different clays treated with Portland cement, and the results were used either independently or together with test data from the literature to achieve the aforementioned objectives. The major conclusions of this research study are as follows:

- Mercury intrusion porosimetry analysis showed that a bimodal distribution of pore sizes exists in saturated reconstituted clays. Variations in the moisture content of the reconstituted material are primarily accompanied by changes in the volume of inter-aggregate rather than intra-aggregate pores. Even air-drying did not significantly change the intra-cluster pore volumes of the reconstituted specimens. The measured intra-aggregate pore volumes only varied depending on the clay mineralogy, rather than the moisture content.
- A systematic error, causing an underestimation of the total pore volume, was detected in the results of mercury intrusion tests on reconstituted clays with high moisture contents. It was found that the amount of the observed error is proportionate to the total void ratio of the specimens. Hence, the inability of the mercury porosimetry technique to detect pores with a large diameter is mentioned as the possible cause of the error.

- Due to artificial cementation, the dispersed bimodal fabric of the reconstituted clay transforms into a flocculated unimodal state, in which a card house fabric exists and aggregates are connected to one another via cementitious bonding. The produced cementitious products are affixed to the particles, coat particle surfaces, and form matrices that fill the gaps between the clay aggregates (inter-aggregate pores). Artificial cementation also partitions the gaps existing between clay aggregates, reducing the total volume of the macro-pores and therefore the hydraulic conductivity of the cemented material.
- Microstructural investigations indicated that soil mineralogy and activity greatly affect the pore size distribution of cement-treated clays. In addition, the changes in the structure due to artificial cementation are directly linked with the resulting mechanical behaviour, i.e. soils undergoing higher structural alterations also experience more significant changes in their mechanical behaviour. Therefore, a greater degree of microstructural modifications due to artificial cementation is accompanied by higher gain of strength and loss of hydraulic conductivity.
- The effect of clay mineralogy on the effectiveness of artificial cementation has been investigated by conducting a parametric study on the data available in the literature along with those obtained herein. The results indicate that the activity of the clay, along with water-cement ratio, greatly influences the outcome of artificial cementation. Higher activity is found to induce higher strength and stiffness. This is explained by the significant effect the pozzolanic reactions, which take place between clay minerals and the cementation products. The slow

rate of these reactions is also considered to be responsible for the observed continuation of the hardening process even after long curing times.

- A critical review of the literature provided possible reasons for the importance of the pozzolanic reactions in the cementation process. A matrix of hardened material is formed in the soil body due to hydration of cement. However, the hydration process does not necessarily produce bonds between the clay particles. Since they form cementitious bridges between the soil particles and within the aggregates, the pozzolanic reactions are responsible for connecting the produced matrix to the clay particles and developing a cement-cluster network.
- A relationship has been proposed to predict the undrained shear strength of cement-treated clays after a certain curing period. The strength gained after 28 days has been used in the relationship as a normalising parameter. In addition, two new parameters have been defined to couple the effect of activity of a clay with that of cement and water contents. New empirical relationships were introduced based on these parameters to estimate the undrained shear strength, sensitivity, vertical effective yield stress, and compression index of cement-treated material.
- Although naturally structured clays exist in a highly collapsible, meta-stable state, artificially cemented clays display a gradual post-yield destructuration. It was illustrated that the structure of a cement-treated clay is preserved up to relatively high stress levels. The brittle bonds, produced due to artificial cementation, do not break simultaneously due to shearing or compression but rather rupture gradually, resulting in an overall elasto-plastic response that follows the critical state



principles. Consequently, the compression behaviour of the cement-treated material can be represented by a simple bilinear model, without any need to deal with the complexities of applying some of the models that currently exist for the structured clays (e.g. Liu and Carter, 2000; Horpibulsuk et al., 2010).

- Results of compression tests on different cement-treated clays have been compared with those previously provided for the reconstituted material (e.g. Nagaraj and Srinivasa Murthy, 1986; Burland, 1990; Nagaraj et al., 1994). It is shown that the same relationship governs the compression behaviour of both reconstituted and artificially cemented clays.
- In addition, results of an experimental study on artificially cemented Ottawa clay were used to define the yield states based on the energy method proposed by Graham et al. (1983b). Based on the critical state concept, a combination of the elliptical cap and modified Cam-clay models have been used to represent the observed yield envelop, which is bounded in  $p$ '- $q$  plane by the unconfined compression path. The expansion of the proposed yield envelop with plastic straining was studied by performing a number of unloading-reloading tests along different stress paths. It was confirmed that the shape of the expanded yield locus can be assumed to be unchanged due to plastic hardening, indicating the occurrence of isotropic hardening. It was also shown that using the critical state concept, the parameters required to find the yield locus can be satisfactorily obtained.
- Two different modes of failure have been detected for the cement-treated material. The specimens failed “dry” of the critical state line show an

- approximately linear elastic pre-yield response followed by an abrupt failure. In contrast, the samples yielding “wet” of the CSL exhibit an elasto-plastic gradual yielding. Work input data for different stress paths also indicate a brittle behaviour “dry” of the CSL and a ductile response “wet” of the critical state line.
- The normality condition was also checked for the proposed yield envelop. It was found that that the associated flow rule is obeyed in artificially cemented specimens failed “wet” of the CSL, while deviations from normality were observed in samples failed “dry” of the critical state line. Based on the observed behaviour, a simple linear, horizontal plastic potential surface has been suggested to predict the plastic flow dry of the CSL.

## **6.2 Recommendations for future research**

The results of this study provided a better understanding of the microstructure of the reconstituted clays with high water contents. It was shown that only the volume of the inter-aggregate pores changes due to variations in the moisture content. It was also proposed that the volume of the macro-pores governs the mechanical properties, such as hydraulic conductivity and strength, of the reconstituted material. This can be further investigated by performing mercury intrusion porosimetry tests on different clay specimens with various moisture contents and following different shear paths, along with measurements of hydraulic conductivity and strength, to find possible systematic patterns governing the soil behaviour during formation and under loading. In addition, it was shown that the intra-aggregate pore volume is constant for a certain clay mineralogy.

Further investigations of various types of clay could provide useful information about the relationship between clay mineralogy and the intra-aggregate pore volume.

Moreover, the microstructural processes involving the formation of artificial structure in clays with high water contents were investigated herein. A more comprehensive study involving the measurement of the pore size distribution of cemented clays, cured under stress, could shed some light on the effects of confinement on the developed structure. In addition, the microstructure of artificially cemented clays consolidated to different loads after curing can be studied using scanning electron microscopy or mercury intrusion porosimetry technique. This can help better understand the reasons for the gradual destructuration exhibited by the cement-treated material.

The parametric study conducted herein involved a relatively limited number of clays and only one type of cementing agent. The results can be further evaluated and adjusted using data obtained for other types of clay treated with Portland cement or a different cementing agent. Moreover, the results of triaxial experiments on various cement-treated clays with different moisture and cement contents can be used to find empirical relationships, similar to those suggested herein, to predict the parameters needed to define the proposed model (i.e.  $R$ ,  $p'_o$ , and  $M$ ). This would enhance the proposed model to provide more realistic predictions of the soil behaviour and reduce the possible errors.

The proposed framework is only rudimentary and has been developed based on the data for one type of cement-treated clay. First, it should also be further expanded analytically to create suitability for numerical predictions by analytically finding the required stress and strain matrices. The model should then be checked with the

experimental data obtained for other types of cemented clay to ensure its applicability to clays with a different mineralogy. Moreover, the suggested plastic potential functions can be further evaluated to find more realistic alternatives. True triaxial or hollow cylinder testing of the artificially cemented samples can also provide a powerful database for further development of the suggested framework in the three dimensional space.

The available knowledge of the naturally structured clays suggests that such clays are typically anisotropic and rate sensitive (e.g. Lo and Morin, 1972; Tavenas and Leroueil, 1977; Graham et al., 1983a). An experimental study of artificially cemented specimens cured under stress and cut in different angles can provide useful information about the possibility of the development of an anisotropic texture in such remoulded material. In addition, the effects of the strain rate and creep on the mechanical behaviour can be investigated by conducting fast and slow triaxial experiments. If needed, further adjustments can be applied to the proposed framework to take the effect of rate dependency and anisotropy into account.

It was shown herein that the intrinsic compression line proposed by Burland (1990) does not accurately predict the behaviour of reconstituted Ottawa clay. Further studies are needed to investigate the reasons for this discrepancy. As discussed before, this could be due to the effect of the silt content on the soil behaviour. Therefore, compression tests can be performed on other natural silty clays or on reconstituted clays artificially prepared in the laboratory with different silt contents to investigate the validity of the equation proposed by Burland (1990) for silty material.

Finally, it was also observed herein that a clear shear band forms in artificially cemented clays sheared in the triaxial equipment. This shear band formed even if the specimen was sheared at high confining pressures due to the partial preservation of the structure. The effects of the localised shear deformations on the overall response need to be evaluated in terms local drainage and geometrical symmetry of the specimen.

### 6.3 References

- Burland, J.B. (1990). "On the compressibility and shear strength of natural clays." *Geotechnique*, 40(3): 329–378.
- Graham, J., Crooks, J.H.A., and Bell, A.L. (1983a). "Time effects on the stress-strain behaviour of natural soft clays." *Geotechnique*, 33(3), 327–340.
- Graham, J., Noonan, M. L., and Lew, K. V. (1983b). "Yield states and stress-strain relationships in a natural plastic clay." *Canadian Geotechnical Journal*, 20(3), 502–516.
- Horpibulsuk, S., Liu, M.D., Liyanapathirana, D.S., and Suebsuk, J. (2010). "Behaviour of cemented clay simulated via the theoretical framework of the Structured Cam Clay model." *Computers and Geotechnics*, 37(1-2), 1–9.
- Liu, M. D., and Carter, J. P. (2000). "Modelling the destructuring of soils during virgin compression." *Geotechnique*, 50(4), 479–483.
- Lo, K.Y., and Morin, J.P. (1972). "Strength anisotropy and time effects of two sensitive clays." *Canadian Geotechnical Journal*, 9(3), 261–277.

- Nagaraj, T. S., and Srinivasa Murthy, B. R. (1986). "A critical reappraisal of compression index equations." *Geotechnique*, 36(1), 27–32.
- Nagaraj, T. S., Pandian, N. S., Narasimha Raju, P. S. R. (1994). "Stress-state–permeability relations for overconsolidated clays. *Geotechnique*, 44(2), 349–352.
- Tavenas, F., and Leroueil, S. (1977). "Effects of stresses and time on yielding of clays." *Proceedings of 9th International Conference on Soil Mechanics and Foundation Engineering*, Tokyo, 1,319–326.

## CURRICULUM VITAE

<b>Name</b>	Saeed Sasanian
<b>Place of birth</b>	Tehran, Iran
<b>Post-secondary Education and Degrees</b>	<p>Civil Engineering, Sharif University of Technology, Tehran, Iran. 2002 – 2005, M.Sc.</p> <p>Civil Engineering, Amirkabir University of Technology (Tehran Polytechnic), Tehran, Iran. 1997 – 2002, B.Sc.</p>
<b>Honours and Awards</b>	<p>John Booker Award for academic achievement and professional contributions to the engineering profession, Geotechnical Research Center, University of western Ontario,</p> <p>Western Engineering Scholarship, The University of Western Ontario, ON, Canada. (2005-2009)</p>
<b>Related Work Experience</b>	<p>Course instructor, The University of Western Ontario, ON, Canada. (2009)</p> <p>Teaching Assistant, The University of Western Ontario, ON, Canada. (2005-2010)</p> <p>Research Assistant, The University of Western Ontario, ON, Canada. (2005-2010)</p> <p>Research Assistant, Sharif University of Technology, Tehran, Iran. (2002-2005)</p>